UNIVERSITAT DE BARCELONA

Evaluation of tau seeding, spreading, and cytotoxicity using *in vitro* and *in vivo* models of tau pathology

Júlia Sala Jarque

ADVERTIMENT. La consulta d'aquesta tesi queda condicionada a l'acceptació de les següents condicions d'ús: La difusió d'aquesta tesi per mitjà del servei TDX (**www.tdx.cat**) i a través del Dipòsit Digital de la UB (**diposit.ub.edu**) ha estat autoritzada pels titulars dels drets de propietat intel·lectual únicament per a usos privats emmarcats en activitats d'investigació i docència. No s'autoritza la seva reproducció amb finalitats de lucre ni la seva difusió i posada a disposició des d'un lloc aliè al servei TDX ni al Dipòsit Digital de la UB. No s'autoritza la presentació del seu contingut en una finestra o marc aliè a TDX o al Dipòsit Digital de la UB (framing). Aquesta reserva de drets afecta tant al resum de presentació de la tesi com als seus continguts. En la utilització o cita de parts de la tesi és obligat indicar el nom de la persona autora.

ADVERTENCIA. La consulta de esta tesis queda condicionada a la aceptación de las siguientes condiciones de uso: La difusión de esta tesis por medio del servicio TDR (**www.tdx.cat**) y a través del Repositorio Digital de la UB (**diposit.ub.edu**) ha sido autorizada por los titulares de los derechos de propiedad intelectual únicamente para usos privados enmarcados en actividades de investigación y docencia. No se autoriza su reproducción con finalidades de lucro ni su difusión y puesta a disposición desde un sitio ajeno al servicio TDR o al Repositorio Digital de la UB. No se autoriza la presentación de su contenido en una ventana o marco ajeno a TDR o al Repositorio Digital de la UB (framing). Esta reserva de derechos afecta tanto al resumen de presentación de la tesis como a sus contenidos. En la utilización o cita de partes de la tesis es obligado indicar el nombre de la persona autora.

WARNING. On having consulted this thesis you're accepting the following use conditions: Spreading this thesis by the TDX (**www.tdx.cat**) service and by the UB Digital Repository (**diposit.ub.edu**) has been authorized by the titular of the intellectual property rights only for private uses placed in investigation and teaching activities. Reproduction with lucrative aims is not authorized nor its spreading and availability from a site foreign to the TDX service or to the UB Digital Repository. Introducing its content in a window or frame foreign to the TDX service or to the UB Digital Repository is not authorized (framing). Those rights affect to the presentation summary of the thesis as well as to its contents. In the using or citation of parts of the thesis it's obliged to indicate the name of the author.

Doctoral Thesis

Universitat de Barcelona

EVALUATION OF TAU SEEDING, SPREADING, AND CYTOTOXICITY USING *IN VITRO* AND *IN VIVO* MODELS OF TAU PATHOLOGY

Julia Sala Jarque

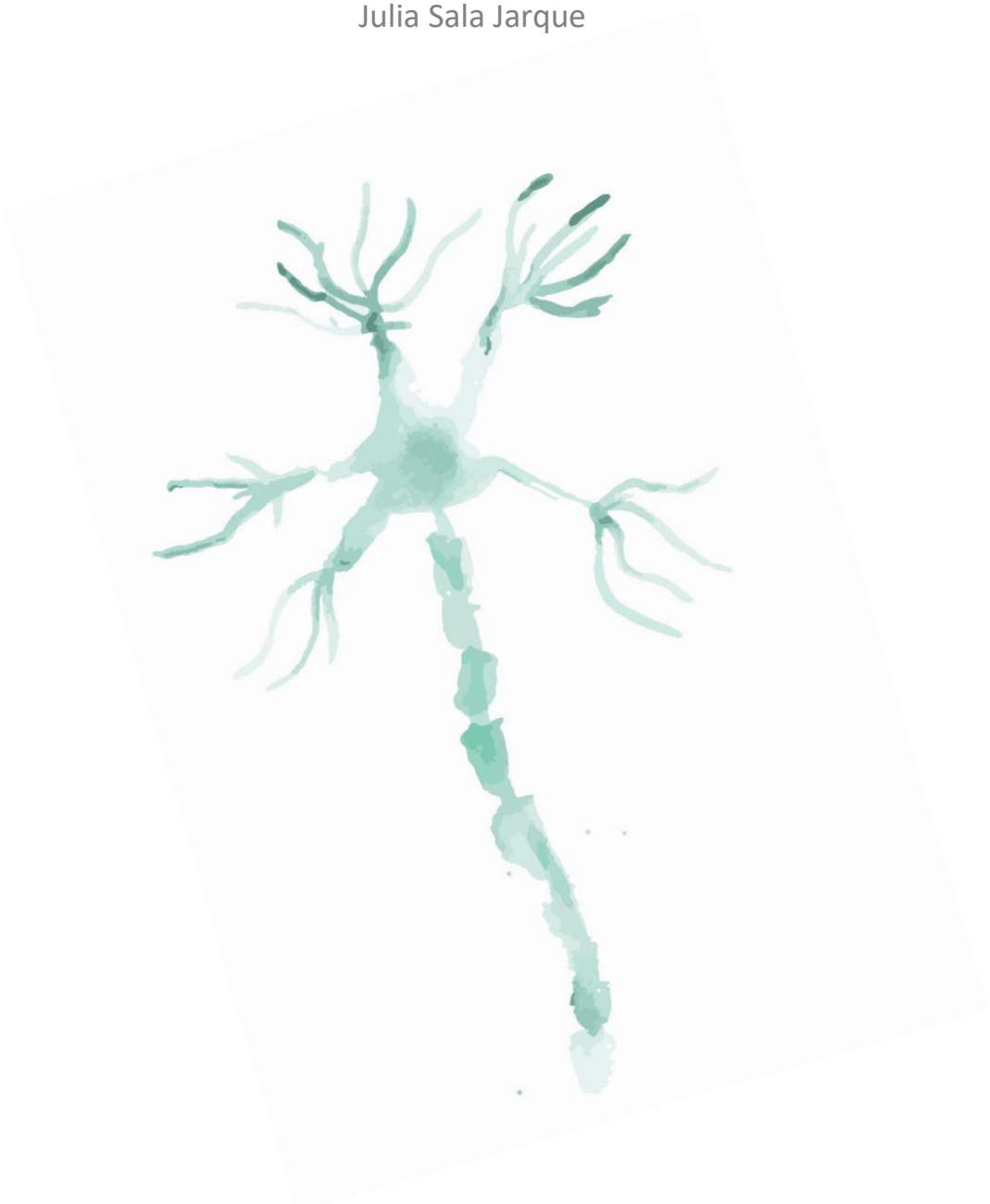

Universitat de Barcelona

Facultat de Biologia

Departament de Biologia Cel·lular, Fisiologia i Immunologia

Institute for Bioengineering of Catalonia (IBEC)

Parc Científic de Barcelona (PCB)

Programa de Doctorat en Biomedicina

Evaluation of tau seeding, spreading, and cytotoxicity using *in vitro* and *in vivo* models of tau pathology

PhD thesis report presented by Julia Sala Jarque to apply for a PhD degree from the Universitat de Barcelona. This doctoral thesis is inscribed in the **Programa de Doctorat en Biomedicina** of the **Universitat de Barcelona**.

Experimental work and the redaction of the present thesis have been performed in the **Institute for Bioengineering of Catalonia** (IBEC), under the direction and tutoring of **Prof. Dr. José Antonio del Río Fernández**, Professor of Cell Biology in the **Departament de Biologia Cel·lular, Fisiologia i Immunologia of the Universitat de Barcelona.**

Barcelona, 2022

Thesis director and tutor	**PhD candidate**
Prof. Dr. José Antonio del Río Fernández	Julia Sala Jarque

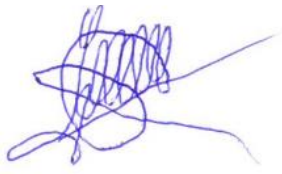

Abstract

Abnormal folding, hyperphosphorylation, aggregation, and subsequent deposition of the microtubule-associated protein tau, is the hallmark of a group of devastating neurodegenerative diseases known as tauopathies, including Alzheimer's disease. One striking aspect of Alzheimer's disease is that the presence of tau-related lesions in the brain occurs in a systematic, sequential manner, maintaining a predictable distribution pattern between synaptically connected neurons that varies very little among individuals. Increasing evidence suggests that the progression of tau pathology in the diseased brain behaves like a prion. The "prion-like" hypothesis suggests that "pathological" tau engages in self-seeded fibrillization and propagates through cell-to-cell spreading. However, despite intensive research, the cellular and molecular mechanisms involved and the pathological processes linking neuronal death and tau dysfunction are not fully understood.

Although Alzheimer's disease was first described in 1906 and has an increasing prevalence in the aging population, there is currently no treatment to prevent or cure this or any other tauopathy. Progress limitations are partially explained by the lack of appropriate models to study human tauopathies. Indeed, tau-targeting therapies that had demonstrated an improvement in the pathology in several models (i.e., *in vitro* and *in vivo*) were unable to produce positive results in clinical trials. These incongruences could be related to the fact that most experimental models rely on the over-expression of mutated tau species and the use of recombinant tau fibrils, which do not reproduce the sporadic nature of most human tauopathies.

Through this doctoral thesis, we examined various aspects of tau pathology, including tau seeding, spreading, and cytotoxicity, by implementing experimental approaches that better mimicked sporadic tauopathies. Nevertheless, at the beginning of this work, the reliability of the only commercially available cell line designed to be used as a cell-based assay to detect and report proteopathic seeding in biological samples was questioned in one publication. Given that this cell-based assay was central to the validation of the samples employed in this thesis, we conducted a thorough characterization of this cell line, known as the Tau biosensor cell line, and its ability to produce fluorescent tau aggregates. Our results show that the Tau biosensor cell line is a reliable cell-based assay that forms amyloid-like inclusions upon the addition of extracellular seed-competent tau species.

Next, we investigated the impact of extracellular seed-competent tau on the neuronal activity of primary cortical cultures derived from wild-type mice. We established an experimental setup that included microfluidic devices and calcium imaging, which allowed us to specifically treat the axons with tau, as well as monitor changes in spontaneous neural activity in a time-course manner. Although we demonstrate that cortical neurons in our microfluidic platforms display typical patterns of neuronal network activity, we do not detect changes after treating them with seed-competent tau. We then investigated how the presence of various extracellular seed-competent tau may affect neural metabolism (i.e., as an indicator of cellular viability) also in primary cortical cultures. Nevertheless, similar to what we observed in the analysis of neuronal activity, within the course of 10 days, no differences between tau-treated and untreated cells are found.

Finally, recent evidence suggests that the cellular prion protein is involved in the pathology of other prion-like proteins, such as amyloid-β and α-synuclein; however, much less is known about its role in tauopathies. We inoculated human Alzheimer's disease-derived samples into the hippocampus of transgenic mouse models with different expressions of the cellular prion protein. We found that all mice, regardless of their genotype, have similar profiles of tau-related lesions in their brains. Hence, our findings indicate that the cellular prion protein does not have a paramount role in the onset, seeding, or spreading of tau pathology.

Taken together, our work underscores the need for more pathologically relevant models to study certain aspects of sporadic human tauopathies, which could lead to the development of effective therapeutic strategies.

Table of Contents

Table of Contents

Abbreviations

2D: Two-dimensional

3D: Three-dimensional

3R-tau: 3-repeat tau

4R-tau: 4-repeat tau

AAV: Adeno-associated virus

Aβ: Amyloid-β

AD: Alzheimer's disease

AGD: Argyrophilic grain disease

ARTAG: Aging-related tau astrogliopathy

α-syn: α-synuclein

ATCC: American Type Culture Collection

a.u: Arbitrary units

BCA: Bicinchoninic acid assay

BSA: Bovine serum albumin

CBD: Corticobasal degeneration

CC: Charged cluster

CEEA: Ethics Committee on Animal Experimentation

CFP: Cyan fluorescent protein

ChR2: Channelrhodopsin-2

CJD: Creutzfeldt-Jakob disease

CO_2: Carbon dioxide

Cryo-EM: Cryogenic electron microscopy

CSF: Cerebrospinal fluid

CTE: Chronic traumatic encephalopathy

DAB: 3.3'-diaminobenzidine

DIV: Days *in vitro*

DMEM: Dulbecco's Modified Eagle Medium

DMSO: Dimethyl sulfoxide

DOT: Day of treatment

DTT: Dithiothreitol

E16.5: Embryonic day 16.5

EDTA: Ethylenediaminetetraacetic

EGTA: Ethylene glycol-bis(β-aminoethyl ether)-*N*,*N*,*N*′,*N*′-tetraacetic acid

EtOH: Ethanol

FBS: Fetal bovine serum

FRET: Fröster resonance energy transfer

FTD: Frontotemporal dementia

FTDP-17: Frontotemporal dementia with parkinsonism linked to chromosome 17

FTLD: Frontotemporal lobar degeneration

GECI: Genetically encoded calcium indicator

GFP: Green fluorescent protein

GGT: Globular glial tauopathy

Glu: Glutamic acid

GPI: Glycosylphosphatidylinositol

GSS: Gerstmann-Straäussler-Scheinker syndrome

HEK293: Human embryonic kidney 293

HR: Hydrophobic region

HRP: Horseradish peroxidase

HSPG: Heparan sulfate proteoglycan

IBI: Inter-burst interval

IHC: Immunohistochemistry

iPSC: Induced pluripotent stem cell

ISF: Interstitial fluid

kDa: Kilodaltons

KO: Knock-out

Leu: Leucine

LRP1: Low-density lipoprotein receptor-related protein 1

LTD: Long-term depression

LTP: Long-term potentiation

MAPT: Microtubule-associated protein tau

MAPT: Human microtubule-associated protein tau

m.p.i: Months post-inoculation

MSA: Multiple system atrophy

MT: Microtubule

MTBD: Microtubule-binding domain

N2a: Neuro-2a cell line

$NaHCO_3$: Sodium bicarbonate

ND: Neurodegenerative disease

NFT: Neurofibrillary tangle

NGS: Normal goat serum

NHS: Normal horse serum

n.s: Not significant

PART: Primary age-related tauopathy

PBS: Phosphate-buffered saline

PD: Parkinson's disease

PDMS: Poly(dimethylsiloxane)

PFA: Paraformaldehyde

PFF: Preformed fibril

PHF: Paired helical filament

PiD: Pick's disease

PMD: Post-mortem delay

PrD: Prion disease

PRNP: Human prion protein gene

Prnp: Murine prion protein gene

PrP: Prion protein

PrP^{C}: Cellular prion protein

PrP^{Sc}: Scrapie prion protein

PSP: Progressive supranuclear palsy

PTM: Post-translational modification

RD: Repeat domain

ROI: Region of interest

ROS: Reactive oxygen species

SD: Standard deviation

SDS-PAGE: Sodium dodecyl sulfate polyacrylamide gel electrophoresis

Ser: Serine

SN: Supernatant

TEM: Transmission electron microscope

Thr: Threonine

ThT: Thioflavin T

TIF: Triton X-100 insoluble fraction

TNT: Tunneling nanotubes

Tris: Tris(hydroxymethyl) aminomethane

TSF: Triton X-100 soluble fraction

TTBS: Tris-buffered saline supplemented with 0.1% Tween 20

WB: Western blot

WT: Wild-type

YFP: Yellow fluorescent protein

ZH3: Zürich-III-*Prnp*$^{-/-}$

General Introduction

1.1 Introduction: Brief Overview

Over 25 different neurodegenerative diseases (NDs) are classified as tauopathies, including Alzheimer's disease (AD), aging-related tau astrogliopathy (ARTAG), argyrophilic grain disease (AGD), primary age-related tauopathy (PART), progressive supranuclear palsy (PSP), chronic traumatic encephalopathy (CTE), Pick's disease (PiD), corticobasal degeneration (CBD), and globular glial tauopathy (GGT) (Cleveland *et al.*, 1977; Ballatore *et al.*, 2007; Sanders *et al.*, 2014). Despite significant efforts to overcome the pathophysiological aspects of tauopathies, there are still no viable treatments.

Tauopathies are defined by the gradual accumulation and deposition of the microtubule (MT)-associated protein tau (MAPT) (i.e., encoded by the *MAPT* gene), along with neuronal loss and cognitive decline. Age is the primary risk factor for most sporadic tauopathies, although they can also be caused by rare genetic mutations (Habes *et al.*, 2016; Hickman *et al.*, 2016). For instance, mutations in the *MAPT* gene on chromosome 17 produce hereditary frontotemporal dementia with parkinsonism linked to chromosome 17 (FTDP-17) (Goedert & Jakes, 2005; Kovacs, 2017).

Tau has predominantly been identified as an MT-binding protein mainly localized in the axons of all neurons, where its primary function is the regulation of MT dynamics (Binder *et al.*, 1985; Guo *et al.*, 2017). It is believed that, under pathological conditions, tau detaches from MTs, causing significant MT-related instability and decreasing axonal transport, which contributes to severe synaptic dysfunction (e.g., (Guo *et al.*, 2017; Laurent *et al.*, 2018)). Eventually, tau aggregates into highly insoluble, hyperphosphorylated amyloid fibrils (Montejo de Garcini *et al.*, 1986; Alonso *et al.*, 1994) via a process known as self-seeded polymerization. Consequently, tau aggregates are the most common histopathological hallmark of all tauopathies. It is relevant to note, however, that the brain areas damaged by tau-related lesions, the primarily affected cell types, and the aggregates' structures, are all specific to each tauopathy. Despite this, the etiology of this clinical and pathological diversity of human tauopathies is currently unknown.

In sporadic AD, the most prevalent tauopathy, tau aggregation occurs in a predictable spatiotemporal manner across neuroanatomically connected brain regions (Braak & Braak, 1991). Multiple studies now suggest that the spreading of "pathogenic" tau between synaptically connected neurons underlies the progression of tau pathology (e.g., (Clavaguera *et al.*, 2009; Frost *et al.*, 2009)). Because these observations match

the established mechanisms of propagation described for prion diseases (PrDs), human tauopathies are now classified into a group of NDs known as “prion-like” diseases. However, the exact cellular pathways involved in this process are unknown. In sporadic tauopathies, the presence of tau aggregates and cognitive decline are strongly correlated. Additionally, the fact that FTDP-17 mutations are directly related to neurodegeneration indicates a causal link between neurodegeneration and tau dysfunction. Nevertheless, the exact pathological mechanisms by which tau may be cytotoxic to neural cells are still unclear.

Despite AD being first described in 1906, to date, there is no treatment for it or any other human tauopathy. The lack of pharmacological approval is usually attributed to clinical trial failure, even though most drugs clearly demonstrated dramatic improvements in preclinical studies using experimental models. There is a need for more reliable and better models to be used not only as platforms for testing drug efficacy but also for understanding the fundamental mechanisms of these diseases.

1.2 Tau Protein

1.2.1 Tau Splicing

In humans, tau is encoded by a single gene (i.e., *MAPT*), which consists of 16 exons, and locates on the long arm of chromosome 17 at band position 17q21.31. Importantly, mutations in the *MAPT* gene are known to cause hereditary frontotemporal dementia (FTD) associated with frontotemporal lobar degeneration (FTLD) (Hutton *et al.*, 1998; Poorkaj *et al.*, 1998; Spillantini *et al.*, 1998; Ghetti *et al.*, 2015). In the healthy adult human brain, there are six tau isoforms ranging from 352 to 441 amino acids in length, resulting from the alternative splicing of exons 2, 3, and 10 (Goedert *et al.*, 1989; Avila, 2006b). Exons 2 and 3 encode 29 amino acid inserts, each located at the N-terminal of the protein. Although exon 3 cannot be transcribed without exon 2, the latter can be expressed even in the absence of exon 3. Therefore, 0N-tau isoforms result from excluding both exons 2 and 3, 1N isoforms result from including exon 2, and 2N isoforms arise from expressing both exons. In parallel, exon 10 encodes the second (R2) of four highly conserved imperfect repeats; the rest are expressed by exons 9, 11, and 12. Thus, the inclusion of exon 10 results in tau isoforms with four repeats (4R), while its exclusion produces isoforms with three repeats (3R). Hence, all possible tau isoforms are 0N3R, 1N3R, 2N3R, 0N4R, 1N4R, and 2N4R (Figure 1). The distribution of spliced isoforms varies among species, is regulated by the brain development stage, and exhibits unique temporal and spatial expression patterns (Goedert & Jakes, 1990; Hanes *et al.*, 2009;

Liu & Gotz, 2013). It is worth mentioning that in healthy adults, 3R and 4R isoforms are found at equivalent ratios (Avila *et al.*, 2016); however, in most tauopathies, save for AD and CTE, this proportion is not maintained. Consequently, human tauopathies can be categorized as 3R, 4R, or 3R/4R (e.g., PiD, GGT, and AD, respectively) based on the tau isoforms present in the large, insoluble aggregates (Kovacs *et al.*, 2022).

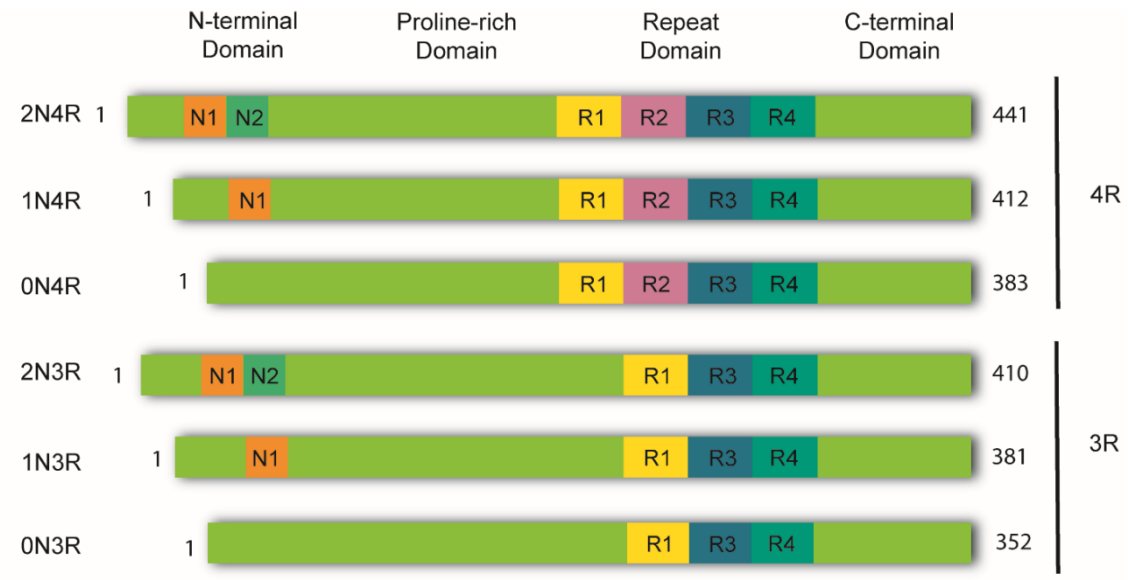

Figure 1 Schematic representation of tau isoforms: In the adult human brain, there exist six tau isoforms resulting from alternative splicing. In all six isoforms, tau protein can be divided into four domains with different biochemical properties: an acidic N-terminal domain, a proline-rich domain, the repeat domain (RD) with three to four repeat sequences (i.e., 3R- or 4R-tau, respectively), and a C-terminal domain. Image obtained from (Sala-Jarque *et al.*, 2022).

1.2.2 Tau Structure

As already indicated, tau's primary function is the regulation of MT dynamics, maintaining cytoskeleton stability, promoting axonal outgrowth, and regulating axonal trafficking (Medina *et al.*, 2016). Tau is a soluble hydrophilic and intrinsically disordered protein that lacks a well-defined tertiary structure, whose conformational remodeling often depends on different binding partners (Schweers *et al.*, 1994; Mandelkow & Mandelkow, 2012; Avila *et al.*, 2016). Importantly, it does not have any potential signal peptides, transmembrane helices, lipidation, or glycolipidation sites that may allow it to be incorporated into cell membranes. As a result, tau is commonly regarded as a cytoplasmic-soluble protein. Furthermore, very little is known about the secondary structure of tau, although it is thought that in solution, it acquires a shape known as the "global hairpin conformation." In this context, the C-terminus of the protein folds over the region with the previously mentioned imperfect repeats, and the N-terminus folds over

the C-terminus (Jeganathan *et al.*, 2006; Jeganathan *et al.*, 2008; Jeganathan *et al.*, 2012).

Tau can be divided into four functional domains (Figure 1): a) the N-terminal domain, also known as the “projection domain,” as it extends out from the MT, allowing tau to interact with other proteins, such as cytoskeletal components, cytosolic organelles, or the plasma membrane (Pooler & Hanger, 2010; Liu *et al.*, 2016). Moreover, it regulates the distance between MTs, influencing axon diameter (Chen *et al.*, 1992). b) The proline-rich mid-domain is characterized by having different phosphorylation residues. This domain also interacts with receptor proteins, playing a variety of critical roles in signal transduction pathways (Hwang *et al.*, 1996; Lee *et al.*, 1998). c) Next, the MT-binding domain (MTBD) or repeat domain (RD) mediates the binding of tau to the MTs network through the four imperfect repeat domains (i.e., encompassing 31-32 residues) encoded by exons 9-12. (Goedert *et al.*, 1989; Lee *et al.*, 1989). Consequently, three (i.e., R1, R3, and R4) or four (i.e., R1-R4) MT-binding repeats, due to the absence or presence of exon 10, respectively, promote MT assembly (Goedert & Jakes, 1990). Notably, given that 4R-tau species have an extra MT-binding repeat, these isoforms bind and stabilize MTs more efficiently than 3R variants (Goedert & Spillantini, 2011). d) Finally, the C-terminal domain, which is known to have an overall basic charge.

1.2.3 Post-Translational Modifications of Tau

The physiological functions of tau are predominantly regulated by at least 12 distinct types of post-translational modifications (PTMs), such as phosphorylation, glycosylation, isomerization, truncation, glycation, deamination, nitration, methylation, and sumoylation (Gong *et al.*, 2005; Martin *et al.*, 2011).

Phosphorylation is the most well-studied PTM of tau protein, as it negatively modulates its binding affinity to the MTs (Avila *et al.*, 2004a). Therefore, under physiological conditions, tau phosphorylation and dephosphorylation levels are tightly regulated by multiple kinases and phosphatases (Biernat *et al.*, 1993; Wagner *et al.*, 1996; Martin *et al.*, 2013a; Martin *et al.*, 2013b). However, hyperphosphorylated tau is the major component of neuronal and glial inclusions in human tauopathies (Grundke-Iqbal *et al.*, 1986). Hence, in disease, the kinase/phosphatase balance is thought to be disturbed, resulting in tau hyperphosphorylation (Avila *et al.*, 2004b). Consequently, tau loses its ability to bind to MTs, leading to destabilization and disruption of axonal transport (Wagner *et al.*, 1996; Wang *et al.*, 2007). Additionally, the phosphorylation of tau at certain key residues affects its propensity to aggregate (Alonso *et al.*, 1994; Alonso

et al., 2001). For instance, experimental evidence has demonstrated that phosphorylation of Ser396 and Ser404, as well as Ser205, Thr205, and Thr212, triggers tau aggregation (Abraha *et al.*, 2000; Necula & Kuret, 2005; Rankin *et al.*, 2005). Notably, in diagnostic practice, antibodies against tau phosphorylation epitopes are often used (e.g., anti-AT8 (pSer202/pThr205), anti-CP13 (pSer422), and anti-PHF-1 (pSer396/pSer402) antibodies, where "p" indicates phosphorylated) (Kovacs, 2015).

Nevertheless, hyperphosphorylation is not always a synonym for neurodegeneration, as highly phosphorylated tau is found during physiological development (Avila *et al.*, 2004a) and hibernation (Arendt *et al.*, 2003) without the formation of amyloid aggregates. Therefore, whether tau phosphorylation is a prerequisite for tau aggregation or even tau pathology is still unclear (Avila, 2006a; Goedert *et al.*, 2017a; Mudher *et al.*, 2017).

1.3 Tauopathies

NDs are extremely complex multifactorial diseases that require in-depth knowledge of several scientific disciplines only to grasp some basic concepts related to their nature. Tauopathies are no different. First and foremost, human tauopathies are a set of NDs characterized by their clinical variability. In this regard, a spectrum of tau pathologies can be distinguished based on the distinct involvement of anatomical areas with tau lesions, different cellular pathology (e.g., neurons and/or glial cells), specific microscopic lesions (e.g., globular astroglial inclusions, spherical inclusions), the presence of 3R-, 4R-, or 3R/4R-tau isoforms in the inclusions, and the morphology of the aggregates (Kovacs, 2015; Kovacs *et al.*, 2022). For instance, AD patients display two kinds of fibril morphology: straight filaments and paired helical filaments (PHFs), which comprise the building blocks of large deposits known as neurofibrillary tangles (NFTs). In PiD, however, tau inclusions are assembled, resulting in a distinct type of aggregate known as Pick Bodies (Falcon *et al.*, 2018a). In addition to phenotypic variability, the stereotypical progression of tau-related lesions in the central nervous system characterizes human tauopathies (Braak & Braak, 1991; 1995). Despite this, the pathological mechanisms underlying these phenomena are still unclear.

Most of the unknowns related to NDs in general, and tauopathies in particular, seem to be associated with protein aggregation during disease progression. Protein aggregates are common in most NDs, and yet, very little is known about how they relate to the pathological process involved. And again, because protein aggregates are common in most NDs, it appears that there must or should be some underlying basic mechanism shared by all of them. Therefore, researchers have focused on these

aggregates in an attempt to provide a rational explanation of why NDs are so prevalent but still incurable. In this endeavor, scientists have been able to demonstrate that, indeed, these diseases share some pathological mechanisms. Nevertheless, acquiring and producing scientific knowledge is not always a linear journey, and sometimes it may take the shape of a network. In this context, tauopathies are now better understood in the realm of amyloids and PrDs. However, what was once limited to PrDs (e.g., strains), now seems to be a property of amyloids in general (e.g., polymorphs), although the terminology has not changed. Consequently, introducing the fundamental principles required to describe the current state-of-the-art knowledge on tau pathology can be challenging.

In the following section, we will present some of the leading notions relevant to the prevailing understanding of human tauopathies. We emphasize that, although some concepts will appear linearly in the text, they are all interconnected and depend on one another. Having said this, we will first describe “amyloids” in the context of amyloid diseases. Next, we will proceed to explain the “prion-like” hypothesis by introducing the terms “seeding,” “spreading,” and “strains.” We will then summarize the main aspects of tau-related cytotoxicity and focus on how this protein may also affect neuronal activity. Finally, we will provide some information on the role of the prion protein (PrP) in NDs and, more specifically, in tauopathies.

1.3.1 Tauopathies Are Amyloid Diseases

All tau aggregates are amyloids despite displaying unique morphologies in the different human tauopathies. Amyloids are notoriously known for their connection to NDs, such as PrDs and α-synucleinopathies. Before proceeding to examine the molecular characteristics of amyloids, it is necessary to clarify several terms related to tau amyloids that will be used throughout this thesis. First, “aggregate” refers to the deposition of many amyloid fibrils, which sometimes become visible under a light microscope. Second, the term “oligomer” has been used in the literature to describe small and soluble (i.e., although sometimes insoluble) protein assemblies with an overall globular conformation (Ren & Sahara, 2013; Maeda & Takashima, 2019). However, as we will discuss in future sections, “oligomer” is a rather nebulous term and will be handled with caution throughout this work.

Amyloids are lengthy assemblies of peptides or proteins stacked upon one another, forming protofilaments. These protofilaments are intertwined with each other and arranged in a two-fold helical symmetry (Willbold *et al.*, 2021). In detail, amyloid fibrils

have a recurring substructure made up of β-strands that run perpendicular to the fibril axis, generating cross-β-sheets running parallel to the fibril axis. Of note, the capability to form cross-β-structure seems to be inherent to all known proteins, despite their primary structure (Chiti & Dobson, 2006). Nevertheless, the precise arrangement of β-strands and β-sheets, as well as their supramolecular architecture, appear to be highly dependent on the amino acid sequence, fibrillization conditions, and presence of cofactors during the amyloid formation. Although amyloids have been known for over a century (Sipe & Cohen, 2000), it was not until 2017 that researchers were able to obtain the first atomic or near-atomic resolution of amyloid tau fibrils, thanks to technical advances in cryo-electron microscopy (EM) (Fitzpatrick *et al.*, 2017; Zhang *et al.*, 2019; Scheres *et al.*, 2020; Goedert, 2021).

The fact that tau aggregates are amyloids is not trivial. Although the following section focuses on the prion-like properties of tau, most of these are features shared by amyloids in general. Indeed, PrDs appear to be just a category of a much wider phenomenon known as amyloidosis (Sipe & Cohen, 2000; Chiti & Dobson, 2006; Willbold *et al.*, 2021). However, for clarity, we have decided to stick to the current trends and terminologies in the literature used to discuss human tauopathies.

1.3.2 Tauopathies Are Prion-Like Diseases

It is pertinent to note that S. Prusiner introduced the word “prion” to describe amyloid fibrils made up of the PrP in a β-sheet-dominated conformation (Prusiner, 1991). As the basis for PrDs, these fibrils grow and self-replicate by recruiting their endogenous monomeric counterparts (i.e., self-seeded polymerization). According to the “protein-only” hypothesis, PrDs are a group of NDs caused solely by an infectious protein known as the proteinase K-resistant prion protein or scrapie prion protein (PrP^{Sc}) (Prusiner, 1998), which is the pathogenic variant of the cellular prion protein (PrP^{C}) (Prusiner, 1982), encoded by the *PRNP* gene. PrDs, like many other NDs, can develop sporadically (e.g., Creutzfeldt-Jakob disease (CJD)) or be inherited (e.g., fatal familial insomnia and Gerstmann-Straäussler-Scheinker syndrome (GSS)) (Colby & Prusiner, 2011). However, PrDs are the only NDs acknowledged to be contagious in mammals and humans (e.g., kuru and bovine spongiform encephalopathy). Although PrP^{Sc} is to blame for all these diseases, there is considerable diversity of clinical symptoms among PrDs (Collinge & Clarke, 2007), such as different incubation times, specific brain lesion profiles, distinguishable amyloid distribution, and horizontally stable spreading. To explain these phenomena, scientists adopted the term “strain” from the research fields of viral and bacterial infections, in which strains are genetic polymorphisms that account

for the variation in pathology and transmissibility observed in infected organisms. In the case of PrDs, prion strains are distinct aggregate conformations of the prion protein, resulting in unique associated pathologies (Bessen & Marsh, 1994). In the brain, prions spread trans-cellularly from diseased neurons to healthy surrounding cells. Although the specifics of this spreading are not entirely understood, several mechanisms have been proposed (Gousset *et al.*, 2009; Colby & Prusiner, 2011; Abounit *et al.*, 2016).

Mounting evidence suggests that NDs characterized by amyloid deposition (e.g., tauopathies, α-synucleinopathies, and Huntington's disease) and PrDs share pathological mechanisms (Clavaguera *et al.*, 2009; Frost *et al.*, 2009; Iba *et al.*, 2013; Wu *et al.*, 2013). Despite some of these shared characteristics being amyloid features rather than prion-specific traits, it is common practice to refer to these proteins as "prion-like." However, prion-like proteins are not currently regarded as *bona fide* prions (Del Rio *et al.*, 2018; Goedert, 2020; Vascellari & Manzin, 2021) since, unlike PrP^{Sc}, there is no definitive evidence of interindividual transmissibility (Coca *et al.*, 2021). Hence, the term "prion-like" has been used to describe proteins with replication and propagation mechanisms similar to PrDs, but whose infectivity has not been proven.

As previously mentioned, human tauopathies are characterized by the presence of tau aggregates in the central nervous system. However, their existence is not limited to specific brain regions, as they appear to spread across the brain during disease progression. Braak and Braak conducted a cross-sectional neuropathological examination of the brains of AD-deceased individuals and reported that tau pathology follows a predictable, stereotyped, and hierarchical pattern along neuroanatomically connected brain areas (Braak & Braak, 1991) (Figure 2). Their findings demonstrated that the presence of NFTs in the diseased brain does not occur at random. Instead, tau lesions consistently begin in the locus coeruleus and proceed to the temporal lobe transentorhinal region, then to the allocortex and neocortex (i.e., initially in associational areas and eventually in the primary sensory cortex and primary motor cortex) (Braak *et al.*, 2013). These observations have recently been validated using positron emission tomography (Scholl *et al.*, 2016).

To date, the underlying pathological mechanisms related to the progression of tau pathology in human patients are not yet fully understood. In this regard, it has been proposed that tau pathology spreads from cell to cell in a manner analogous to that of misfolded PrP in PrDs (Krammer *et al.*, 2009; Prusiner, 2012). Consequently, this rationale has been termed the "prion-like" hypothesis. The pathogenic mechanisms underlying the prion-like nature of tau have been postulated to include both the "seeding"

and trans-cellular “spreading” of proteopathic seeds (Clavaguera *et al.*, 2009; Frost *et al.*, 2009; Kfoury *et al.*, 2012). More recently, experimental evidence has also provided evidence of the existence of tau “strains” (Sanders *et al.*, 2014).

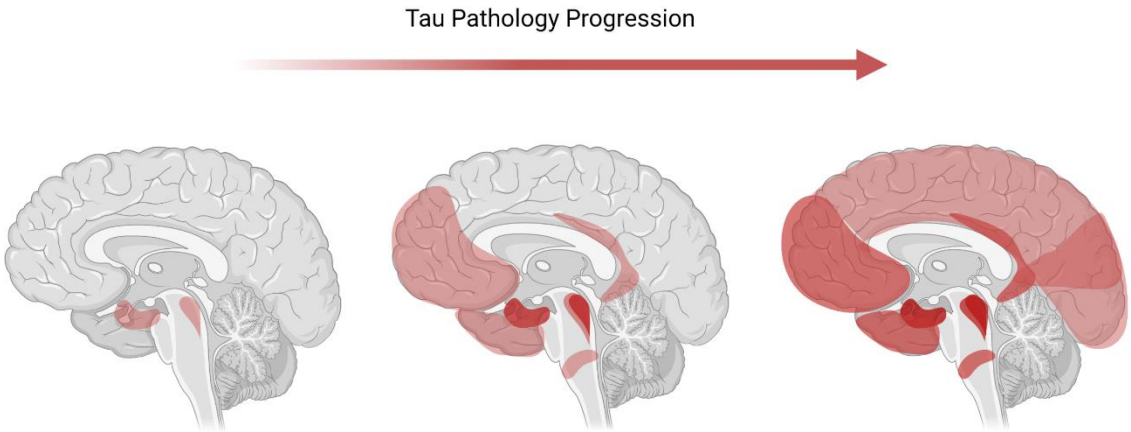

Figure 2 Schematic representation of tau pathology progression in AD patients: The red shaded areas indicate the affected regions by tau pathology. Initially tau lesions appear in the locus coeruleus and from there it spreads to the temporal lobe before further progressing into the allocortex and neocortex (Braak & Braak, 1991).

1.3.2.1 Tau Seeding

Similar to PrDs, the formation of tau aggregates is based on the conversion of monomeric soluble tau into amyloid fibrils. In tauopathies, tau misfolds and acts as a template, recruiting its healthy counterparts via a mechanism akin to crystal formation known as nucleation-dependent polymerization (Jarrett & Lansbury, 1993), by which tau initiates a self-amplifying cascade and forms amyloid fibrils. Importantly, nucleation-dependent polymerization is not exclusive to amyloid formation, as it is also present in many well-studied physiological processes (e.g., MT assembly and filamentous actin polymerization). Nevertheless, replication of the misfolded state is a distinctive feature of amyloid-forming proteins. We will be referring to one such process as “seeding,” and the term “seed” will imply the smallest unit required to template tau’s misfolded state.

Once formed, the seed displays nucleation properties and starts the process of self-seeded fibrillization, in which monomeric tau is progressively recruited and incorporated into the growing fibril. Large tau aggregates can then be disrupted, resulting in new fibrils or seeds, thereby amplifying tau pathology. The kinetics of nucleation-dependent polymerization have long been studied and modeled *in vitro* in cell-free systems. Briefly, to generate an amyloid fibril, the building blocks (i.e., identical proteins or peptides) must

be present, in addition to specific cofactors (e.g., heparin, RNA) that may aid in the process (Willbold *et al.*, 2021). For years, thioflavin T (ThT) binding assays have been the gold standard for monitoring the kinetics of amyloid aggregation *in vitro*. ThT is an amyloid-sensitive fluorescent dye that increases its fluorescence intensity upon binding to cross-β structures. Hence, ThT fluorescence reflects an increase in the sample's cross-β sheet content.

In a fibrillization experiment, the time-dependent ThT fluorescence intensity adopts the form of a sigmoidal-shaped curve, which is typical of any nucleation-dependent process (Figure 3). In this regard, the sigmoidal curve can be divided into three main phases: the lag phase, the exponential growth phase, and the saturation, steady or plateau phase. The lag phase (i.e., also known as the nucleation step) is the period required for the aggregating material to reach a concentration detectable by ThT. During this phase, monomers undergo conformational changes (i.e., misfolding), and self-associate with one another to form more complex assemblies rich in β-sheets. This first step is followed by the growth phase, in which monomeric tau is incorporated into the

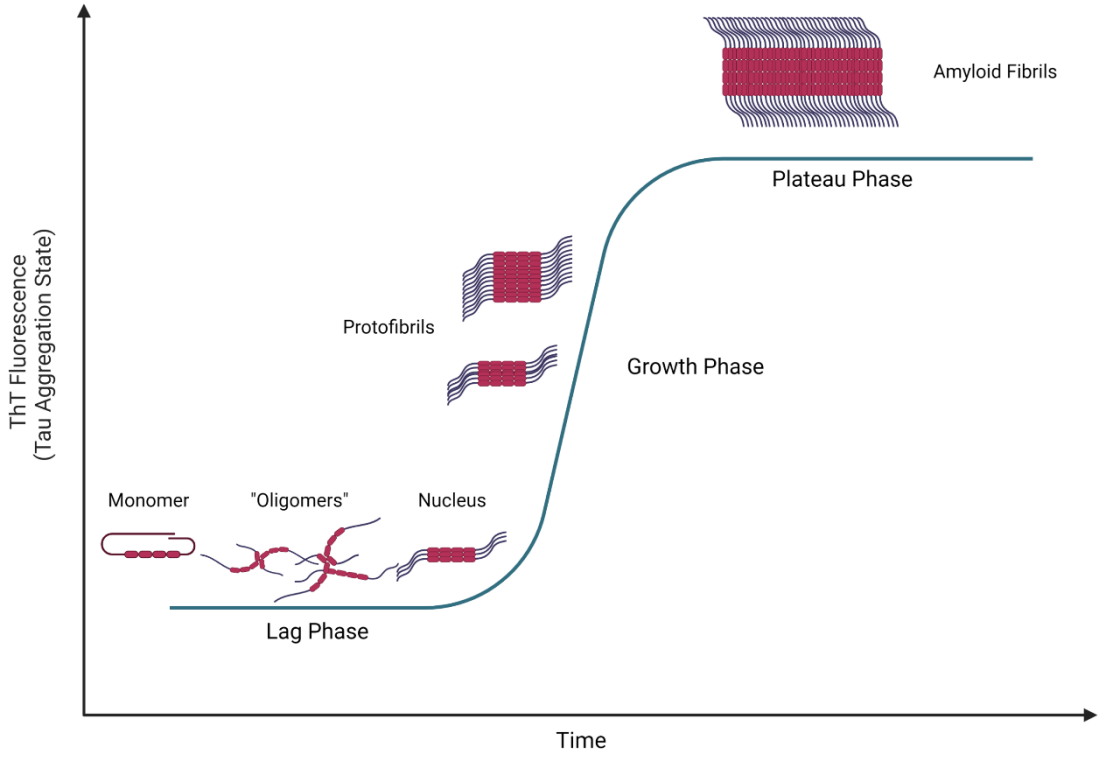

Figure 3 Schematic representation of the nucleation-dependent polymerization model of amyloid fibril formation: The thioflavin T (ThT) fluorescence kinetics displays a sigmoidal-shaped kinetic curve (blue). The lag phase, or nucleation step, is a rate-limiting step in which monomers aggregate into soluble "oligomers" until a nucleus is formed. During the growth phase, the nucleus grows as monomers are incorporated into fibrils. Finally, the final plateau, or steady phase, is when there are no more monomeric substrates available as they have all been incorporated into the amyloid fibril (Willbold et al., 2021).

growing fibril, resulting in more cross-β sheet content, thus increasing fluorescence intensity. Finally, the fluorescent signal reaches a plateau phase, indicating that every monomeric substrate has been converted into amyloid (Schmitz *et al.*, 2016). Notably, the duration of each phase provides insightful information about the characteristics of the initial seed.

It is worth mentioning that the morphology of the resulting fibrils highly depends on the preparation and solution conditions. For instance, it is necessary to minimize the presence of preformed tau aggregates or “oligomers,” as they heavily influence the outcome of the reaction (Willbold *et al.*, 2021). However, the addition of fibrillated tau can bypass the rate-limiting nucleation step by accelerating the polymerization of its monomeric form, as occurs in other fibrillization processes (Del Rio & Ferrer, 2020). Additionally, concentrations of monomeric tau 1000-fold greater than those present in the brain are required reduce the lag phase and observe aggregate formation within hours *in vitro* (Noji *et al.*, 2021). Nevertheless, because full-length tau is highly soluble, this process may require a few days to complete, often in the presence of polyanionic cofactors (e.g., heparin, RNA) (Kampers *et al.*, 1996; Ramachandran & Udgaonkar, 2011; Fichou *et al.*, 2018; Scheres *et al.*, 2020).

In living organisms, under physiological conditions, amyloid formation is a rare event that takes place at a slow pace. This may explain why age is the greatest known risk factor for human sporadic tauopathies (Hickman *et al.*, 2016; Datki *et al.*, 2020). Importantly, tau disease-associated mutations (e.g., FTDP-17-related mutations) produce species that are prone to aggregation and slightly increase the rate of primary nucleation, resulting in a heightened probability of amyloid formation (von Bergen *et al.*, 2001; Allen *et al.*, 2002; Fischer *et al.*, 2007). The fact that tau mutations can promote the formation of amyloids partially explains why the onset of familial tauopathies occurs earlier than in sporadic cases. Consequently, as will be further addressed in the following sections, given their innate propensity to aggregate, mutated tau isoforms are widely used in experimental models. Given the complexity of studying nucleation-dependent polymerization and self-seeding polymerization in living organisms, the exact mechanisms by which monomeric tau misfolds and aggregates are still unclear.

1.3.2.1.1 Tau Seeding Occurs through Tau RD and Tau Repeats Are Required for Amyloid Fibrillization

During the seeding process, full-length tau assembles into amyloid filaments through its RD, which forms the core of the fibril, while the N- and C-terminal domains constitute

the so-called “fuzzy coat” (Goedert *et al.*, 1988; Wischik *et al.*, 1988a; Wischik *et al.*, 1988b). Noteworthy, tau RD is also the region that directly binds to MTs, suggesting that the physiological function of tau and the aggregation state are incompatible with one another. Hence, tau RD constitutes the core of the amyloid fibril and is both necessary and sufficient for amyloid fibrillization. Interestingly, tau RD alone aggregates faster than full-length tau *in vivo* and *in vitro* (Wille *et al.*, 1992; Khlistunova *et al.*, 2006; Seidler *et al.*, 2018), probably because the presence of the N- and C-terminal regions complicates the nucleation step, probably through steric impediments. It is worth mentioning that some familial mutations that increase the propensity of tau to aggregate (i.e., as stated in the previous section) are located in the RD (Barghorn *et al.*, 2005; Akoury *et al.*, 2013).

Importantly, tau’s ability to generate amyloids resides in its structure and is thought to lie in two hexapeptide amino acid sequences (i.e., ^{306}VQIVYK^{311} and ^{275}VQIINK^{280}) located at the beginning of the R2 and R3 in tau RD (von Bergen *et al.*, 2000), termed “PHF6” and “PHF*6,” respectively. Several *in vitro* assembly studies have shown that these peptides are prone to the formation of β-sheet structures (von Bergen *et al.*, 2000; von Bergen *et al.*, 2001; Li & Lee, 2006). Moreover, disruption of these motifs (e.g., amino acid substitution by proline residues) results in tau’s incompetency to form aggregates. In contrast, as previously indicated, some FTDP-17-related mutations (e.g., ΔK280, P301S, or P301L) increase the propensity of these peptides to form β-structures, resulting in accelerated tau aggregation (Allen *et al.*, 2002; Khlistunova *et al.*, 2006; Fischer *et al.*, 2007). Tau assembly is reduced upon deletion of either hexapeptide motif; however, only PHF6 is essential for the formation of amyloid fibrils (Li & Lee, 2006; Ganguly *et al.*, 2015). Consequently, there has been an increasing interest in developing therapies targeting tau RD that function as inhibitors of tau aggregation (Seidler *et al.*, 2018; Seidler *et al.*, 2019).

1.3.2.2 Tau Spreading

Thus far, we have described the process of tau seeding as one of the two leading characteristics of the prion-like hypothesis. The second one is the steady proliferation of aggregates, which is called “spreading.” As previously mentioned, clinical findings suggest that tau pathology progresses through anatomically connected brain regions (Braak & Braak, 1991; Scholl *et al.*, 2016). Importantly, experimental evidence from *in vivo* and *in vitro* models corroborates these observations (Clavaguera *et al.*, 2009; Frost *et al.*, 2009; Liu *et al.*, 2012; Iba *et al.*, 2015).

According to the prion-like paradigm, at the beginning of the disease, only a small proportion of localized neurons are responsible for tau aggregation. Seed-competent tau is then released into neighboring or synaptically connected healthy cells, spreading the disease (Mudher *et al.*, 2017). Of note, tau is an intracellular protein, thus its progression is thought to occur in a four-step process (Figure 4): 1) There is one initial neuron (i.e., termed “donor cell”), which begins the process of self-seeded fibrillization, eventually resulting in tau aggregates. 2) Seed-competent tau is released from the donor cell into the extracellular environment. 3) Extracellular “pathogenic" tau is internalized by a nearby healthy cell (i.e., termed “receptor” or “naïve cell”). 4) Once inside, it recruits its endogenous counterparts, resulting in further pathological seeding. That being said, there are many unknowns in this hypothetical four-step process. Here, we discuss some of the most relevant aspects that have yet to be clarified.

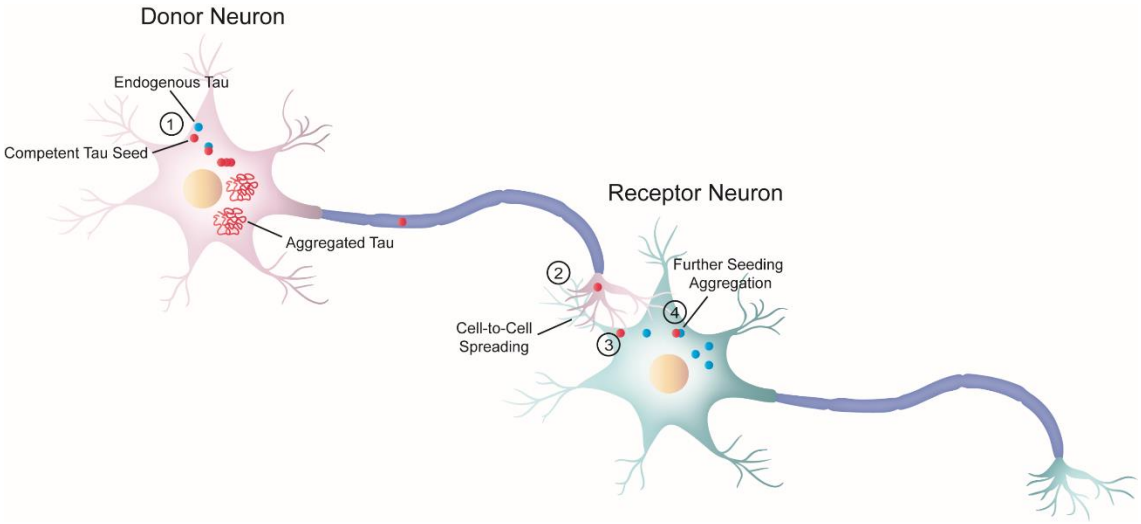

Figure 4 Schematic representation of tans-cellular spreading of tau pathology according to the prion-like hypothesis: 1) Under pathological conditions, monomeric tau misfolds and starts the self-seeded polymerization process, producing large, insoluble amyloid fibrils within the donor neuron (pink). **2-3)** Next, seed-competent tau (red) spreads from the donor neuron to a neighboring healthy neuron termed the receptor neuron (greenish-blue). **4)** Once inside, seed-competent tau recruits and forces its endogenous counterparts (blue) to misfold, inducing further aggregation and ensuring the disease progression. Image obtained from (Sala-Jarque et al., 2022).

The mechanism by which tau can be released and internalized by neural cells is unknown. Noteworthy, tau lacks any potential signal peptide that could locate the protein in the secretory pathway, which makes it more difficult to pinpoint a specific process involved in tau secretion. In parallel, increased neural activity can induce tau release both *in vivo* and *in vitro*, which may be critical for disease progression (Pooler *et al.*, 2013; Yamada *et al.*, 2014; Wu *et al.*, 2016). Thus far, different mechanisms have been proposed for tau release (Figure 5): 1) exosome or ectosome release, 2) direct

translocation across the plasma membrane (e.g., via passive diffusion or by membrane disruption), 3) lysosomal exocytosis, 4) microvesicle shedding, and 5) tunneling nanotubes (TNTs) (Saman *et al.*, 2012; Asai *et al.*, 2015; Tardivel *et al.*, 2016; Wu *et al.*, 2016; Wang *et al.*, 2017; Katsinelos *et al.*, 2018; Brunello *et al.*, 2020; Chastagner *et al.*, 2020; Pellegrini & Lancaster, 2021). It is worth mentioning that, except for TNTs, in which intracellular tau would be directly transported from the donor cell to the receptor cell via physical connections, the other proposed mechanisms imply that pathological tau travels through the extracellular space (i.e., extracellular phase). This notion is supported by the presence of tau in the cerebrospinal fluid (CSF) and interstitial fluid (ISF) of transgenic mice (Barten *et al.*, 2011; Yamada *et al.*, 2011; Takeda *et al.*, 2015) and human patients with AD (Kurz *et al.*, 1998; Takeda *et al.*, 2016).

In parallel, several cellular mechanisms have been proposed (Figure 5) to explain extracellular seed-competent tau internalization, including: 1) endocytosis, 2) passive diffusion, 3) membrane disruption, 4) TNTs, and 5) receptor-mediated internalization (e.g., low-density lipoprotein receptor-related protein 1 (LRP1), PrP^C, and heparan sulfate proteoglycans (HSPGs) (Calafate *et al.*, 2016; Rauch *et al.*, 2018; De Cecco *et al.*, 2020)). Although there have been contradictory findings involving the ability to take up extracellular monomeric tau (Mirbaha *et al.*, 2015; Evans *et al.*, 2018), aggregated tau has been shown to readily enter neurons and other cell types (Frost *et al.*, 2009; Kfoury *et al.*, 2012; Wu *et al.*, 2013). In this context, several studies have shown that micropinocytosis or bulk endocytosis may be responsible for the internalization of exogenously added aggregated and “oligomeric” tau (Frost *et al.*, 2009; Kfoury *et al.*, 2012; Holmes *et al.*, 2013; Wu *et al.*, 2013), in which HSPGs play an active role (Holmes *et al.*, 2013; Rauch *et al.*, 2018). However, because most published results arise from different experimental models, as well as tau variants of distinct origins, the relevance of these mechanisms *in vivo* is still unclear.

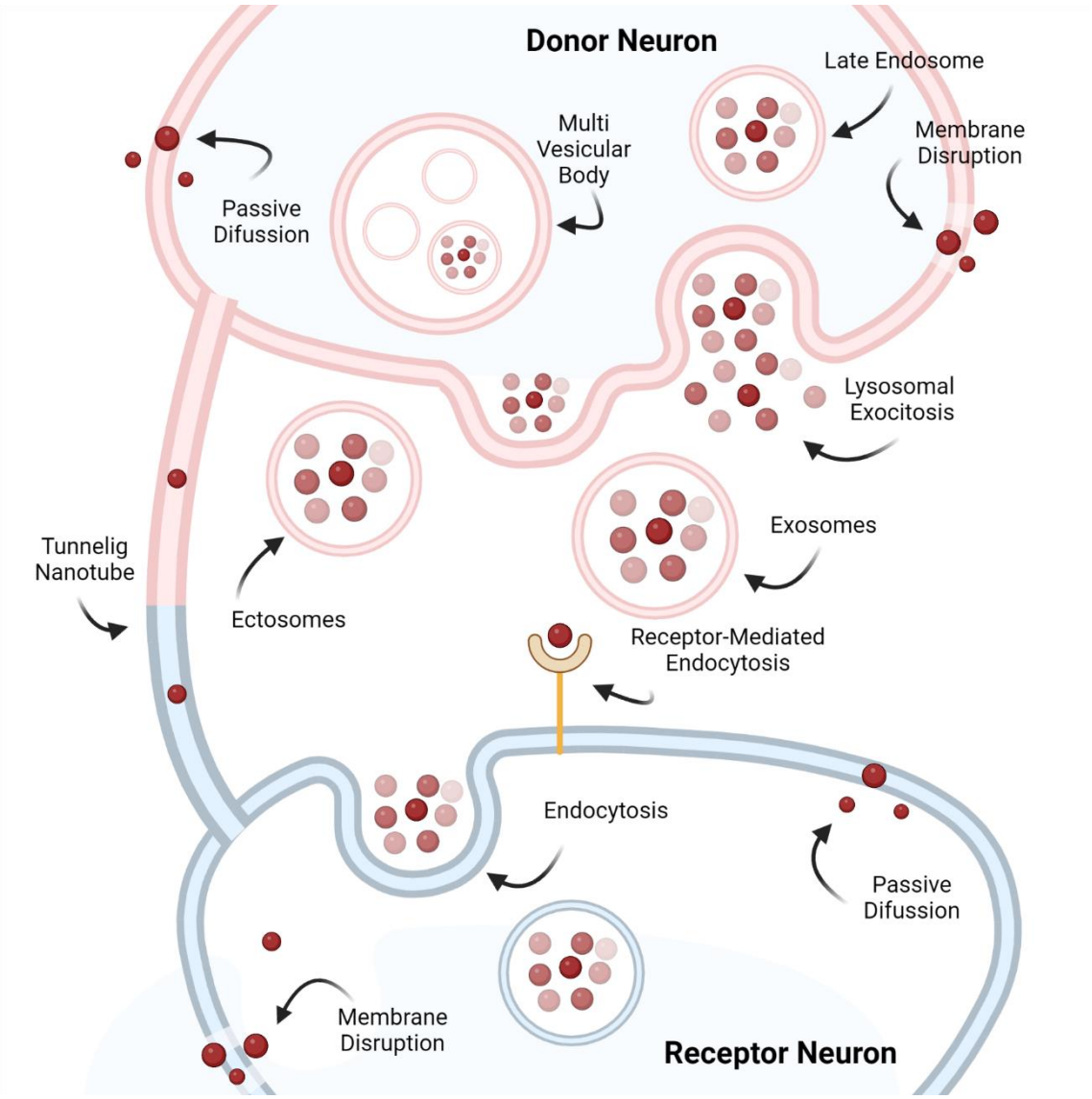

Figure 5 Schematic illustration of the mechanisms involved in the release and internalization of seed-competent tau: How exactly seed-competent tau (red) is released by the donor neuron (pink) and internalized by the receptor neuron (blue) is still unclear. Several mechanisms have been proposed to be involved in both processes. Seed-competent tau can be released by passive diffusion or by disrupting the cell membrane. Alternatively, tau can also be encapsulated into late endosomes and secreted to the cell exterior. Seed-competent tau has been described to be transferred using tunneling nanotubes, as well as secreted into extracellular vesicles, either as ectosomes or exosomes. Once in the extracellular space, tau can be internalized directly through the plasma membrane by passive diffusion or membrane disruption. Other mechanisms include endocytosis, receptor-mediated endocytosis, or fusion of exosomes or ectosomes with the cell membrane (not shown).

Finally, the minimum size of tau assemblies or seeds that allow the transmission of tau pathology from donor neurons to receptor neurons via these cellular pathways is still unclear. One of the few accounts to investigate this issue is that of (Mirbaha *et al.*, 2015), in which the authors determined that for spontaneous propagation of tau aggregation,

there was a minimum size of three units of tau seeds. In contrast, another group demonstrated that extracellular monomeric tau was sufficient to spread tau pathology (Michel *et al.*, 2014). More recently, (Mirbaha *et al.*, 2022) also indicated that monomeric tau can adopt a specific conformation that self-assembles into amyloid fibrils. Identifying the minimal tau seed required to propagate tau pathology is not trivial, as it could be a reasonable target for developing novel therapies to halt the progression of the disease.

1.3.2.3 Tau Polymorphs and Tau Strains

In humans, the tau pathology of each tauopathy occurs in specific brain areas (Arnold *et al.*, 2013), affects different brain networks (Raj *et al.*, 2012; Zhou *et al.*, 2012), and features unique tau inclusions in various cell types (Adori *et al.*, 2015). Strikingly, individuals with the same syndrome develop rapid or slow neurodegeneration (Armstrong *et al.*, 2014). The basis for these diverse disease patterns is not well understood. Likewise, PrDs are heterogeneous diseases, and as previously stated, their variability is considered to be caused by the existence of different prion strains (Bessen & Marsh, 1994; Schmitz *et al.*, 2016; Philiastides *et al.*, 2019). For clarity, the term “strain” reflects an amyloid property known as “polymorphism,” which refers to multiple fibril folds with the same amino acid sequence. The various folds may differ in the polypeptide chain segments that form the β-strands or in the arrangement of β-strands in the protofilament, resulting in a different protofilament conformation (Zhang *et al.*, 2019). Furthermore, the relative arrangement of protofilaments with one another can vary between polymorphs. However, a *bona fide* strain must be able to propagate its properties *in vivo*. Hence, not all polymorphs are strains, but all strains are polymorphs. Nevertheless, the literature is full of examples in which the term “tau strain” is used to describe tau polymorphs. Therefore, to avoid confusion, in this thesis, both terms will be used as synonyms.

It is believed that the specific presence of certain tau polymorphs in different tauopathies could partially explain the heterogeneity observed among human tauopathies. For instance, inoculations of various brain-derived materials from individuals affected by different tauopathies in animal models cause unique patterns of tau pathology, as well as cellular and neuropathological lesions (i.e., reminiscent of those observed in their respective human tauopathies) (Clavaguera *et al.*, 2013; Kaufman *et al.*, 2016). Additionally, *in vitro*, the transduction of extracellular seed-competent tau from diverse origins results in the production of various forms of inclusions (Sanders *et al.*, 2014; Kaufman *et al.*, 2016; Sanders *et al.*, 2016). Importantly, each tau strain has a distinct relative resistance to proteolytic enzymes. More recently, thanks to cryo-EM, the near-atomic resolution of tau amyloids from diverse sources revealed that these

differences are observable at the molecular level (Falcon *et al.*, 2018b; Falcon *et al.*, 2019; Zhang *et al.*, 2020). To date, however, there is no definitive proof that tau strains are the cause rather than the consequence of the variability of human tauopathies. Therefore, their clinical relevance is still under debate.

1.3.3 Tau-Related Cytotoxicity

The extent and distribution of tau lesions strongly correlate with the clinical phenotypes of tauopathy patients, including cognitive decline, neurodegeneration, and reactive gliosis (Braak & Braak, 1991; Arriagada *et al.*, 1992; Kovacs, 2015). Moreover, the discovery of genetic abnormalities linked to familial AD and FTDP-17 has led to the idea that tau dysfunction and aggregation are both central to the neurodegenerative process. Hence, intracellular tau aggregates have been hypothesized to be directly toxic to neural cells. Additionally, because there is increasing evidence to suggest that extracellular tau plays an active role in the progression of the disease (Kfoury *et al.*, 2012), it has been proposed that it may also be cytotoxic to neural cells (Gomez-Ramos *et al.*, 2006). However, the link between tau aggregation, propagation, and neuronal dysfunction remains poorly understood, as are the direct consequences for the neurons and glial cells containing the aggregates. Moreover, the exact nature of tau toxic species (i.e., soluble tau *vs.* large insoluble aggregates) is not well understood. In this section, we will review some of the most relevant information regarding tau toxicity and its possible impact on neuronal activity.

1.3.3.1 Intracellular Tau Cytotoxicity

There appears to be double cytotoxicity associated with intracellular tau. First, because soluble monomeric tau is captured into aggregates, it is thought that loss of the MT-binding function destabilizes the cytoskeleton, leading to what is known as loss-of-function toxicity (Alonso *et al.*, 1997). Second, the immense intracellular physical space usage of large tau amyloid fibrils is believed to result in toxic gain-of-function (Lee *et al.*, 1994; Ballatore *et al.*, 2007). However, the role of tau aggregates as toxic mediators of neuronal dysfunction remains unclear. Indeed, the association between large PHFs and pathology does not always imply a causal link (Tanzi & Bertram, 2001; Stamer *et al.*, 2002; Gotz *et al.*, 2004; Santacruz *et al.*, 2005; Berger *et al.*, 2007). Consequently, the emphasis has shifted towards finding toxic tau species through the fibrillization pathway, from soluble monomers to “oligomers,” to highly insoluble amyloid fibrils. In this context, the tau aggregation process has proven to be damaging in certain experimental models (Khlistunova *et al.*, 2006; Bandyopadhyay *et al.*, 2007). In addition, several studies have

shown that the addition of tau aggregation inhibitors reverses the cytotoxic effects caused by tau fibrillization (Khlistunova *et al.*, 2006; Hosokawa *et al.*, 2012; Mori *et al.*, 2014; Harrington *et al.*, 2015). Intermediate “oligomers” formed during amyloid fibrillization appear to be the culprits of tau-related cytotoxicity (Kumar *et al.*, 2014; Tepper *et al.*, 2014). Nevertheless, as previously stated, tau “oligomers” are still poorly characterized, and “oligomeric” preparations are heterogeneous and highly unstable (Maeda & Takashima, 2019). As a result, there is currently no agreement on the nature of neurotoxic species in tauopathies, which complicates the development of tau-directed therapies.

1.3.3.2 Extracellular Tau Cytotoxicity

Increasing evidence shows that seed-competent tau is present in the extracellular space under pathologic conditions (Bi *et al.*, 2011; Yamada *et al.*, 2011; Magnoni *et al.*, 2012; Evans *et al.*, 2018). In this regard, the existence of extracellular tau has been documented in both primary neuron culture medium (Karch *et al.*, 2012) and immortalized mammalian cell lines over-expressing tau (Simon *et al.*, 2012), as well as in the CSF of tau-transgenic mice (Magnoni *et al.*, 2012) and humans (Yamada *et al.*, 2014). At first, scientists thought that the source of extracellular tau came from dying cells (Medina & Avila, 2014b), as increased tau levels were found in the CSF of patients with AD (Kurz *et al.*, 1998; Takeda *et al.*, 2016). However, the prion-like hypothesis introduced the idea that extracellular tau could be released from neural cells independently of cell death (Pooler *et al.*, 2013; Wu *et al.*, 2016).

In AD patients, there is a significant synaptic loss (Masliah *et al.*, 1989) that correlates with cognitive impairment (DeKosky & Scheff, 1990). It is now believed that the cell-to-cell spreading of pathological tau could be a major contributor to the synaptic dysfunction associated with AD (Sokolow *et al.*, 2015). Consistent with this idea, the addition of extracellular tau “oligomers” impaired memory and long-term potentiation (LTP) in mice (Fa *et al.*, 2016; Puzzo *et al.*, 2017). Interestingly, after tau removal, lost memory and impaired synapses were recovered (Hochgrafe *et al.*, 2013). Another study found that adding small “oligomeric” tau species to neurons in an *in vitro* setting changed the architecture as well as the density of dendritic spines and increased the production of reactive oxygen species (ROS), resulting in altered intracellular calcium homeostasis (Kaniyappan *et al.*, 2017). Despite this, only limited progress has been made in determining the molecular mechanisms by which extracellular tau can be toxic to neural cells. One exception is the work of J. Ávila’s laboratory, which demonstrated that extracellular dephosphorylated tau interacted with the muscarinic receptors M1 and M3,

disrupting calcium homeostasis and eventually leading to cell death (Gomez-Ramos *et al.*, 2006; Gomez-Ramos *et al.*, 2008; Diaz-Hernandez *et al.*, 2010).

1.3.3.3 The Unknowns between Tau Pathology and Neuronal Network Alterations

Either directly or indirectly, tau cytotoxicity may also affect neural functions and probably the ability to regulate brain activity. In this context, patients diagnosed with AD also exhibit neuronal network abnormalities, such as synaptic depression, altered oscillatory rhythmic activity, and hypersynchrony (Palop & Mucke, 2010; 2016). Consequently, neuronal excitability dysregulation, which precedes neurodegeneration in tauopathies, could be the underlying cause of cognitive impairment, although the exact role of tau and its accumulation in "pathogenic" forms, if any, in such processes is unclear (Dickerson *et al.*, 2005; Olazaran *et al.*, 2010; Vossel *et al.*, 2013). However, theoretical and experimental evidence suggests that abnormal neural functions are associated with "pathogenically" related tau species. According to (Crimins *et al.*, 2012; Garcia-Cabrero *et al.*, 2013; Maeda *et al.*, 2016), enhanced network excitability is detected in the brains of transgenic rodents expressing human FTD-related mutations. Moreover, in flies (Holth *et al.*, 2013) and mice (Roberson *et al.*, 2011; DeVos *et al.*, 2013; Holth *et al.*, 2013; Hall *et al.*, 2015), decreasing the levels of tau expression results in the attenuation of neural network excitability. But again, how tau regulates neural excitability is unclear.

As previously mentioned, prior work focused on studying the effects of neuronal activity on the progression of tau pathology. Regardless, the consideration of how tau itself may modulate neural networks is rarely addressed, and most published results report on alterations resulting from over-expressing tau variants. In this regard, the question of whether extracellular tau also disturbs neuronal networks has received limited attention in the literature. There are, however, some experimental data showing that extracellular tau is toxic to cells and increases intracellular calcium via muscarinic receptors (Gomez-Ramos *et al.*, 2006; Gomez-Ramos *et al.*, 2008). More recently, Stancu and colleagues reported network dysfunction in models with over-expression of mutated tau isoforms upon treatment with extracellular tau using *in vitro*, *ex vivo*, and *in vivo* approaches (Stancu *et al.*, 2015). In parallel, exposure to tau "oligomers" in transgenic mice expressing human tau resulted in almost instantaneous impairment of LTP and memory (Fa *et al.*, 2016). Moreover, adding a truncated tau variant to mature primary neurons altered their normal synaptic function by directly interfering with depolarization-evoked glutamate release (Florenzano *et al.*, 2017).

1.3.4 PrP^C and Its Role in Tau Pathology

The prion-like hypothesis predicts the existence of several molecules that support the progression of protein misfolding pathology. Among different candidates (e.g., LRP1 and HSPG), increasing experimental evidence shows PrP^C may be involved in various NDs (Resenberger *et al.*, 2011), both in pathology spreading and mediating cytotoxic effects, although a protective influence has also been suggested (Gavin *et al.*, 2020).

In humans, PrP^C is a 253-amino acid glycosylphosphatidylinositol (GPI)-anchored protein encoded by the *PRNP* gene on chromosome 20, whereas in mice, *Prnp* is located on chromosome 2 (Aguzzi & Miele, 2004; Del Rio *et al.*, 2018). The *PRNP* gene has a length of 20 kb and is composed of two exons in humans and three exons in mice. Nevertheless, in both cases, the PrP^C protein is codified by only the last exon (Puckett *et al.*, 1991). Mature PrP^C has 209 residues (Figure 6) and can be glycosylated at two asparagine residues at positions 181 and 197 (i.e., human PrP^C) (Haraguchi *et al.*, 1989). Therefore, PrP^C can be unglycosylated, monoglycosylated, or diglycosylated, which can be identified by different electrophoretic patterns (Wiseman *et al.*, 2015). The 3D structure of PrP^C consists of an unstructured N-terminal domain (i.e., amino acids 23-122), which contains five copies of an octapeptide repeat region. Notably, this region also contains two positively charged clusters (CC) known as CC1 (i.e., residues 23-30) and CC2 (i.e., residues 101-110) (Martinez *et al.*, 2015). The C-terminal globular domain (i.e., amino acids 123-230) comprises three α-helices and two very short anti-parallel β-plated sheet regions (Pan *et al.*, 1993; Zahn *et al.*, 2000). Between the N-terminal and C-terminal domains, there is a hydrophobic region (HR) (i.e., residues 113-135) (Beland & Roucou, 2012), which is believed to be relevant during prion conversion (Giachin *et al.*, 2015).

In the central nervous system, PrP^C is extensively expressed during early development, as well as in adult neurons and glial cells. It has been proposed that PrP^C plays several roles, such as ion balance homeostasis, neuritogenesis, cell signaling, cell adhesion, and stress-protective function (Legname & Moda, 2017; Legname & Scialo, 2020).

Turning now to the roles of PrP^C in NDs, according to (Lauren *et al.*, 2009), PrP^C is necessary for Amyloid-β (Aβ)-induced cytotoxicity in hippocampal slices and memory impairment *in vivo* (Gimbel *et al.*, 2010). In parallel, in Parkinson's disease (PD), PrP^C may act as a receptor for α-synuclein (α-syn) amyloids, promoting their internalization in

healthy cells, as well as modulating their cytotoxic influence through the activation of a signaling cascade (Aulic *et al.*, 2017).

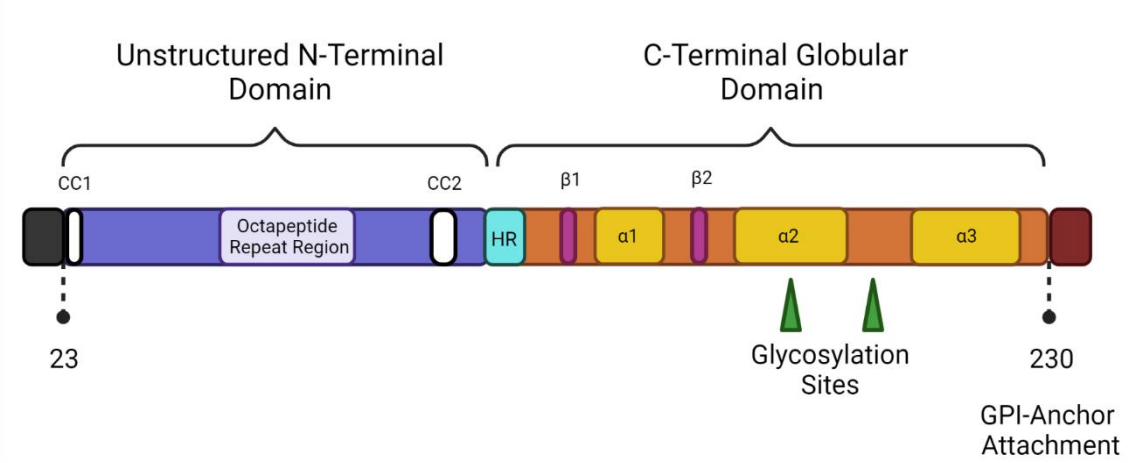

Figure 6 Schematic representation of full-length human PrP^{C}: The mature form of human PrP^{C} consists of 209 amino acids. Since PrP^{C} is a membrane protein, it contains a secretory signal peptide (i.e., positions 1-22) at the extreme of the N-terminal region (gray box). At the C-terminus, there is a hydrophobic peptide region (i.e., positions 231-253) (red box), which is cleaved prior to the addition of the glycosylphosphatidylinositol (GPI) anchor (i.e., position 230). The unstructured N-terminal tail or domain spans from residues 23 to 122 (purple box) and includes an octapeptide repeat region (light purple box). This domain also contains two positively charged clusters (CC), known as CC1 and CC2 (white boxes). The C-terminal globular domain (orange box) (i.e., positions 123-230) contains specific regions that form three α-helices and two β-sheets (yellow and pink boxes, respectively). Green arrowheads indicate the two asparagine residues associated with N-linked glycosylation.

Remarkably, PrP^{C} has been found to be a tau interactor (Han *et al.*, 2006; Wang *et al.*, 2008; Schmitz *et al.*, 2014), although the significance of this interaction is uncertain. In this regard, pull-down and co-immunoprecipitation experiments have proven the existence of an interaction between isolated monomeric and brain-derived tau and PrP^{C} (Han *et al.*, 2006). Additionally, co-immunoprecipitation of PrP^{C} and phosphorylated tau variants has also been reported in lysates from HEK293 cells over-expressing PrP^{C} (Schmitz *et al.*, 2014). Using more pathologically relevant samples, co-localization, and internalization of hyperphosphorylated tau and PrP^{C} were found in brain tissue from AD patients (Gomes *et al.*, 2019). Importantly, NFTs are usually observed in PrDs, suggesting that PrP^{Sc} and tau may influence each other's formation under certain pathological conditions (Ghetti *et al.*, 1989; Tagliavini *et al.*, 1993). Notably, these interactions seem to occur between the unstructured region of PrP, encompassing residues 23-91 (i.e., the N-terminal fragment), and the projection domain and RD of tau (Wang *et al.*, 2008). In this regard, one study showed that in the neuroblastoma cell line N2a, over-expression of PrP^{C} enhanced the internalization of tau amyloid aggregates assembled only with the RD fraction (De Cecco *et al.*, 2020). However, one major

drawback of this study was that the authors used heparin to facilitate tau aggregation. Consequently, increased tau internalization could have resulted from PrP^C interacting with heparin molecules present in the fibrils rather than with tau.

Having said this, however, as previously stated, PrP^C has also been proposed to play a protective role in AD (Guillot-Sestier *et al.*, 2012; Hernandez-Rapp *et al.*, 2014; Schmitz *et al.*, 2014; Vergara *et al.*, 2015; Gavin *et al.*, 2020). In the case of tau, (Nieznanska *et al.*, 2021) demonstrated that the soluble N-terminal fragment of PrP^C protects neurons against tau "oligomer"-induced toxicity. Furthermore, the presence of PrP^C in HEK293 cells down-regulated the expression of tau (Schmitz *et al.*, 2014). Given these contradictory results, the exact role of PrP^C in tau pathology is still unclear.

1.4 Experimental Paradigms for Studying Tauopathies: Tau Seeding, Spreading, and Cytotoxicity

1.4.1 Intracellular Tau: Transgenic *vs.* Wild-Type Models of Tau Pathology

One of the most challenging aspects of studying tau pathology is that full-length tau is a highly soluble protein that does not readily aggregate under physiological conditions, neither *in vivo* nor *in vitro* (Chirita *et al.*, 2005; Khlistunova *et al.*, 2006; Bandyopadhyay *et al.*, 2007). For years, this issue has been solved by inducing the over-expression of human tau alone or bearing aggregation-promoting mutations (e.g., P301L, P301S, ΔK280). Furthermore, the use of fibrillization agonists (Bandyopadhyay *et al.*, 2007), as well as artificially causing certain PTMs, such as truncation or phosphorylation (Chun & Johnson, 2007), have also proven to be successful ways to trigger tau aggregation. However, transgenic models based on the over-expression of tau do not fully recapitulate the characteristics of sporadic human tauopathies. Consequently, the effectiveness of certain drugs in transgenic models contrasts with recent trial results. For example, in AD, out of more than 200 therapies that ameliorated AD-related pathology in genetically engineered models, only two have been approved as medications for humans (Zahs & Ashe, 2010). As a result, the field has seen a shift toward the use of wild-type models of tau expression, in which tau aggregation is usually triggered by the addition of extracellular seed-competent tau species.

1.4.2 Extracellular Tau: Recombinant *vs.* Brain-Derived Tau

As previously mentioned, *in vitro*, using cell-free environments, monomeric tau can be induced to form amyloid aggregates, often in the presence of cofactors. In this

context, adding fibrillated tau can accelerate the aggregation process by eliminating the rate-limiting nucleation step necessary for the amyloid formation. Analogously, the addition of exogenous seed-competent tau in living organisms (e.g., cells or animal models), especially those over-expressing aggregation-prone tau variants, accelerates the process of amyloid fibrillization. When designing an experiment, selecting the nature of the extracellular tau to be used is not a trivial issue, as different tau species may have distinct properties (Nam & Choi, 2019; Zhang *et al.*, 2019). The origin of extracellular tau can broadly be classified into recombinant tau-preformed fibrils (PFFs) and brain-derived tau.

1.4.2.1 Tau PFFs

Tau PFFs are amyloid fibrils that can be easily formed *in vitro* in the absence of cellular systems. Importantly, this process must produce reliable and reproducible amyloids to exclude confounding factors in subsequent experiments. The literature is full of different protocols for generating tau PFFs, and their use is widespread and popular in the field (Li & Lee, 2006; Falcon *et al.*, 2015; Nam & Choi, 2019). In most cases, *Escherichia coli* is used to produce a wide variety of recombinant monomeric tau species, such as full-length wild-type tau, and tau RD with or without aggregation-prone mutations (e.g., P301L P301S), which after purification are induced to aggregate in cell-free environments, often with the help of polyanionic cofactors (e.g., heparin or RNA) (Goedert *et al.*, 1996; Friedhoff *et al.*, 1998; Fichou *et al.*, 2018). The resulting fibrils (i.e., fully formed PFFs) can be sonicated to obtain “oligomeric” species and stored at -80°C until use. Despite their advantages, recent investigations have revealed that the final fibril morphology does not resemble the ones observed in the diseased brain (Zhang *et al.*, 2019). As a consequence, their translational relevance has been called into question.

1.4.2.2 Brain-Derived Tau

The use of brain-derived material obtained from rodent models of tauopathy or deceased human tauopathy patients is becoming increasingly common. However, when comparing brain-derived material to tau PFFs, there are two fundamental limitations. First, human samples are scarce, and the amount of tau retrieved is small, restricting the number of potential experiments. Second, as mentioned above, it is possible to obtain reproducible batches of tau PFFs, but brain-based materials are characterized by heterogeneity within and between samples, and therefore, the consistency of the produced data is highly affected. At the same time, the published protocols for sample acquisition are also diverse. Classically, researchers would sequentially extract

detergent-insoluble fractions (e.g., N-lauroyl sarcosinate (sarkosyl) or Triton X-100 detergent) as they are enriched in highly aggregated tau species. However, alternative protocols have been developed because it is now thought that soluble “oligomeric” species, rather than large insoluble tau aggregates, are the main culprits of the neurodegenerative process. Nevertheless, there is still no consensus on how to isolate tau “oligomers,” complicating, even more, the interpretation of the results in the literature.

1.4.3 Rodent Models of Tauopathy

The gold standard for generating tau pathology in rodent models has been to create transgenic mice over-expressing mutant versions of the human tau protein (Gotz *et al.*, 2018). For example, mice expressing human tau bearing the mutations P301L or P301S under the control of neural promoters (e.g., *Prnp* or *Thy-1*) are known to robustly develop tau pathology as they age (Allen *et al.*, 2002; Yoshiyama *et al.*, 2007). As a result, these models have been helpful in elucidating particular pathogenic pathways involved in tau pathology (Dai *et al.*, 2015; Dai *et al.*, 2018). However, in these animals, practically all brain cells (i.e., or at least all neurons) over-express mutant versions of the *MAPT* gene, frequently in multiple copies. Hence, when studying tau spreading, distinguishing between cell-autonomous and non-autonomous mechanisms becomes nearly impossible (Medina & Avila, 2014a).

Consequently, several groups have investigated other ways of producing alternative approaches, such as mice lacking endogenous murine tau but over-expressing non-mutated human tau (Andorfer *et al.*, 2003; Hu *et al.*, 2016; Saito *et al.*, 2019), as well as restricting the expression of tau-mutated species only to specific brain regions (Harris *et al.*, 2012; Liu *et al.*, 2012). Other alternatives include inoculating either viral particles to monitor the over-expression of tau (Osinde *et al.*, 2008; Caillierez *et al.*, 2013), or injecting seed-competent tau species from various sources (e.g., brain extracts from patients or tau PFFs), which are capable of inducing seeding and spreading of endogenous tau even in wild-type mice. Despite all these advancements, there are still a few drawbacks related to *in vivo* research, since working with animals is generally time-consuming and expensive, along with the potential ethical implications of animal testing (Kirk, 2018).

1.4.4 Cellular Models of Tauopathy

Various cellular models have been created in the last two decades to explore tau pathology. These models include basic unicellular organisms (e.g., yeast) (Vanhelmont

et al., 2010; Porzoor & Macreadie, 2013), immortalized mammalian cell lines (Frost *et al.*, 2009; Guo & Lee, 2011), primary neuronal cell cultures (Wu *et al.*, 2013; Calafate *et al.*, 2015), and, more recently, induced pluripotent stem cells (iPSCs) and organoids (Usenovic *et al.*, 2015; Gonzalez *et al.*, 2018; Oakley *et al.*, 2021). Certain restrictions apply to the reductionist perspective provided by *in vitro* techniques. For example, although it is simpler to identify intricate biological pathways that would otherwise be challenging to investigate, cellular models are far from reproducing the brain's complexity, which implies the loss of many layers of information. They do, however, offer a few advantages over *in vivo* experimentation. For instance, *in vitro* models are easy to maintain and may be genetically engineered to over-express or silence genes of interest more quickly and easily.

1.4.4.1 Mammalian Immortalized Cell Lines

The use of mammalian immortalized cell lines (i.e., cell lines for short) to study specific aspects of tau pathology has proven invaluable over the years. Most of these models rely on the over-expression of mutated isoforms of the tau protein. However, high over-expression of tau over-stabilizes MTs and inhibits cell division, which is not well tolerated by dividing cultured cells (Kanai *et al.*, 1989; Vogelsberg-Ragaglia *et al.*, 2000). Consequently, some models regulate tau expression under the doxycycline-inducible promoter (Khlistunova *et al.*, 2006). Compared to primary cells, cell lines are easy to culture and have rapid experimental turnaround times. Moreover, they are easier to transfect, allowing for the introduction of labeling techniques (e.g., fluorescently tagged tau variants), which are then used to monitor tau amyloid fibrillization with spatiotemporal resolution. Together, they make excellent platforms for high-throughput experimental approaches, such as drug screening for tau-directed compounds. Nevertheless, because most cell lines do not reproduce neuronal phenotypes (e.g., HEK293) or are tumor-derived cell lines (e.g., SH-SY5Y or N2a), specific aspects of tau pathology get lost in translation. Therefore, in most cases, they do not produce translationally relevant results, especially with regard to tau spreading research.

That being said, it is worth mentioning the existence of cell lines designed to be used as cellular assays to study some particular aspects of pathological tau. For instance, to date, there is only one commercially available cell line designed to detect seed-competent tau in biological samples. Commercialized by the American Type Culture Collection (ATCC), the Tau RD P301S FRET (Föster resonance energy transfer) Biosensor (i.e., Tau biosensor cell line, from now on) was first developed in 2014 in M. I. Diamond's laboratory (Holmes *et al.*, 2014). The authors genetically engineered

HEK293 cells to stably over-express the tau RD fragment bearing the P301S mutation, fused to either cyan fluorescent protein (CFP) or yellow fluorescent protein (YFP). Upon the addition of seed-competent tau (e.g., brain homogenates from patients with AD), tau RD-CFP and tau RD-YFP fragments are recruited to aggregate. Thus, both types of constructs are close enough (i.e., < 10 nm) to produce a detectable FRET signal. Flow cytometry can be used to measure the resulting FRET signal, providing precise quantification of all tau aggregates present in a well. Notably, the internalization step can be eliminated by delivering the tau aggregates mixed with Lipofectamine™ directly to the cells, increasing the assay sensitivity. In summary, the Tau biosensor cell line was developed as a cell-based assay to detect proteopathic seeding in a given sample.

By using the Tau biosensor cell line, M. I. Diamond's group was able to demonstrate that tau proteopathic seeding correlates with disease progression, but more importantly, that it can be detected before the appearance of classical histopathological markers in both P301S mice and AD patients, proving that proteopathic seeding may be an effective biomarker for human tauopathies (Holmes *et al.*, 2014; Furman *et al.*, 2017; Kaufman *et al.*, 2017). However, it is still under debate whether proteopathic seeding can be detected in the CSF of AD patients, as there exist contradictory findings on this matter (Takeda *et al.*, 2016; Hitt *et al.*, 2021).

Because the Tau biosensor cell line is commercially available, many groups have included and adapted this cellular assay to their own particular experimental designs. As a result, there is an increasing number of publications in which the use of the Tau biosensor cell line has been reported. For instance, using the Tau biosensor cell line, Wang and colleagues found that microglial cells, which were derived from a mouse model of tauopathy, processed and secreted highly seed-competent tau species (Wang *et al.*, 2022), suggesting a critical role for microglial cells in tauopathies. In another example, the cell line was adapted to evaluate the performance of tau aggregation inhibitors (Louros *et al.*, 2022). Others have used the Tau biosensor cell line to study the heterogeneity observed among patients with AD (Dujardin *et al.*, 2021; Kamath *et al.*, 2021). The authors employed the Tau biosensor cell-based assay to study the kinetics of tau aggregation induced by the addition of extracellular tau from different AD patients. S. Dujardin and co-workers could relate differences in the kinetic profiles to the concept of heterogeneity in association with AD patients. Finally, some researchers have also used the Tau biosensor cell line to investigate some biophysical properties of tau seeds (Hou *et al.*, 2021; Kamath *et al.*, 2021). Together, these different applications of the Tau

biosensor cell line explain the widespread adoption of this cellular model by multiple research groups.

1.4.4.2 Primary Neural Cell Cultures and Organotypic Slices

The specialized morphology of neurons as post-mitotic cells distinguishes them significantly from cell lines. Consequently, cellular pathways and specific protein expression patterns can differ between these two experimental models, which is not a trivial issue for studying tau pathology. As already stated, the primary role of tau, which is largely expressed by neurons, is to control MT dynamics in the axons (Avila *et al.*, 2004a). In disease, tau can be detected in the perikaryon and distal dendrites. Therefore, because most cell lines do not have axons, they cannot mimic these pathological events. Recognizing such constraints has helped develop experimental methodologies based on rodent primary neural cell cultures (Gomez-Ramos *et al.*, 2008) and, more recently, organotypic slices, which preserve the anatomical structures of the brain (Messing *et al.*, 2013; McCarthy *et al.*, 2021). In either case, the culture comes from embryonic or early postnatal mice or rats. Importantly, because both systems are much more sensitive to the protocols of gene transfection than cell lines, a wide variety of viral vectors have been designed to transduce these cultures to over-express different tau constructs. Noteworthy, it is also possible to directly culture primary neurons or organotypic slices from transgenic animals with tau pathology to accelerate and facilitate the aggregation process.

The field has also taken advantage of microfluidic devices to compartmentalize primary neural cell cultures and study the cell-to-cell spreading of pathological tau (e.g., see (Del Rio & Ferrer, 2020)). In this regard, the most frequently utilized microfluidic platforms comprise two or more fluidically isolated compartments interconnected by perpendicular microchannels (Figure 7) (Taylor & Jeon, 2010; Neto *et al.*, 2016). With such a design, only the axons are able to grow through the microchannels and reach the distal chamber, allowing for individual treatment, as well as adjusting and monitoring the various compartments (Wu *et al.*, 2013; Wu *et al.*, 2016; Katsikoudi *et al.*, 2020). Furthermore, neuronal populations may be co-cultured in isolation within discrete reservoirs, recreating neuronal connections known to be affected in NDs (Wu *et al.*, 2016). These approaches are interesting, as they can aid in the investigation of tau

spreading among synaptically coupled neurons. Consequently, they could contribute to our understanding of how tau spreads among synaptically connected neurons.

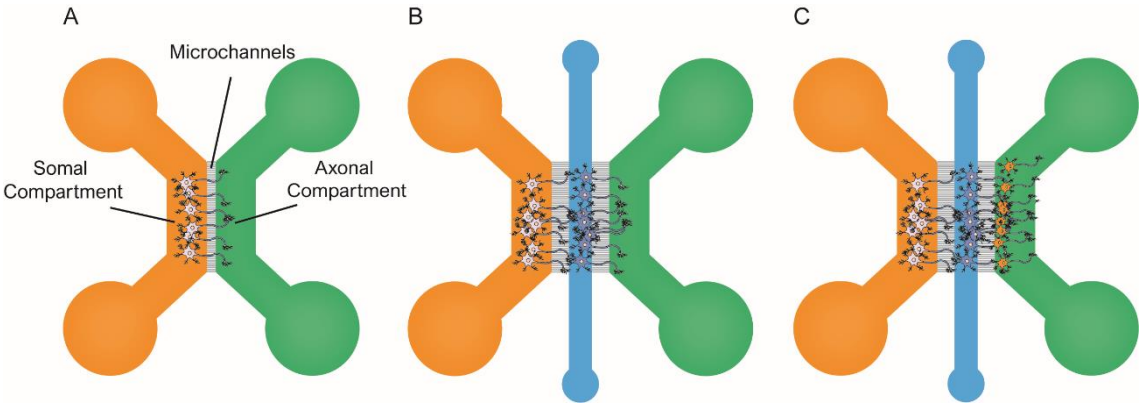

Figure 7 Schematic representation of microfluidic devices: Although there are multiple designs of microfluidic platforms, **A**, **B**, and **C** represent the most commonly used in the research field of tau pathology. Usually, these devices include two or more chambers where primary neural cell cultures are plated. Despite these compartments being fluidically isolated, they are interconnected through perpendicular microchannels, where axons are allowed to grow. Therefore, each reservoir can be treated independently, supporting the study of anterograde and retrograde transport. Image obtained from (Sala-Jarque *et al.*, 2022).

Therefore, primary neural cell cultures are better than cell lines at studying tau pathology for translationally relevant results. However, they are more laborious to prepare, maintain, and require specific skills (e.g., dissection and isolation of the embryonic brain). Of note, high levels of variability characterize primary neural cell cultures, even within different wells, in the same experiment. Moreover, because, in most cases, cells are seeded in 2D, they lack the 3D anatomical architecture of the brain. Additionally, some protocols purposely include the addition of certain factors to the culture media to reduce the population of glial cells (e.g., AraC). These limitations are partially solved with the use of organotypic slices. Nevertheless, primary neural cell cultures and organotypic slices are obtained from immature murine brain tissue, and thus they mainly express 3R-tau isoforms, contrasting with the 1:1 ratio of 3R/4R tau species present in the brain of a human AD patient (McMillan *et al.*, 2008; Bullmann *et al.*, 2009).

1.4.4.3 iPSCs and Organoids

Although this last group is beyond the scope of the present thesis, we would like to summarize some relevant aspects of iPSCs and organoids, as they may represent cutting-edge models of patient-specific cell lines. iPSCs can closely reproduce the characteristics of neurons found in patients, as they may be obtained from any cell type and differentiated into several sorts of neurons and glial cells (Harasta & Ittner, 2017; Kuhn *et al.*, 2021). Notably, the emergence of patient-derived iPSCs provides

unprecedented tools for understanding tau pathology in physiologically relevant models and has the potential for high-throughput drug screening, alongside promising advances in personalized medicine and clinical trials in the future. However, *in vitro* differentiation of iPSC-derived neurons produces important levels of heterogeneity, which limits the ability to obtain consistent results. Additionally, analogous to primary neurons, iPSCs are mostly cultured in 2D, which does not recreate the complexity of the human brain (Sala-Jarque *et al.*, 2022).

To overcome this limitation, some groups have started developing 3D cerebral organoids from iPSCs, as they have all the advantages of the latter, with the superiority of a close recapitulation of the laminar organization observed in the developing human cortex (Dubey *et al.*, 2019; Pellegrini & Lancaster, 2021). Another advantage of organoids is that they last much longer than 2D neural cell cultures, which permits addressing the potential long-term effects of tau pathology. However, to date, an increasing number of culture protocols have resulted in a lack of consistency in the reported results (Bang *et al.*, 2021). Furthermore, most protocols do not allow for the proper formation of oligodendrocytes or microglial cells. Moreover, like iPSCs, organoids are highly variable, and even tau expression may not be consistent between cultures. Importantly, both iPSCs and organoids do not represent the state of a mature brain, since most neurons retain the expression of immature neuronal markers (e.g., SOX2 or Nestin). Finally, both methodologies are laborious and time-intensive to generate and characterize and require a certain level of expertise.

General Objectives

The prion-like hypothesis proposes that tau pathology is transferred trans-cellularly, contributing to the progression of the disease in the brain. Because tau is an intracellular protein, understanding the exact mechanisms involved in cell-to-cell spread may be relevant to developing novel therapies. However, the precise mechanisms involved and the possible impact of extracellular seed-competent tau on neuronal function and cytotoxicity in healthy cells are still unclear. All these aspects have been studied for decades using *in vitro* and *in vivo* models of tau pathology based on the over-expression of tau-bearing aggregation-prone mutations. Nevertheless, the necessity for more pathologically relevant methods for studying human tauopathies has been undermined by the failure of therapeutic strategies developed with these models in later clinical investigations. The main aim of the present thesis is to systematically address the basic mechanisms underlying tau pathology using more pathologically relevant approaches, including brain-derived material from human tauopathy patients, wild-type murine primary cortical cultures, and mouse models expressing wild-type tau.

Chapter 1:

At the beginning of this thesis, the reliability of the cell-based assay that we were using to evaluate whether our samples were seed-competent, known as the Tau biosensor cell line (Holmes *et al.*, 2014), was put into question in a publication by E. Mandelkow's laboratory (Kaniyappan *et al.*, 2020). Therefore, the credibility of our and others' results obtained using this cell line was compromised. Consequently, due to the implications of these claims, we decided to conduct a thorough validation of the Tau biosensor cell line.

- **Objective 1:** To evaluate the reliability of the Tau biosensor cell line by characterizing the fluorescent inclusions observed upon the treatment with seed-competent tau.

Chapter 2:

In the past, other research groups have taken advantage of microfluidic devices to culture primary neurons and add exogenous tau PFFs or extracts from brains with tauopathies to neurons to investigate the mechanisms underlying tau pathology transmission (Holmes *et al.*, 2013; Wu *et al.*, 2016; McCarthy *et al.*, 2021). Most of them proved that tau aggregates were internalized by neurons, trafficked both anterogradely and retrogradely along axons, and spread to and between connected cells (Wu *et al.*, 2013). However, no one has examined the functional outcome of extracellular seed-competent tau in healthy neurons. Here, we sought to determine whether the presence

of extracellular seed-competent tau, added into the axonal compartment of microfluidic devices cultured with primary neurons, could alter neural activity.

- **Objective 2:** To study the impact of extracellular seed-competent tau on the neural activity of wild-type primary cortical cultures by establishing a microfluidic platform suitable for calcium imaging and morphological analyses.

Chapter 3:

The toxicity of tau has been addressed multiple times in the past (Gomez-Ramos *et al.*, 2006; Bandyopadhyay *et al.*, 2007; Tian *et al.*, 2013). However, in most cases, researchers have opted for experimental approaches based on using immortalized cell lines over-expressing mutated tau variants. Very little is known about the toxicity of extracellular seed-competent tau in healthy primary neurons, although the latter represents a more pathologically relevant situation than the former. Therefore, we treated primary cortical cultures with a variety of seed-competent tau to evaluate their impact on cellular viability.

- **Objective 3:** To evaluate the cytotoxicity of different extracellular seed-competent tau in primary cortical cultures through the determination of alterations in their metabolic activity.

Chapter 4:

Finally, there has been an increasing interest in the role of PrP^C in NDs in general. However, at the beginning of this thesis, there was scarce information regarding its role in tauopathies. Therefore, we inoculated brain-derived material from an AD patient into the hippocampus of four mouse models with different expressions of the PrP^C protein.

- **Objective 4:** To evaluate the role of PrP^C in the uptake, seeding, and spreading of tau pathology *in vivo* in wild-type and transgenic PrP^C mice.

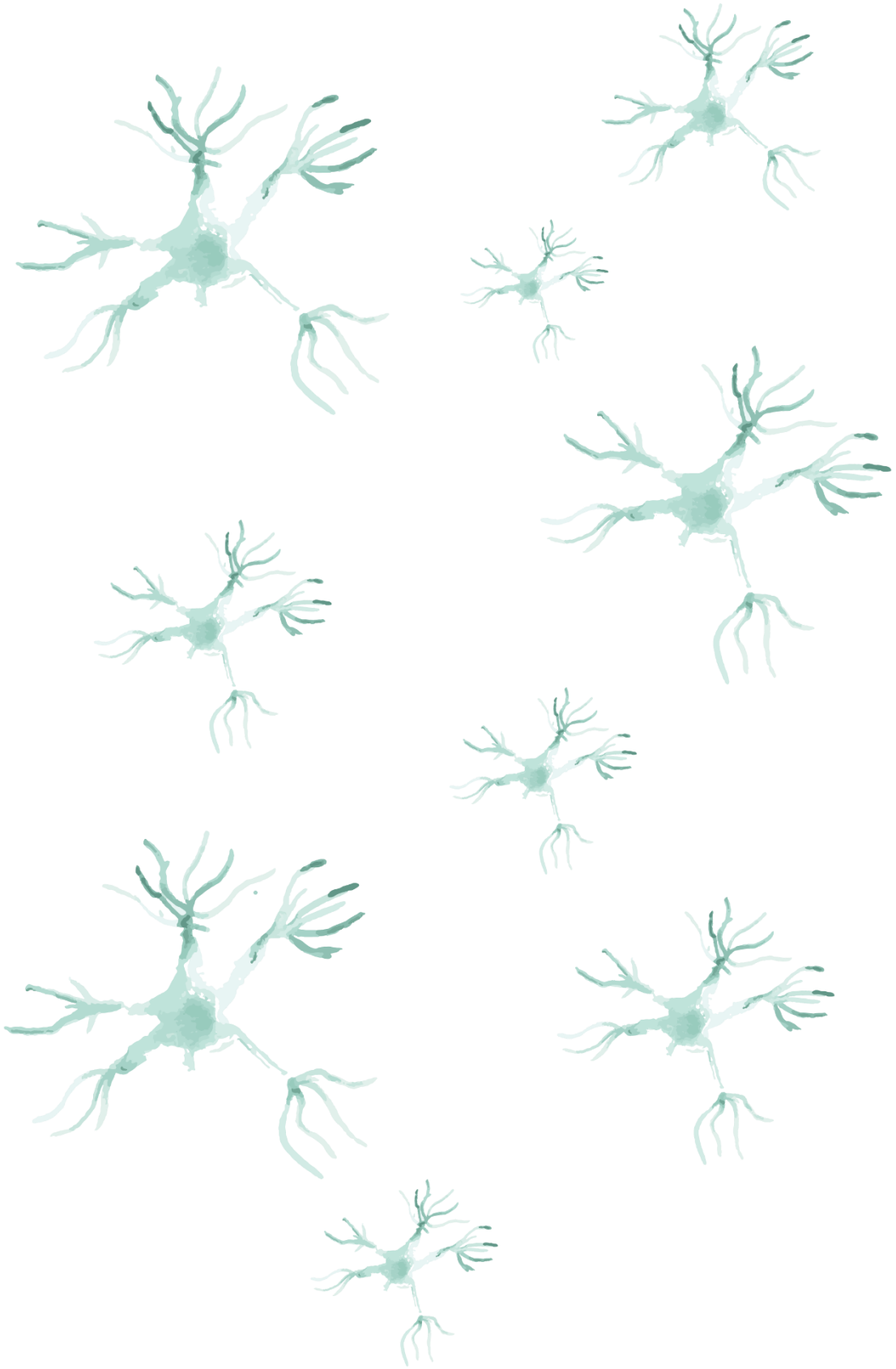

Chapter 1: Addressing the Tau Biosensor Cell Line's Reliability

3.1 Introduction

The Tau biosensor cell line was first developed in M. I. Diamond's laboratory in 2014 to be used as a cell-based assay to detect seed-competent tau in brain-derived samples (Holmes *et al.*, 2014). As mentioned in the Introduction chapter, this cell line is based on genetically engineered HEK293 cells to over-express the tau RD fragment bearing the P301S mutation and fused to either CFP or YFP proteins. Briefly, these cells are characterized by a high fluorescent background under normal conditions, as the tau RD-CFP/YFP fragments remain soluble in the cytoplasm. However, the addition of extracellular seed-competent tau recruits these tau fragments, leading to the formation of intracellular fluorescent inclusions, which can subsequently be quantified via flow cytometry or fluorescence imaging.

The reliability of the Tau biosensor cell line was recently questioned in a publication from E. Mandelkow's group (Kaniyappan *et al.*, 2020). In the original publication of the Tau biosensor cell line from M. I. Diamond's laboratory, the authors assume that the fluorescent inclusions observed in the cells are the result of self-templated aggregates assembled from tau RD-CFP/YFP (Holmes *et al.*, 2014). Thereby, the increased FRET signal directly reports on the levels of intracellular tau aggregation. Conversely, Kaniyappan *et al.* argue that the observed FRET signal may be explained purely by the proximity of tau RD-CFP/YFP constructs in the already crowded cytoplasm, without the necessity for amyloid-like aggregates to develop. To support their claims, the authors propose other mechanisms, such as liquid-liquid phase separation, as plausible causes for the increased FRET signal. Moreover, they believe that RD-CFP/YFP fragments are unable to aggregate due to steric hindrances. However, a serious limitation of Kaniyappan's study is that in their experimental approach, the authors failed to use the Tau biosensor cell line or the tau RD-CFP/YFP constructs employed in the original publication (Holmes *et al.*, 2014). Instead, the experiments were conducted in an *in vitro* cell-free model of tau fibrillization using their own designed tau constructs. Despite these inadequacies, it is true that, in the original paper, Holmes and colleagues do not prove that the fluorescent inclusions are tau amyloid-like fibrils (Holmes *et al.*, 2014). Therefore, if the claims made by Mandelkow's group are correct (Kaniyappan *et al.*, 2020), that would imply that all previous publications based on the Tau biosensor cell line are irrelevant or even misleading.

3.2 Objective

The central objective of this chapter is to evaluate the reliability of the Tau biosensor cell line by characterizing the fluorescent inclusions observed upon the treatment with seed-competent tau. Our primary motivation is to address the claims made by (Kaniyappan *et al.*, 2020) to determine whether the Tau biosensor cell line is a reliable cell-based assay.

3.3 Materials and Methods

3.3.1 Ethical Statement

All animals were kept in the animal facility of the Faculty of Pharmacy at the University of Barcelona under controlled environmental conditions and were provided with food and drink *ad libitum*. Animal care and experimental protocols were performed in compliance with the Ethics Committee on Animal Experimentation (CEEA) of the University of Barcelona. All housing, breeding, and procedures were performed under the guidelines and protocols OB47/19, C-007, 276/16, and 47/20 of CEEA.

3.3.2 Reagents

The tau aggregation inhibitor IN-M4 was purchased from GenScript as a lyophilized powder (Standard peptide, Lot: U902YFI230-1/PE6574). The fragment tauK18, which corresponds to the amino acids Leu243-Glu372, was purchased from R&D Systems (i.e., recombinant human tauK18/tau PHF core protein; R&D Systems, catalog no. SP-496-100).

3.3.3 Mice

All animals used in this study were P301S (+/-) mice and their non-transgenic littermates, P301S (-/-). P301S (+/-) are transgenic mice over-expressing the shortest human tau isoform with the P301S mutation, under the mouse prion promoter (*Prnp*) (Allen *et al.*, 2002), which causes inherited frontotemporal dementia. Importantly, P301S (+/-) mice develop severe filamentous tau aggregation at approximately 9 months of age. The non-transgenic P301S (-/-) mice were used as controls and will be referred to as P301S (-/-). In these experiments, we used 3-month-old P301S (+/-) and P301S (-/-) mice for stereotactic experiments because P301S (+/-) animals had not yet developed tau pathology. Mice of 12-month-old P301S (+/-) and P301S (-/-) mice for brain homogenate and sarkosyl-insoluble extractions because P301S (+/-) animals had a high burden of tau aggregates.

3.3.4 Human Samples

This chapter included frozen material from autopsy-proven, neuropathologically well-characterized cases of AD (n = 3), AGD (n = 2), PiD (n = 3), FTD-tau (n = 1), ARTAG (n = 2) GGT (n = 3), multiple system atrophy (MSA) (n = 2), PD (n = 1), and healthy controls (n = 2) obtained from the HUB-ICO-IDIBELL tissue bank. Table 1 summarizes the basic information about all patients. The institutional research ethics board approved the protocol and gave us consent for the use of all tissues.

Table 1 Human cases used to obtain sarkosyl-insoluble tau extracts

Case ID	Neuropathological diagnosis	Sex	Age at death (years)	PDM (h)
1.1	AD	Male	93	3
1.2	AD	Male	75	11
1.3	AD	Female	85	12
2.1	AGD	Male	76	5
2.2	AGD	Male	81	9
3.1	PiD	Male	91	8
3.2	PiD	Female	83	4.5
3.3	PiD	Female	81	14
4.1	FTD-tau	Male	69	8
5.1	ARTAG	Female	78	4
5.2	ARTAG	Male	66	8
6.1	GGT	Female	66	1
6.2	GGT	Female	57	10
6.2	GGT	Male	63	2
7.1	MSA	Male	73	10.5
7.2	MSA	Male	62	18
8.2	PD	Male	73	4
9.1	Control	Male	39	9
9.2	Control	Female	46	14

Abbreviations: AD: Alzheimer's disease, AGD: argyrophilic gran disease; ARTAG: aging-related tau astrogliopathy; FTD: frontotemporal dementia; GGT: globular glial tauopathy; MSA: multiple system atrophy; PD: Parkinson's disease; PiD: Pick's disease; PMD: post-mortem delay

3.3.5 Assembly of Recombinant tauK18 Fibrils

tauK18 fibrillization reactions were prepared in a 96-well plate to a final volume of 200 µL/well. Briefly, to monitor tauK18 fibrillization in real-time, 10 µM tauK18 was incubated with 0.5 mg/mL heparin, 1 mM dithiothreitol (DTT), 0.1 M phosphate-buffered saline (PBS), and 30 µM ThT. The plate was covered with sealing tape and incubated at 37°C under linear shaking for 60 s of shaking at 1,080 rpm and an amplitude of 1.5 mm. Fluorescence was monitored every 30 min for 24 h through bottom reading at 445 nm excitation and 485 nm emission using an Infinite M200 PRO multimode microplate reader (Tecan, Switzerland). Newly formed aggregates were pelleted by ultracentrifugation at 50,000 xg for 20 min at 4°C. Finally, pellets were resuspended in 10 µL of 0.1 M PBS and stored at -80°C until use. Fibrillization reactions were done in duplicate, and their average values are displayed for each condition.

3.3.6 Transmission Electron Microscopy Imaging

For transmission electron microscopy (TEM) experiments, 5 µL of the sample was placed on 200-mesh carbon film-coated copper grids (S160, Agar Scientific, United Kingdom) for 1 min and washed three times with distilled water. Grids were then negatively stained for 1 min with sterile filtered 2% uranyl acetate. Pictures were taken with a JEOL JEM 1010 TEM at an acceleration voltage of 100 kV and pictures were obtained using a CCD Megaview 1k x 1k camera.

3.3.7 Preparation of Total Mouse Brain Homogenates

Frozen brain tissue from 9-month-old P301S (+/-) or P301S (-/-) mice, was weighted, and 1 mL of 0.1 M PBS supplemented with protease inhibitors (Roche, Switzerland) was used per 20 mg of tissue. Each brain was homogenized for 10 min, using a polytron, and 50 µL aliquots were then stored at -80°C until use. Protein concentrations were determined using the Pierce™ Bicinchoninic Acid Protein (BCA) assay kit (Sigma-Aldrich, Germany), and equal amounts of protein were analyzed by immunoblot.

3.3.8 Preparation of Sarkosyl-Insoluble Fractions from Mice and Human Samples

Sarkosyl-insoluble tau was extracted from frozen brains of P301S (+/-), P301S (-/-) at 9 months of age, or human brains of deceased patients. Briefly, brain tissue was weighed and then homogenized using a Dounce homogenizer in 10 volumes of fresh homogenization buffer [0.8 M NaCl, 1 mM EGTA, 10% sucrose, 0.01 M $Na_2H_2P_2O_7$, 0.1 M NaF, 2 mM Na_3VO_4, 0.025 M β-glycerolphosphate, 0.01 M Tris-HCl, pH 7.4] containing

protease inhibitors (Roche, Switzerland). After centrifugation at 16,000 rpm for 22 min at 4°C, the supernatant was reserved (SN1). The pellet was resuspended in 5 volumes of homogenization buffer and centrifuged again at 14,000 rpm for 22 min at 4°C. The resulting supernatant (SN2) was then combined with the SN1, and the mixture (SN1 + SN2) was incubated with 0.1% sarkosyl (Sigma, Germany) and placed on a rotating shaker for 1 h at room temperature. The mixture was centrifuged at 35,000 rpm for 63 min at 4°C. Next, the supernatant was discarded, and the remaining pellet (sarkosyl-insoluble fraction) was washed and resuspended in 50 mM Tris-HCl, pH 7.4 (200 µL/g starting material). Finally, 100 µL aliquots were stored at -80°C until use. Protein concentrations were determined using the Pierce™ BCA assay kit (Sigma-Aldrich, Germany), and equal amounts of protein were analyzed by immunoblot.

3.3.9 Biochemical Analysis

3.3.9.1 Dodecyl Sulfate-Polyacrylamide Gel Electrophoresis

All samples were characterized by dodecyl sulfate-polyacrylamide gel electrophoresis (SDS-PAGE), followed by western blot (WB). Samples were mixed with 2X Laemmli sample buffer (Bio-Rad) and denatured for 10 min at 100°C. Next, samples were resolved on 10% SDS-PAGE gels and electrophoresed at a constant voltage of 60 V for approximately 15 min, followed by 100 V for 1 h.

3.3.9.2 Western Blot

Proteins were transferred to nitrocellulose membranes via electrophoretic transfer, run at 100 V for 1 h. The membranes were then blocked in 5% fat-free milk in Tris-buffered saline supplemented with 0.1% Tween 20 (TTBS) for 1 h at room temperature. Membranes were probed with primary antibodies in a buffer containing TTBS and 0.02% azide overnight at 4°C on a shaker. The following day, the membranes were rinsed in TTBS three times and incubated with the appropriate secondary antibody conjugated with horseradish peroxidase (HRP) diluted 1:1,000 in 5% fat-free milk in TTBS for 1 h at room temperature. The membranes were washed three times with TTBS for 10 min each. Membranes were revealed with the ECL-plus chemiluminescence western blot kit (Amersham-GE Healthcare, United Kingdom).

Primary antibodies used were, mouse anti-4R-tau (1:1,000) (Merck Millipore, catalog no. 05-804), mouse anti-β-Tubulin (1:10,000) (Biolegend, catalog no. 801201), rabbit anti-GFP (1:500) (Invitrogen, catalog no. A11122).

3.3.10 Tau Biosensor Cell Line

The Tau RD P301S FRET Biosensor [ATCC® CRL-3275™] (i.e., Tau biosensor cell line) was purchased from ATCC. Cells were grown in maintenance medium made of Dulbecco's Modified Eagle Medium (DMEM; ThermoFischer Scientific) supplemented with 10% fetal bovine serum (FBS; ThermoFischer Scientific), 1% GlutaMax (Gibco), and 1% penicillin/streptomycin (ThermoFischer Scientific) in 75 cm^2 culture bottles (Nunc, Denmark). Cells were maintained at 37°C and 5% CO_2 in a humidified incubator and split every 3 days when confluent.

3.3.11 Tau Biosensor Cell Line Seeding Assays

3.3.11.1 Tau Treatments

Samples analyzed included: fibrillated or monomeric tauK18 at a final concentration of 0.01 µM. Increasing concentrations. 100, 10, 1, and 0.1 mM H_2O_2. Human and murine α-syn PFFs (a generous gift from Dr. Masato Hasegawa, Tokyo Metropolitan Institute of Medical Science, Japan), both 0.1 µg/µL. Monomeric 2N4R human tau labeled with sulfoindocyanine Cy5 dye (TauCy5) (kindly provided by Dr. Jesús Ávila, CBM-UAM, Madrid), at a final concentration of 100 nm. Total brain homogenates and sarkosyl-insoluble fractions of P301S (+/-) and P301S (-/-) were used at a final concentration of 0.003 µg/µL total protein. Sarkosyl-insoluble fractions from human brains were used at a final concentration of 0.003 µg/µL total protein. Triton X-100 insoluble fractions derived from the Tau biosensor cell line were used at a final concentration of 0.03 µg/µL total protein. Concentrations for each sample were determined using the results of preliminary experiments.

3.3.11.2 Standard Tau Biosensor Cell Line Seeding Assay

Tau biosensor cells were plated in 96-well poly-D-lysine (Merck Millipore) (0.1 mg/mL) -coated plates at a density of 35,000 cells/well (i.e., total volume 130 µL) in maintenance medium and cultured at 37°C in a 5% CO_2 incubator overnight. The transduction mixture was prepared following the manufacturer's protocol (Holmes *et al.*, 2014). Briefly, 1.5 µL of the sample was combined with 8.5 µL of Opti-MEM medium (ThermoFischer Scientific). Next, a mixture of 1.25 µL of Lipofectamine-2000™ reagent (Invitrogen) and 8.75 µL of Opti-MEM was added to the sample mixture to a final volume of 20 µL and incubated for 1 h at room temperature. Mixtures with empty liposomes were included as negative controls. Tau biosensor maintenance medium was gently removed and replaced with 130 µL of pre-warmed Opti-MEM before 20 µL of the transduction

mixture was added to the cells. Twenty-four hours later, cells were washed once in pre-warmed 0.1 M PBS and fixed in 4% paraformaldehyde (PFA) for 15 min at room temperature. Next, 4% PFA was removed, and cells were washed three times 5 min each with 300 µL of 0.1 M PBS. Finally, 300 µL of 0.1 M PBS with 0.02% azide was placed in each well, and the plate was sealed with sealing tape and kept at 4°C until analysis. For seeding assays, each sample was added in triplicate (i.e., technical replicates), and at least three independent experiments in different days were conducted with that same sample to confirm the results.

3.3.11.3 Tau Biosensor Cell Line Seeding Assay Followed by Sequential Extraction and Biochemical Analysis

The following protocol is summarized in Figure 8. Tau biosensor cells were plated in 60 mm^2 well poly-D-lysine (0.1 mg/mL) -coated plates at a density of 200,000 cells/well in maintenance medium at 37°C and 5% CO_2 in a humidified incubator. On the following day, cells were transduced using the same transduction protocol described in the previous section, always using total brain homogenates of P301S (+/-), P301S (-/-), and empty liposomes as the vehicle control condition. Twenty-four hours later, the transduction reaction was removed, and cells were washed once in pre-warmed sterile 0.1 M PBS and further maintained with fresh maintenance medium. Forty-eight hours later, cells were washed twice with pre-warmed sterile 0.1 M PBS. Next, cells were scraped from the plate surface in Triton X-100 lysis buffer [0.05% Triton X-100 in sterile 0.1 M PBS supplemented with 1X protease inhibitors] and pelleted at 500 xg for 5 min at 4°C. Supernatants were then centrifuged at 1,000 xg for 5 min at 4°C. Next, 10% of the supernatant volume of each sample was kept as the Triton X-100 soluble fraction (TSF). Importantly, each case was named based on the sample used in the transduction of the Tau biosensor cells. Thereby, the homogenate P301S (+/-) produced TSF-P+, the homogenate P301S (-/-) produced TSF-P-, and the empty liposomes (vehicle) condition produced TSF-V. The remaining Triton X-100 soluble fraction was centrifuged at 50,000 rpm for 30 min at 4°C. After that, the pellets were washed in 0.1 M PBS and further centrifuged at 50,000 rpm for 30 min at 4°C. The resulting pellet was resuspended in 50 µL of 50 mM Tris-HCl, pH 7.4 and reserved as the Triton X-100 insoluble fraction (TIF), referred to as TIF-P+, TIF-P, and TIF-V. Aliquots of all fractions were stored at -80°C until further use. Protein concentrations were determined using the Pierce™ BCA assay kit (Sigma-Aldrich, Germany), and equal amounts of protein were analyzed by immunoblot.

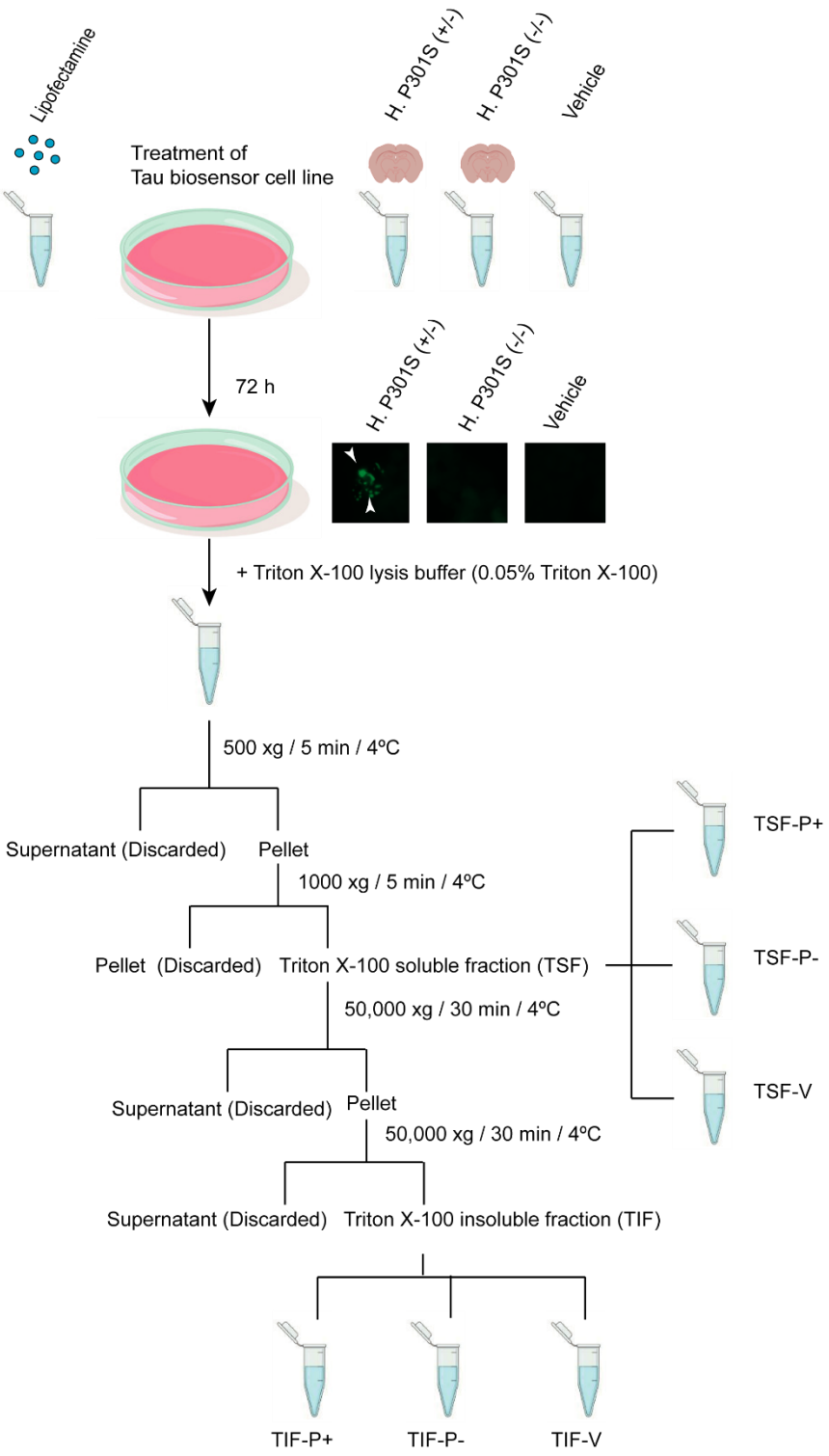

Figure 8 Sequential extraction of the Tau biosensor cell line in Triton X-100: Schematic diagram summarizing the main steps for the sequential extraction of Triton X-100 soluble and insoluble fractions (i.e., TSF and TIF, respectively) from the Tau biosensor cell line treated with P301S (+/-) (P+), P301S (-/-) (P-), or empty liposomes (V). White arrowheads indicate the fluorescent inclusions. The term “H.” stands for homogenate.

3.3.11.4 Tau Biosensor Cell Line Seeding Assay with IN-M4 Inhibitor of Tau Aggregation

IN-M4 is a small peptide designed to inhibit tau aggregation (Seidler *et al.*, 2019). Lyophilized IN-M4 was prepared by dissolving it in dimethyl sulfoxide (DMSO) to make a 10 mM stock solution, then filter-sterilized through a 0.22 µm sterile syringe filter (Merck Millipore, Germany). Finally, the stock was aliquoted into 100 µL or 50 µL portions and stored at -20°C until further use.

Tau biosensor cells were plated in 96-well poly-D-lysine (0.1 mg/mL) -coated plates using the same protocol described above and incubated for 18 h before treatment. On the same day of plating, the IN-M4 peptide was diluted in sterile H_2O to 1 mM (i.e., from the 10 mM stock solution) and further diluted in Opti-MEM at a final concentration of 0, 5, 10, 20, and 50 µM per well (i.e., final reaction volume 100 µL). Next, 2.5 µL of tau samples were added to each IN-M4 dilution to a final volume of 20 µL and incubated for 18 h at 4°C. The next day, the tau samples mixed with or without IN-M4 were left for 10 min at room temperature. Next, samples were mixed with 1 µL of Lipofectamine-2000™ diluted in 19 µL of Opti-MEM. The final mixture was further incubated at room temperature for 1 h. Maintenance medium from the plated Tau biosensor cells was carefully removed, and cells were rinsed in 90 µL of pre-warmed Opti-MEM. Finally, 10 µL of the final mixture was added to the cells to a final volume of 100 µL. Twenty-four hours later, cells were fixed in 4% PFA for 15 min at room temperature. Cells were washed three times 5 min each, with 300 µL of 0.1 M PBS. Finally, 300 µL of 0.1 M PBS with 0.02% azide was placed in each well, and the plate was sealed with sealing tape and kept at 4°C until analysis. Each sample was added in triplicate (i.e., technical replicates), and at least three independent experiments in different days were conducted.

3.3.12 Imaging

For imaging, we used an inverted Olympus fluorescence microscope IX71 (Olympus) equipped with a sensitive, high-speed camera (Hamamatsu ORCA Flash 4.0) and an LED light source (CoolLED's pE-300^{white}, Delta Optics, Spain). Images were acquired with the camera software Olympus cellSens^{TM} (Olympus Corporation; https://www.olympus-lifescience.com/en/software/cellsens/) and saved in 8-bit ".tiff" files. To observe fluorescent inclusions, samples were excited at 488 nm, and a green fluorescent protein (GFP) filter set was employed for signal detection. For aggregated tau quantification in the Tau biosensor cell line, we used the 10x objective. At least six different pictures were randomly taken for each well, for a total of three technical replicates.

3.3.13 Image Processing and Data Acquisition Using ImageJ/Fiji Software

Of note, the levels of FRET signal in the Tau biosensor cell line can be easily quantifiable by flow cytometry, although the fluorescent inclusions can also be seen using standard fluorescence microscopy. Consequently, we developed an ImageJ/Fiji script (Schindelin *et al.*, 2012) (National Institute of Health) to quantify the levels of tau aggregation. Prior to batch processing, we empirically determined the parameters of the macro in a sample of randomly selected images.

The Tau biosensor cell line exhibits green background fluorescence, allowing observation of individual cells without the need for nuclear labeling. Nevertheless, when tau aggregation occurs, inclusions emit a strong fluorescence signal, which can be easily distinguished from the cellular background. Therefore, our ImageJ/Fiji macro was coded to differentiate the signal emitted by the inclusions from that produced by the cells in a two-step process. Briefly, the first step computed the area occupied by the Tau biosensor cells. The objective of the second step was to calculate the area represented by the fluorescent inclusions. Both areas were stored in a ".csv" file with the result of the following equation:

$$\frac{\text{Area occupied by the aggregates}}{\text{Area occupied by the Tau biosensor cells}} \times 100$$

A diagram showing the first step is summarized in Figure 9. In detail, the script started by duplicating the original image and temporarily storing it as "Picture1." Next, the contrast of "Picture1" was enhanced to further differentiate the background from the cells. Then, the image was thresholded by applying the "Huang dark" algorithm, resulting in a binarized mask. The binary mask was then used to obtain the area occupied exclusively by the cells, and the results were saved as "Area1."

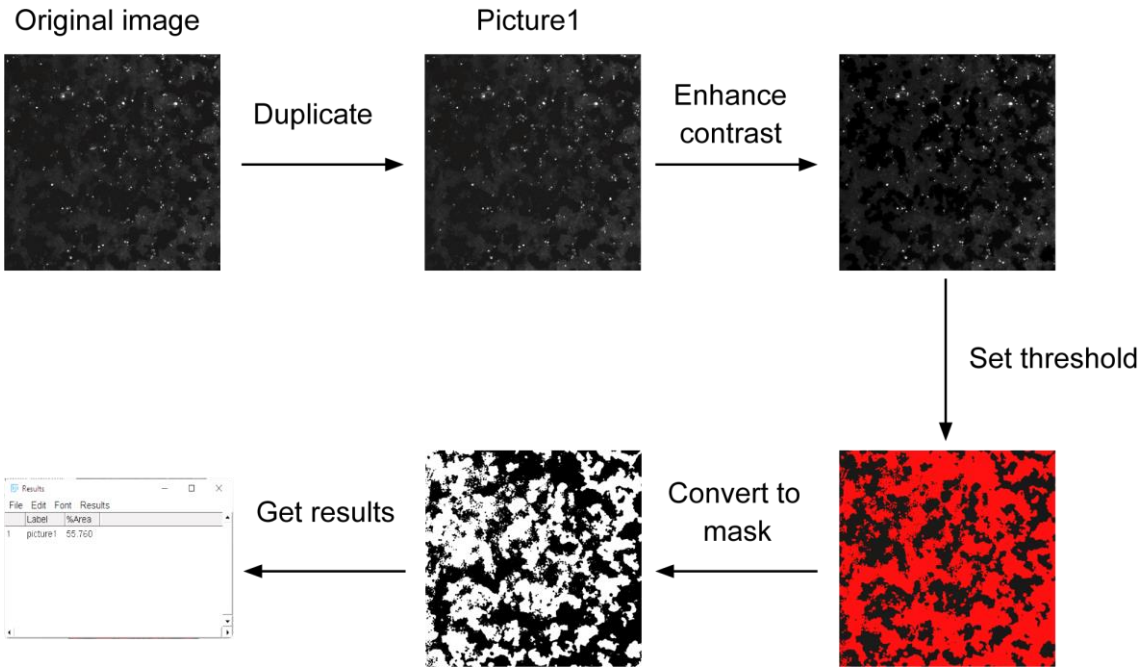

Figure 9 Customized ImageJ/*Fiji* macro used to quantify the area occupied by the Tau biosensor cells (Step I): The original image is duplicated to protect it from further modifications, resulting in "Picture1." The duplicated image is then processed to enhance its contrast. Next, "Picture1" is thresholded with the known "Huang dark" algorithm and subsequently converted into a binarized mask (red and black). *Notably*, this mask differentiates the area occupied by the Tau biosensor cells (black) from the background (white). The program uses this mask to obtain the black area from the image and stores it as "Area1."

The second step, summarized in Figure 10, was programed to first duplicate the original image twice, resulting in "Picture2" and "Picture3." Then, "Picture3" was used to retrieve and store the image's information regarding the area, mean intensity, minimum intensity, maximum intensity, standard deviation, and the intensity histogram. Importantly, maximum intensity values of the fluorescent inclusions were always higher than the background fluorescence. Thus, "Picture3" was used to generate a new image in which the maximum intensity value was reduced to the mean intensity value multiplied by 3.5 units. As a result, fluorescent inclusions were removed from the modified "Picture3." The latter was then subtracted from "Picture2," generating a new image labeled "Result of Picture2," in which the cellular bodies were no longer present because the mean fluorescence had been removed and only the outstanding fluorescent puncta were visible. After that, "Result of Picture2" was thresholded by applying the "Max entropy dark" algorithm, and a binary mask was created. The area occupied by the aggregates was computed, and the results were stored in the ".csv" file labeled "Area2." Finally, the program automatically calculated value of (Area2/Area1) x 100.

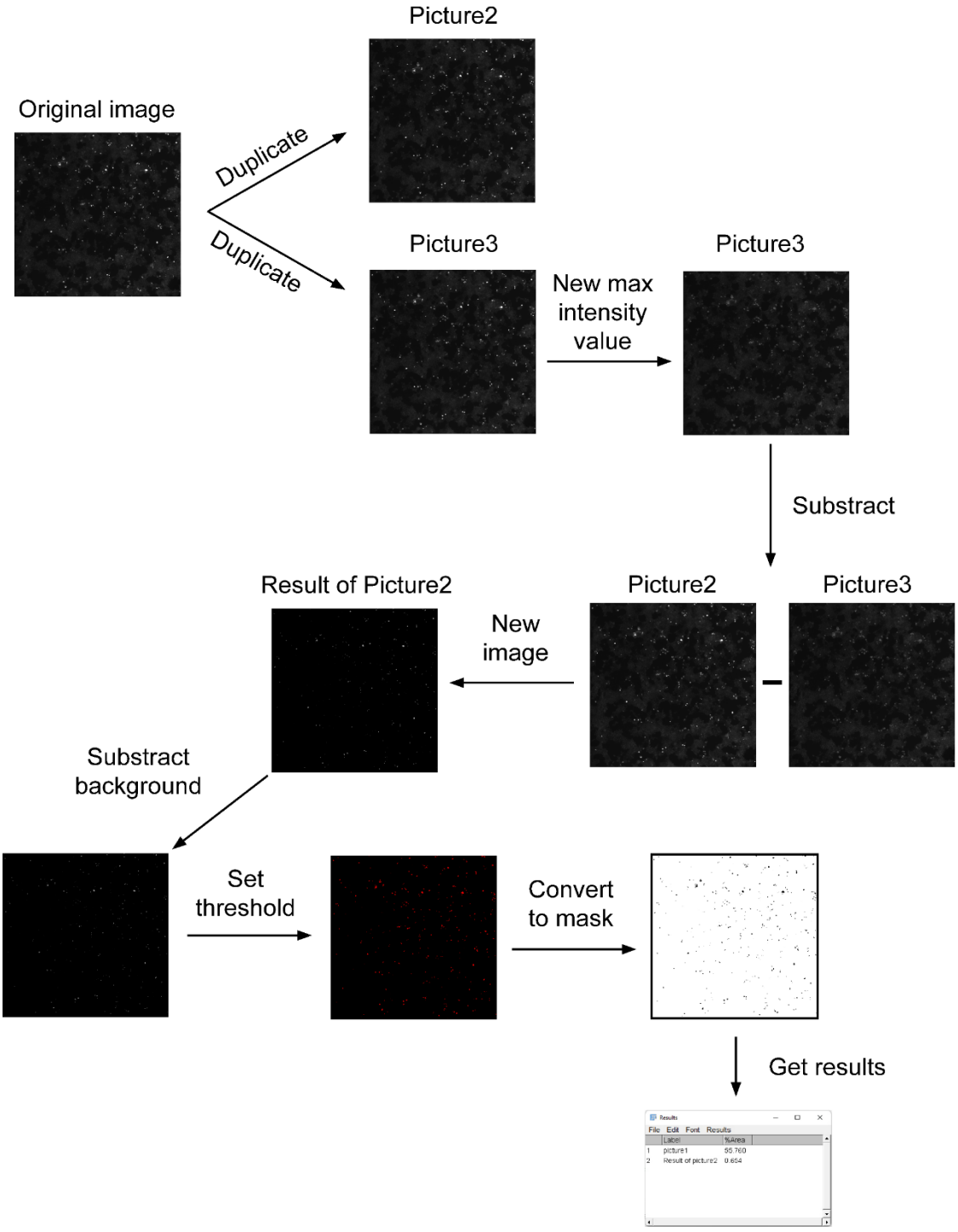

Figure 10 Customized ImageJ/Fiji macro used to quantify the area occupied by the fluorescent inclusions (Step II): The original image is duplicated to protect it from further modifications, resulting in "Picture2" and "Picture3." "Picture3" is then used to produce a newly created image that maintains the name "Picture3," with the adjusted maximum intensity value equal to the image's mean multiplied by 3.5 units. The resulting image does not display fluorescent inclusions within the Tau biosensor cells. A new image labeled "Result of Picture2" is generated by subtracting "Picture3" from "Picture2," in which only fluorescent puncta are visible. The background of "Result of Picture2" is eliminated to reduce residual noise. The image is then thresholded by applying the "Max entropy dark" algorithm and subsequently converted into a binarized mask (red and black). Finally, the program uses this mask to obtain the black area from the image, which is exclusively occupied by fluorescent inclusions, and stores it as "Area2."

3.3.14 Stereotaxic Surgery

For surgery, 3-month-old P301S (+/-) and P301S (-/-) mice were deeply anesthetized with 1.5% isoflurane and placed in a stereotaxic apparatus (Kopf Instruments, California, United States of America). Unilateral stereotaxic injections were performed into the right hippocampus (AP: -1.4 mm from bregma; LM: + 1.5 mm; DV: -1.5 mm), and 2.5 µL of TIF-P+ was inoculated using a Hamilton syringe. Following the injection, the needle was kept in place for an additional 3 min before withdrawal. The surgical area was cleaned with sterile saline, and the incision was sutured. Mice were monitored until recovery from anesthesia and were checked regularly following surgery.

3.3.15 Tissue Processing and Immunohistochemistry

After 3 months of incubation, mice were terminally anesthetized and transcardially perfused, using a peristaltic infusion pump, with 0.1 M PBS, followed by 4% PFA. Next, brains were removed and post-fixed in 4% PFA overnight at 4°C. Finally, brains were changed to 70% ethanol and stored at 4°C until inclusion. Following paraffin embedding, 10 µm coronal sections were cut from the brain tissue of seeded mice and mounted on glass slides.

For immunohistochemistry (IHC), paraffin-embedded tissue sections were deparaffinized in xylene for 20 min and rehydrated through a series of ethanol solutions from 100%, 90%, 80%, and 70%, followed by H_2O, submerging the sections for 5 min each step. Antigen retrieval for IHC was performed with a PT link machine (Pre Treatment Link, DAKO, Agilent, Santa Clara, United States of America), following the manufacturer's instructions. Briefly, sections were treated for 20 min at 97°C with high-pH Tris-EDTA, pH 9 antigen retrieval buffer. After rinsing sections in 0.1 M PBS, endogenous peroxidase activity was quenched with 2% H_2O_2 and 10% methanol for 15 min and blocked for 1 h in blocking solution [10% normal horse serum (NHS), 0.1% Triton X-100, and 0.015 g/mL glycine in 0.1 M PBS containing 1% bovine serum albumin (BSA)]. Sections were incubated the primary antibody anti-AT8 pSer202/pThr205 (1:50) (ThermoFischer Scientific, catalog no. MN1020) in antibody solution [5% FBS, 0.1% Triton X-100, and 0.02% azide in 0.1 M PBS] at 4°C overnight. Sections were then washed in 0.1 M PBS and incubated with the secondary antibody Alexa Fluor 568 anti-mouse (1:300) (Life Technologies) for 2 h at room temperature. The tissues were incubated with 1 µg/mL Hoechst 33342 (Invitrogen) diluted in 0.1 M PBS for 10 min at room temperature. Stained sections were viewed using an Olympus BX43 Upright Microscope (Olympus) equipped with a DP12L-cooled camera.

3.3.16 Statistical Analysis

Quantitative data were analyzed using one-way ANOVA, followed by Dunnett's *post hoc* test was used for comparisons. Statistical significance was set at $p < 0.05$. The data are expressed as means ± SD. GraphPad Prism 8 (version 8.02; GraphPad software Inc., California, United States of America) was used to perform statistical tests and produce graphs. For all statistical analysis in this chapter: *$p < 0.05$, **$p < 0.01$; ***$p < 0.001$, ****$p < 0.0001$.

3.4 Results

3.4.1 Specificity of the Tau Biosensor Cell Line

3.4.1.1 The Tau Biosensor Cell Line Is Sensitive to the Presence of Fibrillated Tau but Not to Monomeric Tau

Our aim in this chapter was to evaluate the specificity of the Tau biosensor cell line for seed-competent tau species by challenging the cell line with samples that had not been evaluated in the original paper (Holmes *et al.*, 2014). Thus, we first wanted to determine whether the Tau biosensor cell line could discriminate between monomeric and fibrillated tau. For this purpose, we used tauK18, a shortened wild-type variant of tau containing only the four MT-binding repeats of the tau RD region. It should be noted that we specifically chose tauK18 for our initial experiments because it is comparable in length and sequence to that expressed by the Tau biosensor cells.

First, samples with monomeric tauK18 were incubated with heparin (tauK18 + Hep), without heparin (tauK18 - Hep), or heparin alone (Hep). The extent to which each condition would form fibrils was determined using the ThT assay (Figure 11A). ThT analysis showed no amyloid formation for the conditions tauK18 - Hep (Figure 11A, blue) or Hep (Figure 11A, purple). On the contrary, tauK18 + Hep exhibited strong ThT fluorescence (Figure 11A, orange). In fact, it is clear from Figure 11A that after 7 h of incubation, the fluorescent signal emitted by the tauK18 + Hep condition exceeded the detection limits of the microplate reader, indicating increased content of β-sheet structures. The presence of fibrils in the tauK18 + Hep condition was confirmed using TEM and negative staining technique (Figure 11B). As expected, we did not find any fibrillated structures in the tauK18 - Hep condition (Figure 11C).

Having proved that we had both monomeric and fibrillated tau samples, we assessed the seeding potencies of both conditions in the Tau biosensor cell line via the standard seeding assay (i.e., see Chapter 1, Materials and Methods, Section 3.3.11.2). Thus, Tau biosensor cells were transduced with Lipofectamine-2000™ mixed with the same tauK18 samples previously used to monitor the fibrillation process for 24 h. As seen in Figures 11D and E, regardless of the treatment, all Tau biosensor cells showed high levels of

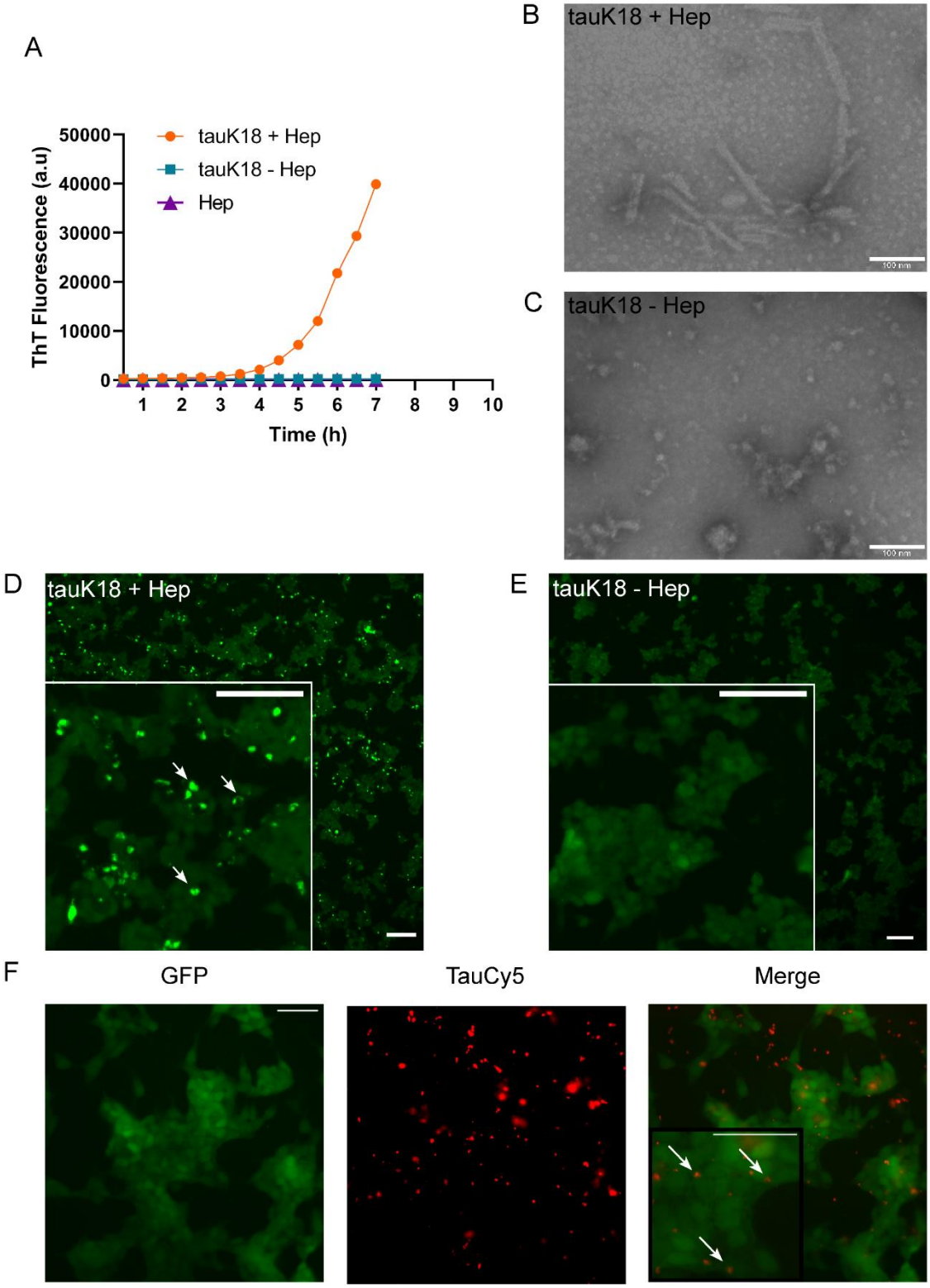

Figure 11 Fibrillated but not monomeric tau triggers the formation of fluorescent inclusions in the Tau biosensor cell line: A) Thioflavin T (ThT) fluorescence of monomeric soluble tauK18 in the presence (tauK18 + Hep, in orange) or absence (tauK18 - Hep, in blue) of heparin. Heparin alone (Hep, in purple) was used as the negative control. **B)** Representative transmission electron microscopy (TEM) images of tauK18 seeded in the presence of heparin display fibril-like morphologies. Scale bar, 100 nm. **C)** Representative TEM images of tauK18 seeded in the absence of heparin display amorphous assemblies. Scale bar, 100 nm. **D)** A representative image of Tau biosensor cells transduced with tauK18 + Hep shows the formation of fluorescent inclusions. Arrowheads in the high magnification image indicate fluorescent aggregates. Scale bars, 50 µm. **E)** The formation of fluorescent puncta in Tau biosensor cells transduced with tauK18 - Hep is not observed. Scale bars, 50 µm. **F)** Tau biosensor cells were treated with monomeric TauCy5 (red). No fluorescent inclusions are observed (left picture), despite high levels of TauCy5 (center). Arrows at high-magnification merge image (right) highlight monomeric TauCy5. Scale bars, 50 µm. Abbreviation a.u stands for arbitrary unit, and GFP stands for green fluorescent protein.

background fluorescence signal diffused in the cytosol. However, in cells treated with tau18 + Hep, we observed the presence of fluorescent inclusions (Figure 11D), which were completely absent in cells treated with tauK18 - Hep (Figure 11E), suggesting that the Tau biosensor cell line only recognizes fibrillar structures. Nevertheless, because tauK18 is a truncated construct, we were concerned that the Tau biosensor cell line was unable to identify it as a monomeric tau species, resulting in a false-negative signal. Therefore, we transduced the cell line with a human full-length 2N4R tau isoform labeled with Cy5 dye (TauCy5). As shown in Figure 11F, no fluorescent inclusions were formed (Figure 11F, left panel) despite the abundant presence of TauCy5 (Figure 11F, middle and right panels). Taken together, these results indicate that fibrillated tau, but not monomeric tau, is recognized as seed-competent by the Tau biosensor cells. Therefore, what triggered the formation of fluorescent inclusions was the presence of structurally “pathogenic” tau rather than the tau protein itself.

3.4.1.2 Neither Oxidative Stress nor Fibrillated α-Syn Induces the Formation of Fluorescent Inclusions in the Tau Biosensor Cell Line

To further validate the Tau biosensor cell line’s specificity for seed-competent tau, we challenged the cell line with two additional treatments devoid of aggregated tau. The production of ROS has been related to the induction of tau aggregation (Du *et al.*, 2022). Therefore, we first examined whether inducing oxidative stress by exposing the Tau biosensor cell line to H_2O_2 resulted in the formation of fluorescent inclusions. We treated cells with four different concentrations of H_2O_2 (100, 10, 1, or 0.1 mM) for 24 h. As illustrated in Figure 12A, after exposure to the higher doses of H_2O_2 (i.e., 100 mM and 10 mM), most cells died and were detached from the wells. Regardless, the few remaining ones did not display fluorescent agglomerates. The two lowest concentrations

of H_2O_2 (i.e., 1 mM and 0.1 mM) did not result in marked cell death, although we did not observe the formation of fluorescent inclusions.

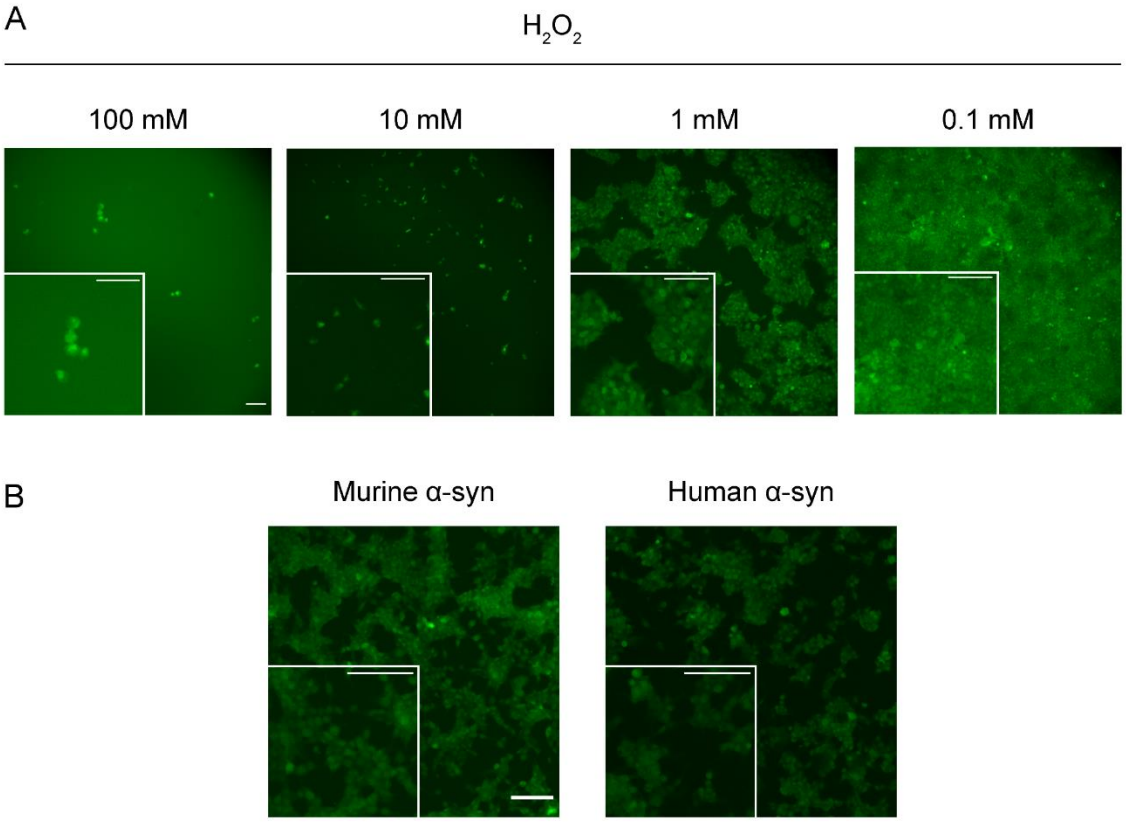

Figure 12 Assessment of H_2O_2 and α-synuclein (α-syn) effects on the Tau biosensor cell line: A) Tau biosensor cells incubated with 100, 10, 1, or 0.1 mM H_2O_2 do not result in the formation of fluorescent puncta. Scale bars, 50 µm. **B)** Tau biosensor cells transduced with either murine or human fibrillated α-syn do not trigger fluorescent inclusions. Scale bars, 50 µm.

Similar to ROS production, previous investigations have suggested that α-syn aggregates can induce the formation of tau aggregates (Giasson *et al.*, 2003; Waxman & Giasson, 2011). Thus, we transduced the Tau biosensor cell line with α-syn PFFs from murine or human sequences for 24 h. We did not observe the formation of fluorescent agglomerates under either condition (Figure 12B). Together, the inability of H_2O_2 and α-syn to trigger fluorescent inclusions further demonstrated the specificity of the Tau biosensor cell line for seed-competent tau species.

3.4.1.3 The Tau Biosensor Cell Line Specifically Detects "Pathogenic" Tau from Sarkosyl-Insoluble Fractions Derived from P301S (+/-) Mice

Next, we tested the specificity of the Tau biosensor cell line by transducing the cells with more disease-relevant samples. For that, we used sarkosyl-insoluble fractions from the brains of 12-month-old P301S (+/-) or P301S (-/-) mice or empty liposomes as the

control vehicle. As shown in Figure 13, only the P301S (+/-) treatment triggered the formation of fluorescent inclusions, whereas the P301S (-/-) and the vehicle treatments did not. These observations were confirmed by the transduction of three independent sarkosyl-insoluble extractions of both P301S (+/-) and P301S (-/-) mice. Together, these results support our prior findings that the Tau biosensor cell line detects only "pathogenic" species of the tau protein.

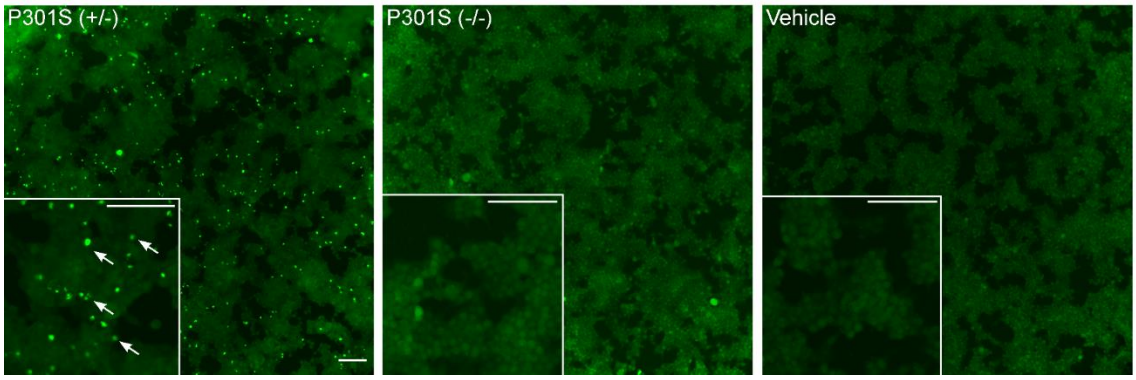

Figure 13 The Tau biosensor cell line specifically detects pathogenic tau from sarkosyl-insoluble fractions derived from P301S (+/-) mice: Representative fluorescence microscopy micrographs of the Tau biosensor cell line transduced with sarkosyl-insoluble fractions from P301S (+/-) or P301S (-/-) mice, or empty liposomes as the vehicle control. Fluorescent inclusions are only visible in cells treated with P301S (+/-). Fluorescent puncta are marked with white arrows. Scale bars, 50 µm.

3.4.1.4 Only Human Tauopathies Induce the Formation of Fluorescent Inclusions in the Tau Biosensor Cell Line

Finally, we challenged the Tau biosensor cell line with sarkosyl-insoluble fractions of post-mortem human-derived samples from patients with diagnosed tauopathies (i.e., ARTAG (n = 2), PiD (n = 3), FTD-tau (n = 1), and GGT (n = 3)), patients with α-synucleinopathies (i.e., MSA (n = 2), and PD (n = 1)), or healthy controls (n = 2). Cells transduced with the different human tauopathies studied are shown in the upper panel of Figure 14. Importantly, all tested cases led to the formation of fluorescent inclusions. Previously, others have used the Tau biosensor cell line to test for the presence of seed-competent tau species in human-derived samples (Furman *et al.*, 2017; Kamath *et al.*, 2021). However, to our knowledge, we are the first to describe tau proteopathic seeding in ARTAG-derived samples using a cell-based approach. This result suggests that, despite tau lesions in ARTAG patients being only found in astrocytes, the "pathological" tau derived from their brains displays seed competency comparable to that observed in other tauopathies. The lower panel of Figure 14 shows representative images of cells treated with either α-synucleinopathy patients- or healthy controls-derived samples, for which we did not observe fluorescent accumulation for any tested cases. To confirm our

findings, samples from each patient were tested in at least three independent experiments, with three technical replicates per case. Again, our results show that the formation of fluorescent inclusions in the Tau biosensor cell line is specific to samples containing “pathogenic” tau species and other amyloids, such as α-syn, do not result in false positives.

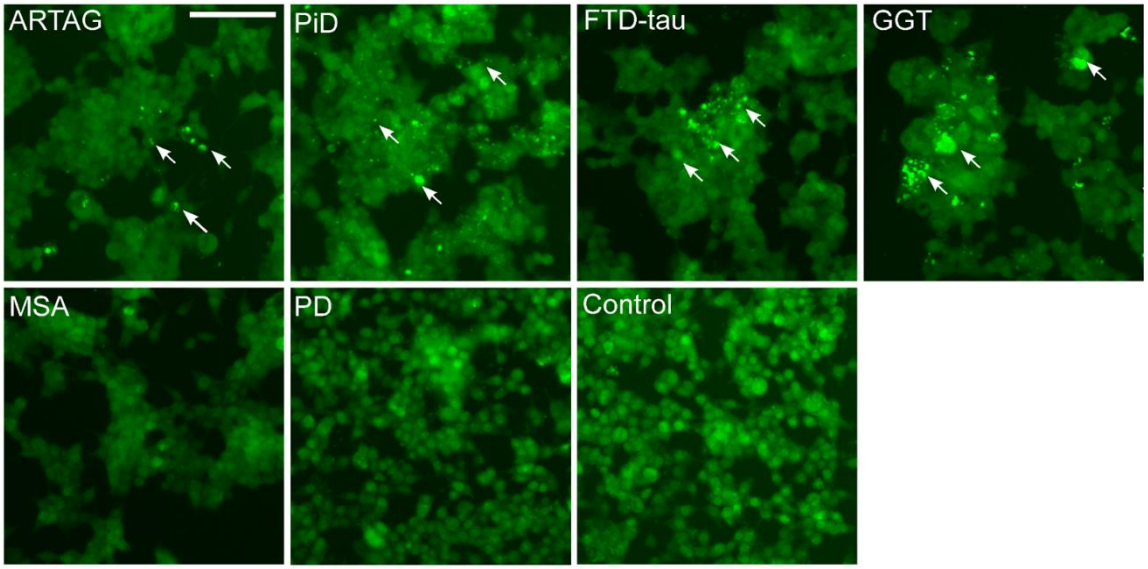

Figure 14 Human tauopathies induce the formation of fluorescent inclusions in the Tau biosensor cell line: Representative fluorescence microscopy images of Tau biosensor cells transduced with human samples from tauopathies (i.e., ARTAG (n = 2), PiD (n = 3), FTD-tau (n = 1), and GGT (n = 3)) or α-synucleinopathies (i.e., MSA (n = 2) and PD (n = 1)) patients, or healthy controls (i.e., Control (n = 2)). White arrows indicate fluorescent inclusions. The lack of localized fluorescence in the MSA, PD, and control cases shows the specificity of the Tau biosensor cell line for seed-competent tau species. Scale bar, 50 µm.

3.4.1.5 Formation of Tau Strains in the Tau Biosensor Cell Line

While conducting these last experiments, we realized specific samples tended to produce aggregates with similar shapes. Therefore, we decided to transduce the Tau biosensor cell line with AD (n = 3), GGT (n = 3), AGD (n = 2), or PiD (n = 3), to further address these observations. We found fluorescent inclusions adopted different morphologies depending on the origin of the extracellular seed-competent tau (Figure 15). Although all tested cases induced the formation of more than one type of inclusion morphology, they also displayed one or two predominant fluorescent structures, which were specific to the exogenous seed. AD patient samples consistently produced fibril-like inclusions, although some cells exhibited dot-like shapes (Figures 15a and b). Of note, AD samples were the most homogeneous regarding the type of inclusion formed. Cells treated with GGT produced rounded aggregates across the cytoplasm (Figures 15c and d). In contrast, AGD samples triggered the formation of multiple shiny speckles

(Figures 15e and f). Surprisingly, PiD-derived samples were the most heterogeneous, producing a wide variety of shapes, although the most frequent ones resembled those observed for GGT (Figures 15g and h). These observations are consistent with the idea that different seeds can trigger the formation of morphologically different tau aggregates. Similar to the previous section, all samples were tested in at least three independent experiments, with three technical replicates per condition. The findings point to the Tau biosensor cell line's potential to generate disease-specific strain aggregates, suggesting its potential as a future diagnostic tool.

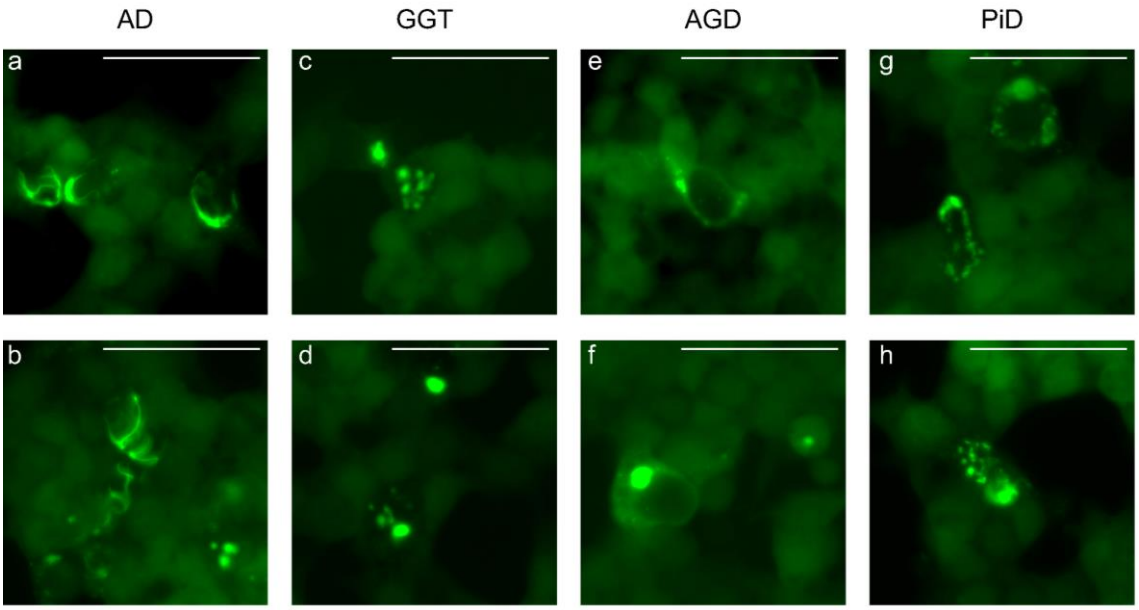

Figure 15 Different human tauopathies produce unique morphologies in the Tau biosensor cell line: AD samples (n = 3) induced the formation of fibril-like fluorescent shapes (**a**, **b**). GGT (n = 3) samples triggered multiple rounded inclusions (**c**, **d**). AGD (n = 2) samples produced multiple shiny speckles and often one big spherical fluorescent structure (**e**, **f**). PiD (n = 3) caused the formation of spherical fluorescent accumulations similar to those observed for GGT (**g**, **h**). Scale bars, 25 µm.

3.4.2 Evaluation of Amyloid-Like Properties of the Fluorescent Inclusions Formed in the Tau Biosensor Cell Line

From the previously presented results, it is clear that the Tau biosensor cell line has a high specificity to produce intracellular fluorescent puncta only in the presence of seed-competent tau. Therefore, contrary to the findings of (Kaniyappan *et al.*, 2020), we hypothesized that endogenously expressed tau RD-CFP/YFP formed fluorescent aggregates with amyloid properties. Amyloid fibrils share several unique properties, such as detergent insolubility, fibril-like morphology, and seeding potency. Hence, we employed a variety of experimental procedures to comprehensively describe the

fluorescent inclusions with the intention of proving their amyloid-like properties for the first time.

3.4.2.1 The Tau Biosensor Cell Line Forms Detergent-Insoluble Tau Aggregates upon Treatment with Seed-Competent Tau Species

To demonstrate the amyloidogenic nature of the fluorescent inclusions, we needed to prove that they were resistant to detergent treatment. For that purpose, we transduced the Tau biosensor cell line with brain homogenates from P301S (+/-) or P301S (-/-) mice or empty liposomes. After 24 h, cells were switched to maintenance medium to remove the treatments and left for another 48 h. Subsequently, cell lysates were sequentially extracted using 0.1% Triton X-100, resulting in the Triton X-100 soluble and insoluble fractions (i.e., a detailed description of this method can be found in Materials and Methods of this chapter). The presence of tau in both fractions was analyzed by immunoblotting and probed with anti-4R-tau (Figure 16A).

We detected 4R-tau migrating at 43 kDa in all tested samples (Figure 16A), consistent with tau RD-CFP/YFP species. Identical levels of 4R soluble tau were observed for the TSF-P+, TSF-P-, and TSF-V samples, suggesting that tau expression was not affected by the transduction of seed-competent species. However, in the Triton X-100 insoluble fraction, we consistently detected higher tau levels in TIF-P+ samples compared with TIF-P- and TIF-V (Figure 16A), indicating the formation of detergent-resistant tau species. The presence of insoluble tau in all Triton X-100 insoluble fractions suggests that “oligomeric” detergent-resistant tau forms are spontaneously generated in the Tau biosensor cell line. Nevertheless, the conformation adopted by these “oligomeric” species may be unable to produce fluorescently visible aggregates, as we did not observe fluorescent inclusions in cells treated with these fractions. Regarding the increased levels of insoluble tau in the TIF-P+ condition compared with TIF-P- and TIF-V, we concluded that the treatment with seed-competent tau increased the formation of insoluble tau RD-CFP/YFP aggregates. To confirm this, we assessed the immunoreactivity of all samples for the anti-GFP antibody (i.e., as it also recognizes YFP but not CFP) (Figure 16B). As expected, all fractions were positively identified by the anti-GFP antibody at 43 kDa, as expected for tau RD-CFP/YFP fragments. In excellent agreement with 4R-tau immunolabeling, we detected similar levels of soluble “GFP-tau” (i.e., RD-YFP) in the Triton X-100 soluble fractions, and TIF-P+ samples showed higher

levels of detergent-resistant RD-YFP than those of TIF-P- and TIF-V. Notably, four different extractions produced identical results.

Next, we further characterized the Triton X-100 insoluble fragments by TEM to analyze their ultrastructure at higher resolution levels (Figure 16C). Negative staining of all fractions revealed that TIF-P+ samples contained fibril-like structures (Figure 16C, left), whereas the TIF-P- and TIF-V samples only displayed small and amorphous constructs, consistent with the existence of small “oligomeric” species (Figure 16C, middle and right). Taken together, these results indicate that seed-competent tau, derived from P301S (+/-) brain homogenates, recruits the RD-CFP/YFP tau into Triton X-100 insoluble species that are detergent-resistant and adopt fibril-like shapes, thereby revealing specific features of amyloid aggregates.

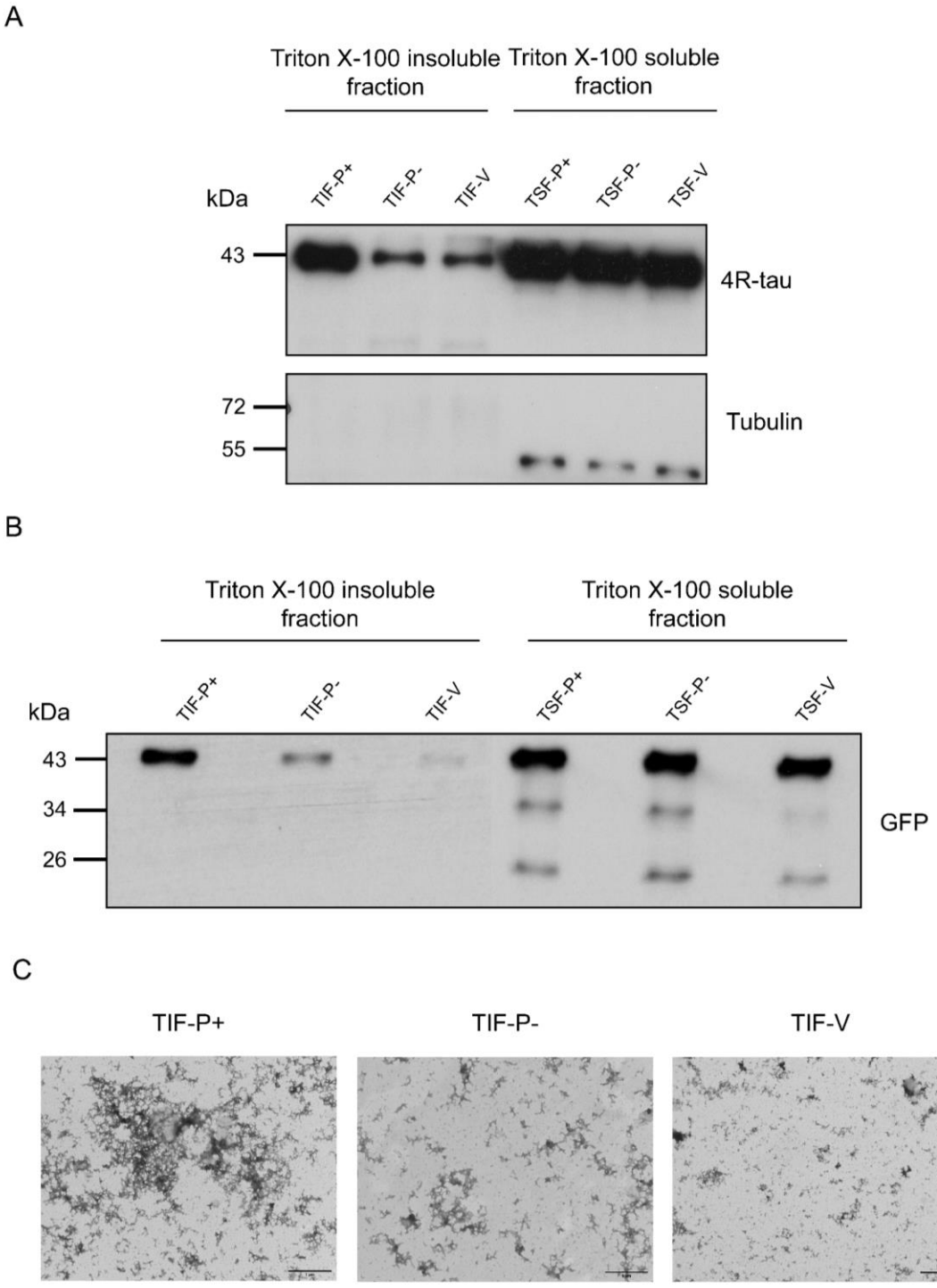

Figure 16 Characterization of the tau present in the Triton X-100 soluble (TSF) and insoluble (TIF) fractions: A) Western blot (WB) analysis of the TSF and TIF fractions of the Tau biosensor cell line treated with P301S (+/-) (P+), P301S (-/-) (P-), or empty liposomes (V), for 4R-tau, with tubulin as a loading control. A 43 kDa band, corresponding to 4R-tau, is detected under all conditions. A band of 55 kDa, corresponding to tubulin, is only present in the TSF fractions, demonstrating that soluble proteins are not present in the TIF samples. Identical results were observed in three independent extractions. **B)** The same samples reveal a band of 43 kDa when probed with the anti-GFP antibody. **C)** Representative transmission electron microscopy (TEM) images of the three TIF samples. Abundant negatively stained fibrils can be seen in the TIF-P+ condition, whereas TIF-P- and TIF-V samples only display amorphous structures. Scale bars, 1 µm.

3.4.2.2 Tau Species Present in the TIF-P+ Fractions Retain Their Seeding Potency

Having found that the fluorescent inclusions were made of insoluble tau RD-CFP/YFP fragments forming fibril-like structures, we next wondered whether the TIF-P+ fraction was also seed-competent. To test this, we transduced the Tau biosensor cell line with TIF-P+, TIF-P-, or TIF-V for 24 h and examined the formation of fluorescent puncta (Figure 17). We found that only cells treated with TIF-P+ samples generated fluorescent cytoplasmic inclusions, while the other two fractions did not. Overall, these findings show that the tau contained in the TIF-P+ fraction is seed-competent, further suggesting that the Tau biosensor cell line forms amyloid-like aggregates.

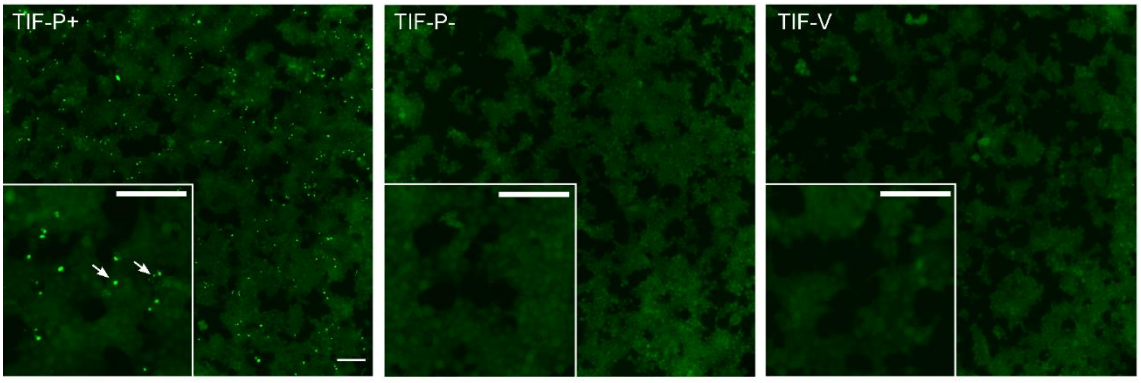

Figure 17 The TIF-P+ fraction triggers the formation of fluorescent inclusions in the Tau biosensor cell line: Representative fluorescence microscopy images of the Tau biosensor cell line transduced with TIF-P+, TIF-P-, or TIF-V samples. Fluorescent inclusions can only be seen in cells treated with the TIF-P+ fraction, indicated by white arrows in the high-magnification image. Scale bars, 50 µm.

3.4.3 The Inhibitor IN-M4 Reduces the Formation of Fluorescent Inclusions in the Tau Biosensor Cell Line

Considering our previous results, we hypothesized that transducing seed-competent tau with an aggregation inhibitor would reduce the presence of fluorescent inclusions in the Tau biosensor cell line. In other words, if the fluorescent accumulations were not tau aggregates, as suggested by (Kaniyappan *et al.*, 2020), adding an inhibitor of tau aggregation should not affect the formation of fluorescent accumulations. To prove our hypothesis, we chose the IN-M4 peptide, since it had previously been described to limit tau aggregation *in vitro* (Seidler *et al.*, 2019). For clarity, IN-M4 is a peptide-based inhibitor of tau-seeded aggregation designed to block the formation of tau aggregates by preventing the incorporation of additional molecules into growing amyloid fibrils. Consequently, although IN-M4 does not eliminate preexisting aggregates, it may prevent the formation of novel aggregates.

To test whether IN-M4 could reduce the formation of fluorescent inclusions, we co-transduced the Tau biosensor cell line with different concentrations of IN-M4 (0, 5, 10, 20, and 50 µM) along with TIF-P+, sarkosyl-insoluble P301S (+/-), or sarkosyl-insoluble GGT (n = 1) samples. After 24 h, all cells treated with seed-competent tau species (i.e., TIF-P+, P301S (+/-), or GGT) in the absence of the inhibitor (i.e., 0 µM IN-M4) displayed abundant fluorescent accumulations (Figure 18A). In contrast, increasing concentrations of IN-M4 peptide resulted in the dose-dependent reduction of fluorescent inclusions produced by all tested samples (i.e., TIF-P+, P301S (+/-), and GGT) (Figure 18A). To quantitatively report on the inhibition levels, we used a customized ImageJ/Fiji macro (i.e., a complete description of the one such macro can be found in Materials and Methods of this chapter). All quantifications were performed for three independent experiments, with three technical replicates per experimental condition, and six pictures per replicate. We found a significant decrease in the area occupied by fluorescent puncta as the IN-M4 increased for all tested samples (Figure 18B). The addition of 10 µM IN-M4 mixed with TIF-P+ significantly reduced the formation of aggregates compared to the 0 µM condition ($p = 0.0401$; n = 3 experiments) (Figure 18Ba). In contrast, only 5 µM of inhibitor significantly reduced the percentage of fluorescent accumulations compared to the 0 µM condition for the P301S (+/-) ($p = 0.0213$; n = 3 experiments) (Figure 18Bb) and GGT ($p = 0.0024$; n = 3 experiments) (Figure 18Bc) compared with their respective control conditions (i.e., 0 µM IN-M4). Together, our results show that the formation of fluorescent inclusions is sensitive to the presence of tau aggregation inhibitors.

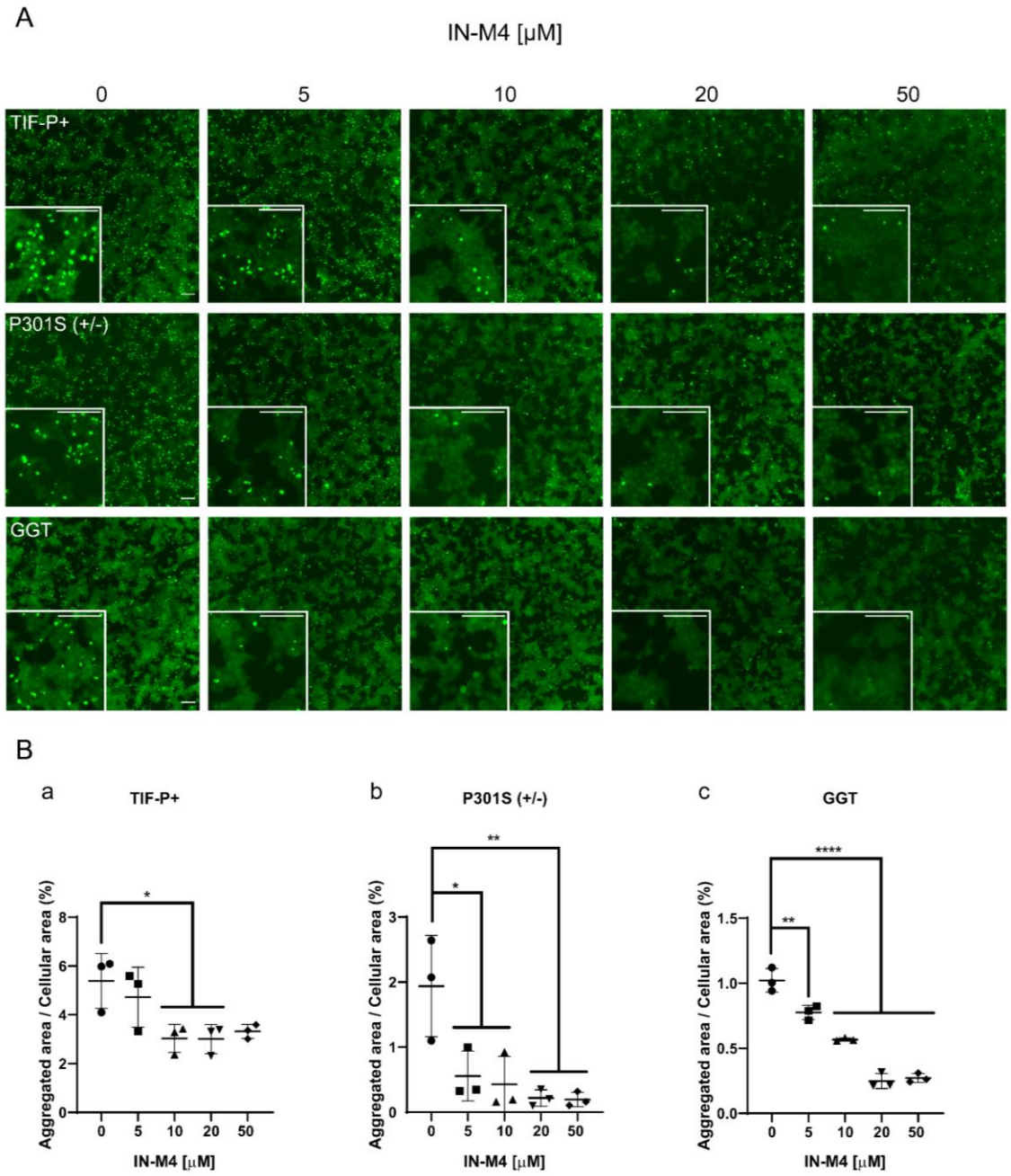

Figure 18 The inhibitor IN-M4 reduces the formation of fluorescent inclusions in the Tau biosensor cell line: A) Representative fluorescence microscopy images of the Tau biosensor cell line treated with TIF-P+, P301S (+/-), or GGT mixed with increasing concentrations of the inhibitor IN-M4 (0, 5, 10, 20, and 50 µM). **B)** All graphs (**a**, **b**, and **c**) represent the percentage of the area occupied by the fluorescent inclusions compared to the area occupied by the Tau biosensor cells. Data were derived from three independent experiments, with three technical replicates and six pictures per replicate. The results are expressed as mean ± SD. Statistically significant differences were calculated by one-way ANOVA followed by Dunnett's post hoc test was used to determine the significance compared to 0 µM (*$p < 0.05$; **$p < 0.01$; ****$p < 0.0001$). Scale bars, 50 µm.

3.4.4 The TIF-P+ Fraction Induces Tau Seeding and Spreading *In Vivo*

The inoculation of tau PFFs into animal models of tau pathology can induce the formation of pathological tau aggregates close to the injection area and synaptically connected regions (Iba *et al.*, 2013). Knowing that TIF-P+ samples were seed-competent *in vitro*, we wanted to examine their seeding potency *in vivo*. Therefore, we conducted a preliminary experiment in which we injected 2 µL of TIF-P+ into the hippocampus of 3-month-old P301S (+/-) (n = 2) and P301S (-/-) mice (n = 3). The animals were euthanized 3 months later and processed for IHC analysis. To evaluate the presence of pathological tau, we used the anti-AT8 antibody, which recognizes phosphorylated tau at residues Ser202 and Thr205 (i.e., known to be phosphorylated in AD's NFTs). We were unable to observe AT8-positive staining in the brains of P301S (-/-) mice (Figure 19A). In contrast, examination of P301S (+/-) animals revealed strong AT8-positive staining not only close to the inoculation area but also in the corpus callosum and, though milder, in the contralateral hippocampus, consistent with tau spreading to the principal anatomical connections of the ipsilateral hippocampal neurons (Figure 19B). These preliminary findings show that TIF-P+ triggers the onset of tau pathology in P301S (+/-) mice, along with its progression to synaptically connected brain areas.

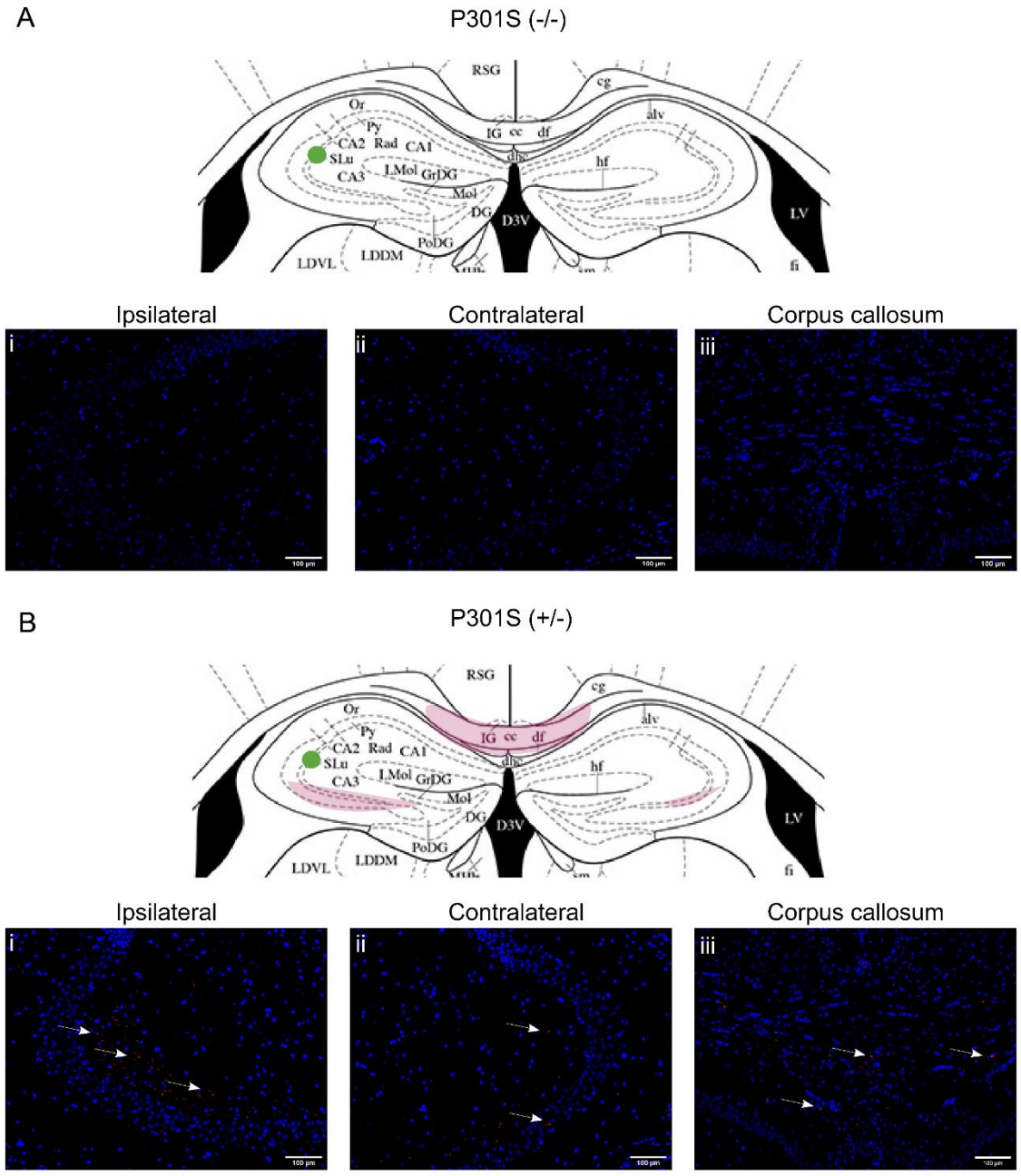

Figure 19 TIF-P+ fraction induces AT8-positive inclusions in P301S (+/-) mice: 3-month-old P301S (-/-) (n = 2) mice and P301S (+/-) (n = 3) mice were unilaterally injected into the right hippocampus with TIF-P+ samples (AP: -1.4 mm from bregma; LM: + 1.5 mm; DV: -1.5 mm). Three months later, mice were sacrificed and analyzed by immunohistochemistry (IHC) for AT8 inclusions (red). Nuclei (blue) stained with Hoechst. Ipsilateral and contralateral to the inoculation site. **A)** The upper panel depicts the inoculation site (green dot). The lower panels are representative images of the ipsilateral and contralateral hippocampus and the corpus callosum. No obvious AT8-positive labeling is observed. **B)** The Upper panel depicts the inoculation site (green dot) and the areas in which AT8-labeled tau pathology was detected (pink). The lower panels are representative images of the ipsilateral and contralateral hippocampus and the corpus callosum. White arrows indicate inclusions stained with AT8 (red). Scale bars, 100 µm.

3.5 Discussion

The Tau biosensor cell line has been widely used in tau pathology research since it was first commercialized (Chung *et al.*, 2019; Shin *et al.*, 2019; Kamath *et al.*, 2021). Although it was initially designed as a cell-based assay to examine proteopathic seeding in biological samples, it has now been adapted for other purposes, such as screening drug platforms (Louros *et al.*, 2022). Despite this, a recent publication (Kaniyappan *et al.*, 2020) questioned the reliability of the Tau biosensor cell line as a cell-based assay. The authors of the study claimed that this cell line is incapable to generate tau aggregates because of steric hindrance between the CFP and YFP molecules of the tau RD-CFP/YFP constructs. However, Kaniyappan and co-workers did not use the Tau biosensor cell line nor the same tau RD-CFP/YFP constructs as in the original publication (Holmes *et al.*, 2014). Consequently, it is unclear whether their results can be translated into a real cause for concern. Regardless, it is also true that, in their original paper, Holmes and colleagues did not fully address some critical aspects regarding the nature of the fluorescent inclusions formed in the Tau biosensor cell line. Therefore, as previously mentioned, if Kaniyappan's claims were valid, much of the conducted research using the Tau biosensor cell line would not only be irrelevant but also misleading. Given this situation, we wanted to clarify whether the fluorescent formations observed in the Tau biosensor cell line are RD-CFP/YFP aggregates with classic amyloid properties. Our findings indicate that the Tau biosensor cell line is a reliable cell-based assay of proteopathic seeding, specifically detecting seed-competent tau species that induce the formation of tau RD-CFP/YFP aggregates, which have amyloid properties and trigger seeding *in vitro* and spreading *in vivo*.

The initial objective of this chapter was to validate the specificity of the Tau biosensor cell line to "pathogenic" or seed-competent tau species. The cells were challenged with monomeric and fibrillated recombinant tau, resulting in the formation of fluorescent inclusions only in the presence of tau PFFs, suggesting that the shape rather than the sequence contains "pathogenic" information. However, we thought it was possible that cells would respond differently to the internalization of monomeric tau or PFFs. For instance, it may be that the larger size of the internalized PFFs forced soluble RD-CFP/YFP fragments to be close enough to produce an intense fluorescence signal perceived as a false positive. To eliminate that possibility, we tested whether other conditions mimicking cellular stress resulted in the formation of fluorescent inclusions. For this purpose, the Tau biosensor cell line was exposed to either oxidative stress or α-syn PFFs. As previously stated, the production of ROS has been linked to the induction

of tau aggregation (Du *et al.*, 2022). Regardless, in the Tau biosensor cell line, increasing concentrations of H_2O_2 did not prompt the formation of fluorescent puncta. These findings demonstrate that, at least in this cellular model, cellular stress is not sufficient to initiate tau aggregation. Additionally, our results ensure the specificity of fluorescent inclusions in situations in which the Tau biosensor cell line may be unwillingly exposed to oxidative stress (e.g., testing particular tissue-derived samples).

Moving now on to consider α-syn PFFs, they have also been proposed to cause tau to aggregate (Giasson *et al.*, 2003; Waxman & Giasson, 2011). However, the transduction of α-syn PFFs into the Tau biosensor cell line did not result in the formation of fluorescent agglomerates. These results corroborate the findings of (Holmes *et al.*, 2014), who also noted that transduction in the Tau biosensor cell line with α-syn did not result in fluorescent inclusions. Nevertheless, in their paper, Holmes and colleagues do not specify the sequence used to produce recombinant α-syn. Consequently, in order to eliminate the possibility that alternative α-syn sequences could have different outcomes, we tested both murine and human α-syn PFFs, obtaining identical results. These findings suggest that the formation of fluorescent inclusions in the Tau biosensor cell line is supported by a seed-dependent mechanism that requires extracellular seeds, which apparently must resemble the tau protein (e.g., fibrillated tauK18). Consistent with previous studies using other cell lines (Nonaka *et al.*, 2010), the Tau biosensor cell line does not seem to support a phenomenon known as cross-seeding of dissimilar amyloid proteins, in which different amyloidogenic proteins actively participate in each other's seeding process (Vasconcelos *et al.*, 2016). However, the Tau biosensor cell line may bias the self-seeded fibrillization of tau, given that the RD-CFP/YFP fragments do not represent the full-length protein and contain the P301S mutation (Sharma *et al.*, 2018). Therefore, its inability to be seeded by α-syn should not be generalized to what may occur in the brains of human patients. Finally, because α-syn PFFs do not trigger the formation of fluorescent puncta whereas tau PFFs do, it seems reasonable to conclude that the fluorescent inclusions in the Tau biosensor treated with tau PFFs were not the result of unspecific interactions but rather *bona fide* tau aggregates.

At this point, we demonstrated that the Tau biosensor cell line detects specifically the presence of aggregated tau. However, it could be argued that since PFFs may have different conformations than those from diseased brains (Zhang *et al.*, 2019), more physiologically relevant samples could produce the opposite results. Therefore, we examined the Tau biosensor cell line specificity for seed-competent tau species from brain-derived material. Due to the limited availability of human samples, we first

transduced the cell line with sarkosyl-insoluble fractions from P301S (+/-) mice, which strongly induced fluorescent inclusions, whereas the P301S (-/-) and vehicle conditions did not, consistent with previous reports (Holmes *et al.*, 2014; Kaufman *et al.*, 2016; Kaufman *et al.*, 2017). Notably, a novel aspect of our research is that we prove the cell line's specificity using sarkosyl-insoluble samples, rather than whole brain homogenates. Hence, our findings indicate that tau aggregation can occur even without highly soluble "oligomeric" species, suggesting that larger insoluble aggregates also have seeding potency.

Having demonstrated that the Tau biosensor cell line discriminates between sarkosyl-insoluble fractions from transgenic and non-transgenic P301S mice, we next examined the specificity for human-derived samples. All tauopathies displayed potent seeding activity upon transduction into the Tau biosensor cell line. In contrast, no fluorescent inclusions were observed in cells treated with either α-synucleinopathies or healthy controls. These results are consistent with the original paper on the Tau biosensor cell line (Holmes *et al.*, 2014), in which the authors noted that brain homogenates derived from Huntington's disease patients could not trigger the development of fluorescent puncta. Notably, Holmes and colleagues did not evaluate samples from patients with α-synucleinopathies. Therefore, our work extends and generalizes the concept that the Tau biosensor cell line specifically detects "pathological" tau and that transducing aggregates from other NDs does not result in the formation of fluorescent inclusions.

Notably, the two tested ARTAG cases resulted in the formation of fluorescent inclusions in the Tau biosensor cell line. To our knowledge, no previous study has used this or any other cell-based assay to investigate the seeding capacity of tau derived from ARTAG patients. As a reminder, the tau protein is mainly expressed in neurons. However, ARTAG describes a rare and unique astrocytic tauopathy in which neurons are unaffected (Kovacs *et al.*, 2016). At present, ARTAG is one of the less well-studied tauopathies, probably due to the absence of consensus regarding its diagnosis (Kovacs *et al.*, 2017a; Ferrer *et al.*, 2018). Therefore, much of the work in this area is still limited to histopathological descriptions of the disease. Despite studies on ARTAG being lacking in the literature, our observation that ARTAG-derived samples are seed-competent is consistent with that of (Ferrer *et al.*, 2018). In their study, Ferrer and colleagues injected sarkosyl-insoluble fractions from patients diagnosed with ARTAG into the brains of wild-type mice and found induced tau-related lesions not only in astrocytes but also in oligodendroglia and neurons. Taking this into account, we speculate that astrocytes may

play a key role in tau seeding and spreading, as they are able to retain seed-competent tau species that trigger tau pathology both *in vivo* and *in vitro*.

When we first transduced the Tau biosensor cell line with samples from various tauopathy patients, we noticed fluorescent inclusions adopting distinct shapes depending on the origin of the seed. To confirm this observation and to better examine the various morphologies, we transduced the Tau biosensor cell line with AD, GGT, AGD, or PiD samples and compared the resulting fluorescent inclusions to each other. Importantly, different patients with the same tauopathy resulted in almost identical formations, with one or two predominant morphologies, suggesting the formation of tau strains in the Tau biosensor cell line. These findings are consistent with those of (Kamath *et al.*, 2021), who discovered distinct fluorescent assemblies after transducing the Tau biosensor cell line with brain homogenates from either rTg4510 mice (i.e., a transgenic model of human tauopathy (Ramsden *et al.*, 2005)) or AD patients. The idea that tau forms *bona fide* strains has previously been examined *in vitro* (Guo & Lee, 2011; Sanders *et al.*, 2014; Kaufman *et al.*, 2017; Falcon *et al.*, 2018a; Sharma *et al.*, 2018) and *in vivo* (Sanders *et al.*, 2014; Kaufman *et al.*, 2016; Narasimhan *et al.*, 2017). Hence, our results suggest that the Tau biosensor cell line may be suitable for studying tau strains. However, it should be clear that the Tau biosensor cell line may bias the detection of strains, as has been reported for other cell lines (Sanders *et al.*, 2014; Sharma *et al.*, 2018). Hence, in the future, it would be interesting to further analyze the properties of these inclusions to confirm that they differ in other aspects than just their morphology (Sanders *et al.*, 2014; Nam & Choi, 2019) and whether they share some features with the exogenous seeds. Finally, it is difficult to comprehend how seed-competent tau from patients with the same tauopathy would consistently induce the formation of fluorescent inclusions with the same shapes if they were not the result of templated-aggregation (i.e., as (Kaniyappan *et al.*, 2020) defend).

Having observed that the formation of fluorescent inclusions was specific to seed-competent tau, we sought to prove that tau RD-CFP/YFP assembled into tau fluorescent aggregates with amyloid-like properties. For that purpose, we evaluated three fundamental features of amyloids: 1) detergent resistance, 2) fibril-like assemblies, and 3) self-seeding potency.

First, we escalated the Tau biosensor cell seeding assay to increase the number of fluorescent puncta in cells transduced with homogenates from P301S (+/-), P301S (-/-), or empty liposomes (i.e., vehicle condition). To determine whether the fluorescent inclusions had a biochemical correlate, we next performed detergent fractionation and

used biochemical analysis to determine whether tau was present in these fractions. We consistently observed that the TIF-P+ extraction displayed increased levels of detergent-resistant tau species that migrated to 43 kDa and were positive for anti-4R-tau and anti-GFP antibodies. It is worth mentioning that we also detected insoluble tau in the TIF-P- and TIF-V conditions, although to a much lesser extent. A possible explanation is that the Tau biosensor cell line spontaneously assembles tau RD-CFP/YFP fragments into "oligomers." Based on the finding that tubulin was only found in the TSF fractions and not in the TIF fractions, proving that our extraction protocol excludes soluble proteins, we argue that "oligomeric" species were formed, even in the absence of extracellular seed-competent tau. Notably, spontaneous formation of "oligomeric" species without aggregation has been reported in other cell lines (Khlistunova *et al.*, 2006; Chun & Johnson, 2007; Chun *et al.*, 2007; Tak *et al.*, 2013; Wegmann *et al.*, 2016; Holzer *et al.*, 2018; Lo *et al.*, 2019), suggesting that it may also happen in the Tau biosensor cell line. Regarding morphological differences, we observed fibril-like structures only in the TIF-P+ samples, whereas "amorphous" agglomerates were seen in the TIF-P- and TIF-V fractions. This last finding is in excellent agreement with the notion that small, insoluble "oligomeric" species are spontaneously formed in the Tau biosensor cell line. Nevertheless, future research to determine their existence would be needed.

We then sought to determine whether the TIF fractions contained seed-competent tau species. Notably, our previous results revealed the presence of insoluble tau in all TIF conditions. Additionally, these non-soluble tau species were assembled from RD-CFP/YFP fragments bearing the P301S mutation. Therefore, we were unsure if all TIFs would trigger the formation of fluorescent inclusions upon their transduction into the Tau biosensor cell line. We consistently found that it was only cells treated with TIF-P+ that displayed fluorescent puncta, as TIF-P- and TIF-V had no effect. We hypothesize that the small insoluble "oligomeric" assemblies observed in the TIF-P- and TIF-V fractions do not have the proper conformation to trigger the process of amyloid fibrillization since, for five independent extractions, they never induced detectable fluorescent inclusions. In parallel, we also suggest that the insoluble tau present in the TIF-P+ has a specific aggregation morphology, probably shaped by the initial seed (i.e., sarkosyl-insoluble P301S (+/-)-derived tau), which ensures the observed seeding potency. Finally, to the best of our knowledge, our study constitutes the first thorough analysis of the fluorescent inclusions formed in the Tau biosensor cell line. No previous publications exist that examine the nature of these "aggregates" directly derived from the cell line to validate its reliability.

Next, we decided to use an alternative approach in addition to the biochemical analysis to further validate the reliability of the Tau biosensor cell line. We hypothesized that co-transducing the Tau biosensor cell line with seed-competent tau and an inhibitor of tau seeded-aggregation would reduce the presence of fluorescent inclusions. To this end, we chose the peptide IN-M4, as it has been reported to inhibit the formation of tau aggregates induced by homogenates from AD, CTE, CBD, and PSP patients *in vitro* (Seidler *et al.*, 2019). Notably, although our ultimate purpose was to prove our hypothesis, we sought the opportunity to expand on the results of (Seidler *et al.*, 2019) by challenging the IN-M4 with previously untested samples. In an attempt to corroborate the inhibitory effect of the IN-M4 peptide, we opted to use seed-competent tau species that had not been tested in the original paper (Seidler *et al.*, 2019). Hence, we transduced the Tau biosensor cell line with TIF-P+, sarkosyl-insoluble fractions from P301S (+/-) mice, or one case of human GGT.

Our results show a dose-dependent inhibitory effect of IN-M4 on the aggregation induced by all tested samples, suggesting that seed-competent tau species from all three conditions have shared structural features recognized by the peptide. This observation adds to our hypothesis that the TIF-P+ fraction contains tau species that acquire amyloid-like properties similar to those of diseased brain-derived material. Hence, we suggest that the IN-M4 peptide reduces the number of tau aggregates because it directly inhibits the generation of tau RD-CFP/YFP amyloid fibrils. These findings support our hypothesis that the formation of fluorescent inclusions is a direct indicator of tau RD-CFP/YFP fragment assembly. However, it will be interesting to repeat these experiments using another inhibitor to corroborate our results. Finally, we find it difficult to explain why an inhibitor of tau aggregation would consistently reduce the presence of fluorescent puncta if the claims made by (Kaniyappan *et al.*, 2020) were valid.

It is worth mentioning that we have also developed an ImageJ/Fiji macro. Notably. This macro presents an alternative approach to flow cytometry analysis, used to quantify the amount of aggregated tau. Because our method does not require the experimental setup of flow cytometry experiments, it may be advantageous for other laboratories with limited access to this technology. Moreover, since the cells can be imaged in life, our approach also permits the evaluation of the same cell culture over the course of different days, allowing for a time-course assessment of the seeding process. We hope that our macro will help others with their research.

The inoculation of tau PFFs into P301S mice rapidly induces pathology within weeks (Iba *et al.*, 2013). Thus, we conducted a preliminary evaluation of TIF-P+ seeding

potency *in vivo*, to test whether the tau present in that fraction formed in cell culture would have similar effects. For that purpose, we injected the TIF-P+ fraction into the hippocampus of 3-month-old P301S (+/-) and P301S (-/-) mice. Three months after the inoculation, we detected the presence of pathological tau (i.e., AT8-positive inclusions) in the P301S (+/-) but not in the P301S (-/-) animals. Noteworthy, the AT8 antibody recognizes “pathologically” phosphorylated residues located in the proline-rich domain of the tau protein (i.e., Ser202 and Thr205). However, the TIF-P+ fraction only contains tau RD-CFP/YFP fragments, which lack the proline-rich domain recognized by the AT8 antibody. Consequently, the observed AT8-positive lesions must be the result of endogenous murine tau being recruited by the seed-competent tau present in the TIF-P+ sample. In addition, since we found AT8-positive labeling in distant but anatomically connected areas to the injection site, TIF-P+ may induce not only seeding but also the spreading of tau pathology (Clavaguera *et al.*, 2009; Iba *et al.*, 2013). Together, our results suggest that the TIF-P+ fraction induces tau pathology *in vivo*, which agrees with our previous *in vitro* findings.

Our findings are in line with previous studies in which the authors inoculated cell lysates from another cellular model of tau aggregation in P301S mice (Sanders *et al.*, 2014). Notably, similar to our observations, Sanders and colleagues found tau aggregates in P301S mice, but not in wild-type inoculated animals. There are multiple potential explanations for these results. For instance, it is possible that the inoculation of TIF-P+ requires more than 3 months to initiate tau pathology. Another possibility is related to the notion that brain-derived tau aggregates have proven to be ten times more seeding potency than their equivalent aggregates generated *in vitro* (Falcon *et al.*, 2015). As a result, while TIF-P+ are not fibrillated *in vitro* (i.e., cell-free environment), it is likely that their ability to initiate tau pathology *in vivo* is compromised because they do not resemble brain-derived material (Fichou *et al.*, 2018; Sharma *et al.*, 2018; Zhang *et al.*, 2019). Finally, it is also possible that wild-type mice never developed pathology because of a seeding barrier between inoculated tau RD and wild-type murine tau (Nizynski *et al.*, 2018).

The most obvious shortcoming of our *in vivo* preliminary study is that we did not inject TIF-P- nor TIF-V due to limitations in the number of animals available for injection. Although these two samples were unable to induce further tau aggregation in the Tau biosensor cell line, we cannot exclude the possibility that they may have had the opposite effect *in vivo*. Therefore, prospective studies are needed to confirm our results.

In conclusion, we believe that the results reported by Kaniyappan and colleagues (Kaniyappan *et al.*, 2020) were biased, probably because they used different constructs than the ones expressed by the Tau biosensor cell line and also because their experiments were conducted in a cell-free environment, which does not recapitulate the physiological milieu of the cell. Our findings undermine the importance of addressing this and similar issues in cell-based assays (e.g., see (Harrington *et al.*, 2015)). Having said that, we have demonstrated that fluorescent aggregates derived from the Tau biosensor cell line display amyloid-like properties. Hence, we propose that our protocol for extracting the TIF-P+ fractions could be adapted by others to serve as a source for readily obtaining seed-competent tau species. Taken together, we believe we have provided enough evidence to prove that the fluorescent puncta observed in the Tau biosensor cell line are newly formed tau RD-CFP/YFP aggregates, rather than the result of non-related, unspecific events promoting these fragments to be close enough to produce a strong fluorescent signal. Therefore, the Tau biosensor cell line is a reliable model for evaluating the presence of seed-competent species in biological samples.

Chapter 2: The Impact of Extracellular Seed-Competent Tau on Neuronal Activity

4.1 Introduction

Neuronal networks are known to be altered in patients with AD, and neuronal hyperexcitability occurs early in the disease's pathogenesis (Dickerson *et al.*, 2005; Olazaran *et al.*, 2010). Although the underlying source of AD-related neuronal hyperexcitability is unknown, similar phenotypes have been reported in AD transgenic rodent models characterized by increased expression of amyloid beta (Busche *et al.*, 2008; Busche *et al.*, 2012; Siskova *et al.*, 2014). More recently, transgenic models of tau pathology have also been confirmed to have altered neural activity (Hall *et al.*, 2015; Busche *et al.*, 2019). In parallel, most researchers now accept that neural activity regulates the levels of extracellular tau both *in vitro* (Wu *et al.*, 2016) and *in vivo* (Yamada *et al.*, 2014) and increases tau pathology *in vivo* (Wu *et al.*, 2016). Because accumulating evidence suggests that tau exhibits prion-like features and that tau pathology spreads through synaptically connected neurons, tau itself has been proposed to affect the brain circuitry (Seeley *et al.*, 2009; Goedert *et al.*, 2010; Raj *et al.*, 2012; Guo & Lee, 2014). Nevertheless, the influence of extracellular seed-competent tau on neural activity has received limited attention in the literature, with a few exceptions (Gomez-Ramos *et al.*, 2006; Gomez-Ramos *et al.*, 2008; Stancu *et al.*, 2015; Decker *et al.*, 2016; Sohn *et al.*, 2019; McCarthy *et al.*, 2021). It is worth noting that these studies are mostly conducted with models characterized by the over-expression of mutated tau variants. Therefore, they do not represent most human tauopathies since they are sporadic in nature. In parallel, given the complexity associated with the data analysis of neuronal network activity (e.g., time-consuming and computation skills), this issue is rarely discussed in contrast to tau-related topics. Consequently, the impact of "pathogenic" tau on neuronal activity requires further investigation.

4.2 Objective

In this chapter, we aim to study the impact of extracellular seed-competent tau on the neural activity of wild-type primary cortical cultures by establishing a microfluidic platform suitable for calcium imaging and morphological analyses.

4.3 Materials and Methods

4.3.1 Ethical Statement

All animals were kept in the animal facility of the Faculty of Pharmacy at the University of Barcelona under controlled environmental conditions and were provided with food and

drink *ad libitum*. Animal care and experimental protocols were performed in compliance with the CEEA of the University of Barcelona. All housing, breeding, and procedures were performed under the guidelines and protocols OB47/19, C-007, 276/16, and 47/20 of CEEA.

4.3.2 Design and Fabrication of Microfluidic Devices

Our methodology included poly(dimethylsiloxane) (PDMS) microfluidic devices because they offer numerous advantages for calcium imaging, such as minimal autofluorescence and neuronal compartmentalization (Wu *et al.*, 2016; Hallinan *et al.*, 2019; Katsikoudi *et al.*, 2020). Based on previously available layouts (Deleglise *et al.*, 2013), we used CAD software to update and customize the design of a three-chambered microfluidic device for our experimental needs (Sala-Jarque *et al.*, 2020). The resulting chrome masks were fabricated at the Microfabspace of the Institute for Bioengineering of Catalonia (IBEC). The microfluidic device included four 8-mm-diameter circular reservoirs interconnected in pairs by two cell seeding chambers. These two chambers were: the cell body or soma compartment and the axonal or distal chamber, which were interconnected by 100 microchannels of 100 µm (high) x 10 µm (wide) section and were 900 µm long. The microchannels were intersected perpendicularly by a third channel with two ports of 1.25 mm diameter each. This third channel was a perpendicular reservoir consisting of a 100 µm (high) x 100 µm (wide) section and was 12,000 µm long. A SU8 mold was used to fabricate the devices, which were made using standard photolithography and soft lithography techniques of PDMS (Dow Corning). PDMS, mixed at a 10:1 (w/w) base/curing agent ratio, was poured onto the mold and cured at 60°C for at least 4 h. The devices were then cut off from the mold and trimmed to the appropriate size. The ports were then formed with 1.25 mm and 7 mm diameter biopsy punches. Next, the devices were permanently bound to glass by oxygen plasma treatment. For calcium recording experiments, PDMS was bound to Nunc™ Glass Bottom 35 mm Dishes (ThermoFischer Scientific). Once ready, the microfluidic chips were sterilized by placing them under UV light inside the culture hood for 1 h.

4.3.3 Tau Biosensor Cell Line Culture and Seeding for Sequential TIF Extraction

Please see Chapter 1, Materials and Methods, Section 3.3.11.3.

4.3.4 Primary Cortical Cultures

Primary cortical neurons were prepared from embryonic day (E) 16.5 embryos of wild-type CD1 mice (Charles River Laboratories, France). In brief, brains were dissected

in ice-cold sterile 0.1 M PBS containing 6.5 mg/mL glucose (Merck Millipore); cerebral cortices were isolated, and meninges were removed. Afterward, we transferred the cortices into trypsin and digested them for 15 min at 37°C with gentle inversion every 3 min. After adding NHS (ThermoFischer Scientific) and centrifugation, cells were mechanically dissociated in sterile 0.1 M PBS containing 0.025% DNAse (Roche). For their culture, cells were plated onto the cell body compartment of poly-D-lysine (0.1 mg/mL) -coated microfluidic devices at a density of 170,000 cells/device by pipetting 10 µL of cellular suspension in plating medium [Neurobasal medium (ThermoFischer Scientific) supplemented with 5% NHS, 6.5 mg/mL glucose, $NaHCO_3$ (Merck Millipore), 1X B27 (ThermoFischer Scientific), 1% GlutaMax (Gibco), and 1% penicillin/streptomycin (ThermoFischer Scientific)]. The plated devices were kept at 37°C in a 5% CO_2 atmosphere for 30 min until the cells had adhered to the plates. To enhance the microfluidic isolation between reservoirs and prevent passive diffusion of subsequent treatments, 260 µL of plating medium was added to the soma compartment, whereas only 140 µL was placed into the axonal compartment. After 1 day *in vitro* (DIV), the plating medium was replaced with culture medium [Neurobasal medium (ThermoFischer Scientific) supplemented with 6.5 mg/mL glucose, $NaHCO_3$ (Merck Millipore), 1X B27 (ThermoFischer Scientific), 1% GlutaMax (Gibco), and 1% penicillin/streptomycin (ThermoFischer Scientific)]. The culture medium was changed every 2 to 3 days until the end of the experiment.

4.3.5 Viral Transduction

Viral transduction of neural cultures with a genetically encoded calcium indicator (GECI) was done at 1 DIV by the administration of an adeno-associated virus (AAV) carrying the gene of interest under the neuron-specific promoter synapsin (Syn). Specifically, we transduced RCaMP (AAV9.Syn.NES-jRCaMP1b.WPRE.SV40, 2 x 10^7 particles; Addgene). After 72 h, viral transduction was stopped by changing the culture medium.

4.3.6 Tau Treatment

Neural cultures in microfluidic devices were treated with TIF-P+ or TIF-P- fractions at 6 DIV. First, we aspirated the medium of both compartments and added 260 µL of freshly prepared maintenance medium to the cell body compartment. Next, we treated the axonal chamber with medium alone (i.e., untreated control) or TIF-P+ or TIF-P- fractions at a final concentration of 0.1 µg/µL in a final volume of 140 µL. Importantly, subsequent medium changes were done in the cell body chamber to avoid removing TIF treatments

from the axonal compartment. Of note, calcium imaging was performed at 5, 8, 12, and 14 DIV, corresponding to days with no medium change.

4.3.7 Electrical Stimulation

For electrical stimulation, platinum electrodes were placed in the 8-mm-diameter circular reservoirs of the microfluidic device on each side of the cell body chamber. Neural cell cultures were stimulated by applying an electrical field using the electric stimulator A-M Systems 2100 model (A-M Systems, United States of America). Biphasic square waveform electric pulses of ± 2.5 V were applied at a frequency of 10 Hz with a pulse duration of 50 s.

4.3.8 Calcium Imaging and Recoding Setup

For the calcium imaging setup, we used an inverted Olympus IX71 inverted fluorescence microscope (Olympus) equipped with a sensitive, high-speed camera (Hamamatsu ORCA Flash 4.0), an LED light source (CoolLED's pE-300^{white}, Delta Optics, Spain), and a customized plate incubator from OKO Lab (Izasa, Spain). The incubator kept the cell plates at 37°C and 5% CO_2 during the recordings. Images of 16-bits were acquired using the camera software Olympus cellSens^{TM} (Olympus Corporation; https://www.olympus-lifescience.com/en/software/cellsens/) at 10 frames per second (fps) with a 50 ms exposure for 1 min to 5 min based on the type of experiment. The image size was 512 x 512 pixels, utilizing a 4x objective. The videos were stored as ".btf" files for further processing.

4.3.9 Calcium Image Analysis

Calcium image analysis was performed using the NETCAL software (Orlandi *et al.*, 2014) (www.itsnetcal.com). NETCAL is a MATLAB-built, comprehensive framework for large-scale calcium imaging data analysis. Once the analysis was finished, we further processed the data with a custom-made package kindly provided by Dr. Jordi Soriano (University of Barcelona). Prior to calcium analysis, we uploaded the videos to ImageJ/Fiji (Schindelin *et al.*, 2012) as ".btf" files, cropped to a final size of 228 x 509 pixels (i.e., corresponding to the cell body compartment), and saved as ".avi" files. The cropped videos were individually uploaded to NETCAL and preprocessed to obtain the "Average trace" and "Average image."

4.3.9.1 Region of Interest Detection

Using NETCAL, we generated a grid of 100 rows x 100 columns covering the entire image to identify the regions of interest (ROIs).

4.3.9.2 Neuronal Activity Analysis

The set of raw fluorescence traces was computed by averaging the intensity pixels for each ROI for the entire recording. Afterwards, each trace was normalized (i.e., smoothed) and adjusted for global drifts and artifacts. To achieve this, the data were normalized to DFF_i (%) ≡ 100 x (F_i (t) - $F_{i,0}$) / ($F_{i,0}$) where $F_{i,0}$ is the average fluorescence of each ROI at rest.

4.3.9.3 Spike Identification

The normalized fluorescence signal was then used to determine the onset times of activation (i.e., spikes). We used the Schmitt Trigger algorithm to infer the timing of neuronal activation. Briefly, the Schmitt Trigger method identifies the existence of spikes when the fluorescence signal of a given ROI rises above an upper threshold and does not fall below a lower threshold for a pre-set minimum duration. For our videos, we determined ten as the upper threshold value and five as the lower threshold value. As a result, the program generated a raster file that plotted all spike events for each ROI over the length of the video. The detected spikes were then shown as raster plots of neuronal activity over time.

4.3.9.4 Averaged Neuronal Activity

The average neuronal activity was estimated by measuring the number of spikes per neuron per minute. Notably, neurons exhibiting at least 5 spikes throughout the recording were considered active.

4.3.9.5 Global Neuronal Network Activity Analysis

Network bursts are neuronal activations that occur at short time intervals, indicating the existence of coordinated neural activity. Thus, the network burst is also an indicator of network synchrony. We quantified the network bursts per minute by computing the signal of all spikes (i.e., from the previously acquired raster plots of neuronal activity) within time intervals smaller than 1 s, divided by the recording duration. We also computed the inter-burst interval (IBI) as the average time between consecutive network

bursts. Importantly, we filtered the data by establishing a threshold so that only bursts involving 10% of the network, or more, were considered for analysis.

4.3.10 Immunocytochemistry

For immunofluorescence staining, cells in the microfluidic devices were fixed in 4% PFA for 15 min at room temperature. Afterward, cells were washed three times with 0.1 M PBS. The cells were then permeabilized and blocked with 0.1 M PBS, 5% normal goat serum (NGS), and 0.1% Triton X-100 for 1 h at room temperature on a shaker with low speed. After blocking, cells were incubated with primary antibodies diluted in antibody solution [1% NGS and 0.1% Triton X-100 in 0.1 M PBS] overnight at 4°C with gentle agitation. The following antibodies were used for immunostaining: mouse anti-MAP2 (1:200) (Sigma, catalog no. M1406) and mouse anti-TUJ1 (neuron-specific class III β-tubulin) (1:500) (BioLegend, catalog no. 801201). The following day, cells were rinsed with 0.1 M PBS five times before adding the secondary antibody Alexa Fluor 568 (Life Technologies) diluted in antibody solution (1:500) for 2 h in the dark. Next, cells were washed thrice with 0.1 M PBS, and nuclei were stained with 1 µg/mL Hoechst 33342 (Invitrogen) prepared in 0.1 M PBS for 10 min at room temperature. Cells were washed three additional times with 0.1 M PBS. Finally, 300 µL of 0.02% azide diluted in 0.1 M PBS was added to each chamber. The devices were kept at 4°C until imaging.

4.3.11 Statistical Analysis

Quantitative data were analyzed using one-way ANOVA, followed by Tukey's *post hoc* test was used for comparisons between several independent groups. Statistical significance was set at $p < 0.05$. The data are expressed as means ± SD. GraphPad Prism 8 (version 8.02; GraphPad software Inc., California, United States of America) was used to perform statistical tests and produce graphs. For all statistical analysis in this chapter: *$p < 0.05$, **$p < 0.01$; ***$p < 0.001$, ****$p < 0.0001$.

4.4 Results

4.4.1 Characterization of Primary Cortical Cultures Plated in Microfluidic Devices

4.4.1.1 Time-Course Analysis: Evolution of Primary Cortical Cultures in Microfluidic Devices

For our experimental setup, primary cortical cultures were plated in our three-chambered PDMS microfluidic devices (Figure 20A) (Sala-Jarque *et al.*, 2020). We

conducted daily visual examinations of the devices to study the evolution of neural cells. After 6 DIV, most axons had reached the distal compartment, a sign of mature morphology, and neurons displayed an overall healthy appearance (Figures 20B, C, and D). Surprisingly, after 16 DIV, we observed a rapid decline in neuronal health, specifically in the axonal terminals (data not shown). Immunocytochemical analysis of the axonal marker TUJ1 confirmed mild degeneration of neuronal processes (data not shown). Moreover, at 21 DIV, we noted a substantial increase in pycnotic nuclei and some cytoplasmatic debris, implying a decrease in cell viability (data not shown). Because further efforts to improve neural survival were unsuccessful, we decided that future tau treatments should begin at 6 DIV and last up to 14 DIV (i.e., the maximum time point at which most neurons appear healthy).

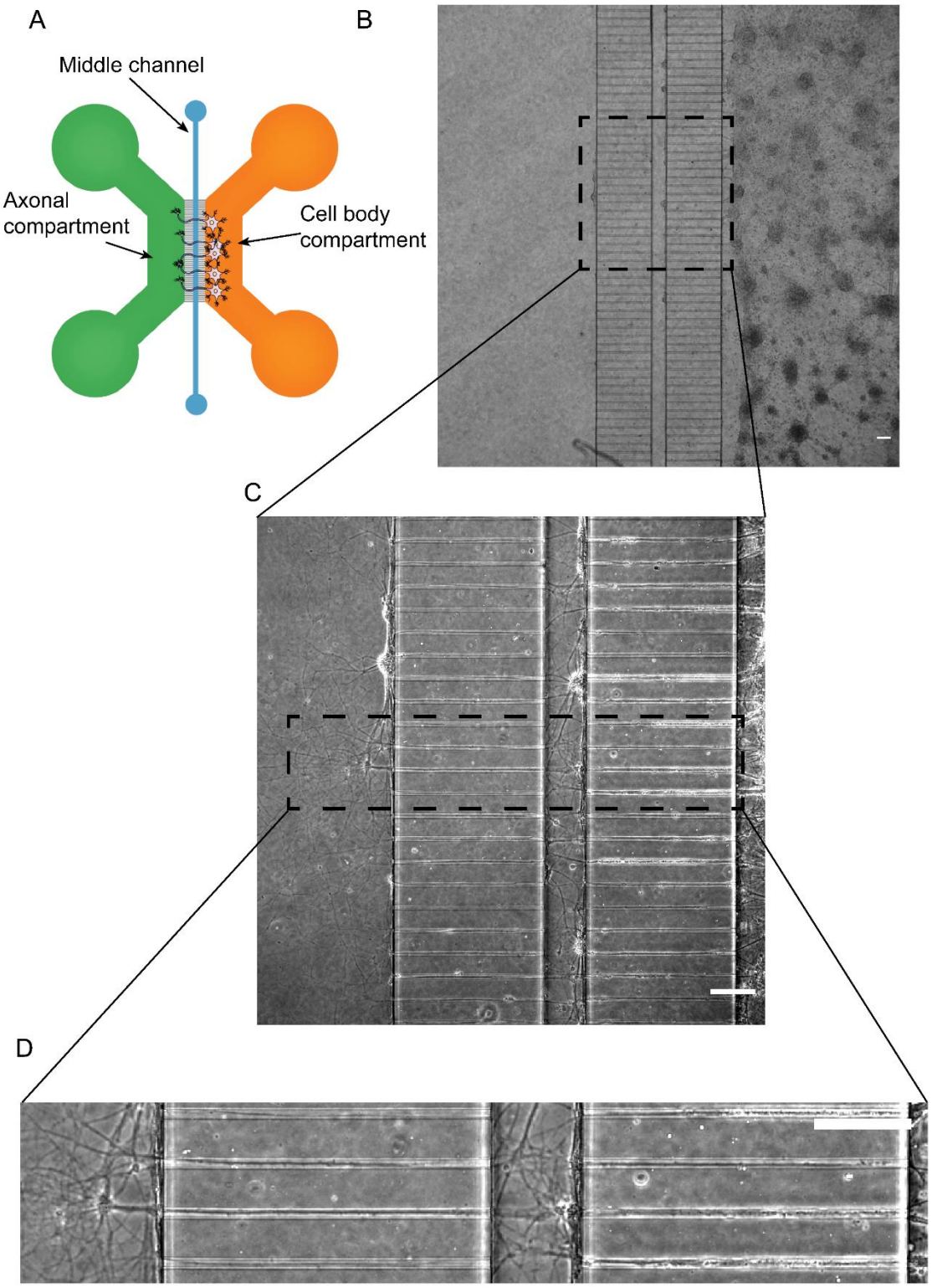

Figure 20 Primary cortical cell cultures grow in microfluidic devices: A) Schematic diagram of primary neurons cultured in three-chambered microfluidic devices. Cells are seeded in the cell body compartment, from where axons grow through the microchannels, first reaching the middle chamber and finally the axonal compartment. This specific design allows for microfluidic isolation between reservoirs. **B-D)** Representative bright-field images of primary neural cell culture, showing the typical appearance at 6 days *in vitro* (DIV). Insets show magnifications of the area indicated in the main image. Note that only axons are allowed to grow from the soma compartment to the distal chamber. Scale bars, 100 µm.

4.4.1.2 Expression of Neuronal Markers in Primary Cortical Cultures Plated in Microfluidic Devices

Because we decided to initiate tau treatments at 6 DIV, we first wanted to verify that, by that time, cultured cells already displayed typical features expected in mature neurons. Therefore, by immunocytochemistry, we analyzed the presence of TUJ1 and MAP2, which are axonal- and dendritic-specific markers, respectively. Importantly, all devices stained positive for TUJ1 (Figure 21A) and MAP2 (Figure 21B) at 6 DIV, indicating proper maturation of the primary cortical neurons.

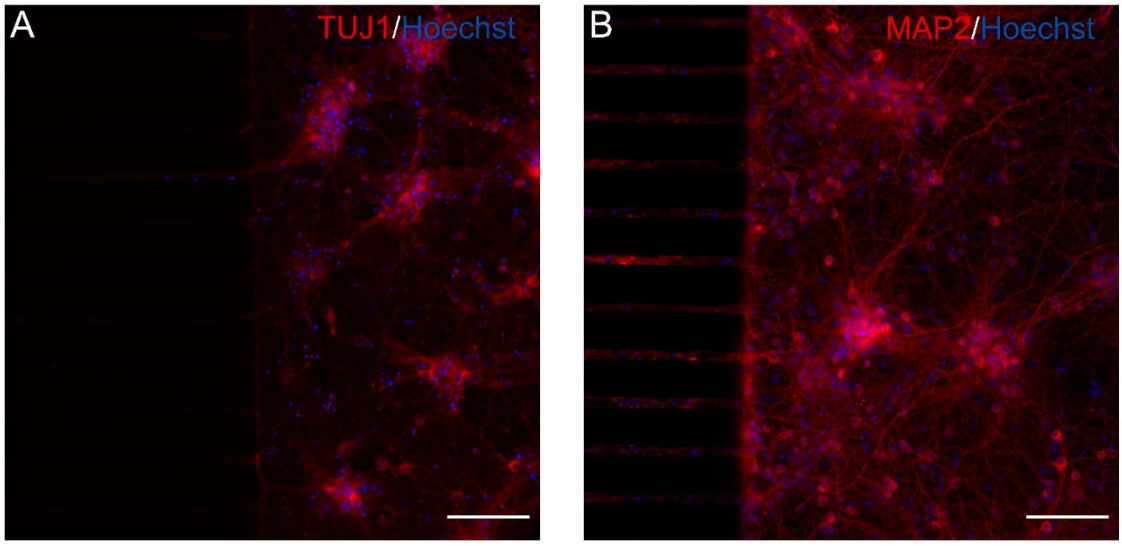

Figure 21 Primary neural cell cultures express neuronal maturity markers after 6 days *in vitro* (DIV) within microfluidic devices: At 6 DIV, cells were fixed and immunolabeled for neuronal maturity markers. Nuclear staining was performed using Hoechst (blue). **A)** A representative image showing TUJ1-positive neurons (red). **B)** A representative image of neurons expressing MAP2 (red). Scale bars, 100 µm.

4.4.2 Calcium Imaging: Primary Neurons in Microfluidic Devices Are Functionally Active and Electrically Modulable

To fully understand this section, it is necessary to clarify that we opted for calcium imaging to analyze changes in spontaneous neural activity in our microfluidic devices in a time-course experiment. First, regarding calcium imaging, mature neurons display considerably low intracellular calcium concentrations (i.e., 100 nM), which rise by two orders of magnitude upon firing (Berridge *et al.*, 2000). Consequently, calcium-binding fluorescent molecules have been adapted to track calcium currents during neuronal activation, since imaging systems can detect them through sudden spikes in fluorescence signals, which can be recorded and analyzed. Calcium indicators can be classified into two major categories: chemical probes (e.g., Fura-2 AM) and GECIs (e.g., GCaMP or RCaMP). The former is not suitable for long-term imaging, whereas the latter

is characterized by its steady expression for weeks. Notably, because GECIs are proteins not naturally expressed by neurons, they must be encoded into DNA vectors and introduced into cells for expression. Since neural cells cannot tolerate transfection reagents well enough, viral gene transfer is usually preferred. For these reasons, viral transduction of GECI was our tool of choice. It is worth mentioning that although there exist multiple GECIs, the most effective are single-wavelength green indicators that use the original GCaMP sensor (Nakai *et al.*, 2001), whose constituent molecules are calmodulin and GFP. However, because GFP is a typical marker in most rodent models of human tauopathies and is commonly employed to label fluorescently recombinant tau, GCaMP is considered to be an incompatible choice. Thus, our preference for using RCaMP (Akerboom *et al.*, 2013), a red, single-wavelength GECI, appears to be a reasonable choice regarding future applications.

Turning now to time-course experiments, in general, previous *in vitro* research has typically only investigated changes in neuronal activity at a single time point, often following the addition of tau treatment. In the present work, we aimed at rectifying this by examining the time-course evolution of neural activity resulting from the presence of extracellular seed-competent tau.

Having said this, we first needed to address whether we could detect spontaneous neural activity in neural cell cultures expressing RCaMP within our microfluidic devices. Primary neurons were transduced with viral vectors expressing RCaMP at 1 DIV. Figure 22A shows representative fluorescence traces of spontaneous activity from one microfluidic device at 6 DIV, which was sustained at least until 14 DIV. Next, we sought to demonstrate that our system was responsive to external inputs, which translated into measurable variations in the emitted fluorescence. Hence, we electrically stimulated (i.e., 10 Hz, ± 2.5 V, for 50 s) five independent devices, consistently resulting in a stable peak calcium transient in response to the electrical stimulus (Figure 22B). Together, these data indicate that primary neural cell cultures in our microfluidic devices at 6 DIV are functionally active, viable, and sufficiently mature for studying parameters related to neuronal network activity.

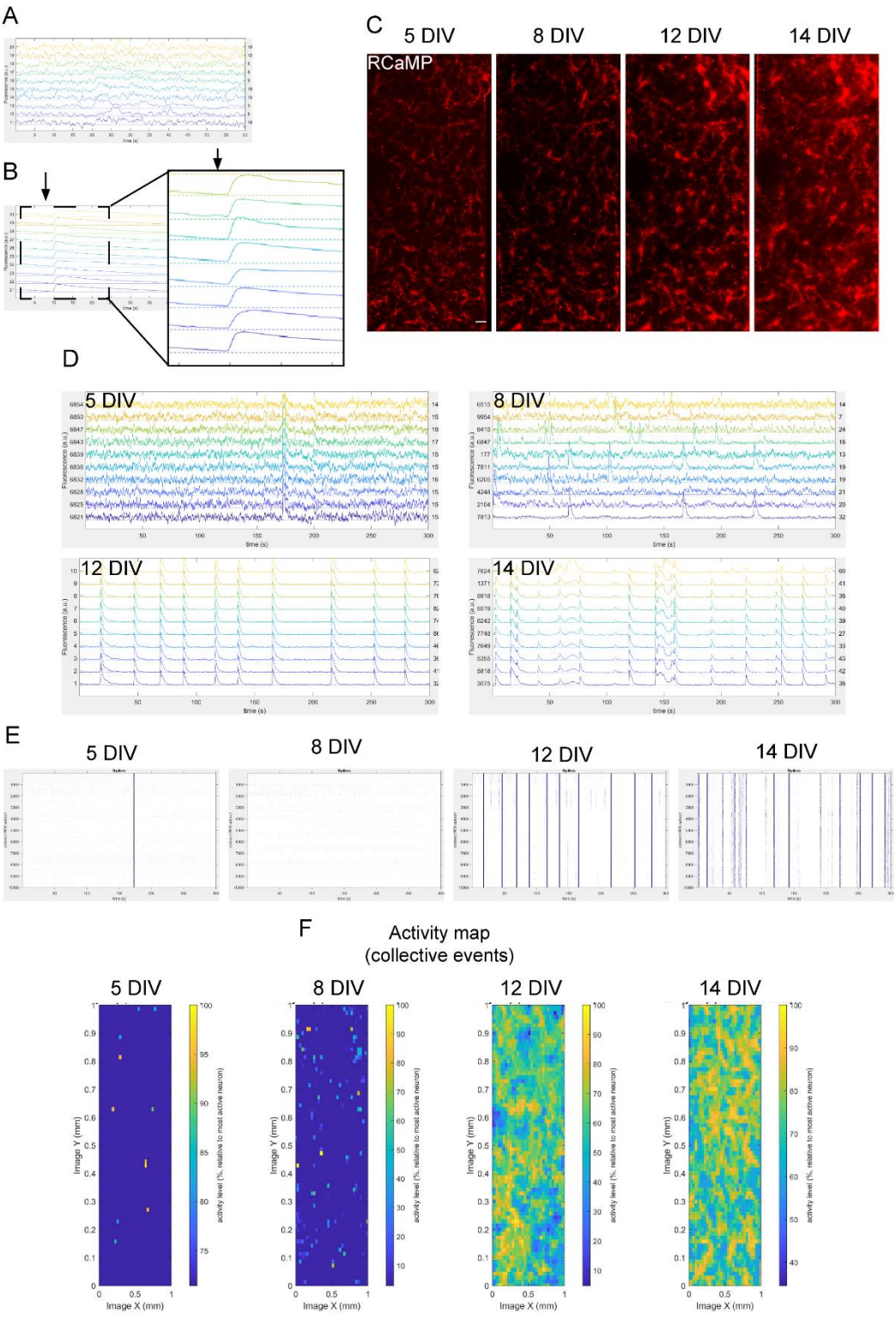

Figure 22 Microfluidic devices and RCaMP expression are both suitable tools for studying neuronal activity: A) Representative spontaneous calcium transients from primary neurons at 6 days *in vitro* (DIV). **B)** Electrical stimulation of one microfluidic device (10 Hz, ± 2.5 V, for 50 s - black arrow indicates the time of the stimulus addition) at 6 DIV. Calcium fluorescence increases when electrical stimulation is applied.

Figure 22 continued on next the page

Figure 22 continued

C-F) Representative data obtained from the same microfluidic device recorded along 14 DIV to evaluate the progression of neural activity. Selected time points are 5, 8, 12, and 14 DIV. **C)** Fluorescence microscopy images showing the expression of RCaMP (red) on different days. Scale bar, 100 µm. **D)** Representative fluorescence traces at different DIV. Each panel displays the calcium transients of ten regions of interest (ROIs). Normalized data are represented as fluorescence in arbitrary units (a.u). **E)** Temporal raster plots of spikes detected for every ROI of the previous fluorescence traces were analyzed to determine the onset of neuronal activations using the Schmitt Trigger algorithm. Blue dots are neuronal activations. **F)** Activity maps depicting collective events at the specified time points. Activity levels are represented as a percentage relative to the most active neuron. Blue represents the lowest activity level, and yellow the highest.

To verify the healthy maturation of primary neural cell cultures in our microfluidic devices, we examined how neuronal activity developed at 5, 8, 12, and 14 DIV. For the purpose of clarity, we present the data collected from a single microfluidic device. However, equivalent results were obtained for eight independent devices. Having said that, we first sought to determine whether RCaMP fluorescence intensity levels changed over time (Figure 22C). Consequently, we established that the most appropriate time window for signal analysis was between 12 DIV and 14 DIV since they featured comparable fluorescence intensity levels.

Next, we monitored changes in fluorescence intensity levels at 5, 8, 12, and 14 DIV. Figure 22D shows representative fluorescence traces of the same microfluidic device over 14 DIV. For clarification, fluorescence traces of firing neurons exhibit fast onsets, followed by either slow or fast decay, depending on the type of activation. The first occurrence of calcium transients was observed at 5 DIV, in which only a few simultaneous co-activation events were detected. This activity pattern is typical of young and immature neural connections, as has previously been reported (Chiappalone *et al.*, 2006; Pasquale *et al.*, 2008; Soriano *et al.*, 2008). As the cell culture matured, the number of simultaneous events increased, indicating increasing levels of neuronal synchronization that culminated in almost fully synchronous activations by 14 DIV. Together, our findings show that primary neurons, plated in our microfluidic devices, display the patterns of activity maturation expected from a healthy neural cell culture (Tibau *et al.*, 2013).

We then computed the fluorescence traces using the Schmitt Trigger algorithm to generate a spike profile for each ROI, represented as raster plots in Figure 22E, illustrating the global network dynamics of the primary cortical cultures. As a reminder,

bursts are episodes of collective neuronal activation in which neurons fire synchronously for short periods of time. Although we were not quantitatively evaluating these collective events, from Figure 22E, we can see an increasing number of neurons spiking in synchronization over time (i.e., probably in bursts). Together, these results corroborate our previous observations of calcium traces, which also showed an increase in synchronization events over the course of time.

Finally, we performed a preliminary analysis to examine whether the increased synchronization represented collective events that occurred in isolated groups of neurons or involved a substantial proportion of cells. Figure 22F shows the corresponding activity maps for each day. To understand the data, it is necessary to clarify that the activity map represents the number of times each ROI has fired. Initially, the number of regions with detectable calcium activity was low and dispersed throughout the whole recorded region. However, the number of active areas increased in a time-dependent manner. These findings suggest that at 12 DIV, most neurons show strong firing activity compared with earlier time periods. Therefore, we conclude that the synchronicity observed in the fluorescence traces and raster plots resulted from collective activations rather than just a tiny fraction of highly synchronized spiking neurons.

4.4.3 Seed-Competent Tau Has No Effects on Spontaneous and Bursting Neuronal Activity in Primary Cortical Cultures

Having characterized some relevant features of our model, we wanted to investigate the potential effects of extracellular seed-competent tau on neural network function in terms of spontaneous neural activity and bursting events in primary cortical neurons. At 6 DIV, cell cultures were either left untreated or treated with 0.1 µg/µL of either TIF-P+ or TIF-P- in the axonal compartment. Of note, before being used for treatment, the presence of seed-competent tau species in the TIF-P+ fraction and their absence in the TIF-P- fraction was evaluated by transducing both fractions into the Tau biosensor cell line using Lipofectamine-2000^{TM} (data not shown). We then monitored spontaneous activity in n = 8 to 10 independent microfluidic devices for each condition at 5, 8, 12, and 14 DIV (Figure 23).

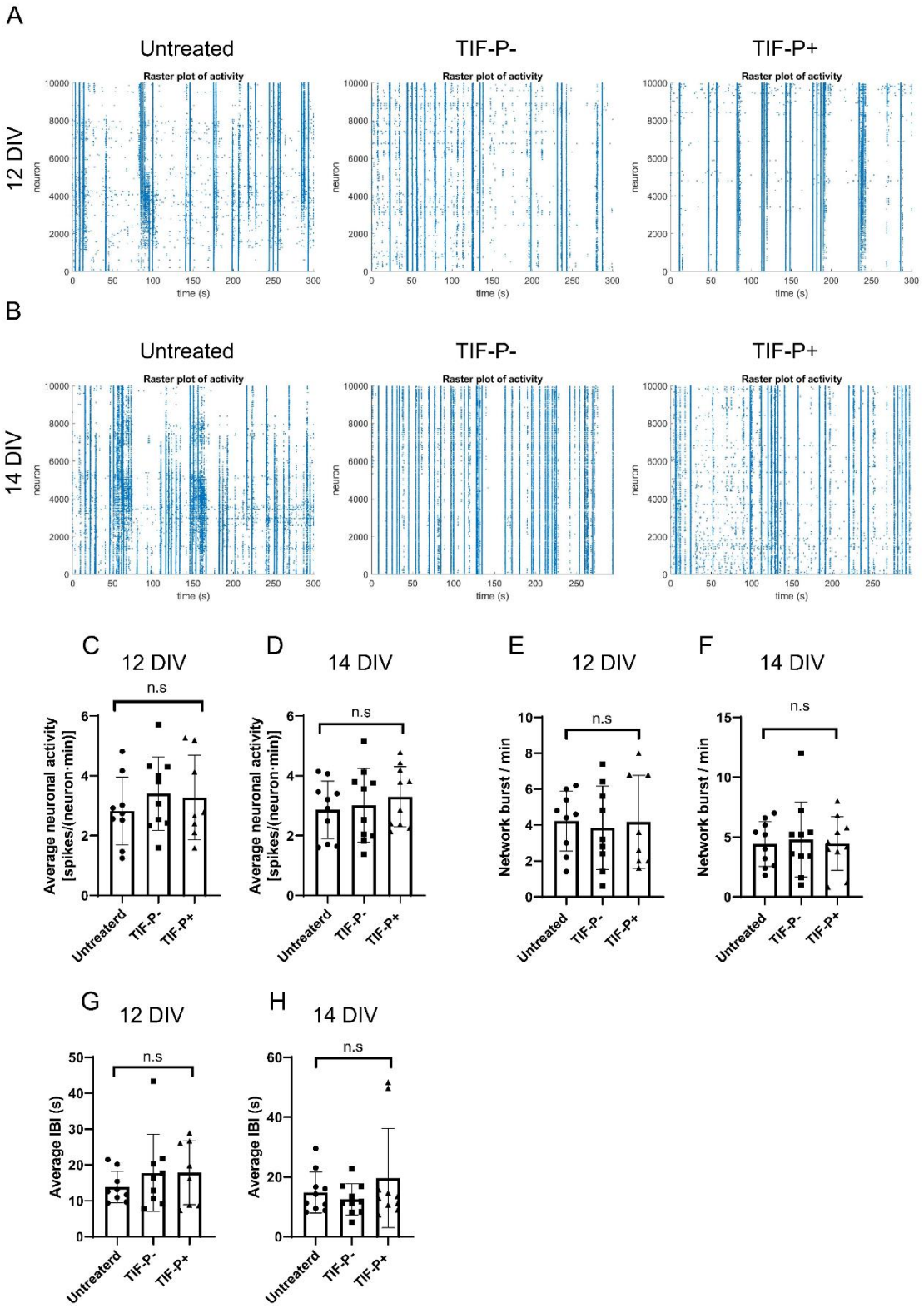

Figure 23 Extracellular seed-competent tau does not alter the neuronal activity network: A-B) Representative raster blots of spontaneous neuronal networks at 12 days *in vitro* (DIV) and 14 DIV of primary neural cell cultures left untreated or treated with either TIF-P- or TIF-P+. Blue dots are neuronal activations. **C-H)** Analysis of n = 8 to 10 independent devices (i.e., from at least three different litters) at 12 DIV and 14 DIV was used to compare differences in global network characteristics between primary cortical cultures left untreated or treated with TIF-P- or TIF-P+ along 5 min recording. *Figure 23 continued on the*

Figure 23 continued

C-D) The average number of spikes per neuron per min. No differences are observed. Each dot represents an individual microfluidic device. Statistical significance was calculated by one-way ANOVA with Tukey's *post hoc* test. Abbreviation n.s stands for not significant ($p > 0.05$). **E-F)** Average bursting rate. No differences are observed. Each dot represents an individual microfluidic device. Statistical significance was calculated by one-way ANOVA with Tukey's *post hoc* test. Abbreviation n.s stands for not significant ($p > 0.05$). **G-H)** Average inter-burst interval (IBI), defined as the timing between consecutive episodes. No differences are observed. Each dot represents an individual microfluidic device. Statistical significance was calculated by one-way ANOVA with Tukey's *post hoc* test. Abbreviation n.s stands for not significant ($p > 0.05$).

To characterize and compare major network features, we quantitatively addressed four parameters: average network activity, average burst/min, and average IBI. However, we have only been able to evaluate the recordings from 12 DIV and 14 DIV due to the incredibly time-consuming nature of the data analysis. Importantly, we decided to analyze these two specific time points, mainly because: 1) Our previous findings showed that, at 12 DIV, primary cortical cultures exhibited mature (i.e., synchronous) neural activity, more closely resembling those from the adult brain. 2) We were interested in exploring long-term rather than punctual alterations of the network. In other words, we were not looking for activity changes that may have occurred at earlier time points (e.g., 5 DIV) but were endogenously resolved by the cell culture becoming undetectable at later time points (e.g., 14 DIV).

Figures 23A and B show representative raster plots of activity for each condition at 12 DIV (i.e., 6 days of treatment) and 14 DIV (i.e., 8 days of treatment). First, we estimated the average neural activity to infer the degree of spontaneous activity of our microfluidic devices. Surprisingly, devices treated with TIF-P+ did not display significant differences in mean neural activity compared with the TIF-P- and untreated conditions (Figures 23C and D), suggesting that even in the presence of seed-competent tau, neurons remain electrically functional. Next, we quantified the average network bursts per minute (i.e., average network activity). Importantly, when analyzing spontaneous activity, the number of random activations is relatively frequent. Consequently, raster plots of neural activity need to be filtered to operate exclusively with coordinated events. Here, we thresholded the size of coherent network activations to be within a time window of 1 s. When at least 10% of the network participated in a coordinated activity episode, we considered it to be a network burst. No significant differences between the three groups were evident at either 12 DIV or 14 DIV (Figures 23E and F). Finally, we analyzed the IBI network, defined as the average time between consecutive network bursts, whose

value describes the temporal structure of the activity events. Again, we did not detect statistically significant differences between treatments at either 12 DIV or 14 DIV (Figures 23G and H). Together, our findings show that, at least in our model and at these time points, the presence of extracellular seed-competent tau does not significantly affect the neuronal network activity of wild-type primary neurons.

4.5 Discussion

This chapter aimed to develop a suitable platform for examining changes in neuronal activity in response to extracellular seed-competent tau. We opted to employ three-chambered microfluidic devices to compartmentalize cell cultures and treat each reservoir independently. In the past, others in the field have successfully employed microfluidic devices to address tau spreading in primary neurons (Wu *et al.*, 2013; Calafate *et al.*, 2015; Wu *et al.*, 2016). Here, we used primary neural cell cultures from wild-type mice, as they are more relevant to the study of sporadic tauopathies, and demonstrated that they grow within our microfluidic devices, displaying typical markers of mature neurons as early as 6 DIV. Moreover, our findings indicate that the viral transduction of RCaMP into primary neural cell cultures results in long-term expression of the protein, easily detected via fluorescence microscopy. Currently, the most widely used GECIs rely on the original GCaMP sensor (Nakai *et al.*, 2001). However, the excitation spectrum of GCaMP overlaps with the action spectrum of channelrhodopsin-2 (ChR2), the gold standard for optogenetic manipulation. Having shown that RCaMP is a suitable calcium sensor, our model could be combined with optogenetic tools, such as ChR2. This would allow finer modulation of neural activity compared to pharmacological modulators, such as bicuculline or picrotoxin. In parallel, we found that primary neurons plated on our microfluidic devices are functionally active and display strongly synchronized bursting dynamics, matching those of non-pathological cortical tissue activity. Overall, we have proven that, although with some limitations, our experimental approach meets the purpose for which it was designed.

Having said that, concerning the effects of extracellular seed-competent tau on the neuronal activity network, we have been unable to identify significant differences between treated and untreated cells. In the following paragraphs, we will discuss some possible explanations as to why we may have failed to detect altered neuronal activity and provide suggestions for future work.

The relationship between spontaneous activity and proper brain function began less than 15 years ago (Deco *et al.*, 2008; Honey *et al.*, 2009). In this context, it has recently

been proposed that their alteration indicates disease-related circuit damage (Fornito *et al.*, 2015). Therefore, understanding why and how spontaneous activity is impaired under pathological conditions is no trivial matter. Here, we have attempted to establish a relationship between extracellular seed-competent tau and altered dynamics in neuronal networks by using calcium imaging to infer the dynamics of neuronal activity. As a reminder, during action potentials, calcium levels within a firing neuron increase by two orders of magnitude (Berridge *et al.*, 2000). Consequently, calcium transients can be monitored during neuronal activations using calcium-binding fluorescent proteins. Hence, calcium imaging is a powerful tool that allows us to address neural activity without the need for an electrophysiological setup. However, calcium imaging data analysis may be challenging in terms of image processing, data structure, downstream analysis, and availability (Kolar *et al.*, 2021). Additionally, because it demands an important level of computing knowledge that is uncommon among biologists, most published research on tau pathology is limited to evaluating fluorescence changes. Hence, they lack the robust preprocessing and signal extraction steps that are needed to provide reliable results. Instead, most research merely compares data concerning calcium oscillations (e.g., changes in amplitude (Stancu *et al.*, 2015; Florenzano *et al.*, 2017)) and never provides information regarding network dynamics. Hence, they are likely to produce limited or even misleading results. In this work, we have attempted to overcome these limitations in collaboration with Dr. Jodi Soriano's laboratory (University of Barcelona), as they have ample experience with calcium imaging and their own specific software for calcium data analysis, NETCAL (Orlandi *et al.*, 2014). Because of this, our experimental design, could be considered a step forward in the analysis of neuronal activity in the research field of tau pathology.

By evaluating our data with NETCAL, we demonstrated that our cell cultures display the typical progression of neuronal network dynamics, consistent with past research (Opitz *et al.*, 2002; Tibau *et al.*, 2013), which validates the methodology used in our experimental approach. However, contrary to our initial assumption that tau negatively affects neuronal network dynamics, we did not find significant differences in neural activity between tau-treated and control cells. Our results partially contradict previous studies in which tau has been shown to have a significant impact on calcium dynamics. We say "partially" because, as we will see, most published research has been conducted in experimental models over-expressing transgenic species of the tau protein, which is not comparable to our approach. Nevertheless, our findings agree with what several studies consider to be "controls," defined as tau treatments in wild-type models.

An example is that of (Stancu *et al.*, 2015), who treated primary neurons from wild-type and P301S mice with PFFs assembled from a truncated 4RD tau isoform carrying the P301L mutation. It is worth remarking here that, in our study, cells were treated with TIF-P+ fractions, which contained insoluble RD-CFP/YFP tau bearing the P301S mutation, comparable to the tau construct used by Stancu *et al.* Following tau treatment, the authors loaded Fura-2 AM to address calcium fluorescence variations. Notably, Stancu and colleagues reported statistically significant differences in the amplitudes of oscillations in primary neural cell cultures derived from P301S animals treated with exogenous tau. Remarkably, the same treatment in wild-type neurons did not result in any changes in neural activity. This last observation is consistent with our findings, suggesting that wild-type neurons are resistant to the presence of seed-competent tau. In the end, the authors concluded that extracellular "pathogenic" tau altered the neuronal network. We believe their conclusion is limited to transgenic models and underscores the need for more native and disease-relevant approaches, since the cause of the vast majority of human tauopathies is not related to tau over-expression or mutations of the protein.

To our knowledge, no one else besides (Stancu *et al.*, 2015) has examined the impact of extracellular seed-competent tau on neuronal network activity using primary neural cell cultures, at least to a level comparable to our experimental approach. Hence, our results, together with those of (Stancu *et al.*, 2015) (i.e., from their tau-treated wild-type controls), suggest that extracellular seed-competent tau does not affect the network dynamics of primary neurons.

Having said that, it is pertinent to emphasize that our analyses were performed only using data from spontaneous activity (i.e., spiking events in the absence of external stimuli, such as picrotoxin, KCl, and bicuculline). In this context, many studies have reported alterations in neuronal activity related to pathological tau only in the presence of external perturbations (Messing *et al.*, 2013; Stancu *et al.*, 2015; Florenzano *et al.*, 2017). However, induced network disturbances do not represent real patterns of activity changes in the brain, and thus results need to be viewed with extreme caution. Therefore, given the broader goals of our study to work with more pathologically relevant models (e.g., using non-transgenic primary neurons), we decided that external stimulation was an inappropriate choice for our aims.

As previously indicated, our findings are somewhat contradictory compared to previous research based on models over-expressing transgenic tau, in which the authors reported altered neuronal network activity (Hall *et al.*, 2015; Stancu *et al.*, 2015; Busche

et al., 2019; Sohn *et al.*, 2019). Although there are a few possible explanations for these discrepancies (e.g., differences in extracellular tau seeds, disparate data analysis methods, etc.), we suspect that the key factor is that we have used wild-type primary neurons. For example, it may be that primary neural cell cultures from wild-type animals are unreliable models for studying neuronal activity dynamics in NDs. Estevez-Priego and colleagues showed that embryonic cortical cultures responded to externally induced perturbations by increasing their effective connectivity and eventually reaching a "hyperefficient" state (Estevez-Priego *et al.*, 2020). The authors concluded that embryonic cell cultures are highly plastic and exhibit self-regulatory mechanisms in the presence of outside disturbances. Thus, based on this, it is possible that, in our experimental model, primary neurons were able to rapidly resolve seed-competent tau-induced activity changes, which were too subtle for us to detect. However, another possibility is that 14 DIV is not enough time to observe changes in neural activity, even in embryonic cells. Unlike other published studies (Wu *et al.*, 2016; Katsikoudi *et al.*, 2020), we were unable to maintain our primary neural cell cultures for more than 16-18 DIV. Therefore, we suggest that future directions should aim to improve cell culture to evaluate changes in neural activity over extended periods. Despite not finding differences between treated and untreated cells, probably due to the use of wild-type neurons, we firmly believe that this is where the strength of our approach lies.

Tau PFFs have been widely used to study the effects of seed-competent tau on multiple experimental models (Gomez-Ramos *et al.*, 2006; Nonaka *et al.*, 2010; Guo & Lee, 2011; Iba *et al.*, 2013; Sanders *et al.*, 2014; Stancu *et al.*, 2015; McCarthy *et al.*, 2021). These tau fibrils are usually assembled in the presence of polyanionic cofactors (e.g., heparin or RNA), as they help shorten the nucleation phase of the fibrillization process (Kuret *et al.*, 2005; Zhang *et al.*, 2017; Fichou *et al.*, 2018; Ismail & Kanapathipillai, 2018). Nevertheless, it has recently been shown that the morphology of tau PFFs, assembled in the presence of heparin, largely differs from the aggregates obtained from AD and PiD patients (Zhang *et al.*, 2019). Here, we treated our microfluidic devices with seed-competent tau present in TIF-P+ fractions. We chose to use these aggregates because of the limited availability of human and mouse-derived samples. Although TIF-P+ are not strictly classical tau PFFs (i.e., HEK293-derived *vs. Escherichia coli*-derived), we recognize that, despite being seed-competent, the tau present in these fractions may not represent pathologically relevant species. It is possible that different results would have been obtained if we had employed brain-derived material from patients with AD. Future directions include using more disease-relevant samples to address changes in neuronal network activity.

In the present work, we added seed-competent tau in the axonal compartment in an attempt to recreate the trans-synaptic spreading of tau pathology (Wu *et al.*, 2013). It could be argued that adding the tau treatment to the cell body reservoir would have had different results. It is worth mentioning, however, that in a 3-year parallel collaboration with Dr. Jordi Soriano's laboratory (University of Barcelona), 2D primary neural cell cultures treated with TIF-P+ fractions or sarkosyl-insoluble samples from P301S (+/-) mice, also led to negative results (not published). Therefore, we are confident that our negative findings are not directly related to our model, although we recognize that specific changes would improve our experimental design (e.g., using brain-derived tau from AD patients and/or examining neural activity beyond 14 DIV).

It should be noted that our experimental design differs from previous research in the sense that we have addressed the effects of extracellular tau on neuronal network dynamics from the same devices in a time-course experiment. Although we have not been able to analyze the data from all days (i.e., 5 DIV and 8 DIV), it has proved sufficient to meet the purpose of the present work. However, further investigation is needed to analyze these two earlier time points.

Taking everything into account, it is also possible that extracellular tau does not modify neuronal activity whatsoever. Noteworthy, most human tauopathies are sporadic and characterized by the aggregation of endogenous tau. Indeed, to our knowledge, no experimental data have so far shown that wild-type tau aggregation in wild-type models induces changes in neuronal network activity. It is possible that the increased hyperexcitability observed in human tauopathies is not directly related to tau aggregation and that other pathological mechanisms are the real reason (Siskova *et al.*, 2014; Kazim *et al.*, 2017).

In summary, although we have been unable to conclusively establish whether extracellular seed-competent tau affects neuronal activity, several areas of our work can be regarded as innovative and may be relevant to aiding the development of new therapies. First, we have used wild-type healthy primary neural cell cultures, since they represent a relatively better, translationally relevant approach compared to transgenic models. Second, we have taken advantage of microfluidic devices to implement an experimental platform that can be adapted to recreate and study brain connections. Third, we have successfully included the red, single-wavelength GECI-RCaMP protein, which could be combined with optogenetic tools, such as ChR2, or the use of GFP-tagged proteins, without interfering with the calcium fluorescence signal. Fourth, our approach involves a time-course evaluation of neuronal activity, which, to our knowledge,

has never been addressed before at this level. Finally, we have implemented a comprehensive pipeline for the analysis of calcium imaging by introducing the NETCAL software into our experimental design. Overall, we are confident that our innovations will be advantageous for future research on neuronal network analysis relevant to tau pathology.

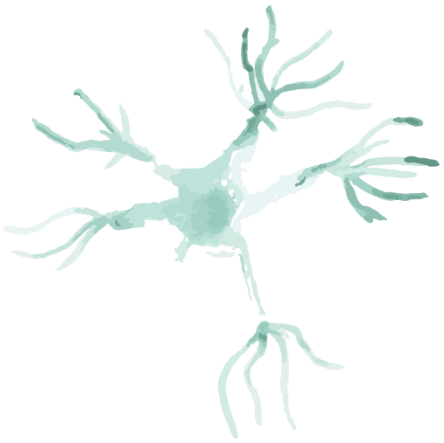

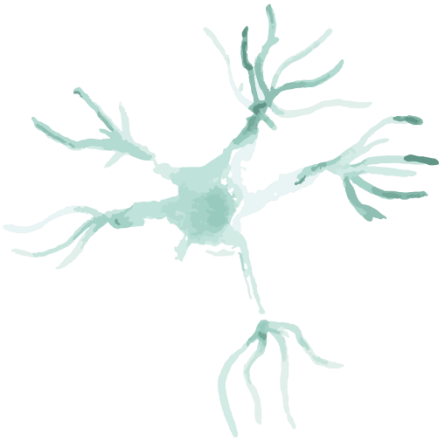

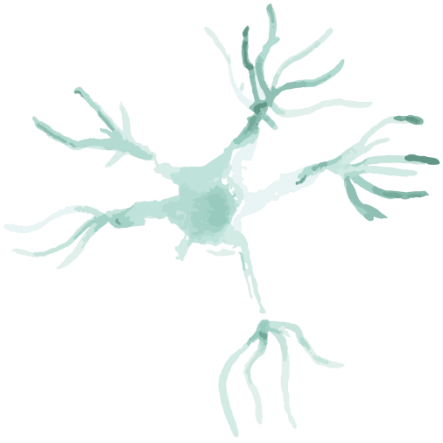

Chapter 3: Evaluation of Extracellular Seed-Competent Tau Cytotoxicity in Primary Cortical Cultures

5.1 Introduction

The realm of tau toxicity is considerably complex and has been addressed in a wide variety of models, ranging from immortalized cell lines (Gomez-Ramos *et al.*, 2006; Khlistunova *et al.*, 2006), to murine primary neural cell cultures (Stancu *et al.*, 2015), organotypic slices (McCarthy *et al.*, 2021), iPSCs, organoids, and assembloids (Evans *et al.*, 2018; Gonzalez *et al.*, 2018), as well as in various model organisms *in vivo* (Kruger & Mandelkow, 2016). Most of these approaches rely on the over-expression of truncated or mutated tau species, although toxicity has also been studied in wild-type models referred to as “controls” in some publications (e.g., (Stancu *et al.*, 2015; McCarthy *et al.*, 2021)). Notably, the toxicity of tau can also be examined solely by over-expressing tau isoforms in cellular models or by adding extracellular tau to the system (i.e., endogenous *vs.* exogenous tau-induced toxicity). Moreover, treatment with exogenous tau differs in the origin and nature of the added variants. For instance, extracellular tau can be monomeric, “oligomeric,” truncated, or fibrillated, and it can be “synthetic” (i.e., tau PFFs) or derived from the brains of transgenic animals or sporadic human tauopathies. Therefore, it does not come as a surprise that there are multiple conflicting reports regarding the cytotoxicity induced by tau (Khlistunova *et al.*, 2006; Guo *et al.*, 2016a).

In Chapter 2, we examined the link between extracellular seed-competent tau and altered neuronal network activity. Likewise, in the present chapter, we were interested in the relationship between extracellular seed-competent tau and neurotoxicity in primary neural cell cultures. In this regard, tau-related lesions have long been associated with synaptic loss and cognitive decline in AD and other human tauopathies (Masliah *et al.*, 1989; DeKosky & Scheff, 1990; Braak & Braak, 1991; Bierer *et al.*, 1995; Coleman & Yao, 2003). Indeed, increased tau levels have been found in the CSF of AD patients (Buerger *et al.*, 2006; Scholl *et al.*, 2019). Additionally, as just mentioned, the association between extracellular tau and neurodegeneration is supported by recent results from many experimental models (Gomez-Ramos *et al.*, 2006; Fa *et al.*, 2016; Wu *et al.*, 2016; Pampuscenko *et al.*, 2021). Initially, pathogenic extracellular tau was thought to be related to neuronal death (Buerger *et al.*, 2006). However, mounting evidence suggests that neurons actively secrete seed-competent tau into the extracellular milieu and that surrounding cells internalize it, resulting in cell-to-cell spreading of tau pathology in a prion-like manner (Clavaguera *et al.*, 2009; Frost *et al.*, 2009; Wu *et al.*, 2013; Brunello *et al.*, 2020; Chastagner *et al.*, 2020). Therefore, addressing the potential toxicity of extracellular tau is critical for the development of therapeutic strategies and a better understanding of disease progression.

5.2 Objective

In this chapter, we aim to evaluate the cytotoxicity of different extracellular seed-competent tau in primary cortical cultures through the determination of alterations in their metabolic activity.

5.3 Materials and Methods

5.3.1 Ethical Statement

All animals were kept in the animal facility of the Faculty of Pharmacy at the University of Barcelona under controlled environmental conditions and were provided with food and drink *ad libitum*. Animal care and experimental protocols were performed in compliance with the CEEA of the University of Barcelona. All housing, breeding, and procedures were performed under the guidelines and protocols OB47/19, C-007, 276/16, and 47/20 of CEEA.

5.3.2 Mice

In this chapter, we used 12-month-old P301S (+/-) mice and their non-transgenic littermates, P301S (-/-). Non-transgenic P301S (-/-) mice were used as control mice and will be referred to as P301S (-/-).

5.3.3 Human Samples

This chapter included frozen material from an autopsy-proven, neuropathologically well-characterized case of AD. We used brain-derived material from one male patient, who was 93 years old, and a 3 h delay in post-mortem inspection.

5.3.4 Preparation of Sarkosyl-Insoluble Fractions from Mice and Human Samples

Please see Chapter 1, Materials and Methods, Section 3.3.8

5.3.5 Tau Biosensor Cell Line Culture and Seeding for Sequential TIF Extraction

Please see Chapter 1, Materials and Methods, Section 3.3.11.3

5.3.6 Standard Tau Biosensor Cell Line Seeding Assay

Please see Chapter 1, Materials and Methods, Section 3.3.11.2

5.3.7 Primary Cortical Cultures

Primary cortical neurons were prepared from E16.5 embryos of wild-type CD1 mice (Charles River Laboratories, France). In brief, brains were dissected in ice-cold 0.1 M PBS containing 6.5 mg/mL glucose (Merck Millipore), cerebral cortices were isolated, and meninges were removed. Thereafter, cortices were transferred into trypsin and digested for 15 min at 37°C with gentle inversion every 3 min. After adding NHS (ThermoFischer Scientific) and centrifugation, cells were mechanically dissociated in 0.1 M PBS containing 0.025% DNAse (Roche). Depending on the objective of the experiment, cells were cultured differently. For immunocytochemistry experiments, cells were cultured onto poly-D-lysine (0.1 mg/mL) -coated glass coverslips on 4-well plates. For cytotoxicity experiments, cells were plated onto poly-D-lysine (0.1 mg/mL) -coated 24-well plates. In both cases, cells were plated at a density of 250,000 cells/well in plating medium [Neurobasal medium (ThermoFischer Scientific) supplemented with 5% NHS, 6.5 mg/mL glucose, $NaHCO_3$ (Merck Millipore), 1X B27 (ThermoFischer Scientific), 1% GlutaMax (Gibco), and 1% penicillin/streptomycin (ThermoFischer Scientific)]. After 1 DIV, the plating medium was replaced with culture medium [Neurobasal medium (ThermoFischer Scientific) supplemented with 6.5 mg/mL glucose, $NaHCO_3$ (Merck Millipore), 1X B27 (ThermoFischer Scientific), 1% GlutaMax (Gibco), and 1% penicillin/streptomycin (ThermoFischer Scientific)]. The culture medium was changed every 2 to 3 days.

5.3.8 Viral Transduction and Biochemical Analysis

We transduced primary neurons at 1 DIV with 2 x 10^7 viral particles of AAV2retro encoding full-length human tau with the P301L mutation (AAV-P301L) under the control of the human *SYN1* gene promoter (a kind gift from Dr. José Luis Lanciego, CIMA, Navarra). Two days later, the conditioned medium was replaced with an equal volume of fresh media. Biochemical analysis was used to confirm the proper expression of the tau construct P301L in primary neural cell cultures. Briefly, at 6 DIV, the culture medium was removed, and cells were resuspended in 2X Laemmli sample buffer (Bio-Rad) and analyzed by SDS-PAGE, followed by WB (i.e., see Chapter 1, Materials and Methods, Section 3.3.9 for a detailed protocol). Immunoblots were probed with the human-specific anti-Tau-13 antibody (1:1,000) (Abcam, catalog no. ab19030), which specifically detects human tau.

5.3.9 Tau Treatments

To investigate the cytotoxic effects of extracellular seed-competent tau, primary neural cell cultures were treated with TIF, TauCy5, P301S mice, and human AD-derived samples at 6 DIV for 48 h. In brief, for TIF-P+, TIF-P-, TIF-V, and TauCy5 (a kind gift from Dr. Jesús Ávila, CBM-UAM, Madrid), 5 µg of total protein was diluted in 500 µL of the culture medium. For treatments with sarkosyl-insoluble P301S (-/-), P301S (+/-), or AD fractions, 20 µg of total protein was diluted in 500 µL of the culture medium. Likewise, primary neurons transduced with AAV-P301L were incubated with 20 µg of total protein from sarkosyl-insoluble fractions from P301S (+/-) mice, diluted in 500 µL of the culture medium. Untreated cells were used as controls. For cytotoxicity experiments, cells were plated in quadruplicate for each condition (i.e., 24-well plates). Initially, each culture plate had eight wells with untreated cells, four of which were used as untreated controls, and the other four were eventually used as positive controls for cell death. The remaining wells were treated with the above-mentioned tau samples.

5.3.10 Transmission Electron Microscopy Imaging

Please see Chapter 1, Materials and Methods, Section 3.3.6

5.3.11 alamarBlue™ Cell Viability Assay

Tau-related cytotoxicity was assessed by measuring the cellular metabolism integrity of primary neural cell cultures at 2, 5, 7, and 10 days of treatment (DOT) with alamarBlue™ Cell Viability Reagent (ThermoFischer Scientific), according to the manufacturer's instructions. Briefly, on the day of the assay, positive cell death controls were prepared by replacing their culture medium with 300 µL of 70% ethanol for 15 min. Next, the media of all wells (i.e., tau-treated and controls) was aspirated and replaced with freshly prepared culture media. Following that, alamarBlue™ was directly added to each well at a final concentration of 10% (v/v), and the culture plates were returned to the incubator at 37°C with 5% CO_2 for 4 h. For fluorescence readings, we placed 100 µL of medium from each replica in triplicate into the wells of a 96-well black bottom plate (Costar) (i.e., three independent measurements were taken from four replicates from at least three independent experiments for each time point). Fluorescence intensity was quantified through top readings at 530 nm excitation and 570 nm emission using an Infinite M200 PRO microplate reader (Tecan, Switzerland). The reduction of the cell viability reagent was normalized relative to that of the untreated control cells, which were considered to have 100% metabolic integrity. For plates analyzed at 10 DOT, the

alamarBlue™ assay was complemented by evaluating: 1) the total number of cells (i.e., determined by Hoechst staining), and 2) the ratio of neurons (i.e., NeuN-positive cells) relative to the total number of cells (i.e., determined by Hoechst staining).

5.3.12 Immunocytochemistry

For standard fixation, cultured primary neurons were washed once in pre-warmed 0.1 M PBS and then fixed in 4% PFA for 15 min at room temperature. For removal of soluble proteins, cells were washed once in pre-warmed 0.1 M PBS and then fixed in pre-chilled methanol for 15 min at -20°C (Guo *et al.*, 2016b). Following fixation, cells were permeabilized and blocked for 1 h in blocking solution [5% NGS, 0.1% Triton X-100, 0.015 g/mL glycine in 0.1 M PBS containing 2% BSA]. After blocking, cells were incubated with primary antibodies diluted in antibody solution [2% NGS, 0.1% Triton X-100 in 0.1 M PBS] overnight at 4°C with gentle agitation. The following antibodies were used for immunostaining: mouse anti-HT7 (1:600) (ThermoFischer Scientific, catalog no. MN1000), rabbit anti-GFP (1:500) (Invitrogen, catalog no. A11122), or mouse anti-NeuN (1:500) (Merck Millipore, catalog no. MAB377). Secondary antibodies Alexa Fluor 488 or Alexa Fluor 568 (Life Technologies) of the appropriate species were diluted in antibody solution (1:500) and incubated for 2 h at room temperature, then subsequently washed three times in 0.1 M PBS. Nuclei were stained for 10 min at room temperature with 1 µg/mL Hoechst 33342 (Invitrogen).

5.3.13 Imaging

For imaging, we used an inverted Olympus fluorescence microscope IX71 (Olympus) equipped with a sensitive, high-speed camera (Hamamatsu ORCA Flash 4.0) and an LED light source (CoolLED's pE-300^{white}, Delta Optics, Spain). Images were acquired with the camera software Olympus cellSens™ (Olympus Corporation; https://www.olympus-lifescience.com/en/software/cellsens/) and saved in 8-bit ".tiff" files.

5.3.14 Image Processing and Data Acquisition

To quantify the ratio of neurons to nuclei (i.e., NeuN-positive/Hoechst or Neurons/Nuclei), we randomly selected 15 areas per well, and pictures for the UV and red channels were acquired at 20x magnification. Hence, for a total of three independent experiments, with four replicates per condition, we took 15 x 2 pictures per well. We used the same exposure settings across all experiments to ensure consistency and appropriate compatibility of the results. We took advantage of the open-source Cell Profiler v4.2.1 software (Stirling *et al.*, 2021) to create a pipeline that allowed us to

compute the number of cell nuclei and NeuN-positive cells per field. The ratio of Neurons/Nuclei was calculated with Excel. Next, we used GraphPad Prism for statistical analysis.

5.3.15 Statistical Analysis

Quantitative data were analyzed using one-way ANOVA, followed by Tukey's *post hoc* test was used for comparisons between several independent groups. Statistical significance was set at $p < 0.05$. The data were expressed as means ± SD. GraphPad Prism 8 (version 8.02; GraphPad software Inc., California, United States of America) was used to perform statistical tests and produce graphs. For all statistical analysis in this chapter: *$p < 0.05$, **$p < 0.01$; ***$p < 0.001$, ****$p < 0.0001$.

5.4 Results

5.4.1 Effect of Extracellular Seed-Competent Tau Species on Primary Cortical Cultures

To date, few studies have addressed the impact on cellular viability produced by the presence of seed-competent extracellular tau in healthy primary neural cell cultures. Additionally, most of the published research on this particular topic have focused on measuring tau cytotoxicity at a single time point, often following the addition of tau. In the present study, we sought to rectify this by examining the time-course impact of extracellular tau on primary neurons derived from wild-type mice.

Given the large body of evidence reporting tau toxicity (Khlistunova *et al.*, 2006; Flach *et al.*, 2012; Wegmann *et al.*, 2015), we hypothesized that the presence of exogenous seed-competent tau could negatively affect the viability of neural cells. However, it should be noted that cell cultures were treated at 6 DIV, but several medium changes were performed prior to the addition of alamarBlue™. Hence, before conducting the time-course analysis of cell viability, we sought to determine whether the extracellular seed-competent tau from the treatment was present in the cell culture at 10 DOT or whether it had been removed because of the culture medium exchanges. To evaluate this, we carried out a group of experiments in which cells were treated at 6 DIV, and we changed the medium at 2, 5, 7, and 10 DOT (i.e., identically as for the alamarBlue™ assays). Then, at 10 DOT, we fixed the cells in methanol to remove soluble tau (Guo *et al.*, 2016b) and immunolabeled them with specific antibodies to detect the presence of insoluble tau.

The alamarBlue™ Cell Viability Reagent was then used to investigate the possible harmful effects of various tau samples on primary cortical neurons at 2, 5, 7, and 10 DOT. The alamarBlue™ is an oxidation-reduction indicator that changes from blue to red with cellular metabolic activity and is widely used to measure the reduction potential in living cells. In addition to the cell viability assay, since we were interested in long-term toxic effects (i.e., analogous to what we did in Chapter 2), we further evaluated the cell cultures at 10 DOT by quantifying the total number of nuclei as a readout for gross extracellular tau toxicity. Of note, when working with mixed primary neural cell cultures, the alamarBlue™ assay is unsuitable for identifying neuron-specific cell death. Moreover, in human tauopathies, the neurodegenerative process is intimately linked to the activation and proliferation of inflammatory cells (Millington *et al.*, 2014; Spangenberg & Green, 2017; Yang, 2019). Therefore, we sought to exclude the possibility that extracellular tau was killing neurons and that, in response, glial cells were increasing in number, thereby masking the neurotoxic effect. We calculated the ratio of Neurons/Nuclei on the same plates used to analyze the alamarBlue™ reaction. To this end, at 10 DOT, immediately after collecting the medium for the alamarBlue™ measurements, cultures were fixed in 4% PFA. Cells were then immunolabeled with NeuN (i.e., to show only neurons) and Hoechst (i.e., to expose all nuclei).

For clarity, since we used different samples, we decided to divide the Results section into three experimental blocks corresponding to each set of tau treatments. In “Block 1,” the effects of TIF-P+, TIF-P-, TIF-V, and TauCy5 will be reported. In “Block 2,” we will present the results of treatment with sarkosyl-insoluble fractions from P301S (-/-), P301S (+/-), and one human AD-derived sample. Finally, in “Block 3,” we will show the outcome of sarkosyl-insoluble tau from P301S (+/-) mice on neuronal cells virally transduced to produce full-length human tau bearing the P301L mutation.

5.4.1.1 Block 1: Neither TIF-Derived Samples nor Monomeric TauCy5 Affects Primary Cortical Culture Viability

In Chapter 1, we show that the TIF-P+ fraction contains insoluble tau with fibril-like structures and that it is seed-competent *in vitro* and induces tau pathology *in vivo*. Here, we wanted to address possible toxic effects on primary neuronal cell cultures. For that purpose, we first treated primary neurons with TIF-P+, TIF-P-, TIF-V, or TauCy5 at 6 DIV and fixed them at 10 DOT. Cells incubated with TauCy5 were immunolabeled with the anti-HT7 antibody, as it detects specifically human tau (Figure 24, upper panel). Similarly, neural cultures treated with TIF fractions were immunolabeled with anti-GFP antibodies to recognize tau RD-CFP/YFP fragments (Figure 24, lower panel). Consistent

with our previous findings from Chapter 1, the TIF-P+ treatment resulted in detectable GFP-positive inclusions, whereas the other treatments did not. Of note, the specificity of both antibodies (i.e., GFP and HT7) was confirmed in untreated cells (Figure 24). Together, our results show that only the TIF-P+ fraction contains insoluble tau species, which are abundantly detected at 10 DOT.

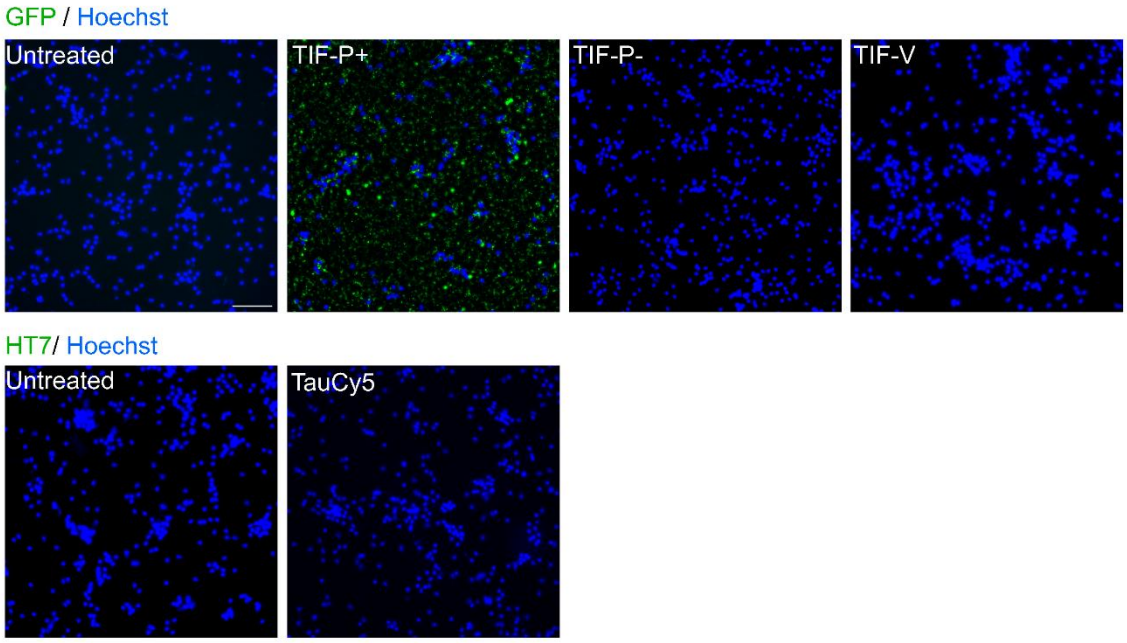

Figure 24 Detection of extracellular seed-competent tau at 10 days of treatment (DOT) with TIF-P+, TIF-P-, TIF-V, or TauCy5: Primary neural cell cultures were left untreated or treated with TIF-P+, TIF-P-, TIF-V, or TauCy5 after 6 days *in vitro* (DIV). At 10 DOT (i.e., 16 DIV), cells were fixed in methanol to remove soluble tau and immunostained. Nuclei (blue) were stained with Hoechst. In the upper panel, the anti-GFP antibody was used to detect tau RD-CFP/YFP (green) in cells treated with TIF-P+, TIF-P-, and TIF-V (green). Insoluble tau can be detected even at 10 DOT, but only in TIF-P+-treated cells. The anti-HT7 antibody, a human tau-specific antibody, was used to detect tau in cells treated with TauCy5, but no signal could be detected at 10 DOT. Pictures are representative of at least n = 3 independent experiments. Scale bar, 100 µm.

Next, we measured the possible cytotoxic effect on cellular metabolism by performing the alamarBlue™ assay at 2, 5, 7, and 10 DOT. As seen in Figure 25A, treatment with 70% ethanol resulted in massive cell death, confirming the validity of the assay. However, no significant differences were observed between treatments compared to untreated cells, even at the latest time point of the study (i.e., 10 DOT). After that, we looked at the number of nuclei at 10 DOT and found no significant changes (Figure 25B). Finally, we did not detect any differences in the proportion of NeuN-positive cells relative to the total number of Hoechst-positive nuclei (Figure 25C), indicating that neurons were not affected by tau treatments. Together, our findings show that extracellular seed-

competent TIF-P+ is not toxic to primary neurons, at least according to our experimental model.

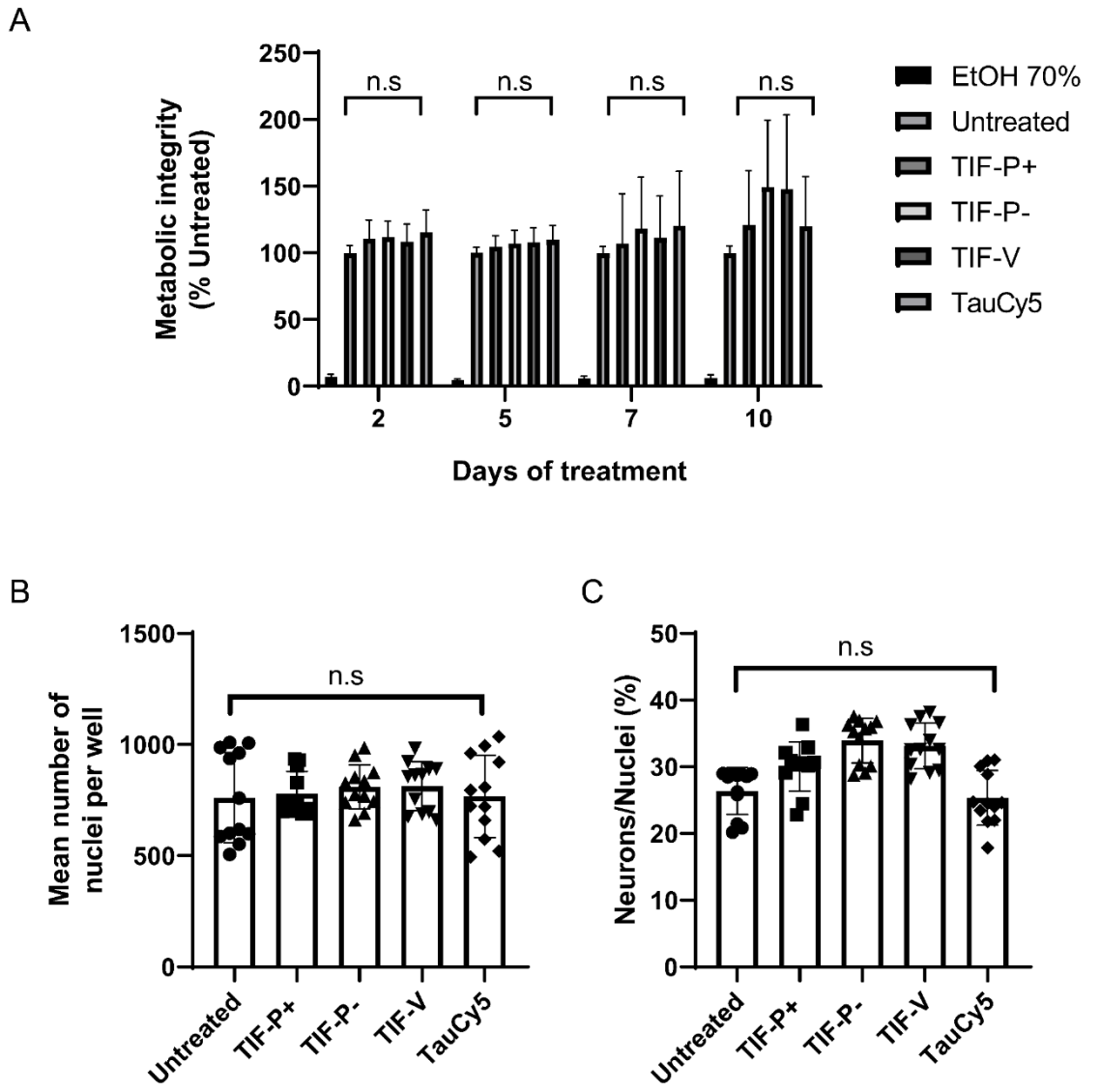

Figure 25 Extracellular seed-competent tau derived from TIF-P+ is not toxic to primary neural cell cultures: Primary neural cell cultures were treated with TIF-P+, TIF-P-, TIF-V, or TauCy5 or left untreated. For positive controls of cell death, four extra seeded wells were left untreated until the day of the alamarBlue™ assay, when 70% ethanol (EtOH) was added for 15 min at 37°C to induce cell death. **A)** Time-course of alamarBlue™ reduction in primary neural cell cultures at 2, 5, 7, and 10 days of treatment (DOT). No changes in metabolic integrity are detected between conditions at any point in time. The results are expressed as mean ± SD from at least eight independent experiments. Statistical significance was calculated by one-way ANOVA with Tukey's *post hoc* test for group comparisons. All conditions are statistically different from cells treated with 70% EtOH (***$p < 0.001$), but for clarity, this significance is omitted in the graph. Abbreviation n.s stands for not significant ($p > 0.05$). *Figure 25 continued on the next page*

Figure 25 continued

B) Effects of each treatment on the total number of nuclei at 10 DOT. No differences are observed between treatments. The results are expressed as mean ± SD; each symbol represents the average of 15 from at least eight independent experiments. Statistical significance was calculated by one-way ANOVA with Tukey's *post hoc* test for group comparisons. Abbreviation n.s stands for not significant ($p > 0.05$). **C)** Effects of each treatment on the number of neurons (i.e., NeuN-positive) expressed as a percentage of the total number of cells (i.e., Hoechst) at 10 DOT. No changes in the proportion of neurons relative to the total number of cells are observed. The results are expressed as mean ± SD; each symbol represents the average of 15 pictures from at least eight independent experiments. Statistical significance was calculated by one-way ANOVA with Tukey's *post hoc* test for group comparisons. Abbreviation n.s stands for not significant ($p > 0.05$).

5.4.1.2 Block 2: Neither Sarkosyl-Insoluble Fractions from P301S (+/-) Mice nor AD-Derived Tau Affects Primary Cortical Culture Viability

Given the previous results, we considered that TIF-P+ could not have been the most appropriate model to study tau toxicity, as it may not fully mimic the type of aggregates present in the diseased brain (Sharma *et al.*, 2018; Zhang *et al.*, 2019). Therefore, we chose to investigate the toxicity of more physiologically relevant specimens in primary neural cell cultures. For this purpose, we opted for sarkosyl-insoluble samples derived from P301S (-/-), P301S (+/-), and one human AD case. First, we performed a seeding assay in the Tau biosensor cell line and confirmed that the P301S (+/-) and AD samples were seed-competent (data not shown). Accordingly, TEM analysis of both fractions revealed the existence of fibrillar structures (Figure 26A). In contrast, no fibril-like structures were observed for P301S (-/-) (data not shown). Next, primary cortical cultures were treated with P301S (-/-), P301S (+/-), or AD and fixed in methanol at 10 DOT before being immunolabeled with anti-HT7 for insoluble tau detection. As expected, only cultures treated with P301S (+/-) or AD samples were positively stained for HT7, proving the presence of tau seeds throughout the experiment (Figure 26B).

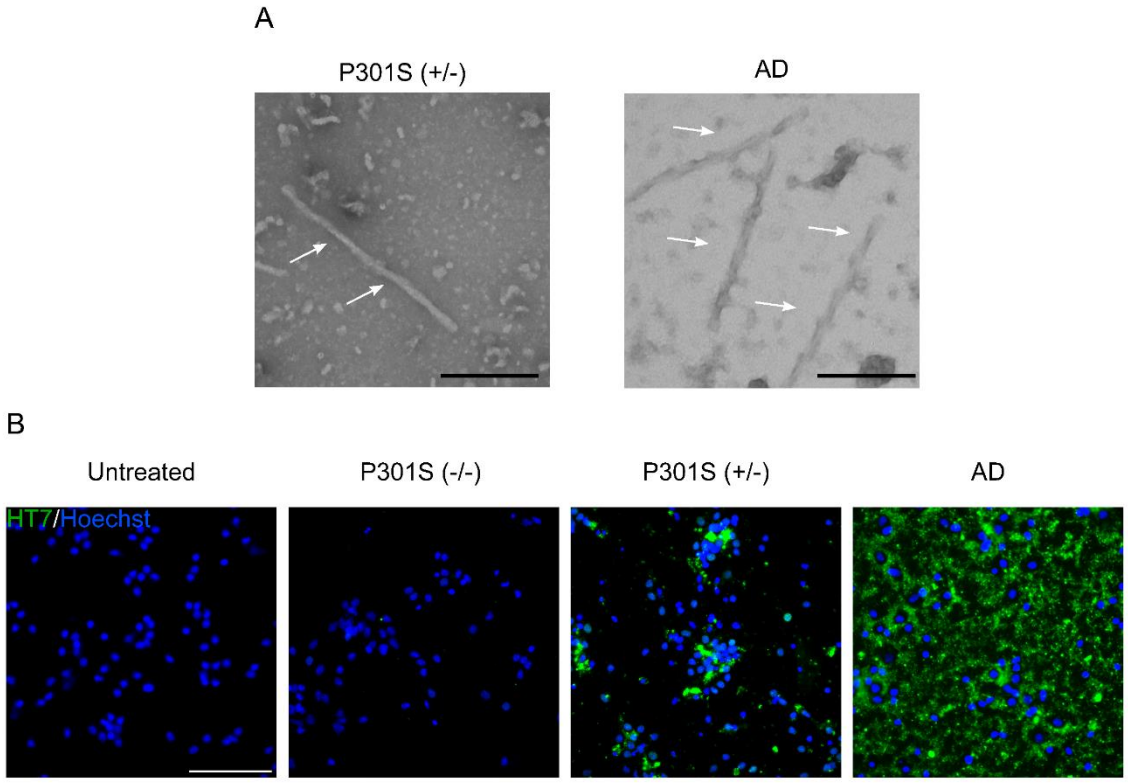

Figure 26 Detection of extracellular seed-competent tau at 10 days of treatment (DOT) with sarkosyl-insoluble fractions from P301S (-/-), P301S (+/-), and human AD: A) Transmission electron microscopy (TEM) analysis by negative staining. The sarkosyl-insoluble fraction of P301S (+/-) mice and the AD patient contain numerous fibrils (white arrows). Scale bars, 200 nm. **B)** Primary neural cell cultures were left untreated or treated with sarkosyl-insoluble fractions from P301S (-/-), P301S (+/-), and human AD after 6 days *in vitro* (DIV). At 10 DOT (i.e., 16 DIV), cells were fixed in methanol to remove soluble tau and immunolabeled with the anti-HT7 antibody (green), and nuclei (blue) were stained with Hoechst. The insoluble tau is only observable in cultures treated with P301S (+/-) and human AD. Scale bar, 100 µm.

We then examined how these treatments affected cellular metabolism. Surprisingly, we did not observe tau-dependent increased cytotoxicity in the alamarBlue™ assay (Figure 27A). Likewise, no changes were found in the number of total nuclei at 10 DOT, corroborating the alamarBlue™ results (Figure 27B). Finally, the proportion of neurons relative to total cell nuclei also did not reveal any differences between treated and untreated cells (Figure 27C). These results show that sarkosyl-insoluble seed-competent tau, derived from either P301S (+/-) mice or human AD, does not result in an overall negative impact on the health of primary neural cell cultures. Furthermore, because the ratio of Neurons/Nuclei is similar between conditions, our findings suggest that glial cells are not activated, at least to the point of proliferation, by the presence of brain-derived tau.

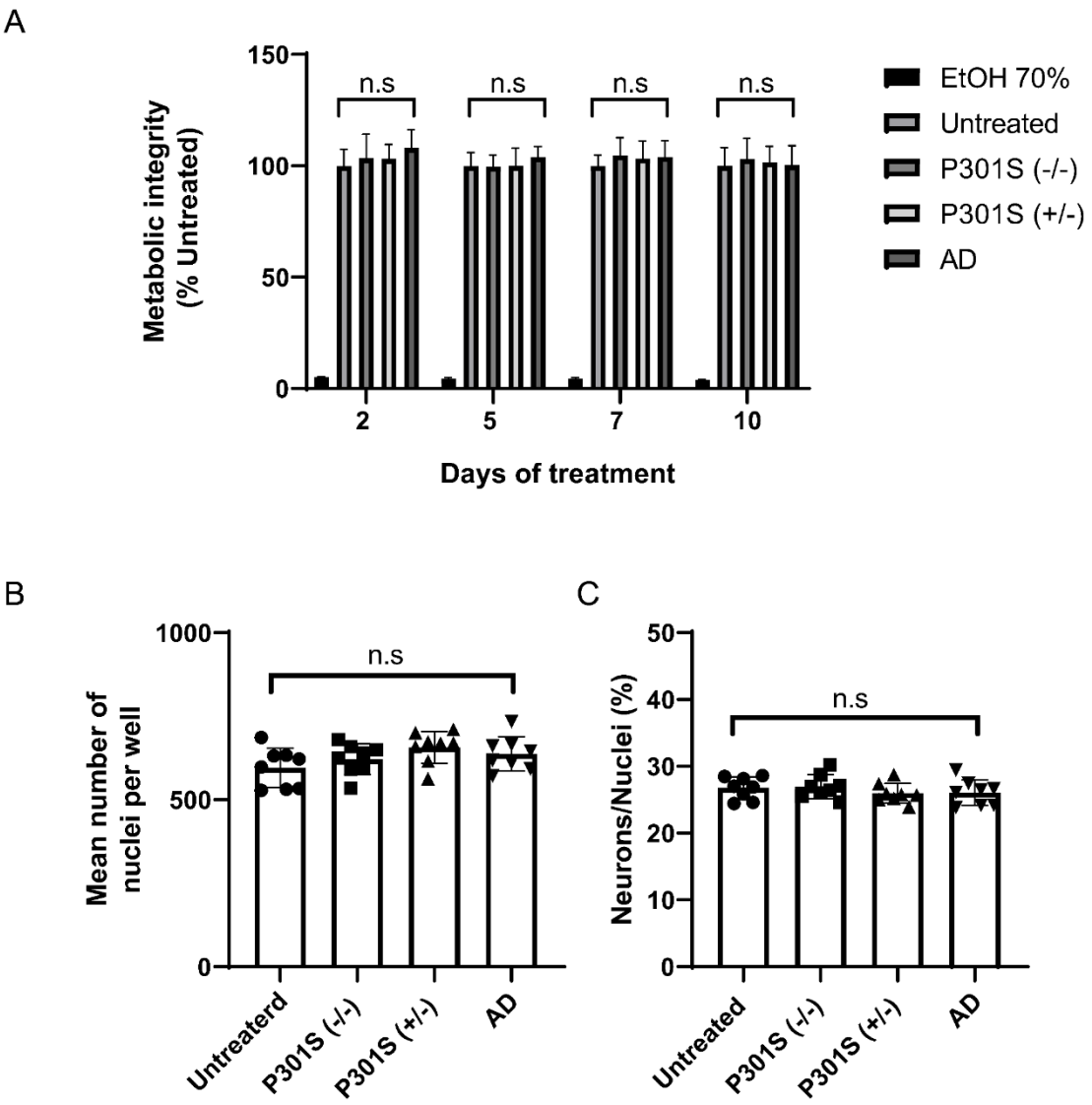

Figure 27 Extracellular seed-competent tau derived from sarkosyl-insoluble samples derived from P301S (+/-) mice and human AD is not toxic to primary neural cell cultures: Primary neural cell cultures were treated with sarkosyl-insoluble samples from P301S (-/-) or P301S (+/-) mice, or human AD or left untreated. For positive controls of cell death, wells were treated with 70% ethanol (EtOH) for 15 min. **A)** Time-course of alamarBlue™ reduction in primary neural cell cultures at 2, 5, 7, and 10 days of treatment (DOT). No changes in metabolic integrity are detected between conditions at any point in time. The results are expressed as mean ± SD from at least seven independent experiments. Statistical significance was calculated by one-way ANOVA with Tukey's *post hoc* test for group comparisons. All conditions are statistically different from cells treated with 70% EtOH (***$p < 0.001$), but for clarity, this significance is omitted in the graph. Abbreviation n.s stands for not significant ($p > 0.05$). **B)** Effects of each treatment on the total number of nuclei at 10 DOT. No differences are observed between treatments. The results are expressed as mean ± SD; each symbol represents the average of 15 from at least seven independent experiments. Statistical significance was calculated by one-way ANOVA with Tukey's *post hoc* test for group comparisons. Abbreviation n.s stands for not significant ($p > 0.05$). *Figure 27 continued on the next page*

Figure 27 continued

C) Effects of each treatment on the number of neurons (i.e., NeuN-positive) expressed as a percentage of the total number of cells (i.e., Hoechst) at 10 DOT. No changes in the proportion of neurons relative to the total number of cells are observed. The results are expressed as mean ± SD; each symbol represents the average of 15 pictures from at least seven independent experiments. Statistical significance was calculated by one-way ANOVA with Tukey's *post hoc* test for group comparisons. Abbreviation n.s stands for not significant ($p > 0.05$).

5.4.1.3 Block 3: Primary Cortical Cultures Expressing P301L Full-Length Human Tau Treated with Sarkosyl-Insoluble Fractions from P301S (+/-) Mice Do Not Show Reduced Cell Viability

At this point, we were surprised that none of the previous treatments had caused significant toxic effects on wild-type primary neural cell cultures. Consequently, we decided to modify our experimental approach by inducing the over-expression of a mutant tau isoform (i.e., P301L) to predispose the primary neurons to a more pathological scenario prior to treating them with seed-competent tau. To this end, we transduced primary cortical cultures with AAV-P301L and confirmed that they over-expressed P301L tau by biochemical analysis. Immunoblotting with the monoclonal anti-Tau-13 antibody revealed that only infected cultures produced human tau (Figure 28A). Our findings indicate that primary neurons strongly over-express P301L tau at 6 DIV, coinciding with the day of tau treatment.

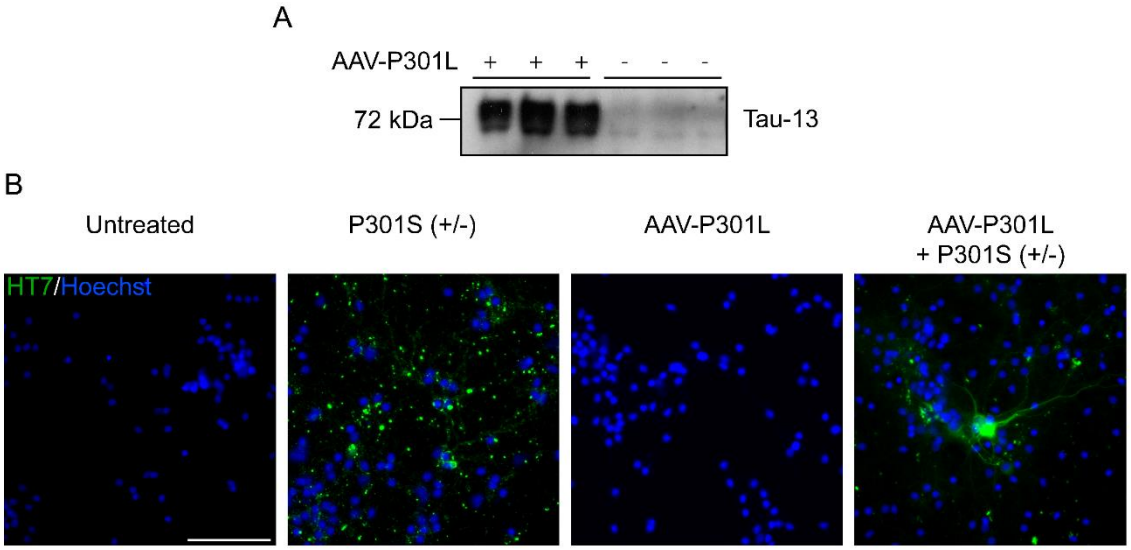

Figure 28 Primary neurons transduced with AAV-P301L viral particles express human tau and form insoluble tau at 10 days of treatment (DOT): A) Primary neural cell cultures were infected with AAV-P301L viral particles at 1 day *in vitro* (DIV). At 6 DIV, cortical cultures were **lysed**, and tau expression was assessed by western blotting (WB) using the human-specific tau anti-Tau-13 antibody. Human tau is only detected in cells transduced with AAV-P301L. **B)** Primary cortical cultures were left untreated, treated with sarkosyl-insoluble fraction from P301S (+/-) mice, transduced with AAV-P301L without further treatment, or transduced with AAV-P301L and treated with sarkosyl-insoluble samples from P301S (+/-) after 6 DIV. At 10 DOT (i.e., 16 DIV), cells were fixed in methanol to remove soluble tau and immunolabeled with the anti-HT7 antibody (green), and nuclei (blue) were stained with Hoechst. Insoluble tau can be seen in cells treated with P301S (+/-) and the AAV-P301L + P301S (+/-) condition. Scale bar, 100 µm.

Next, we examined whether endogenous expression of P301L tau sufficed to induce the formation of insoluble tau aggregates or whether extracellular seed-competent tau was required. To answer this question, we compared HT7 staining patterns at 10 DOT between primary neural cell cultures: a) treated with sarkosyl-insoluble samples from P301S (+/-) mice but not virally transduced; b) untreated cells but virally transduced to produce P301L tau; and c) treated with the sarkosyl-insoluble P301S (+/-) fraction and virally transduced to over-express P301L tau (Figure 28B). Cortical neurons incubated with P301S (+/-) samples revealed discrete HT7-positive staining. Surprisingly, untreated cells over-expressing P301L tau did not produce detectable HT7-specific fluorescence. In contrast, primary neurons over-expressing P301L tau and treated with sarkosyl-insoluble P301S (+/-) samples, on the other hand, showed HT7-positive staining comparable to that seen with P301S (+/-) treatment alone. Notably, extensive cytoplasmic staining was observed at around 5 to 10% of neuronal cells, meaning that despite elevated levels of P301L expression detected by immunoblotting, only a reduced number of neurons were triggered to form intracellular tau aggregates. Together, these results show that the over-expression of P301L tau alone does not lead to the formation

of insoluble inclusions even at 16 DIV (i.e., 10 DOT) in primary cortical neurons, suggesting that P301L tau remains soluble in the cytoplasm and that adding extracellular seed-competent species is required to induce the formation of insoluble aggregates.

Finally, we addressed the putative impairment of cellular metabolism using the alamarBlue™ assay. Surprisingly, no differences in viability were found in tau P301L over-expressing neurons compared to non-transduced neurons treated with P301S (+/-), neither under P301S (+/-) treatment alone nor compared to the untreated control (Figure 29A). Consistent with these results, at 10 DOT, we did not detect changes in the total number of nuclei (Figure 29B) or differences in the proportion of neurons relative to the overall number of cells (Figure 29C), indicating that glial cells were not induced to proliferate. Overall, these findings show that primary neural cell cultures over-expressing P301L tau do not have altered cell viability, even when seeded with P301S (+/-).

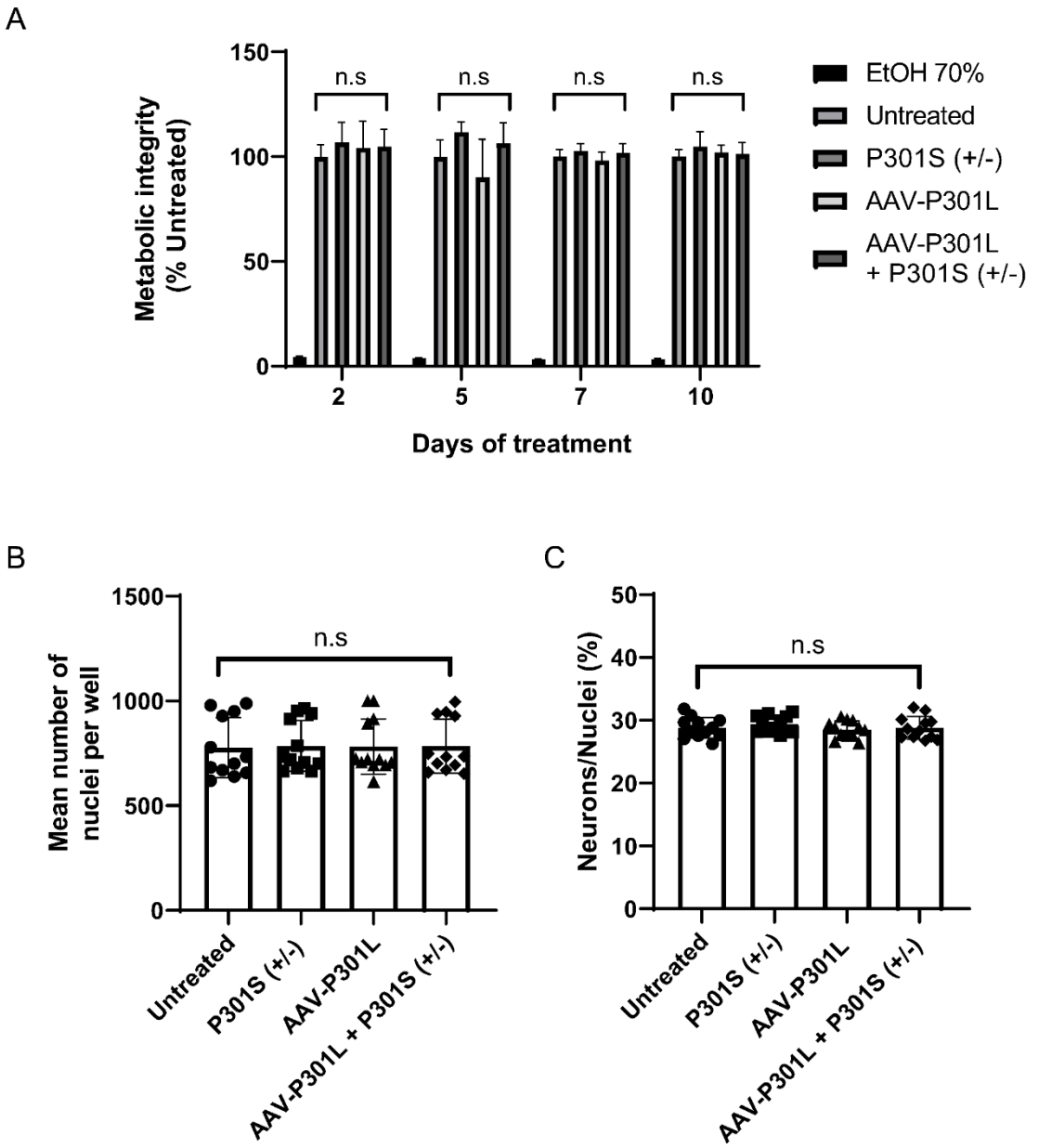

Figure 29 Extracellular seed-competent tau derived from sarkosyl-insoluble samples derived from P301S (+/-) mice is not toxic to primary neural cell cultures over-expressing P301L tau: Primary neural cell cultures were left untreated, treated with sarkosyl-insoluble fraction from P301S (+/-) mice, transduced with AAV-P301L without further treatment, or transduced with AAV-P301L and treated with sarkosyl-insoluble samples from P301S (+/-) after 6 days *in vitro* (DIV). For positive controls of cell death, wells were treated with 70% ethanol (EtOH) for 15 min. **A)** Time-course of alamarBlue™ reduction in primary neural cell cultures at 2, 5, 7, and 10 days of treatment (DOT). No changes in metabolic integrity are detected between conditions at any point in time. The results are expressed as mean ± SD from at least eight independent experiments. Statistical significance was calculated by one-way ANOVA with Tukey's *post hoc* test for group comparisons. All conditions are statistically different from cells treated with 70% EtOH (***$p < 0.001$), but for clarity, this significance is omitted in the graph. Abbreviation n.s stands for not significant ($p > 0.05$). *Figure 29 continued on next the page*

Figure 29 continued

B) Effects of each treatment on the total number of nuclei at 10 DOT. No differences are observed between treatments. The results are expressed as mean ± SD; each symbol represents the average of 15 from at least eight independent experiments. Statistical significance was calculated by one-way ANOVA with Tukey's *post hoc* test for group comparisons. Abbreviation n.s stands for not significant ($p > 0.05$). **C)** Effects of each treatment on the number of neurons (i.e., NeuN-positive) expressed as a percentage of the total number of cells (i.e., Hoechst) at 10 DOT. No changes in the proportion of neurons relative to the total number of cells are observed. The results are expressed as mean ± SD; each symbol represents the average of 15 pictures from at least eight independent experiments. Statistical significance was calculated by one-way ANOVA with Tukey's *post hoc* test for group comparisons. Abbreviation n.s stands for not significant ($p > 0.05$).

5.5 Discussion

Interest in the role of extracellular tau in human tauopathies has recently grown, particularly in light of the prion-like manner in which tau pathology spreads throughout the brain. Here, we have examined the cytotoxicity of various extracellular seed-competent tau species in healthy primary neural cell cultures and found no significant differences between treated and untreated cells.

To characterize tau-related cytotoxicity, we used: 1) the alamarBlue™ Cell Viability Reagent, to detect changes in neural metabolism; 2) the total cell count, to determine if the presence of seed-competent tau directly affected the number of viable cells; and 3) the proportion of neurons relative to all cells in the culture, to address whether tau was specifically toxic to neurons. Our results show that primary neural cell cultures, treated with TIF-P+ samples, contain insoluble GFP-positive tau species detectable at 10 DOT. However, it did not result in overt cellular damage at any tested time point. In Chapter 1 of this thesis, we show that TIF-P+ tau-insoluble species are seed-competent *in vitro* and trigger tau pathology *in vivo*. Taking this into account, our findings suggest that the mere presence of seed-competent tau species is not sufficient to trigger cytotoxic events, at least in our experimental model. Notably, the Tau biosensor cell line itself is not characterized by overt cellular toxicity, even in the presence of seed-competent tau (Holmes *et al.*, 2014). Nevertheless, we recognize that insoluble tau present in TIF-P+ fractions does not necessarily resemble pathological tau derived from diseased human brains (Zhang *et al.*, 2019). Therefore, it is possible that toxicity-related mechanisms associated with more physiologically relevant samples may not exist in tau species from TIF-P+ fractions.

Unexpectedly, we observed similar results when the experimental approach was changed, and primary neurons were treated with sarkosyl-insoluble fractions from P301S (+/-) mice and human AD-derived samples. Hence, our findings show that extracellular seed-competent tau obtained from more disease-relevant sources is not overly toxic to primary neural cell cultures. It should be noted, however, that tau toxicity has recently been linked to soluble tau aggregates (i.e., soluble "oligomeric" species) rather than the filamentous aggregates found in sarkosyl-insoluble fractions (Kaniyappan *et al.*, 2017; Lo *et al.*, 2019; Lo, 2021). Therefore, since our experimental approach relies on utilizing detergent-insoluble fractions, it could be argued that our samples do not include toxic tau species. Regardless, our fractions are obtained using 0.1% sarkosyl instead of 1%, the latter being the current gold standard method for producing detergent-insoluble fractions. Hence, our less restrictive conditions permit the enrichment of tau-insoluble species, as well as the presence of more "soluble" ones (i.e., "oligomers") (data not shown). Consequently, our protocol provides a more realistic ensemble of tau isoforms, despite favoring insoluble aggregates. Nevertheless, we would like to highlight that there exists a degree of uncertainty around the term "oligomer." In fact, one can find multiple definitions and protocols in the literature (Ren & Sahara, 2013; Fa *et al.*, 2016; Wegmann *et al.*, 2016; Chen & Mobley, 2019; Lo, 2021; Pampuscenko *et al.*, 2021). Therefore, we believe that generalizing that "oligomers" are more cytotoxic than monomeric tau or insoluble aggregates can be deceptive and misleading. Instead, we hypothesize that tau-induced toxicity is the product of several species acting simultaneously, and that numerous cellular pathways may contribute to neurodegeneration. Notably, recent studies have provided evidence that highly fibrillated tau rather than oligomers are toxic to the cells, proving that this issue is far from being solved (Chua *et al.*, 2017; Esteras *et al.*, 2021).

Initially, our experimental design excluded the over-expression of tau variants, since most sporadic tauopathies are not associated with increased tau protein levels, and the relevance of over-expression-mediated toxicity in transgenic systems has been debated. However, we were concerned that our inability to detect tau-related cytotoxicity was related to a "species-barrier" phenomenon between the endogenous murine tau, expressed by primary neural cell cultures, and the extracellular tau present in the P301S (+/-) and AD samples (Collinge & Clarke, 2007; Saito *et al.*, 2019). Despite our worries, human tau has been shown to induce endogenous murine tau aggregation (Katsikoudi *et al.*, 2020). Nevertheless, to eliminate that possibility, we decided to include an experimental design in which both endogenously produced and extracellular seed-competent tau were from the same organism. To this end, primary neural cell cultures

were virally transduced with AAVs to over-express full-length human tau bearing the P301L mutation and were treated or not with sarkosyl-insoluble samples from P301S (+/-) mice for comparison. Notably, primary neurons over-expressing P301L tau alone do not display insoluble tau inclusions at 16 DIV. Contrastingly, virally transduced cells treated with sarkosyl-insoluble fractions from P301S (+/-) mice result in a small number of neurons displaying a strong fluorescence signal filling their cytoplasm (i.e., recognized by the human-specific anti-tau antibody HT7). Hence, the over-expression of P301L tau is not sufficient to trigger the formation of non-soluble inclusions, and extracellular seed-competent tau is required for this to occur. This finding is consistent with previous research showing that primary neural cell cultures and organotypic slices derived from transgenic animals over-expressing aggregation-prone tau fail to develop insoluble aggregates unless cells are also treated with extracellular tau (Stancu *et al.*, 2015; Wu *et al.*, 2016; McCarthy *et al.*, 2021).

It is worth remaking that transgenic rodent models of familial FTD-associated mutations, for instance, P301S (Allen *et al.*, 2002) or P301L (Terwel *et al.*, 2005), naturally exhibit robust tau pathology. Therefore, it could be surprising that we did not detect insoluble aggregates in neurons over-expressing P301L without any additional tau treatment. However, it should be noted that the detection of aberrantly phosphorylated tangle-like pathology (e.g., AT8-positive aggregates) in the brain of these transgenic mice starts at around 8 to 9 months of age (Allen *et al.*, 2002; Iba *et al.*, 2015; Jackson *et al.*, 2016). Hence, our findings have been remarkably close to what is known to happen *in vivo*, and thus, it is possible that more time is needed to observe the formation of insoluble aggregates in these neurons transduced to over-express P301L tau.

Finally, contrary to our expectations, the integrity of cellular metabolism was not altered in cell cultures virally transduced to over-express P301L and treated with P301S (+/-) samples compared to the other conditions tested. Likewise, we did not find differences in the total number of cells or the proportion of Neurons/Nuclei at 10 DOT between treatments. Therefore, we conclude that cell viability is not affected by the combination of the over-expression of P301L and the addition of extracellular seed-competent tau. However, it is worth noting that we only detected considerable HT7 labeling in 5% to 10% of the cultured neurons. Notably, similar percentages were reported in a prior study in which the authors also combined endogenous over-expression of mutated tau with extracellular seed-competent species (Stancu *et al.*, 2015). Remarkably, Stancu and colleagues found that these few neurons were sufficient

to cause significant changes in overall neuronal activity compared to untreated cells, which were not significantly altered. The authors concluded that only minute amounts of insoluble tau are required to impact the neuronal network of cultured cells. Taking this into account, it is possible that a small number of neurons with insoluble tau may be enough to generate neural activity alterations, but not to produce detectable changes in cell viability. Therefore, future research should focus on increasing the number of cells with insoluble inclusions to determine whether the presence of insoluble tau and cytotoxicity are related.

Despite our results contradicting previous research (Kuret *et al.*, 2005; Bandyopadhyay *et al.*, 2007; Messing *et al.*, 2013), multiple, although not necessarily incompatible, reasons could explain these inconsistencies. However, it is pertinent to note that in the studies of tau-related cytotoxicity, there is a lack of uniformity regarding the experimental models employed, the standards for toxicity assessments, as well as the procedures and sources for obtaining seed-competent tau species. Therefore, it does not come as a surprise that even in the literature, there are conflicting results.

The toxic effects of extracellular tau have been shown in mammalian cell lines (e.g., SH-SY5Y, N2a, and HEK-293) (Gomez-Ramos *et al.*, 2006; Khlistunova *et al.*, 2006; Flach *et al.*, 2012; Kaufman *et al.*, 2016). However, although the use of immortalized cell lines is advantageous in certain experimental paradigms, we, and others (Crowe *et al.*, 2020), believe that there may be some disparities regarding their cytotoxic vulnerability compared to primary neurons. While the physiological relevance of these findings is unclear, they are supported by more recent, albeit limited, results showing that extracellular tau is also toxic in primary neural cell cultures (Kim *et al.*, 2015; Pampuscenko *et al.*, 2021). Yet again, in most cases, the authors used recombinant tau, which, as previously stated, does not resemble the actual aggregates from diseased brains and, consequently, may exhibit unique biological activities (e.g., toxicity mechanisms) (Mocanu *et al.*, 2008; Fichou *et al.*, 2018; Zhang *et al.*, 2019). Therefore, since most of our samples were obtained from diseased brains (i.e., from P301S (+/-) mice and human AD), we are confident that, despite the lack of conclusive results, our model represents a more translationally relevant approach.

Having said that, previous studies have shown that extracellular tau does not influence cell viability in their experimental models, which is consistent with the findings reported in this chapter. For instance, Kaniyappan and colleagues found that, even at high concentrations, seed-competent extracellular tau causes synaptotoxicity without apparent cell death in SH-SY5Y cells or primary cortical neurons (Kaniyappan *et al.*,

2017). Likewise, (Takeda *et al.*, 2015; Hallinan *et al.*, 2019; Crowe *et al.*, 2020; Katsikoudi *et al.*, 2020) found no changes in neuronal viability following “pathological” tau treatment. More recently, similar results have been reported for organotypic slices (McCarthy *et al.*, 2021). McCarthy and colleagues, for example, were unable to detect cell death employing even higher extracellular tau concentrations than those used in this thesis (McCarthy *et al.*, 2021). Nevertheless, it is also possible that seed-competent tau is not necessarily neurotoxic to the cells and that other tau species are responsible for neuronal cell death (Jackson *et al.*, 2016).

As discussed in Chapter 2, it is also possible that embryonic neurons are not suitable models for examining certain aspects of tau pathology, such as cellular toxicity; mainly because of their higher intrinsic resistance to external disturbances (Estevez-Priego *et al.*, 2020). This argument is consistent with the findings of (Ferrer *et al.*, 2022a), in which the authors found that 3 months after inoculating tau derived from patients with AD into newborn and 3-month-old wild-type mice, the former had minimal tau aggregates compared to the latter. Ferrer and colleagues concluded that variations in tau seeding could be attributed to differences in tau isoform expression, as well as neural connections in newborn mice. Taking this into account, it seems plausible that the inability to detect cellular toxicity originates in our experiments originates from the model itself. However, many of the alternative methods in the literature rely on the over-expression of aggregation-prone tau species, which may have limited reliability and validity given the lack of success in developing novel therapies. The publication bias to report statistically significant results may be partially responsible for that. We suggest that future studies should re-examine tau toxicity using wild-type expression models and samples derived from brain material.

In this regard, it should be mentioned that aging is the greatest risk factor for sporadic AD and other NDs, as most of them develop over years or even decades (Braak & Braak, 1991). Furthermore, the timing at which initial tau misfolding leads to cellular degeneration, tangle formation, and cytotoxicity is unknown. Therefore, the lack of neuronal toxicity observed by us and others may reflect the decade-long progression of tau disease in humans. Consequently, tau-induced toxicity may require extended incubation times to cause neurodegeneration, which is impossible to assess in the lifespan of primary neural cell cultures. Further work will be required the development of better disease-relevant cellular models with increased survival times to study the long-term effect of seed-competent extracellular tau on neural viability.

In summary, in this chapter, we discuss the potential cytotoxic effects of various seed-competent tau species in primary neural cell cultures and find no difference in cell viability compared to untreated controls. Our work is different from previous research in the sense that our experimental approach included healthy primary neurons, which more closely represents the sporadic nature of human tauopathies. We used tau seeds derived from diverse sources in an attempt to compare their effects. Notably, our experimental design involved a time-course examination of tau toxicity, which is rarely reported in the literature. Finally, we encourage others to include similar approaches to those used in the present study in their investigations, as we believe that, although they may not provide significant results, disease-relevant models may be a step forward in understanding the lack of success regarding tau-directed therapies.

Chapter 4: Involvement of the PrP^C in Tau Uptake, Seeding, and Spreading: An *In Vivo* Approach

6.1 Introduction

As indicated in the Introduction, human tauopathies are clinically, biochemically, and heterogeneously NDs characterized by the deposition in specific brain regions of the abnormally misfolded and aggregated tau (e.g., (Braak & Del Tredici, 2015; Kovacs, 2017; Hoglinger *et al.*, 2018; Shi *et al.*, 2021). Each tauopathy has a unique clinicopathologic phenotype defined by: a) the types of tau deposits (i.e., 3R- or 4R-tau); b) the aggregation status of tau species (e.g., puncta, granular, diffuse, or fibrillar); and c) the affected brain regions and cells, the latter including neurons, astrocytes, and oligodendrocytes (Rohan *et al.*, 2016; Kovacs, 2017; Hoglinger *et al.*, 2018; Ferrer *et al.*, 2019; Rosler *et al.*, 2019; Shi *et al.*, 2021). Tau aggregates are found in sporadic and familial AD, in association with Aβ; certain prion diseases, as in GSS; and in pure forms, either sporadic, as in PART, ARTAG, PSP, AGD, and GGT, or linked to familial mutations in the *MAPT* gene: FTLD-tau (Cervos-Navarro & Schumacher, 1994; Nishimiya & Yuasa, 1999; Probst & Tolnay, 2002; Kovacs, 2017; Kovacs *et al.*, 2017b; Ferrer *et al.*, 2018; Hoglinger *et al.*, 2018; Kovacs *et al.*, 2018; Matamoros-Angles *et al.*, 2018; Forrest *et al.*, 2021).

Human tauopathies are characterized by exhibiting a trans-regionally spreading proteinopathy, resulting in stereotyped spatiotemporal progression patterns (De Leon & Braak, 1999; Goedert *et al.*, 2017b; Arnsten *et al.*, 2021). In fact, a recent study suggests that the neuronal transmission of tau in 4R tauopathies is linked to synapses, whereas the oligodendroglial and astroglial tau inclusions may be linked to further uptake of tau released by degenerating neurons (Gilvesy *et al.*, 2022). This notion contrasts with the active role of oligodendrocytes in tau phosphorylation shown in other studies (Ferrer, 2018; Ferrer *et al.*, 2019). Far from this controversy, after the inoculation of “pathological”-containing samples in mouse brains, aberrantly phosphorylated tau aggregates (e.g., AT8-positive) emerged both at the injection sites and in connected brain regions (e.g., (Clavaguera *et al.*, 2017; Del Rio *et al.*, 2018)). Thus, this approach has been used to elucidate the mechanisms of cell uptake, seeding, and brain propagation of different tau species or strains, as well as the role of endogenous tau in these processes (Ferrer *et al.*, 2014; Ferrer *et al.*, 2020; Andres-Benito *et al.*, 2022; Ferrer *et al.*, 2022a). However, a complete explanation of these processes is unavailable for all tau isoforms and different tauopathies (Hoglinger *et al.*, 2018), particularly when affected cells are other than neurons (Ferrer, 2022).

In view of the different mechanisms of uptake of misfolded proteins (i.e., see (Del Rio *et al.*, 2018) and General Introduction for details), receptor-mediated uptake therapy is a current target of pharmacological and therapeutic research. In this regard, a recent study reported the existence of shared neuronal receptors for tau, Aβ, and α-syn (Ondrejcak *et al.*, 2018). Among others, LRP1 (A *et al.*, 2020; Rauch *et al.*, 2020) and PrP^C (Corbett *et al.*, 2020; Legname & Scialo, 2020) have been identified as functional neuronal receptors of tau in some experimental models. The PrP^C is a cell surface GPI-anchored protein expressed in several tissues with particularly high levels in the nervous system (Ford *et al.*, 2002; Su *et al.*, 2004), in which it is expressed by neurons and glial cells (Moser *et al.*, 1995; Adle-Biassette *et al.*, 2006; Lima *et al.*, 2007; Bribian *et al.*, 2012). PrP^C is known for its crucial role in the pathogenesis of human and animal PrDs (Prusiner & DeArmond, 1994; Aguzzi, 2000; Baldwin & Correll, 2019). In these diseases, physiological PrP^C is transformed into a misfolded, β-sheet-rich isoform known as the "infectious prion protein" (i.e., PrP^{Sc}) (Prusiner & DeArmond, 1994).

The increasing knowledge of PrP^C participation in prion pathogenesis contrasts with the puzzling data regarding its natural physiological role, probably related to its molecular pleiotropy or specific interactions (Griffoni *et al.*, 2003; Linden *et al.*, 2008; Legname, 2017; Wulf *et al.*, 2017; Watts *et al.*, 2018; Gavin *et al.*, 2020). As mentioned in the General Introduction, the PrP^C contains the HR, CC2, and CC1 (i.e., a schematic representation of PrP^C can be found in the General Introduction, Section 1.3.4, Figure 6), which are thought to be involved in binding to different "oligomeric" species (i.e., scrapie prions and Aβ/α-syn, respectively) (Resenberger *et al.*, 2011; Resenberger *et al.*, 2012; Ferreira *et al.*, 2017), reviewed in (Del Rio *et al.*, 2018)). From histopathological studies, we know that PrP^C is localized in dystrophic neurites and amyloid plaques in advanced AD (Takahashi *et al.*, 2011; Takahashi *et al.*, 2021; Zhang *et al.*, 2021). Therefore, although the interaction between amyloid proteins and PrP^C has been previously described (i.e., see for Aβ (Lauren *et al.*, 2009), α-syn (Ferreira *et al.*, 2017; Thom *et al.*, 2022), or tau (Ondrejcak *et al.*, 2018)), their participation in tau seeding and spreading is still elusive. In this regard, three recent studies suggest that PrP^C may bind to tau, but its role in tau seeding and spreading was not analyzed (Corbett *et al.*, 2020; De Cecco *et al.*, 2020; Legname & Scialo, 2020). Finally, given that a subsequent study noted that PrP^C cannot bind to α-syn (La Vitola *et al.*, 2019) in contrast to prior research (Aulic *et al.*, 2017; Ferreira *et al.*, 2017; Urrea *et al.*, 2018; Rosener *et al.*, 2020; Thom *et al.*, 2022), we consider that this putative interaction between PrP^C and tau merits further study *in vivo*.

6.2 Objective

The principal objective of this chapter is to evaluate the role of PrP^C in the uptake, seeding, and spreading of tau pathology *in vivo* in wild-type and transgenic PrP^C mice.

6.3 Materials and Methods

6.3.1 Ethical Statement

All animals were kept in the animal facility of the Faculty of Pharmacy at the University of Barcelona under controlled environmental conditions and were provided with food and drink *ad libitum*. Animal care and experimental protocols were performed in compliance with the CEEA of the University of Barcelona. All housing, breeding, and procedures were performed under the guidelines and protocols OB47/19, C-007, 276/16, and 47/20 of CEEA.

6.3.2 Mice

The following mice were studied: a) Adult C57BL/6J (i.e., wild-type) mice were purchased from Charles River Laboratory. b) Tau knock-out (KO) mice (Dawson *et al.*, 2001) (a kind gift from Dr. Jesús Ávila, CBM-UAM, Madrid). c) Zürich-III-*Prnp*$^{-/-}$ (ZH3) mice (i.e., *Prnp* KO) (Nuvolone *et al.*, 2016) (a generous gift from Prof. Adriano Aguzzi, Institute of Neuropathology, University Hospital of Zürich, Zürich). d) Tg44 mice over-expressing the secreted form of PrP^C lacking the GPI anchor (Chesebro *et al.*, 2005) (kindly provided by Vincent Beringue, INRA UR892, Virologie Immunologie Moléculaires, Paris).

6.3.3 Human Samples

This chapter included frozen material from an autopsy-proven, neuropathologically well-characterized case of AD. We used brain-derived material from one male patient, who was 93 years old, and a 3 h delay in post-mortem inspection.

6.3.4 Preparation of Sarkosyl-Insoluble Fractions from Human Samples

Please see Chapter 1, Materials and Methods, Section 3.3.7.

6.3.5 Standard Tau Biosensor Cell Line Seeding Assay

Please see Chapter 1, Materials and Methods, Section 3.3.11.2.

6.3.6 Transmission Electron Microscopy Imaging

Please see Chapter 1, Materials and Methods, Section 3.3.6.

6.3.7 Biochemical Analysis

Please see Chapter 1, Materials and Methods, Section 3.3.9. The primary antibody used was the mouse anti-PrP 6H4 (1:5,000) (Prionics, catalog no. 01-010).

6.3.8 Stereotaxic Surgery

For surgery, 3- to 4-month-old wild-type (n = 11), Tau KO (n = 3), ZH3 (n = 7), and Tg44 (n = 14) mice were anesthetized with 1.5% isoflurane and placed in a stereotaxic apparatus (Kopf Instruments, California, United States of America). Mice were unilaterally injected with 2.5 µL sarkosyl-insoluble human-derived samples into the right hippocampus (AP: -1.4 mm from bregma; LM: +1.5 mm; DV: -1.5 mm) using a Hamilton syringe. Following the injection, the needle was kept in place for an additional 3 min before the withdrawal. The surgical area was cleaned with sterile saline, and the incision was sutured. Mice were monitored until recovery from anesthesia and were checked regularly following surgery.

6.3.9 Tissue Processing and Immunohistochemistry

After 3 (wild-type (n = 6), Tau KO (n = 3), ZH3 (n = 5), Tg44 (n = 7)) and 6 (wild-type (n = 5), ZH3 (n = 2), Tg44 (n = 7)) months post-injection (m.p.i), mice were terminally anesthetized and transcardially perfused, using a peristaltic infusion pump, with 0.1 M PBS, followed by 4% PFA. Next, brains were removed and post-fixed in 4% PFA overnight at 4°C. Finally, brains were changed to 70% ethanol and stored at 4°C until inclusion. Following paraffin embedding, 10 µm coronal sections were cut from the brain tissue of seeded mice and mounted on glass slides.

For IHC, paraffin-embedded tissue sections were deparaffinized in xylene for 20 min and rehydrated through a series of ethanol solutions from 100%, 90%, 80%, and 70%, followed by H_2O, submerging the sections for 5 min each step. Antigen retrieval for IHC was performed with a PT link machine (Pre Treatment Link, DAKO, Agilent, Santa Clara, United States of America), following the manufacturer's instructions. Briefly, sections were treated for 20 min at 97°C with high-pH Tris-EDTA, pH 9 antigen retrieval buffer. After rinsing sections in 0.1 M PBS, endogenous peroxidase activity was quenched with 2% H_2O_2 and 10% methanol for 15 min and blocked for 1 h in blocking solution [10%

NHS, 0.1% Triton X-100, and 0.015 g/mL glycine in 0.1 M PBS containing 1% BSA]. All primary antibodies were diluted in antibody solution [5% FBS, 0.1% Triton X-100, and 0.02% azide in 0.1 M PBS] overnight at 4°C. For bright-field visualization, tissue sections were then rinsed in 0.1 M PBS, and incubated for 2 h at room temperature with species-specific biotinylated secondary antibody (1:200) (Vector Laboratories) in 0.1 M PBS. To reveal immunoperoxidase labeling, sections were incubated with the avidin-biotin-peroxidase complex (ABC) kit (Vector Laboratories), followed by development with 0.03% 3-3'-diaminobenzidine (DAB) with the addition of H_2O_2. For fluorescence staining, sections were rinsed in 0.1 M PBS and incubated with species-specific secondary antibodies Alexa Fluor 488 or 568 (1:300) (Life Technologies) for 2 h at room temperature. Stained sections were viewed using an Olympus BX43 Upright Microscope (Olympus) equipped with a DP12L-cooled camera.

The following primary antibodies were used: mouse anti-AT8 (1:50) (ThermoFischer Scientific, catalog no. MN1020), rabbit anti-TauphosphoSer422 (pSer422) (1:75) (Life Technologies, catalog no. 44-764G), mouse anti-6H4 (1:1,000) (ThermoFischer Scientific, catalog no. 01-010), human tau-specific anti-Tau-13 (1:200) (Biolegend, catalog no. 835201), murine tau-specific antibody anti-T49 (1:200) (Merck Millipore, catalog no. MABN827), murine anti-3R-tau (1:50) (Merck Millipore, catalog no. 05-803), murine anti-4R-tau (1:50) (Merck Millipore, catalog no. 05-804), rabbit anti-Olig2 (1:400) (Merck Millipore, catalog no. AB9610), rabbit anti-GFAP (1:500) (Dako, catalog no. Z0334), rabbit anti-Iba1 (1:500) (FUJIFILM Wako, catalog no. 019-19741).

6.4 Results

6.4.1 Evaluation of Sarkosyl-Insoluble Fraction Derived from One Human Patient with AD

It is well known that the inoculation of seed-competent tau into the brain of murine models induces the formation of tau-related lesions near the injection site and into synaptically connected brain areas (Clavaguera *et al.*, 2009; Iba *et al.*, 2013; Ferrer *et al.*, 2022a). Hence, it is possible to investigate what role different molecules may play in pathology. In the present work, we aimed to determine whether PrP^C plays a leading role in the seeding and spreading of seed-competent tau. Analogous to the previous chapters of this thesis, here we employed an experimental approach that better mimicked the situation of sporadic tauopathies. Consequently, we used sarkosyl-insoluble fractions from one human patient with AD (i.e., from now on, AD-tau) and mouse models with a different burden of PrP^C but with endogenous expression of the tau protein.

Our primary goal was to characterize AD-tau to demonstrate its suitability for inoculation. First, we decided to explore by immunoblotting the presence of aberrantly or "pathologically" phosphorylated tau in the sarkosyl-insoluble sample using the anti-tau pSer422 antibody. Figure 30A shows the classical bands between 55 kDa and 68 kDa expected for tau protein, indicating the existence of "pathological" tau in the sarkosyl-insoluble samples. Next, we confirmed the presence of NFT fibrils by negative staining at TEM (Figure 30B). Finally, we validated the seeding efficacy of the AD-tau inoculum using the Tau biosensor cell line (Figure 30C).

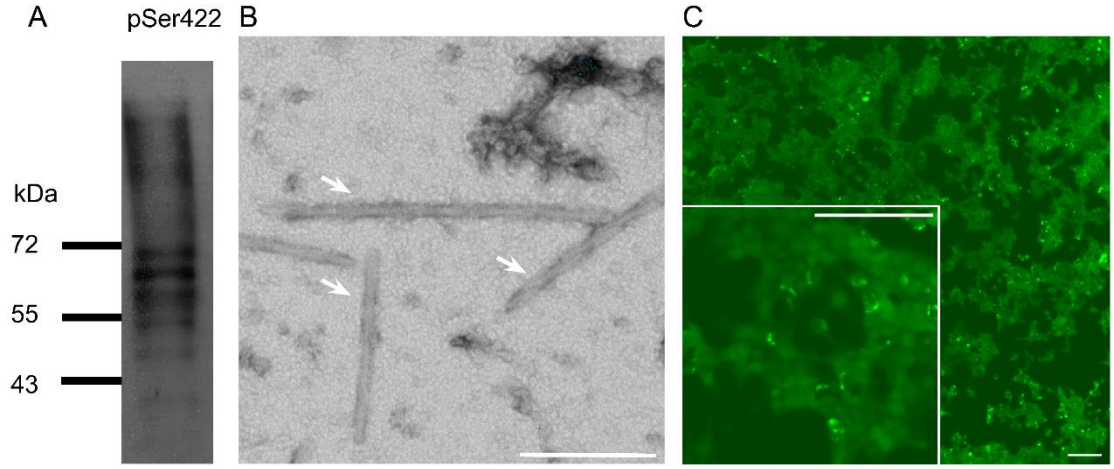

Figure 30 Characterization of the sarkosyl-insoluble fraction used for the inoculation: A) Western blotting (WB) analysis of AD-tau using the anti-pSer422 antibody. The typical discrete bands between 55 kDa and 66 kDa can be clearly recognized (e.g., see also (Ferrer *et al.*, 2022a)). **B)** Transmission electron microscope (TEM) images after negative staining of AD-tau. White arrows indicate the presence of paired helical filaments (PHF) typical of AD-diseased brains. Scale bar, 200 nm. **C)** The Tau biosensor cell line was transduced with AD-tau to evaluate its seeding potency. The formation of fluorescent inclusions demonstrates that the sarkosyl-insoluble fraction contains seed-competent tau species. Scale bars, 100 µm.

6.4.2 Evaluation of the PrP^C Expression in the Brain of Wild-Type, Tg44, and ZH3 Mice

As previously stated, in this chapter, we used four mouse strains to assess the role of PrP^C in the seeding and spreading of tau pathology. Figure 31A illustrates the differential expression of PrP^C in our murine models. Tg44 mice express PrP^C lacking the GPI anchor, and so, the protein is found in the extracellular space. Since the ZH3 strain is PrP^C KO, the protein is not produced at all. In wild-type and Tau KO animals, PrP^C is expressed on the cell membrane, where it performs its physiological functions.

To validate our *in vivo* models, we determined the expression of PrP^C in their brain tissue. First, we studied the localization of the PrP^C protein in each strain. Tg44 and ZH3 mice did not show positive labeling in IHC using the PrP^C-targeting 6H4 antibody, while a strong signal was seen in wild-type animals (Figure 31B). Tau KO mice revealed similar patterns to those detected in wild-type animals (data not shown). In detail, for Tg44 mice, pale homogeneous cell labeling was found in all hippocampal layers, including the hippocampal fimbria. In wild-type mice, robust neuropil labeling of PrP^C was observed in the CA1 region of the hippocampus proper, with lower levels in the CA3 and dentate gyrus. Notably, the most marked staining was found in the stratum lacunosum-moleculare of the CA1, with the hippocampal white matter exhibiting the highest staining levels. We confirmed our histological findings by immunoblotting using the anti-6H4 antibody. The results revealed the existence of the three typical bands in wild-type mice (Figure 31C), which correspond to the different glycosylated and unglycosylated forms of PrP^C. In contrast, the analysis of Tg44 mice exhibited only the two lower bands corresponding to PrP^C lacking the GPI anchor, previously described by (Chesebro *et al.*, 2005), whereas no labeling was found for the ZH3 strain.

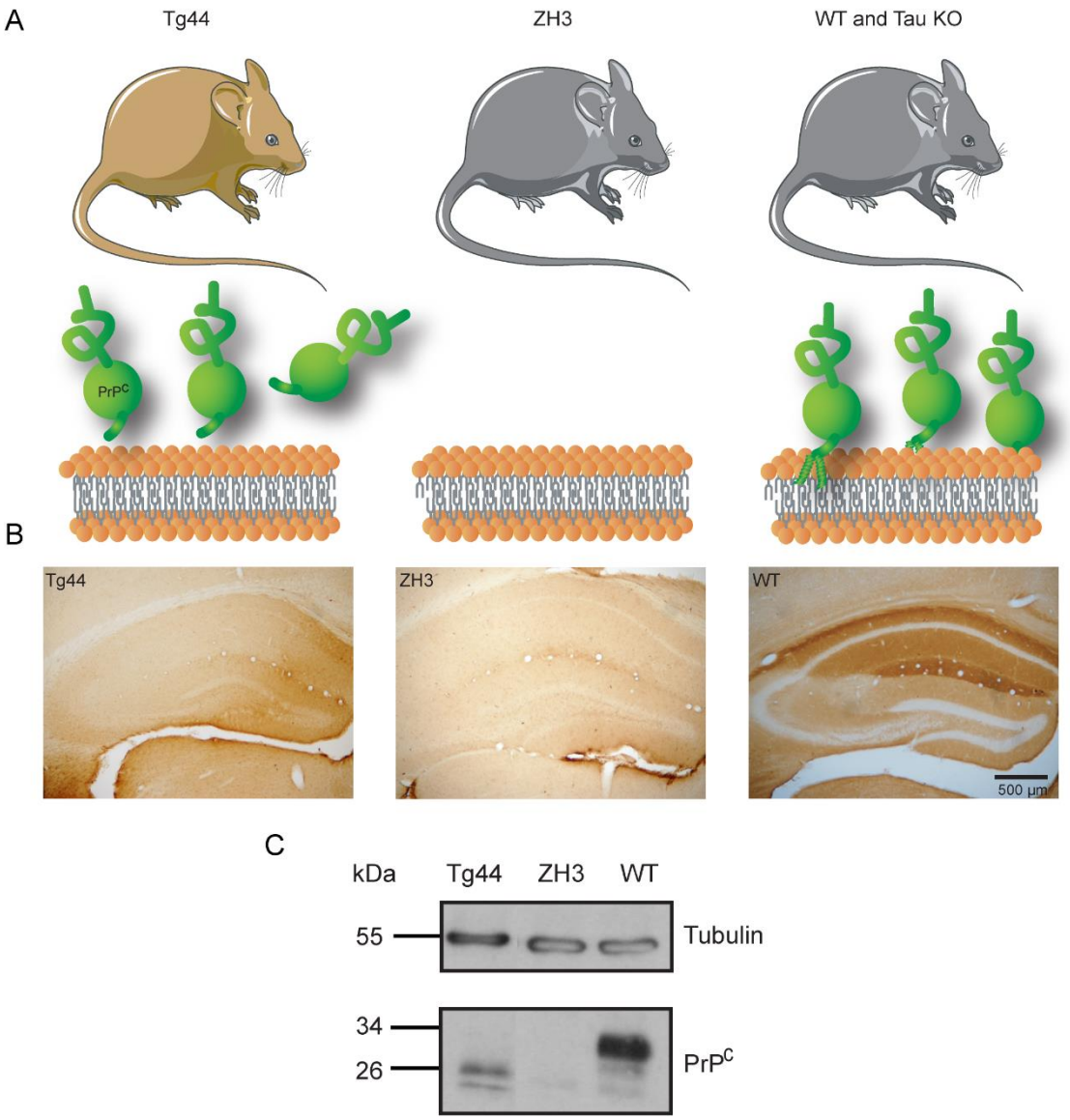

Figure 31 PrP^C expression in the hippocampus of the different mouse strains used in this chapter: A) Schematic representation of the differential PrP^C expression in the mouse strains used in this chapter. In Tg44 animals, PrP^C is located in the extracellular space. The ZH3 strain does not express PrP^C. In WT and Tau KO mice, the protein is found in the cell membrane of brain cells. **B)** Representative low-power photomicrographs showing the distribution of PrP^C. Brown DAB staining reveals the expression of PrP^C only in WT, associated with the neuropil and absent in the principal layers. No detectable signal is observed in ZH3 and Tg44 tissue sections. Scale bar, 500 µm. **C)** Western blot (WB) characterization of PrP^C variants expressed by the three mouse strains. As expected, WT mice exhibit the typical three bands of unglycosylated or glycosylated PrP^C. The characteristic GPI-less bands are seen for Tg44. Finally, there is no PrP^C-positive signal for ZH3. Tubulin was used as a loading control on the same gel.

6.4.3 Uptake, Seeding, and Propagation of AT8-Positive Tau after AD-Tau Inoculation Is Not Affected by the Absence of PrP^C nor by the Extracellular Presence of PrP^C

At 3 m.p.i and 6 m.p.i, mice were sacrificed and processed for IHC using the anti-AT8 antibody to evaluate the levels of tau seeding and spreading induced by the presence of AD-tau (Figure 32). Except for the Tau KO mice, we observed AT8-positive labeling in all mouse strains at 3 m.p.i and 6 m.p.i. The lack of staining in the Tau KO strain indicates that endogenous murine tau is necessary for the seeding and spreading of exogenous human tau (Figure 32A). In parallel, for the other mice strains, most AT8-positive inclusions were observed in the ipsilateral hippocampus and corpus callosum of all AD-tau-injected mice. Nevertheless, extremely limited AT8 reactivity was detected in the ipsilateral hippocampus, where a few cells could be distinguished (data not shown). Notably, the distribution of AT8 labeling in the corpus callosum was similar between phenotypes and almost identical in all examined mice. Moreover, we found similar levels of AT8-positive inclusions at 6 m.p.i (Figure 32B) to those observed at 3 m.p.i (Figure 32A). There was, however, a slight decrease in the expansion of AT8-positive labeling in the white matter of some animals, perhaps related to phagocytic processing at extended times post-inoculation.

It is worth mentioning that for pathogenic prion propagation experiments, the presence of the extracellular form of PrP^C (i.e., as in Tg44 mice) is linked to the blockage of the inoculated PrP^C, with the appearance of PrP^{Sc} inclusion but decreased neurodegeneration (Chesebro *et al.*, 2005; Baumann *et al.*, 2009). As previously stated, we aimed to determine whether, in Tg44, the extracellular presence of PrP^C lacking its GPI anchor could change or modify the seeding and propagation of AD-tau. Surprisingly, the extracellular presence of the GPI-less PrP^C was not robust enough to block the seeding and further spreading of exogenous seed-competent tau after inoculation (Figure 32). Although other possibilities can be considered when compared to PrP^{Sc} spreading, the lack of blockage could be associated with a putatively low presence of extracellular PrP^C in contrast to the inoculated sarkosyl-insoluble fraction.

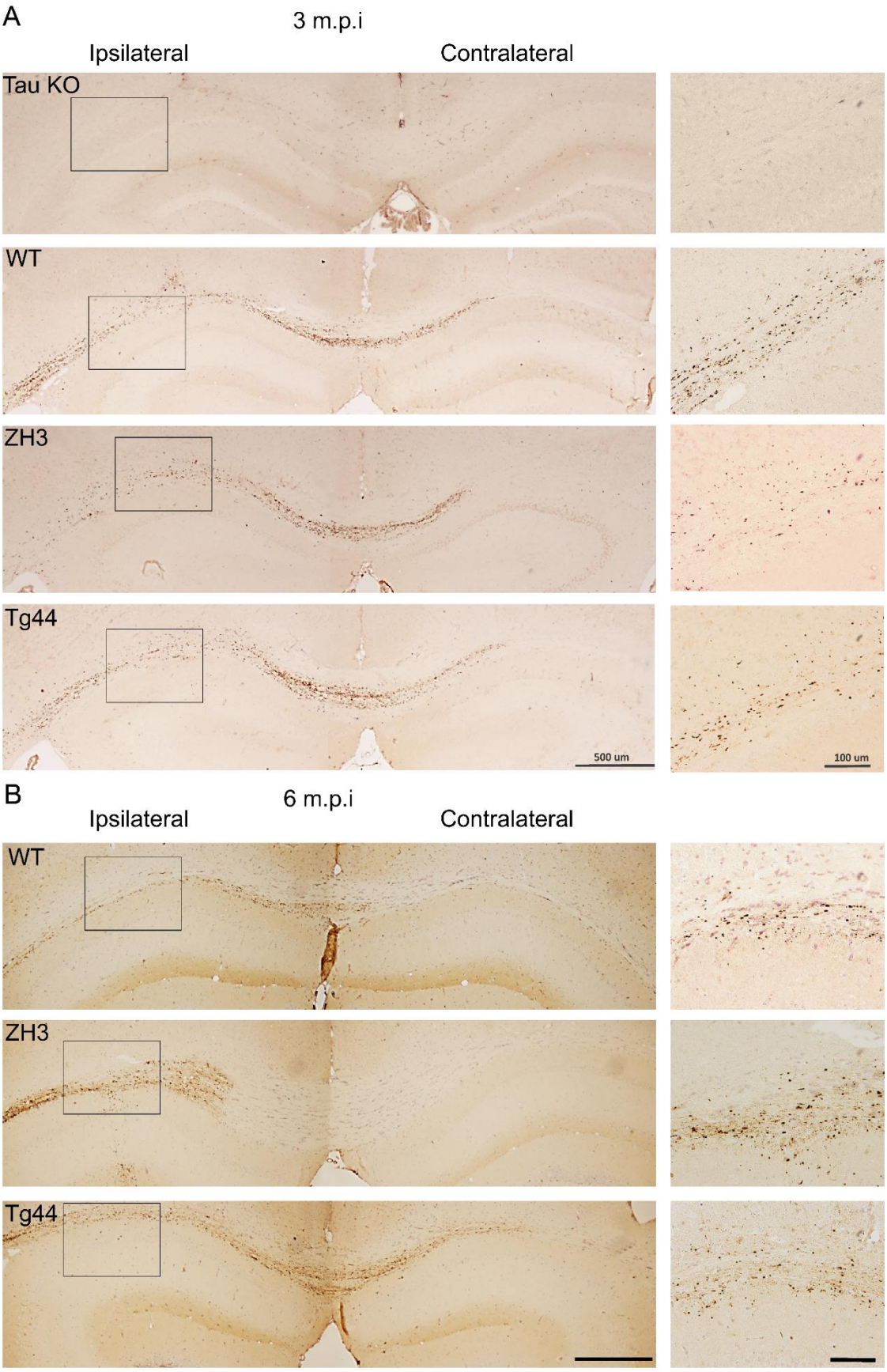

Figure 32 Distribution of AT8-positive inclusions in AD-tau inoculated mouse strains at 3- and 6-months post-inoculation (m.p.i): *Figure 32 continued on next the page*

Figure 32 continued

A) Representative immunostaining with AT8 antibody of inoculated mouse strains with AD-tau at 3 m.p.i. Higher magnification of the boxed regions can be seen in the right panels. The inoculated ipsilateral and contralateral hemispheres are shown. Tau KO mice were used as internal controls, indicating that endogenous tau is required for seed formation. **B)** Representative immunostaining with AT8 antibody of inoculated mouse strains with AD-tau at 6 m.p.i. Higher magnification of the boxed regions can be seen in the right panels. The ipsilateral and contralateral hemispheres are shown. Low-power view scale bar, 500 µm. High-power view scale bar, 100 µm.

6.4.4 "Pathologically" Phosphorylated Tau in AD-Tau Inoculated Mice Is Composed of Endogenous Murine Tau

As discussed in the previous section, the absence of endogenously expressed murine tau impairs the formation of AT8-positive inclusions in the inoculated Tau KO strain (Figure 33). Notably, in the past, it has been proven that inoculated AD-tau is almost absent in the brains of injected mice two weeks after inoculation (e.g., see also (Ferrer *et al.*, 2022a) for details). Nevertheless, to further eliminate the possibility that residual AD-tau was present in the brain tissue of the examined mice, we performed double-labeling using anti-pSer422 and the human-specific anti-Tau-13 antibody (Figure 33A) or the murine-specific anti-tau T49 antibody (Figure 33B). The results probed the absence of human tau in the phosphorylated inclusions, confirming that the aggregates were formed of endogenously expressed murine tau. Notably, we consistently observed colocalization between pSer422 and T49 (Figure 33B) in all tested cases. For clarity, the data presented in Figure 33 display the tissue derived from one wild-type mouse at 3 m.p.i; however, identical results were seen for all strains at both 3 m.p.i and 6 m.p.i (data not shown). We never observed positive labeling in Tau KO-derived samples (data not shown). Together, our findings indicate that the "pathologically" phosphorylated tau (i.e., either AT8- or pSer422-positive inclusions) detected in the brain tissue of inoculated mice is indeed endogenously expressed murine tau probably recruited by AD-tau. Interestingly, this suggests that the phosphorylation of newly formed inclusions is an active process that may involve several kinases.

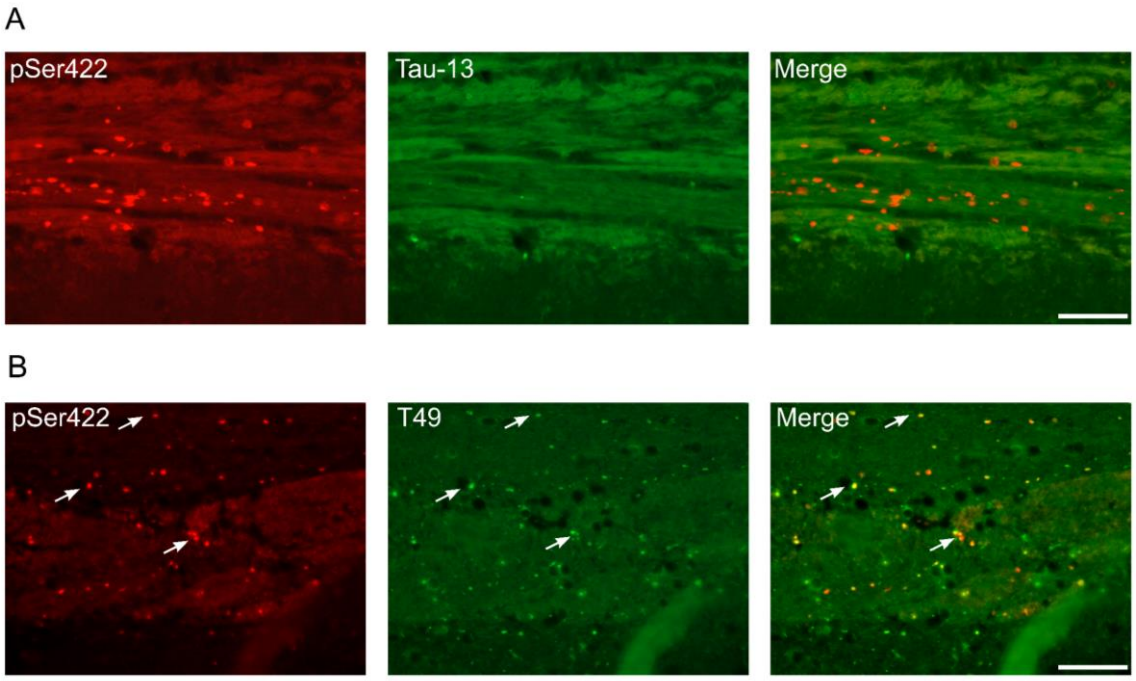

Figure 33 AD-tau inoculation triggers endogenous murine tau to aggregate and eventually be phosphorylated in "pathologically" related residues at 3 months post-inoculation (m.p.i): A) Representative fluorescence microscopy micrographs showing double-immunolabeled brain tissue sections with pSer422 (red) and Tau-13 (green) antibodies. Note that there is no Tau-13 signal colocalizing with pSer422-positive inclusions. **B)** Representative fluorescence microscopy photomicrographs illustrating double-immunolabeled sections using pSer422 (red) and T49 (green) antibodies. White arrows point to examples of double-stained inclusions. Scale bars, 100 µm.

6.4.5 "Pathologically" Phosphorylated Tau Is Composed of 3R- and 4R-Tau Isoforms in AD-Tau Inoculated Mice

In the following experiments, we sought to determine whether the observed AT8- or pSer422-positive inclusions are composed of 3R- and 4R-tau (Figure 34). To address this, we double-labeled tissue sections at 3 m.p.i with anti-pSer422 and antibodies specific to 3R or 4R isoforms of tau. For clarity, Figure 34 displays tissue immunolabeling from one inoculated wild-type mouse; however, identical results were seen for all strains at both 3 m.p.i and 6 m.p.i (data not shown). We did not detect positive labeling in the Tau KO strain (data not shown), in agreement with the results from the previous section. Our findings demonstrate that the pSer422-positive inclusions formed after AD-tau inoculation are composed of 3R (Figure 34A) and 4R (Figure 34B) isoforms of tau, similar to what is observed in human patients with AD (Hoglinger *et al.*, 2018). Notably, 3R-tau isoforms do not exist in adult mice (Hernandez *et al.*, 2020). Therefore, our results suggest that the presence of extracellular seed-competent tau containing 3R- and 4R-tau aggregates has the ability to induce the expression of 3R-tau in adult mice.

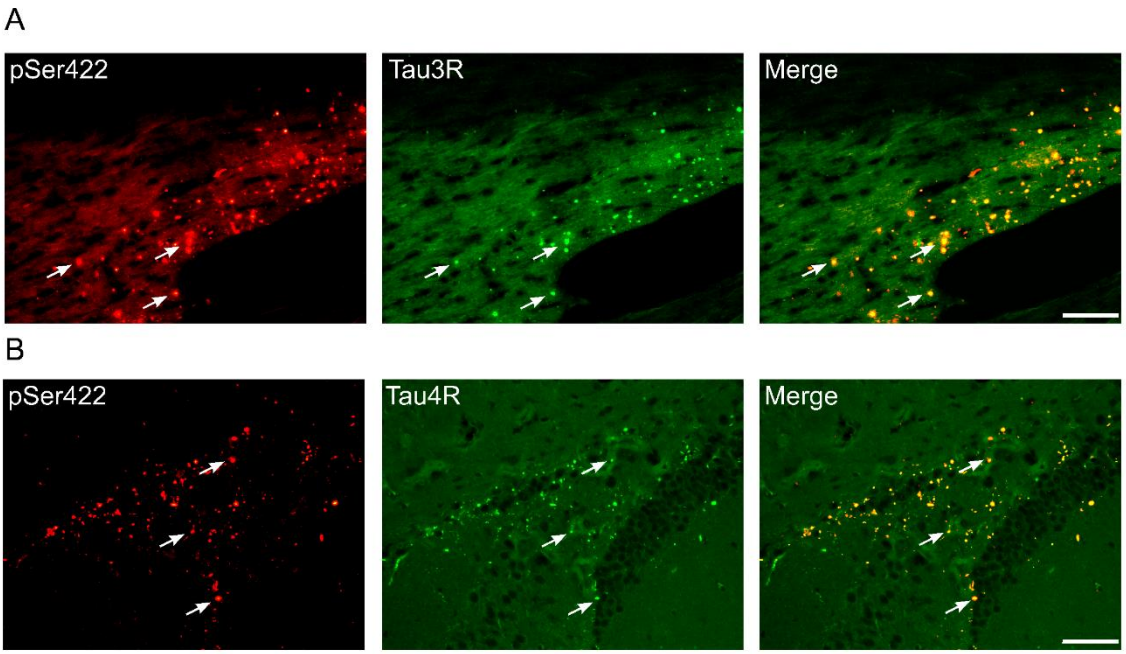

Figure 34 AD-tau-derived pSer422-positive inclusions in inoculated mice are composed of 3R- and 4R-tau isoforms at 3 months post-inoculation (m.p.i): A) At 3 m.p.i, double-labeling with anti-pSer422 (red) and anti-3R-tau (green) revealed the colocalization of "pathologically" phosphorylated tau and 3R-tau isoforms. **B)** At 3 m.p.i, double-labeling with anti-pSer422 (red) and anti-4R-tau (green) revealed the colocalization of "pathologically" phosphorylated tau and 4R-tau isoforms. White arrows point to examples of positive double-stained inclusions. Scale bars, 100 µm.

6.4.6 AT8-Positive Tau Does Not Colocalize with Glial Cells in AD-Tau Inoculated Mice, Irrespective of Their Genotype

Lastly, we were interested in determining whether "pathologically" phosphorylated inclusions formed after AD-tau inoculation were also localized in cells other than neurons (i.e., glial cells) (Figure 35). To accomplish this, we conducted double-labeling with AT8 and three different glial markers: a) Anti-Olig2, an antibody specific for the oligodendrocyte lineage (Figure 35A). b) Anti-GFAP, an astrocyte-specific marker (Figure 35B). c) Anti-iba1, an antibody that recognizes microglial cells (Figure 35C). For all tested antibodies, we found little to no colocalization with AT8-positive labeling. For clarity, Figure 35 only shows the IHCs pertaining to one wild-type animal at 3 m.p.i, although identical results were obtained for all mouse strains at both 3 m.p.i and 6 m.p.i. Taken together, our findings indicate that, since we found minimal colocalization with glial markers and AT8-positive inclusions, most "pathologically" phosphorylated tau is localized in neuronal cells.

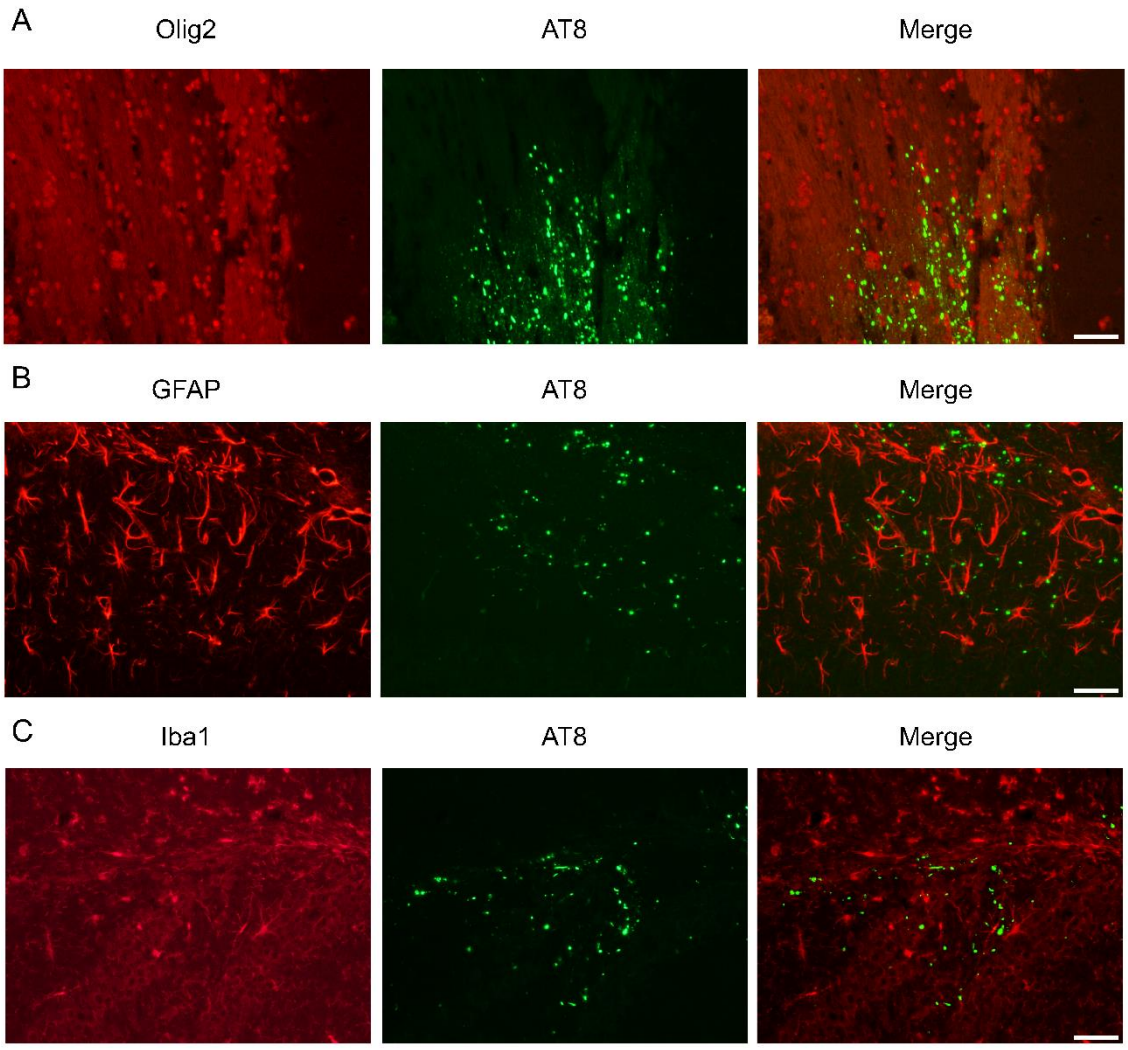

Figure 33 AT8-positive inclusions do not colocalize with glial markers: Double immunofluorescence of one wild-type animal at 3 months post-inoculation (m.p.i) with AD-tau. **A)** Olig-2 (red) and AT8 (green). **B)** GFAP (red) and AT8 (green). **C)** Iba-1 (red) and AT8 (green). In all cases, double-labeling shows no colocalization between glial markers and "pathologically" phosphorylated tau. Scale bars, 100 µm.

6.5 Discussion

PrP^C has been linked to the disease progression of various NDs, as it directly interacts with amyloid proteins, such as Aβ (Kostylev *et al.*, 2015; Scott-McKean *et al.*, 2016), α-syn (Ferreira *et al.*, 2017; Urrea *et al.*, 2018; Thom *et al.*, 2022). However, its role in tau pathology has rarely been addressed (Ondrejcak *et al.*, 2018; De Cecco *et al.*, 2020). Moreover, in these studies, the connection between PrP^C and the uptake, seeding, and spreading of tau is not reported. Herein, we show that AD-tau, inoculated into the hippocampi of three mouse strains expressing endogenous wild-type tau but with distinct presence of PrP^C (i.e., physiological, extracellular, or null), seeds and spreads irrespective of the mouse genotype. Therefore, our findings show that, although we

cannot rule out a possible interaction between these two proteins, PrP^C is not required for either the initialization or progression of tau pathology.

In the current work, we decided to inoculate sarkosyl-insoluble fractions from one human patient diagnosed with AD that contained “pathological” tau species that better recapitulate the heterogeneity of aggregates found in sporadic human tauopathies. In this regard, we first analyzed the existence of typical pathogenic characteristics in these fractions by immunoblotting analysis to reveal the presence of “pathologically” phosphorylated tau residues with the pSer422 antibody. Next, we proved that AD-tau contained PHF via TEM. Finally, we determined the fraction’s seeding potency with the Tau biosensor cell line. Together, our results show that the sample used in our work featured three significant characteristics of what is generally defined as “pathological” tau (Kovacs, 2017).

Having validated the suitability of the AD-tau sample, we then moved to corroborate the differential expression of PrP^C in our mouse strains. As expected, only wild-type and Tau KO mice exhibited detectable levels of PrP^C in tissue sections revealed by IHC using the anti-6H4 antibody. These results were further corroborated by WB, in which wild-type and Tau KO animals produced the normal band pattern of unglycosylated, monoglycosylated, and diglycosylated PrP^C, while Tg44 featured two lower bands (i.e., as previously described by (Chesebro *et al.*, 2005)), and ZH3 did not display any bands at all (Nuvolone *et al.*, 2016). Again, our results demonstrate that these mouse strains are suitable for addressing the role of PrP^C in the seeding and spreading of tau pathology *in vivo*.

We inoculated AD-tau into the hippocampus of all four mouse strains, and at 3 m.p.i and 6 m.p.i, animals were sacrificed and analyzed by IHC. First, we determined the presence of tau inclusions using the anti-AT8 antibody, which is widely used to detect “pathologically” phosphorylated tau. Surprisingly, we found AT8-positive aggregates in all mouse strains at 3 m.p.i and 6 m.p.i, except for Tau KO, for which we never observed positive labeling for any antibody against tau. These findings have several implications that will be introduced here and further discussed in the following sections. In this regard, our results show that PrP^C is not central to the seeding and spreading processes, since there are no differences in the level and extent of tau-related lesions between genotypes. Furthermore, because tau inclusions are not seen in Tau KO animals, the expression of endogenous tau is mandatory for *de novo* generation of aggregated tau. Notably, this last observation agrees with previously published data from I. Ferrer’s laboratory in collaboration with our group (Ferrer *et al.*, 2022a). However, our findings contradict those

of (Wegmann *et al.*, 2015). Importantly, in this publication, the authors used mutated mice expressing human P301L tau that exhibited similar levels of tau aggregates and were able to spread even when tau expression was silenced. Yet again, this model does not represent the sporadic nature of human tauopathies, and the production of aggregation-prone tau isoforms may involve higher seeding potencies than those present in non-inherited tauopathies.

Although our results strongly suggested that the observed AT8-positive inclusions were composed of endogenous murine tau, we wanted to eliminate the possibility that remaining traces of the inoculated AD-tau were still present in the tissue. Double IHC with pSer422 and human-specific anti-Tau-13 or murine-specific anti-T49 revealed that all “pathologically” phosphorylated tau inclusions colocalized with T49. In contrast, we did not observe Tau-13-positive labeling for any examined animal inoculated with AD-tau at either 3 m.p.i or 6 m.p.i. Together, our findings show the absence of human tau in the brain tissue of the injected mice and prove that endogenously expressed murine tau forms inclusions, which are actively phosphorylated by the rodent’s kinases.

Let us now return to the notion that, at least in our experimental models, PrP^C is not required for the seeding and spreading of tau pathology. As indicated previously, in the past, there have been a few attempts to elucidate the relationship between these two proteins. For instance, in 2018, Ondrejcak and colleagues showed that PrP^C directly modulates the alteration of hippocampal synaptic plasticity induced by soluble tau using an *in vivo* approach (Ondrejcak *et al.*, 2018). The authors demonstrate that AD brain-soluble extracts containing tau inhibit LTP in wild-type rats. Noteworthy, this alteration was reduced with the inoculation of PrP^C antibodies. In a follow-up study, the same authors provided evidence that the injection of soluble tau into the rat hippocampus inhibits long-term depression (LTD) in a PrP^C-dependent manner (Ondrejcak *et al.*, 2019).

Together, these two publications suggest a link between tau pathology and PrP^C. However, the authors did not address whether PrP^C is also involved in tau seeding and spreading. In this regard, in recent work by (De Cecco *et al.*, 2020), the authors used PrP^C KO N2a cells and fluorescently labeled tauK18 to investigate the possible role of PrP^C as a receptor for tau endocytosis. Interestingly, De Cecco and colleagues found that the lack of PrP^C expression in these cells significantly decreased the number of internalized tauK18 compared to control cells (i.e., *Prnp*$^{+/+}$).

Having said that, our conclusion that PrP^C is not required for tau internalization or spreading seems to be partially contradicted, especially by De Cecco and colleagues' findings. Notably, because we did not address changes in LTP or LTD, we cannot rule out the possibility that PrP^C modulates tau pathology by altering neural activity in the hippocampus. In other words, it is possible that PrP^C and tau may be related in the context of extracellular tau cytotoxicity and how seed-competent tau modulates the neuronal network in a PrP^C-dependent manner. In future work, it will be interesting to assess whether there are differences in LTP or LTD between the mouse strains following AD-tau inoculation compared to age-matched controls.

Nevertheless, our results are inconsistent with those of (De Cecco *et al.*, 2020), but there may be several reasons for this. Let us emphasize that De Cecco and colleagues used an *in vitro* approach, and cells were treated with tauK18 PFFs to study the uptake process. As already discussed in this thesis, tau PFFs do not resemble the type of tau aggregates present in the diseased brain (Zhang *et al.*, 2019). Therefore, when studying specific cellular mechanisms, it is essential to understand the limitations and translational value of models based on these approaches. Hence, we believe that our experimental design better reproduces the situation of sporadic tauopathies. However, since this issue has not been extensively addressed in the literature, further work using more disease-relevant approaches is needed.

Taking everything into account, it is worth mentioning that our results have certain commonalities with investigations of the relationship between Aβ and PrP^C. In particular, (Gimbel *et al.*, 2010) used an AD mouse model known as APPsw/PS1DE9 (Jankowsky *et al.*, 2004), which is known to produce Aβ plaques in the cortex and hippocampus at 9 months of age. Gimbel and colleagues crossed this mouse model with a PrP^C KO mouse strain (Manson *et al.*, 1994), producing the APPsw/PS1DE9/*Prnp*$^{-/-}$ (Gimbel *et al.*, 2010), to study whether the PrP^C protein was related to Aβ-related neurotoxicity. Notably, the authors indicated that the absence of PrP^C does not lead to a noticeable change in the burden of Aβ plaques compared with APPsw/PS1DE9/*Prnp*$^{+/+}$ animals. However, they did find a significant impairment in spatial and learning memory in APPsw/PS1DE9/*Prnp*$^{+/+}$ but not in APPsw/PS1DE9/*Prnp*$^{-/-}$ mice. The authors concluded that, although PrP^C does not regulate the levels of amyloid inclusions, its presence directly relates to behavioral impairment. This is only one of many publications in which PrP^C has been shown to mediate Aβ cytotoxicity, primarily through the inhibition of LTP, which can be rescued by suppressing the PrP^C expression (Lauren *et al.*, 2009) or by inhibiting the interaction of PrP^C and Aβ (e.g., with antibodies (Chung *et al.*, 2010; Freir

et al., 2011; Klyubin *et al.*, 2014) or polymers (Gunther *et al.*, 2019)). It should be mentioned, however, that Aβ-related synaptic deficits have also been reported in the absence of PrP^C (Balducci *et al.*, 2010; Kessels *et al.*, 2010).

Considering that in most of these publications, the burden of Aβ plaques in the presence or absence of PrP^C was partially or not addressed, our group, in collaboration with E. Wandosell's laboratory, conducted a thorough examination of this matter also using the APPsw/PS1DE9 strain (Ordonez-Gutierrez *et al.*, 2013). Ordoñez-Gutierrez and colleagues generated several transgenic mouse lines with different expression levels of PrP^C by crossing the APPsw/PS1DE9 mouse line with either PrP^C KO mice (Manson *et al.*, 1994) or the *Prnp*^{tga20} strain (Fischer *et al.*, 1996), which over-expresses three to four times more PrP^C than wild-type mice. The authors demonstrate that all strains exhibited an increasing burden of Aβ plaques with age, irrespective of the animal's genotype. At 9 months of age, although no differences were detected between the APPsw/PS1DE9/*Prnp*^{tga20} and the APPsw/PS1DE9/*Prnp*$^{+/+}$ strains, the APPsw/PS1DE9/*Prnp*^{tga20} displayed significantly higher levels of Aβ inclusions compared to the APPsw/PS1DE9/*Prnp*$^{-/-}$, indicating that the over-expression of PrP^C could be directly related to increased plaque formation levels.

Taking everything into account, comparing our results to what has been reported for Aβ, there are certain commonalities. To begin with, we have also observed that the lack of PrP^C does not directly affect the burden of tau inclusions, similar to (Gimbel *et al.*, 2010) and (Ordonez-Gutierrez *et al.*, 2013). In this regard, in future work, it may be useful to include the *Prnp*^{tga20} strain in the experimental design in an attempt to replicate the results observed by (Ordonez-Gutierrez *et al.*, 2013). It would be interesting to determine whether the over-expression of PrP^C impacts the seeding and spreading of extracellular seed-competent tau. In parallel, given that the lack of PrP^C did not alter the burden of Aβ plaques but impaired LTP, it further reaffirms our belief that future studies using our experimental approach should include this type of functional analysis.

Continuing with this line of thought, let us now consider the relationship between PrP^C and α-syn and compare it to tau. In previous work from our laboratory, (Urrea *et al.*, 2018) used three mouse strains with different PrP^C expression levels to evaluate its role in the seeding and spreading of α-syn. The authors employed a PrP^C KO strain known as Zürich-I (Bueler *et al.*, 1992) (i.e., *Prnp*$^{-/-}$), their control littermates (i.e., *Prnp*$^{+/+}$), and the already mentioned *Prnp*^{tga20} model. Urrea and colleagues inoculated α-syn PFFs into the brains of these mouse lines and then examined the formation of α-syn inclusions 45 days later. Although α-syn pathology was observed in all strains, the authors discovered that

increased PrP^C expression resulted in a significantly higher presence of α-syn inclusions in a dose-dependent manner (i.e., *Prnp*$^{-/-}$ < *Prnp*$^{+/+}$ < *Prnp*^{tga20}). This result contrasts with our findings, in which we did not observe any differences between the Tau KO (i.e., ZH3) and wild-type animals. Other publications have also shown that α-syn internalization and spreading are facilitated by PrP^C (Aulic *et al.*, 2017; Ferreira *et al.*, 2017). Therefore, although it is possible that PrP^C interacts differently with α-syn and tau, it is worth noting that the mentioned studies were conducted using α-syn PFFs, and we used brain-derived material.

Thus far, we have compared our findings on the interaction of tau and PrP^C with previously published data on PrP^C's association with Aβ and α-syn. In the following paragraphs, we will continue to discuss the characterization of the tau inclusions found in our experiments with a more detailed approach.

As previously mentioned, no differences in the type of tau aggregates were found between mouse strains or between m.p.i, indicating that the absence of a functional PrP^C did not alter the process of tau aggregation. An intriguing aspect of our results is that all tau inclusions contain 3R- and 4R-tau. As previously stated, adult mice do not express 3R-tau isoforms (Hernandez *et al.*, 2020). The formation of 3R- and 4R-tau inclusions in wild-type mice after inoculation with human-derived samples has recently been reported (Ferrer *et al.*, 2020; Ferrer *et al.*, 2022a; Ferrer *et al.*, 2022b). Notably, in the past, PrP^C has been suggested to regulate the 3R/4R tau ratio (Lidon *et al.*, 2021). To our knowledge, we are the first to report that, despite the absence of PrP^C, no obvious changes can be detected in the ratio of 3R/4R tau isoforms present in the formed inclusions. Hence, the lack of functional PrP^C does not alter the changes in the metabolism induced by AD-tau, as suggested by (Ferrer *et al.*, 2020). Noteworthy, these metabolic changes are also associated with the activation of specific endogenous kinases involved in tau phosphorylation. Overall, there is no simple explanation for how extracellular tau changes the ratio of tau isoforms in the mouse brain. Notably, the formation of 3R/4R tau inclusions has only been reported in wild-type mice injected with brain-derived material. It would be interesting to see if tau PFFs or extremely purified brain-derived tau also change this proportion or if it is a combination of factors present in the sarkosyl-insoluble fractions.

At this point, it is worth mentioning that although we firmly believe that *de novo* inclusions observed after the inoculation of AD-tau are the result of self-seeded polymerization induced by seed-competent tau present in the sarkosyl-insoluble fraction, we cannot rule out the possibility that since other molecules exist in these fractions, they

could be the real inductors of the observed tau aggregates. In other words, we cannot ignore the fact that molecules other than tau may alter the metabolism of neural cells in the mouse brain, inducing endogenous tau misfolding, and eventually the formation of aggregates, independently of the presence of exogenous tau. In this regard, there are several studies in which immunodepleting tau from sarkosyl or homogenate samples derived from patients or transgenic rodent models did not trigger the formation of tau aggregates (Clavaguera *et al.*, 2009; Takeda *et al.*, 2015; Guo *et al.*, 2016b), demonstrating that the observed tau pathology is a direct cause of the presence of seed-competent tau in the inoculated fractions.

The Tg44 mouse strain was included in our experimental design mainly because it represents a situation in which PrP^C is present but unable to perform its physiologic functions. However, since it is present extracellularly and exposes its unstructured N-terminal domain, which has been suggested to interact with amyloid proteins, PrP^C's putative ability to bind tau remains unchanged. It is, therefore, tempting to predict that, in the presence of extracellular tau aggregates, extracellular PrP^C would bind to tau amyloids. This event would impair tau uptake and subsequent seeding and spreading. Regardless, in this work, we report that this is not the case, since Tg44 animals exhibited similar seeding and spreading patterns to those of wild-type and ZH3 mice.

It is worth mentioning that a recent paper has related the presence of soluble extracellular PrP^C, N-methyl-D-aspartate receptor (NMDA-R), and LRP1 to anti-inflammatory activity (Mantuano *et al.*, 2020). Interestingly, current evidence points to LRP1 as a critical factor in tau uptake and transport in neural cells, and its absence reduces tau internalization in cultured cells (A *et al.*, 2020; Rauch *et al.*, 2020). Hence, it is possible to hypothesize that soluble PrP^C (i.e., as in the Tg44 strain) modulates tau uptake by interacting with LRP1 (Rauch *et al.*, 2020), which could, in turn, reduce an inflammatory response (Mantuano *et al.*, 2020). Nevertheless, we did not observe obvious differences in the number of glial cells in the Tg44 strain compared with wild-type or ZH3 mice. Having said this, it would be interesting to determine whether molecules related to anti-inflammatory processes are up- or down-regulated in Tg44 compared to the other mouse strains.

In summary, although we cannot completely exclude the possibility that PrP^C could be a minor regulator of tau pathology, we conclude that PrP^C does not play a central role in tau uptake, seeding, and spreading, in contrast to other amyloids (Ordonez-Gutierrez *et al.*, 2013; Urrea *et al.*, 2018). Finally, we predict that various internalization processes

occur concurrently and probably through multiple cellular mechanisms and that future therapies should attempt to cover several targets simultaneously.

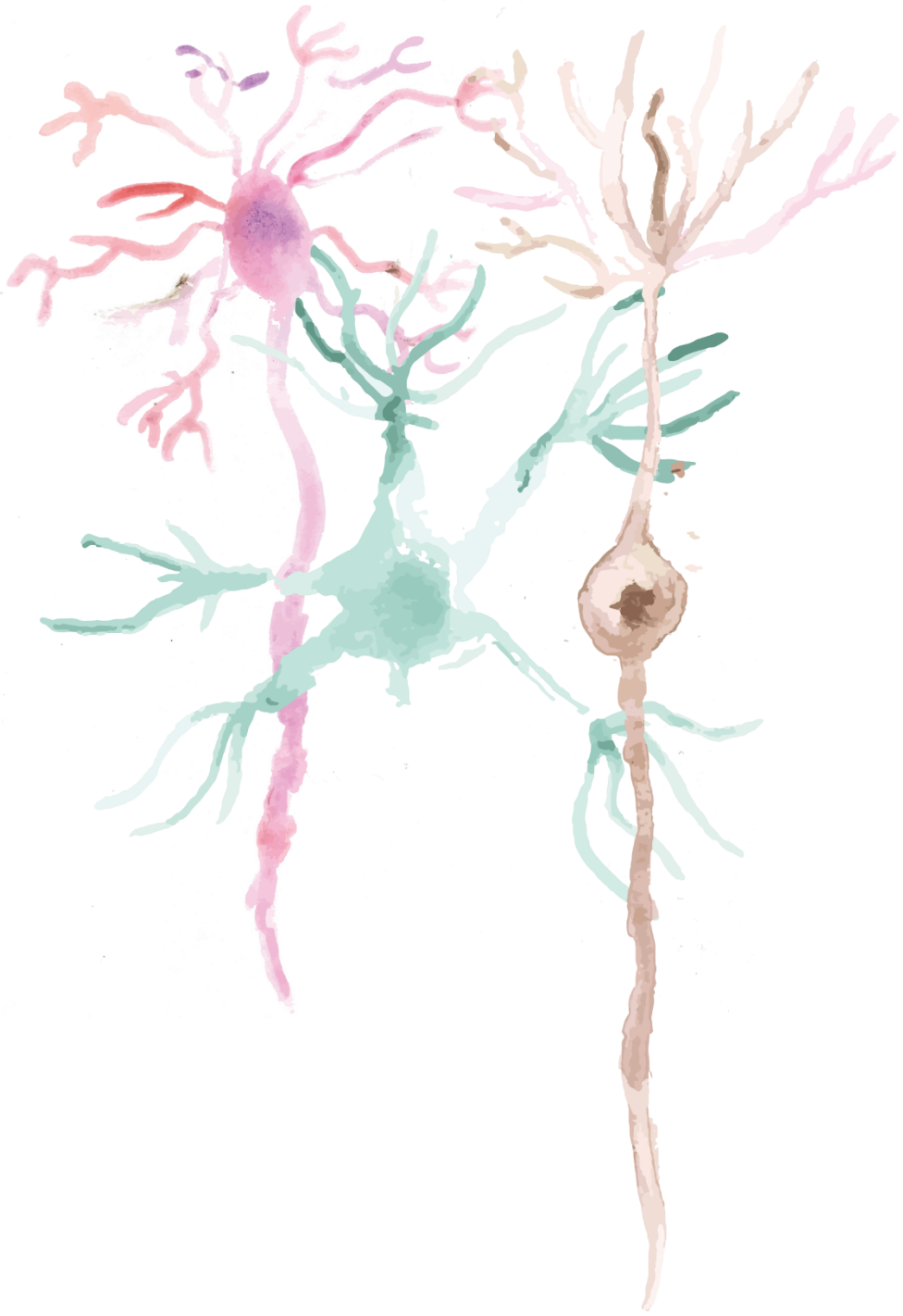

General Discussion

For the last 10 years, there has been increasing evidence supporting the hypothesis that tau pathology spreads along neural networks to drive the progression of human tauopathies (Clavaguera *et al.*, 2009; Kfoury *et al.*, 2012; Guo & Lee, 2014; Sanders *et al.*, 2016). However, the exact mechanisms that underlie the phenotypic diversity, seeding, spreading, and toxicity of these diseases have remained elusive. Decades of research have suggested that tauopathies and other NDs share pathogenic mechanisms with PrDs, resulting in the terminology "prion-like" that refers to these proteins whose infectivity has not been proven. One of the most relevant aspects of the prion-like hypothesis is the theoretical existence of a step in which extracellular seed-competent tau progresses from one affected neuron to a neighboring healthy cell during cell-to-cell transmission. Notably, the presence of "pathological" tau in the CSF and ISF of human patients with AD has been confirmed (Kurz *et al.*, 1998; Takeda *et al.*, 2016), and more recently, in murine and cellular models of tau pathology (Barten *et al.*, 2011; Yamada *et al.*, 2011; Takeda *et al.*, 2015). Consequently, it provides an attractive target for tau-directed therapies since it avoids treating pathological processes inside neural cells.

Despite the existence of multiple treatments showing positive results *in vitro* and *in vivo* (Khlistunova *et al.*, 2006; Seidler *et al.*, 2019; Crowe *et al.*, 2020), there has been a persistent failure to reproduce this success in human clinical trials (Zahs & Ashe, 2010; Boxer *et al.*, 2013). There are several possible explanations for these inconsistencies. In this regard, given that tau is a highly soluble protein that does not readily aggregate under physiological conditions, the gold standard for producing *in vitro* and *in vivo* models of tau pathology has been the over-expression of aggregation-prone tau isoforms (Allen *et al.*, 2002; Khlistunova *et al.*, 2006; Kfoury *et al.*, 2012; Guo *et al.*, 2013). However, most human tauopathies are sporadic, meaning that they are not associated with genetic mutations. Additionally, the relevance of using tau PFFs in other experimental approaches has now been questioned, given the growing evidence that these fibrils are far from reproducing the actual aggregates derived from diseased human brains (Sharma *et al.*, 2018; Zhang *et al.*, 2019). As a result, we believe there is a need for consistency in the methodologies and pathologically relevant experimental models used for research in the field of tauopathies.

The principal objective of this thesis was to study the effects of extracellular seed-competent tau species *in vitro* and *in vivo*. We were interested in using disease-relevant approaches (e.g., wild-type tau expression models and tau derived from brain material). In the following paragraphs, we summarize the most relevant findings of each chapter and discuss noteworthy aspects relevant to our work, as well as make suggestions for

future improvements. Finally, the scope of this section is focused on providing a global analysis, and a specific discussion can be found at the end of every chapter.

At the beginning of this thesis, the reliability of the Tau biosensor cell line (Holmes *et al.*, 2014) was questioned (Kaniyappan *et al.*, 2020), and therefore our and others' work, which were based on this cellular assay. Hence, we decided to thoroughly characterize the fluorescent inclusions formed in the Tau biosensor cell line to address the claims of Kaniyappan *et al*. In Chapter 1, through different experimental approaches, we demonstrate that the Tau biosensor cell line assembles endogenously expressed tau RD-CFP/YFP into amyloid-like aggregates upon the addition of extracellular seed-competent tau. It is pertinent to remember that Kaniyappan and colleagues examined the reliability of the Tau biosensor cell line in a cell-free environment using different tau RD-CFP/YFP constructs than those used in the publication by (Holmes *et al.*, 2014). Our findings demonstrate that it is imperative to address aspects of tau seeding in a cellular context. In other words, it is possible that the suggestions made by Kaniyappan and co-workers, claiming that tau RD-CFP/YFP fragments are unable to aggregate due to steric impediments, may be overcome in the context of the cellular milieu due to unknown reasons. In conclusion, we believe that the Tau biosensor cell line is a reliable cell model for examining the presence of seed-competent tau species in biological samples, and we therefore proceeded to use it for the rest of this thesis.

We then examined the role of extracellular seed-competent tau in primary cortical cultures. Notably, according to the prion-like hypothesis, tau pathology starts in a small number of neurons in the brain, and from there, it spreads trans-cellularly to healthy synaptically connected neurons. Hence, we decided to use primary neural cell cultures derived from wild-type mice to better represent the context of human sporadic tauopathies, and the effects of extracellular seed-competent tau were addressed through time-course experiments. Hence, our findings cannot be directly compared with previous research due to the paucity of available literature reporting studies using similar experimental approaches.

In Chapter 2, we successfully develop an experimental setup consisting of a microfluidic device plated with primary cortical neurons virally transduced to over-express the RCaMP GECI. The decision to use RCaMP instead of GCaMP was based on future adaptations in which calcium imaging could be combined with the use of GFP-expressing models without producing fluorescence interference. We demonstrate that neural cultures display highly synchronous activity patterns as they mature. However, we could not prove that the presence of extracellular seed-competent tau, which is

present in TIF-P+ fractions, affects neuronal networks compared to untreated cultures. Future experiments should aim to increase the survival of primary neurons plated on the devices to determine whether longer incubation periods result in detectable changes in neural activity. Additionally, it would be interesting to include disease-relevant tau species (e.g., brain-derived material from patients with AD) in the experimental design.

In Chapter 3, we examine possible tau-associated cytotoxicity of various seed-competent tau species (i.e., TIF-P+, sarkosyl-insoluble samples from P301S (+/-) mice and one human AD patient) in primary cortical cultures by addressing changes in cellular metabolism, the total number of cells, and the ratio of neurons relative to the total number of cells. Similar to Chapter 2, no differences between treated and untreated cells are found. Notably, primary neurons over-expressing P301L tau treated with sarkosyl-insoluble samples from P301S (+/-) mice are also not affected. Due to time limitations, we were unable to examine whether other cellular responses related to toxicity, such as the generation of ROS species, or altered morphology, were affected. Further investigations exploring these issues are necessary to clarify the impact of extracellular seed-competent tau on primary neural cultures.

Although our findings from Chapter 2 and Chapter 3 partly contradict previous research, it is pertinent to mention that most studies did not use wild-type primary neurons. Instead, the vast majority relied on the use of non-neuronal or neuronal *in vitro* models that over-express wild-type or mutant tau, frequently using non-physiological tau fragments to initiate aggregation (Guo & Lee, 2011; Kfoury *et al.*, 2012; Falcon *et al.*, 2015). We believe that the lack of success in translating positive results from these models underscores the need for the field to shift towards more pathologically relevant experimental approaches. However, it is also possible that embryonic cell cultures are not appropriate models for studying certain aspects of human tauopathies. The principal risk factor for most sporadic NDs is aging. Hence, it is more than likely that an embryonic cell culture does not replicate the complex structure of an aged brain (Estevez-Priego *et al.*, 2020). Indeed, one interesting factor that could have affected our results is the missing 3D organization of the nervous system when we plate primary cortical cultures in our microfluidic devices. It is possible that the loss of complexity associated with 2D cell cultures alters the susceptibility of primary neurons to be affected by the presence of extracellular seed-competent tau. Notably, this is a well-documented problem in the research field of PrDs, in which several reports demonstrate the lack of cytotoxicity in 2D prion-infected cultures (Falsig *et al.*, 2012; Matamoros-Angles *et al.*, 2018). Indeed, our laboratory determined that prion infection is unable to induce *de novo* prion formation in

treated 2D cell cultures (Matamoros-Angles *et al.*, 2018). By contrast, translating these models into organotypic slice cultures with a large expression of PrP^C (e.g., cerebellar) has proven to reliably reproduce prion infection and neurodegeneration (Falsig *et al.*, 2008; Falsig *et al.*, 2012; Liu *et al.*, 2022). Consequently, in recent years, there has been increasing research for new 3D models of cell culture that better represent the complexity of the nervous system (Messing *et al.*, 2013; Stancu *et al.*, 2015; McCarthy *et al.*, 2021). In this context, there have also been several attempts at producing organoid-based AD models, since iPSCs can represent the genetic information of human patients, whereas organotypic slices do not. Currently, however, there are still very few studies using organotypic approaches or organoids generated from iPSCs from AD patients that are able to mimic tau seeding and spreading (Messing *et al.*, 2013; Gonzalez *et al.*, 2018; Madhavan *et al.*, 2018; McCarthy *et al.*, 2021; Shimada *et al.*, 2022). Having said that, it is also true that when neural activity has been addressed in these systems for wild-type controls treated with tau, no cytotoxic effects or alterations in the neuronal network have been observed. Most of these approaches are still in the early stages of development, and further work is required to determine the role of extracellular tau.

There is another interesting possibility that may be relevant to explain the negative results observed by us and others when using either primary neural cell cultures or organotypic slices from fetal rodents. As previously mentioned, the ratio between 3R- and 4R-tau isoforms is determined by development. For instance, embryonic mice mainly express 3R-tau, whereas adult rodents express 4R-tau isoforms (Guo *et al.*, 2017). Hence, since in Chapter 2 and Chapter 3, we used embryonic primary neural cell cultures derived from wild-type mice, it is safe to assume that neurons were solely expressing 3R-tau. Regardless, the treatments with extracellular seed-competent tau either contained 4R isoforms (e.g., TIF-P+ and sarkosyl-insoluble samples derived from P301S (+/-) mice) or 3R/4R aggregates (i.e., human AD-derived sarkosyl-insoluble fraction). Therefore, most of our exogenous tau seeds did not include the predominant isoforms endogenously produced by primary neurons. An interesting point to note here is that some prior studies have indicated the existence of an asymmetric seeding barrier between 3R and 4R isoforms (Dinkel *et al.*, 2011; Woerman *et al.*, 2016). In this regard, although we did not address whether extracellular seeds induce intracellular aggregation, it may be that incompatibilities between endogenously produced tau and extracellular seeds reduce or even prevent tau-mediated cytotoxicity. For instance, as indicated before, (Ferrer *et al.*, 2022a) demonstrated seeding differences between newborn and adult wild-type mice upon inoculation of tau derived from AD patients. Notably, while adult animals displayed AT8-positive inclusions after the injections,

newborns did not, suggesting an incompatibility between isoforms and/or higher resistance related to newborns. However, the exact reasons for that are not yet clear. Hence, inducing the expression of 4R-tau in these *in vitro* models and re-evaluating putative tau-related toxicity may be considered a potential area for future research.

Overall, it seems that despite being more relevant, embryonic approaches may have certain limitations in recreating aged brains. Nevertheless, we believe that it may be better to use healthy primary neurons than, for instance, N2a cells, since the latter may express tumor-related features that are even more distant from the brain state in the context of NDs. Although we recognize that a shift towards these models could come with a decrease in high-impact publications, given the publication bias for positive findings, we predict that with time, this change will produce better models and maybe even help in developing successful treatments.

In Chapter 4, we aimed to demonstrate whether the presence of PrP^C affected tau seeding and spreading *in vivo*. Taking into account that the unstructured region (i.e., located at the N-terminal domain) of the PrP^C is able to bind to several amyloids (i.e., including tau) (Aulic *et al.*, 2017; De Cecco *et al.*, 2020), we used various mouse models with different expression of the PrP^C protein: a) wild-type mice that have a physiological expression of PrP^C, b) Tau KO mice that do not express tau protein, c) ZH3 mice that do not express PrP^C, and d) Tg44 mice that over-express PrP^C, although without the GPI anchor (i.e., located at the C-terminal domain), thus the protein is released into the extracellular space. Notably, the Tg44 model is characterized by increased levels of extracellular PrP^C, and therefore the unstructured region is thought to interact with tau (De Cecco *et al.*, 2020). Consequently, we also sought to determine whether this domain could block tau pathology after inoculation. Our results suggest that, although possibly involved, PrP^C is not required for the spreading of tau *in vivo*.

Conclusions

Herein, we conclude:

1. The Tau biosensor cell line assembles tau RD-CFP/YFP into amyloid-like aggregates upon the addition of extracellular seed-competent tau

2. Insoluble tau species present in the TIF-P+ fraction trigger tau aggregation *in vitro* and *in vivo*

3. Primary cortical cultures in our microfluidic devices display mature patterns of neuronal activity

4. The presence of extracellular seed-competent tau does not alter the network dynamics of primary neurons

5. Seed-competent extracellular tau is not toxic to healthy primary cortical cultures

6. Seed-competent extracellular tau is not toxic to neurons endogenously over-expressing P301L tau

7. PrP^{C} does not play a central role in the uptake, seeding, or spreading of tau pathology *in vivo*

References

A, T.M., Stamelou, M. & G, U.H. (2020) LRP1: A Novel Mediator of Tau Uptake. *Mov Disord*, **35**, 1136.

Abounit, S., Wu, J.W., Duff, K., Victoria, G.S. & Zurzolo, C. (2016) Tunneling nanotubes: A possible highway in the spreading of tau and other prion-like proteins in neurodegenerative diseases. *Prion*, **10**, 344-351.

Abraha, A., Ghoshal, N., Gamblin, T.C., Cryns, V., Berry, R.W., Kuret, J. & Binder, L.I. (2000) C-terminal inhibition of tau assembly in vitro and in Alzheimer's disease. *J Cell Sci*, **113 Pt 21**, 3737-3745.

Adle-Biassette, H., Verney, C., Peoc'h, K., Dauge, M.C., Razavi, F., Choudat, L., Gressens, P., Budka, H. & Henin, D. (2006) Immunohistochemical expression of prion protein (PrPC) in the human forebrain during development. *J Neuropathol Exp Neurol*, **65**, 698-706.

Adori, C., Gluck, L., Barde, S., Yoshitake, T., Kovacs, G.G., Mulder, J., Magloczky, Z., Havas, L., Bolcskei, K., Mitsios, N., Uhlen, M., Szolcsanyi, J., Kehr, J., Ronnback, A., Schwartz, T., Rehfeld, J.F., Harkany, T., Palkovits, M., Schulz, S. & Hokfelt, T. (2015) Critical role of somatostatin receptor 2 in the vulnerability of the central noradrenergic system: new aspects on Alzheimer's disease. *Acta Neuropathol*, **129**, 541-563.

Aguzzi, A. (2000) Molecular pathology of prion diseases. *Vox Sang*, **78 Suppl 2**, 25.

Aguzzi, A. & Miele, G. (2004) Recent advances in prion biology. *Curr Opin Neurol*, **17**, 337-342.

Akerboom, J., Carreras Calderon, N., Tian, L., Wabnig, S., Prigge, M., Tolo, J., Gordus, A., Orger, M.B., Severi, K.E., Macklin, J.J., Patel, R., Pulver, S.R., Wardill, T.J., Fischer, E., Schuler, C., Chen, T.W., Sarkisyan, K.S., Marvin, J.S., Bargmann, C.I., Kim, D.S., Kugler, S., Lagnado, L., Hegemann, P., Gottschalk, A., Schreiter, E.R. & Looger, L.L. (2013) Genetically encoded calcium indicators for multi-color neural activity imaging and combination with optogenetics. *Front Mol Neurosci*, **6**, 2.

Akoury, E., Gajda, M., Pickhardt, M., Biernat, J., Soraya, P., Griesinger, C., Mandelkow, E. & Zweckstetter, M. (2013) Inhibition of tau filament formation by conformational modulation. *J Am Chem Soc*, **135**, 2853-2862.

Allen, B., Ingram, E., Takao, M., Smith, M.J., Jakes, R., Virdee, K., Yoshida, H., Holzer, M., Craxton, M., Emson, P.C., Atzori, C., Migheli, A., Crowther, R.A., Ghetti, B., Spillantini, M.G. & Goedert, M. (2002) Abundant tau filaments and nonapoptotic neurodegeneration in transgenic mice expressing human P301S tau protein. *J Neurosci*, **22**, 9340-9351.

Alonso, A., Zaidi, T., Novak, M., Grundke-Iqbal, I. & Iqbal, K. (2001) Hyperphosphorylation induces self-assembly of tau into tangles of paired helical filaments/straight filaments. *Proc Natl Acad Sci U S A*, **98**, 6923-6928.

Alonso, A.C., Zaidi, T., Grundke-Iqbal, I. & Iqbal, K. (1994) Role of abnormally phosphorylated tau in the breakdown of microtubules in Alzheimer disease. *Proc Natl Acad Sci U S A*, **91**, 5562-5566.

Alonso, A.D., Grundke-Iqbal, I., Barra, H.S. & Iqbal, K. (1997) Abnormal phosphorylation of tau and the mechanism of Alzheimer neurofibrillary degeneration: sequestration of microtubule-associated proteins 1 and 2 and the disassembly of microtubules by the abnormal tau. *Proc Natl Acad Sci U S A*, **94**, 298-303.

Andorfer, C., Kress, Y., Espinoza, M., de Silva, R., Tucker, K.L., Barde, Y.A., Duff, K. & Davies, P. (2003) Hyperphosphorylation and aggregation of tau in mice expressing normal human tau isoforms. *J Neurochem*, **86**, 582-590.

Andres-Benito, P., Carmona, M., Jordan, M., Fernandez-Irigoyen, J., Santamaria, E., Del Rio, J.A. & Ferrer, I. (2022) Host Tau Genotype Specifically Designs and Regulates Tau Seeding and Spreading and Host Tau Transformation Following Intrahippocampal Injection of Identical Tau AD Inoculum. *Int J Mol Sci*, **23**.

Arendt, T., Stieler, J., Strijkstra, A.M., Hut, R.A., Rudiger, J., Van der Zee, E.A., Harkany, T., Holzer, M. & Hartig, W. (2003) Reversible paired helical filament-like phosphorylation of tau is an adaptive process associated with neuronal plasticity in hibernating animals. *J Neurosci*, **23**, 6972-6981.

Armstrong, M.J., Castellani, R.J. & Reich, S.G. (2014) "Rapidly" Progressive Supranuclear Palsy. *Mov Disord Clin Pract*, **1**, 70-72.

Arnold, S.E., Toledo, J.B., Appleby, D.H., Xie, S.X., Wang, L.S., Baek, Y., Wolk, D.A., Lee, E.B., Miller, B.L., Lee, V.M. & Trojanowski, J.Q. (2013) Comparative survey of the topographical distribution of signature molecular lesions in major neurodegenerative diseases. *J Comp Neurol*, **521**, 4339-4355.

Arnsten, A.F.T., Datta, D., Del Tredici, K. & Braak, H. (2021) Hypothesis: Tau pathology is an initiating factor in sporadic Alzheimer's disease. *Alzheimers Dement*, **17**, 115-124.

Arriagada, P.V., Growdon, J.H., Hedley-Whyte, E.T. & Hyman, B.T. (1992) Neurofibrillary tangles but not senile plaques parallel duration and severity of Alzheimer's disease. *Neurology*, **42**, 631-639.

Asai, H., Ikezu, S., Tsunoda, S., Medalla, M., Luebke, J., Haydar, T., Wolozin, B., Butovsky, O., Kugler, S. & Ikezu, T. (2015) Depletion of microglia and inhibition of exosome synthesis halt tau propagation. *Nat Neurosci*, **18**, 1584-1593.

Aulic, S., Masperone, L., Narkiewicz, J., Isopi, E., Bistaffa, E., Ambrosetti, E., Pastore, B., De Cecco, E., Scaini, D., Zago, P., Moda, F., Tagliavini, F. & Legname, G. (2017) alpha-Synuclein Amyloids Hijack Prion Protein to Gain Cell Entry, Facilitate Cell-to-Cell Spreading and Block Prion Replication. *Sci Rep*, **7**, 10050.

Avila, J. (2006a) Tau phosphorylation and aggregation in Alzheimer's disease pathology. *FEBS Lett*, **580**, 2922-2927.

Avila, J. (2006b) Tau protein, the main component of paired helical filaments. *J Alzheimers Dis*, **9**, 171-175.

Avila, J., Jimenez, J.S., Sayas, C.L., Bolos, M., Zabala, J.C., Rivas, G. & Hernandez, F. (2016) Tau Structures. *Front Aging Neurosci*, **8**, 262.

Avila, J., Lucas, J.J., Perez, M. & Hernandez, F. (2004a) Role of tau protein in both physiological and pathological conditions. *Physiol Rev*, **84**, 361-384.

Avila, J., Perez, M., Lim, F., Gomez-Ramos, A., Hernandez, F. & Lucas, J.J. (2004b) Tau in neurodegenerative diseases: tau phosphorylation and assembly. *Neurotox Res*, **6**, 477-482.

Balducci, C., Beeg, M., Stravalaci, M., Bastone, A., Sclip, A., Biasini, E., Tapella, L., Colombo, L., Manzoni, C., Borsello, T., Chiesa, R., Gobbi, M., Salmona, M. & Forloni, G. (2010) Synthetic amyloid-beta oligomers impair long-term memory independently of cellular prion protein. *Proc Natl Acad Sci U S A*, **107**, 2295-2300.

Baldwin, K.J. & Correll, C.M. (2019) Prion Disease. *Semin Neurol*, **39**, 428-439.

Ballatore, C., Lee, V.M. & Trojanowski, J.Q. (2007) Tau-mediated neurodegeneration in Alzheimer's disease and related disorders. *Nat Rev Neurosci*, **8**, 663-672.

Bandyopadhyay, B., Li, G., Yin, H. & Kuret, J. (2007) Tau aggregation and toxicity in a cell culture model of tauopathy. *J Biol Chem*, **282**, 16454-16464.

Bang, S., Lee, S., Choi, N. & Kim, H.N. (2021) Emerging Brain-Pathophysiology-Mimetic Platforms for Studying Neurodegenerative Diseases: Brain Organoids and Brains-on-a-Chip. *Adv Healthc Mater*, **10**, e2002119.

Barghorn, S., Biernat, J. & Mandelkow, E. (2005) Purification of recombinant tau protein and preparation of Alzheimer-paired helical filaments in vitro. *Methods Mol Biol*, **299**, 35-51.

Barten, D.M., Cadelina, G.W., Hoque, N., DeCarr, L.B., Guss, V.L., Yang, L., Sankaranarayanan, S., Wes, P.D., Flynn, M.E., Meredith, J.E., Ahlijanian, M.K. & Albright, C.F. (2011) Tau transgenic mice as models for cerebrospinal fluid tau biomarkers. *J Alzheimers Dis*, **24 Suppl 2**, 127-141.

Baumann, F., Pahnke, J., Radovanovic, I., Rulicke, T., Bremer, J., Tolnay, M. & Aguzzi, A. (2009) Functionally relevant domains of the prion protein identified in vivo. *PLoS One*, **4**, e6707.

Beland, M. & Roucou, X. (2012) The prion protein unstructured N-terminal region is a broad-spectrum molecular sensor with diverse and contrasting potential functions. *J Neurochem*, **120**, 853-868.

Berger, Z., Roder, H., Hanna, A., Carlson, A., Rangachari, V., Yue, M., Wszolek, Z., Ashe, K., Knight, J., Dickson, D., Andorfer, C., Rosenberry, T.L., Lewis, J., Hutton, M. & Janus, C. (2007) Accumulation of pathological tau species and memory loss in a conditional model of tauopathy. *J Neurosci*, **27**, 3650-3662.

Berridge, M.J., Lipp, P. & Bootman, M.D. (2000) The versatility and universality of calcium signalling. *Nat Rev Mol Cell Biol*, **1**, 11-21.

Bessen, R.A. & Marsh, R.F. (1994) Distinct PrP properties suggest the molecular basis of strain variation in transmissible mink encephalopathy. *J Virol*, **68**, 7859-7868.

Bi, M., Ittner, A., Ke, Y.D., Gotz, J. & Ittner, L.M. (2011) Tau-targeted immunization impedes progression of neurofibrillary histopathology in aged P301L tau transgenic mice. *PLoS One*, **6**, e26860.

Bierer, L.M., Hof, P.R., Purohit, D.P., Carlin, L., Schmeidler, J., Davis, K.L. & Perl, D.P. (1995) Neocortical neurofibrillary tangles correlate with dementia severity in Alzheimer's disease. *Arch Neurol*, **52**, 81-88.

Biernat, J., Gustke, N., Drewes, G., Mandelkow, E.M. & Mandelkow, E. (1993) Phosphorylation of Ser262 strongly reduces binding of tau to microtubules: distinction between PHF-like immunoreactivity and microtubule binding. *Neuron*, **11**, 153-163.

Binder, L.I., Frankfurter, A. & Rebhun, L.I. (1985) The distribution of tau in the mammalian central nervous system. *J Cell Biol*, **101**, 1371-1378.

Boxer, A.L., Gold, M., Huey, E., Gao, F.B., Burton, E.A., Chow, T., Kao, A., Leavitt, B.R., Lamb, B., Grether, M., Knopman, D., Cairns, N.J., Mackenzie, I.R., Mitic, L., Roberson, E.D., Van Kammen, D., Cantillon, M., Zahs, K., Salloway, S., Morris, J., Tong, G., Feldman, H., Fillit, H., Dickinson, S., Khachaturian, Z., Sutherland, M., Farese, R., Miller, B.L. & Cummings, J. (2013) Frontotemporal degeneration, the next therapeutic frontier: molecules and animal models for frontotemporal degeneration drug development. *Alzheimers Dement*, **9**, 176-188.

Braak, H. & Braak, E. (1991) Neuropathological stageing of Alzheimer-related changes. *Acta Neuropathol*, **82**, 239-259.

Braak, H. & Braak, E. (1995) Staging of Alzheimer's disease-related neurofibrillary changes. *Neurobiol Aging*, **16**, 271-278; discussion 278-284.

Braak, H. & Del Tredici, K. (2015) Neuroanatomy and pathology of sporadic Alzheimer's disease. *Adv Anat Embryol Cell Biol*, **215**, 1-162.

Braak, H., Zetterberg, H., Del Tredici, K. & Blennow, K. (2013) Intraneuronal tau aggregation precedes diffuse plaque deposition, but amyloid-beta changes occur before increases of tau in cerebrospinal fluid. *Acta Neuropathol*, **126**, 631-641.

Bribian, A., Fontana, X., Llorens, F., Gavin, R., Reina, M., Garcia-Verdugo, J.M., Torres, J.M., de Castro, F. & del Rio, J.A. (2012) Role of the cellular prion protein in oligodendrocyte precursor cell proliferation and differentiation in the developing and adult mouse CNS. *PLoS One*, **7**, e33872.

Brunello, C.A., Merezhko, M., Uronen, R.L. & Huttunen, H.J. (2020) Mechanisms of secretion and spreading of pathological tau protein. *Cell Mol Life Sci*, **77**, 1721-1744.

Bueler, H., Fischer, M., Lang, Y., Bluethmann, H., Lipp, H.P., DeArmond, S.J., Prusiner, S.B., Aguet, M. & Weissmann, C. (1992) Normal development and behaviour of mice lacking the neuronal cell-surface PrP protein. *Nature*, **356**, 577-582.

Buerger, K., Ewers, M., Pirttila, T., Zinkowski, R., Alafuzoff, I., Teipel, S.J., DeBernardis, J., Kerkman, D., McCulloch, C., Soininen, H. & Hampel, H. (2006) CSF phosphorylated tau protein correlates with neocortical neurofibrillary pathology in Alzheimer's disease. *Brain*, **129**, 3035-3041.

Bullmann, T., Holzer, M., Mori, H. & Arendt, T. (2009) Pattern of tau isoforms expression during development in vivo. *Int J Dev Neurosci*, **27**, 591-597.

Busche, M.A., Chen, X., Henning, H.A., Reichwald, J., Staufenbiel, M., Sakmann, B. & Konnerth, A. (2012) Critical role of soluble amyloid-beta for early hippocampal hyperactivity in a mouse model of Alzheimer's disease. *Proc Natl Acad Sci U S A*, **109**, 8740-8745.

Busche, M.A., Eichhoff, G., Adelsberger, H., Abramowski, D., Wiederhold, K.H., Haass, C., Staufenbiel, M., Konnerth, A. & Garaschuk, O. (2008) Clusters of hyperactive neurons near amyloid plaques in a mouse model of Alzheimer's disease. *Science*, **321**, 1686-1689.

Busche, M.A., Wegmann, S., Dujardin, S., Commins, C., Schiantarelli, J., Klickstein, N., Kamath, T.V., Carlson, G.A., Nelken, I. & Hyman, B.T. (2019) Tau impairs neural circuits, dominating amyloid-beta effects, in Alzheimer models in vivo. *Nat Neurosci*, **22**, 57-64.

Caillierez, R., Begard, S., Lecolle, K., Deramecourt, V., Zommer, N., Dujardin, S., Loyens, A., Dufour, N., Auregan, G., Winderickx, J., Hantraye, P., Deglon, N., Buee, L. & Colin, M. (2013) Lentiviral delivery of the human wild-type tau protein mediates a slow and progressive neurodegenerative tau pathology in the rat brain. *Mol Ther*, **21**, 1358-1368.

Calafate, S., Buist, A., Miskiewicz, K., Vijayan, V., Daneels, G., de Strooper, B., de Wit, J., Verstreken, P. & Moechars, D. (2015) Synaptic Contacts Enhance Cell-to-Cell Tau Pathology Propagation. *Cell Rep*, **11**, 1176-1183.

Calafate, S., Flavin, W., Verstreken, P. & Moechars, D. (2016) Loss of Bin1 Promotes the Propagation of Tau Pathology. *Cell Rep*, **17**, 931-940.

Cervos-Navarro, J. & Schumacher, K. (1994) Neurofibrillary pathology in progressive supranuclear palsy (PSP). *J Neural Transm Suppl*, **42**, 153-164.

Chastagner, P., Loria, F., Vargas, J.Y., Tois, J., M, I.D., Okafo, G., Brou, C. & Zurzolo, C. (2020) Fate and propagation of endogenously formed Tau aggregates in neuronal cells. *EMBO Mol Med*, **12**, e12025.

Chen, J., Kanai, Y., Cowan, N.J. & Hirokawa, N. (1992) Projection domains of MAP2 and tau determine spacings between microtubules in dendrites and axons. *Nature*, **360**, 674-677.

Chen, X.Q. & Mobley, W.C. (2019) Alzheimer Disease Pathogenesis: Insights From Molecular and Cellular Biology Studies of Oligomeric Abeta and Tau Species. *Front Neurosci*, **13**, 659.

Chesebro, B., Trifilo, M., Race, R., Meade-White, K., Teng, C., LaCasse, R., Raymond, L., Favara, C., Baron, G., Priola, S., Caughey, B., Masliah, E. & Oldstone, M. (2005) Anchorless prion protein results in infectious amyloid disease without clinical scrapie. *Science*, **308**, 1435-1439.

Chiappalone, M., Bove, M., Vato, A., Tedesco, M. & Martinoia, S. (2006) Dissociated cortical networks show spontaneously correlated activity patterns during in vitro development. *Brain Res*, **1093**, 41-53.

Chirita, C.N., Congdon, E.E., Yin, H. & Kuret, J. (2005) Triggers of full-length tau aggregation: a role for partially folded intermediates. *Biochemistry*, **44**, 5862-5872.

Chiti, F. & Dobson, C.M. (2006) Protein misfolding, functional amyloid, and human disease. *Annu Rev Biochem*, **75**, 333-366.

Chua, S.W., Cornejo, A., van Eersel, J., Stevens, C.H., Vaca, I., Cueto, M., Kassiou, M., Gladbach, A., Macmillan, A., Lewis, L., Whan, R. & Ittner, L.M. (2017) The Polyphenol Altenusin Inhibits in Vitro Fibrillization of Tau and Reduces Induced Tau Pathology in Primary Neurons. *ACS Chem Neurosci*, **8**, 743-751.

Chun, W. & Johnson, G.V. (2007) Activation of glycogen synthase kinase 3beta promotes the intermolecular association of tau. The use of fluorescence resonance energy transfer microscopy. *J Biol Chem*, **282**, 23410-23417.

Chun, W., Waldo, G.S. & Johnson, G.V. (2007) Split GFP complementation assay: a novel approach to quantitatively measure aggregation of tau in situ: effects of GSK3beta activation and caspase 3 cleavage. *J Neurochem*, **103**, 2529-2539.

Chung, D.C., Carlomagno, Y., Cook, C.N., Jansen-West, K., Daughrity, L., Lewis-Tuffin, L.J., Castanedes-Casey, M., DeTure, M., Dickson, D.W. & Petrucelli, L. (2019) Tau exhibits unique seeding properties in globular glial tauopathy. *Acta Neuropathol Commun*, **7**, 36.

Chung, E., Ji, Y., Sun, Y., Kascsak, R.J., Kascsak, R.B., Mehta, P.D., Strittmatter, S.M. & Wisniewski, T. (2010) Anti-PrPC monoclonal antibody infusion as a novel treatment for cognitive deficits in an Alzheimer's disease model mouse. *BMC Neurosci*, **11**, 130.

Clavaguera, F., Akatsu, H., Fraser, G., Crowther, R.A., Frank, S., Hench, J., Probst, A., Winkler, D.T., Reichwald, J., Staufenbiel, M., Ghetti, B., Goedert, M. & Tolnay, M. (2013) Brain homogenates from human tauopathies induce tau inclusions in mouse brain. *Proc Natl Acad Sci U S A*, **110**, 9535-9540.

Clavaguera, F., Bolmont, T., Crowther, R.A., Abramowski, D., Frank, S., Probst, A., Fraser, G., Stalder, A.K., Beibel, M., Staufenbiel, M., Jucker, M., Goedert, M. & Tolnay, M. (2009) Transmission and spreading of tauopathy in transgenic mouse brain. *Nat Cell Biol*, **11**, 909-913.

Clavaguera, F., Tolnay, M. & Goedert, M. (2017) The Prion-Like Behavior of Assembled Tau in Transgenic Mice. *Cold Spring Harb Perspect Med*, **7**.

Cleveland, D.W., Hwo, S.Y. & Kirschner, M.W. (1977) Purification of tau, a microtubule-associated protein that induces assembly of microtubules from purified tubulin. *J Mol Biol*, **116**, 207-225.

Coca, J.R., Erana, H. & Castilla, J. (2021) Biosemiotics comprehension of PrP code and prion disease. *Biosystems*, **210**, 104542.

Colby, D.W. & Prusiner, S.B. (2011) Prions. *Cold Spring Harb Perspect Biol*, **3**, a006833.

Coleman, P.D. & Yao, P.J. (2003) Synaptic slaughter in Alzheimer's disease. *Neurobiol Aging*, **24**, 1023-1027.

Collinge, J. & Clarke, A.R. (2007) A general model of prion strains and their pathogenicity. *Science*, **318**, 930-936.

Corbett, G.T., Wang, Z., Hong, W., Colom-Cadena, M., Rose, J., Liao, M., Asfaw, A., Hall, T.C., Ding, L., DeSousa, A., Frosch, M.P., Collinge, J., Harris, D.A., Perkinton, M.S., Spires-Jones, T.L., Young-Pearse, T.L., Billinton, A. & Walsh, D.M. (2020) PrP is a central player in toxicity mediated by soluble aggregates of neurodegeneration-causing proteins. *Acta Neuropathol*, **139**, 503-526.

Crimins, J.L., Rocher, A.B. & Luebke, J.I. (2012) Electrophysiological changes precede morphological changes to frontal cortical pyramidal neurons in the rTg4510 mouse model of progressive tauopathy. *Acta Neuropathol*, **124**, 777-795.

Crowe, A., Henderson, M.J., Anderson, J., Titus, S.A., Zakharov, A., Simeonov, A., Buist, A., Delay, C., Moechars, D., Trojanowski, J.Q., Lee, V.M. & Brunden, K.R. (2020) Compound screening in cell-based models of tau inclusion formation: Comparison of primary neuron and HEK293 cell assays. *J Biol Chem*, **295**, 4001-4013.

Dai, C.L., Chen, X., Kazim, S.F., Liu, F., Gong, C.X., Grundke-Iqbal, I. & Iqbal, K. (2015) Passive immunization targeting the N-terminal projection domain of tau decreases tau pathology and improves cognition in a transgenic mouse model of Alzheimer disease and tauopathies. *J Neural Transm (Vienna)*, **122**, 607-617.

Dai, C.L., Hu, W., Tung, Y.C., Liu, F., Gong, C.X. & Iqbal, K. (2018) Tau passive immunization blocks seeding and spread of Alzheimer hyperphosphorylated Tau-induced pathology in 3 x Tg-AD mice. *Alzheimers Res Ther*, **10**, 13.

Datki, Z., Galik-Olah, Z., Janosi-Mozes, E., Szegedi, V., Kalman, J., Hunya, A.G., Fulop, L., Tamano, H., Takeda, A., Adlard, P.A. & Bush, A.I. (2020) Alzheimer risk factors age and female sex induce cortical Abeta aggregation by raising extracellular zinc. *Mol Psychiatry*, **25**, 2728-2741.

Dawson, H.N., Ferreira, A., Eyster, M.V., Ghoshal, N., Binder, L.I. & Vitek, M.P. (2001) Inhibition of neuronal maturation in primary hippocampal neurons from tau deficient mice. *J Cell Sci*, **114**, 1179-1187.

De Cecco, E., Celauro, L., Vanni, S., Grandolfo, M., Bistaffa, E., Moda, F., Aguzzi, A. & Legname, G. (2020) The uptake of tau amyloid fibrils is facilitated by the cellular prion protein and hampers prion propagation in cultured cells. *J Neurochem*, **155**, 577-591.

De Leon, M.J. & Braak, H. (1999) *An atlas of Alzheimer's disease*. Parthenon Pub. Group, New York.

Decker, J.M., Kruger, L., Sydow, A., Dennissen, F.J., Siskova, Z., Mandelkow, E. & Mandelkow, E.M. (2016) The Tau/A152T mutation, a risk factor for frontotemporal-spectrum disorders, leads to NR2B receptor-mediated excitotoxicity. *EMBO Rep*, **17**, 552-569.

Deco, G., Jirsa, V.K., Robinson, P.A., Breakspear, M. & Friston, K. (2008) The dynamic brain: from spiking neurons to neural masses and cortical fields. *PLoS Comput Biol*, **4**, e1000092.

DeKosky, S.T. & Scheff, S.W. (1990) Synapse loss in frontal cortex biopsies in Alzheimer's disease: correlation with cognitive severity. *Ann Neurol*, **27**, 457-464

Del Rio, J.A. & Ferrer, I. (2020) Potential of Microfluidics and Lab-on-Chip Platforms to Improve Understanding of "prion-like" Protein Assembly and Behavior. *Front Bioeng Biotechnol*, **8**, 570692.

Del Rio, J.A., Ferrer, I. & Gavin, R. (2018) Role of cellular prion protein in interneuronal amyloid transmission. *Prog Neurobiol*, **165-167**, 87-102.

Deleglise, B., Lassus, B., Soubeyre, V., Alleaume-Butaux, A., Hjorth, J.J., Vignes, M., Schneider, B., Brugg, B., Viovy, J.L. & Peyrin, J.M. (2013) Synapto-protective drugs evaluation in reconstructed neuronal network. *PLoS One*, **8**, e71103.

DeVos, S.L., Goncharoff, D.K., Chen, G., Kebodeaux, C.S., Yamada, K., Stewart, F.R., Schuler, D.R., Maloney, S.E., Wozniak, D.F., Rigo, F., Bennett, C.F., Cirrito, J.R., Holtzman, D.M. & Miller, T.M. (2013) Antisense reduction of tau in adult mice protects against seizures. *J Neurosci*, **33**, 12887-12897.

Diaz-Hernandez, M., Gomez-Ramos, A., Rubio, A., Gomez-Villafuertes, R., Naranjo, J.R., Miras-Portugal, M.T. & Avila, J. (2010) Tissue-nonspecific alkaline phosphatase promotes the neurotoxicity effect of extracellular tau. *J Biol Chem*, **285**, 32539-32548.

Dickerson, B.C., Salat, D.H., Greve, D.N., Chua, E.F., Rand-Giovannetti, E., Rentz, D.M., Bertram, L., Mullin, K., Tanzi, R.E., Blacker, D., Albert, M.S. & Sperling, R.A. (2005) Increased hippocampal activation in mild cognitive impairment compared to normal aging and AD. *Neurology*, **65**, 404-411.

Dinkel, P.D., Siddiqua, A., Huynh, H., Shah, M. & Margittai, M. (2011) Variations in filament conformation dictate seeding barrier between three- and four-repeat tau. *Biochemistry*, **50**, 4330-4336.

Du, F., Yu, Q., Kanaan, N.M. & Yan, S.S. (2022) Mitochondrial oxidative stress contributes to the pathological aggregation and accumulation of tau oligomers in Alzheimer's disease. *Hum Mol Genet*, **31**, 2498-2507.

Dubey, S.K., Ram, M.S., Krishna, K.V., Saha, R.N., Singhvi, G., Agrawal, M., Ajazuddin, Saraf, S., Saraf, S. & Alexander, A. (2019) Recent Expansions on Cellular Models to Uncover the Scientific Barriers Towards Drug Development for Alzheimer's Disease. *Cell Mol Neurobiol*, **39**, 181-209.

Dujardin, S., Commins, C., Lathuiliere, A., Beerepoot, P., Fernandes, A.R., Kamath, T.V., De Los Santos, M.B., Klickstein, N., Corjuc, D.L., Corjuc, B.T., Dooley, P.M., Viode, A., Oakley, D.H., Moore, B.D., Mullin, K., Jean-Gilles, D., Clark, R., Atchison, K., Moore, R., Chibnik, L.B., Tanzi, R.E., Frosch, M.P., Serrano-Pozo, A., Elwood, F., Steen, J.A., Kennedy, M.E. & Hyman, B.T. (2021) Author Correction: Tau molecular diversity contributes to clinical heterogeneity in Alzheimer's disease. *Nat Med*, **27**, 356.

Esteras, N., Kundel, F., Amodeo, G.F., Pavlov, E.V., Klenerman, D. & Abramov, A.Y. (2021) Insoluble tau aggregates induce neuronal death through modification of membrane ion conductance, activation of voltage-gated calcium channels and NADPH oxidase. *FEBS J*, **288**, 127-141.

Estevez-Priego, E., Teller, S., Granell, C., Arenas, A. & Soriano, J. (2020) Functional strengthening through synaptic scaling upon connectivity disruption in neuronal cultures. *Netw Neurosci*, **4**, 1160-1180.

Evans, L.D., Wassmer, T., Fraser, G., Smith, J., Perkinton, M., Billinton, A. & Livesey, F.J. (2018) Extracellular Monomeric and Aggregated Tau Efficiently Enter Human Neurons through Overlapping but Distinct Pathways. *Cell Rep*, **22**, 3612-3624.

Fa, M., Puzzo, D., Piacentini, R., Staniszewski, A., Zhang, H., Baltrons, M.A., Li Puma, D.D., Chatterjee, I., Li, J., Saeed, F., Berman, H.L., Ripoli, C., Gulisano, W., Gonzalez, J., Tian, H., Costa, J.A., Lopez, P., Davidowitz, E., Yu, W.H., Haroutunian, V., Brown, L.M., Palmeri, A., Sigurdsson, E.M., Duff, K.E., Teich, A.F., Honig, L.S., Sierks, M., Moe, J.G., D'Adamio, L., Grassi, C., Kanaan, N.M., Fraser, P.E. & Arancio, O. (2016) Extracellular Tau Oligomers Produce An Immediate Impairment of LTP and Memory. *Sci Rep*, **6**, 19393.

Falcon, B., Cavallini, A., Angers, R., Glover, S., Murray, T.K., Barnham, L., Jackson, S., O'Neill, M.J., Isaacs, A.M., Hutton, M.L., Szekeres, P.G., Goedert, M. & Bose, S. (2015) Conformation determines the seeding potencies of native and recombinant Tau aggregates. *J Biol Chem*, **290**, 1049-1065.

Falcon, B., Zhang, W., Murzin, A.G., Murshudov, G., Garringer, H.J., Vidal, R., Crowther, R.A., Ghetti, B., Scheres, S.H.W. & Goedert, M. (2018a) Structures of filaments from Pick's disease reveal a novel tau protein fold. *Nature*, **561**, 137-140.

Falcon, B., Zhang, W., Schweighauser, M., Murzin, A.G., Vidal, R., Garringer, H.J., Ghetti, B., Scheres, S.H.W. & Goedert, M. (2018b) Tau filaments from multiple cases of sporadic and inherited Alzheimer's disease adopt a common fold. *Acta Neuropathol*, **136**, 699-708.

Falcon, B., Zivanov, J., Zhang, W., Murzin, A.G., Garringer, H.J., Vidal, R., Crowther, R.A., Newell, K.L., Ghetti, B., Goedert, M. & Scheres, S.H.W. (2019) Novel tau filament fold in chronic traumatic encephalopathy encloses hydrophobic molecules. *Nature*, **568**, 420-423.

Falsig, J., Julius, C., Margalith, I., Schwarz, P., Heppner, F.L. & Aguzzi, A. (2008) A versatile prion replication assay in organotypic brain slices. *Nat Neurosci*, **11**, 109-117.

Falsig, J., Sonati, T., Herrmann, U.S., Saban, D., Li, B., Arroyo, K., Ballmer, B., Liberski, P.P. & Aguzzi, A. (2012) Prion pathogenesis is faithfully reproduced in cerebellar organotypic slice cultures. *PLoS Pathog*, **8**, e1002985.

Ferreira, D.G., Temido-Ferreira, M., Vicente Miranda, H., Batalha, V.L., Coelho, J.E., Szego, E.M., Marques-Morgado, I., Vaz, S.H., Rhee, J.S., Schmitz, M., Zerr, I., Lopes, L.V. & Outeiro, T.F. (2017) alpha-synuclein interacts with PrP(C) to induce cognitive impairment through mGluR5 and NMDAR2B. *Nat Neurosci*, **20**, 1569-1579.

Ferrer, I. (2018) Oligodendrogliopathy in neurodegenerative diseases with abnormal protein aggregates: The forgotten partner. *Prog Neurobiol*, **169**, 24-54.

Ferrer, I. (2022) Hypothesis review: Alzheimer's overture guidelines. *Brain Pathol*, e13122.

Ferrer, I., Aguilo Garcia, M., Carmona, M., Andres-Benito, P., Torrejon-Escribano, B., Garcia-Esparcia, P. & Del Rio, J.A. (2019) Involvement of Oligodendrocytes in Tau Seeding and Spreading in Tauopathies. *Front Aging Neurosci*, **11**, 112.

Ferrer, I., Andres-Benito, P., Garcia-Esparcia, P., Lopez-Gonzalez, I., Valiente, D., Jordan-Pirla, M., Carmona, M., Sala-Jarque, J., Gil, V. & Del Rio, J.A. (2022a) Differences in Tau Seeding in Newborn and Adult Wild-Type Mice. *Int J Mol Sci*, **23**.

Ferrer, I., Andres-Benito, P., Sala-Jarque, J., Gil, V. & Del Rio, J.A. (2022b) Corrigendum: Capacity for Seeding and Spreading of Argyrophilic Grain Disease in a Wild-Type Murine Model; Comparisons With Primary Age-Related Tauopathy. *Front Mol Neurosci*, **15**, 870475.

Ferrer, I., Garcia, M.A., Gonzalez, I.L., Lucena, D.D., Villalonga, A.R., Tech, M.C., Llorens, F., Garcia-Esparcia, P., Martinez-Maldonado, A., Mendez, M.F., Escribano, B.T., Bech-Serra, J.J., Sabido, E., de la Torre Gomez, C. & Del Rio, J.A. (2018) Aging-related tau astrogliopathy (ARTAG): not only tau phosphorylation in astrocytes. *Brain Pathol*, **28**, 965-985.

Ferrer, I., Lopez-Gonzalez, I., Carmona, M., Arregui, L., Dalfo, E., Torrejon-Escribano, B., Diehl, R. & Kovacs, G.G. (2014) Glial and neuronal tau pathology in tauopathies: characterization of disease-specific phenotypes and tau pathology progression. *J Neuropathol Exp Neurol*, **73**, 81-97.

Ferrer, I., Zelaya, M.V., Aguilo Garcia, M., Carmona, M., Lopez-Gonzalez, I., Andres-Benito, P., Lidon, L., Gavin, R., Garcia-Esparcia, P. & Del Rio, J.A. (2020) Relevance of host tau in tau seeding and spreading in tauopathies. *Brain Pathol*, **30**, 298-318.

Fichou, Y., Lin, Y., Rauch, J.N., Vigers, M., Zeng, Z., Srivastava, M., Keller, T.J., Freed, J.H., Kosik, K.S. & Han, S. (2018) Cofactors are essential constituents of stable and seeding-active tau fibrils. *Proc Natl Acad Sci U S A*, **115**, 13234-13239.

Fischer, D., Mukrasch, M.D., von Bergen, M., Klos-Witkowska, A., Biernat, J., Griesinger, C., Mandelkow, E. & Zweckstetter, M. (2007) Structural and microtubule binding properties of tau mutants of frontotemporal dementias. *Biochemistry*, **46**, 2574-2582.

Fischer, M., Rulicke, T., Raeber, A., Sailer, A., Moser, M., Oesch, B., Brandner, S., Aguzzi, A. & Weissmann, C. (1996) Prion protein (PrP) with amino-proximal deletions restoring susceptibility of PrP knockout mice to scrapie. *EMBO J*, **15**, 1255-1264.

Fitzpatrick, A.W.P., Falcon, B., He, S., Murzin, A.G., Murshudov, G., Garringer, H.J., Crowther, R.A., Ghetti, B., Goedert, M. & Scheres, S.H.W. (2017) Cryo-EM structures of tau filaments from Alzheimer's disease. *Nature*, **547**, 185-190.

Flach, K., Hilbrich, I., Schiffmann, A., Gartner, U., Kruger, M., Leonhardt, M., Waschipky, H., Wick, L., Arendt, T. & Holzer, M. (2012) Tau oligomers impair artificial membrane integrity and cellular viability. *J Biol Chem*, **287**, 43223-43233.

Florenzano, F., Veronica, C., Ciasca, G., Ciotti, M.T., Pittaluga, A., Olivero, G., Feligioni, M., Iannuzzi, F., Latina, V., Maria Sciacca, M.F., Sinopoli, A., Milardi, D., Pappalardo, G., Marco, S., Papi, M., Atlante, A., Bobba, A., Borreca, A., Calissano, P. & Amadoro, G. (2017) Extracellular truncated tau causes early presynaptic dysfunction associated with Alzheimer's disease and other tauopathies. *Oncotarget*, **8**, 64745-64778.

Ford, M.J., Burton, L.J., Morris, R.J. & Hall, S.M. (2002) Selective expression of prion protein in peripheral tissues of the adult mouse. *Neuroscience*, **113**, 177-192.

Fornito, A., Zalesky, A. & Breakspear, M. (2015) The connectomics of brain disorders. *Nat Rev Neurosci*, **16**, 159-172.

Forrest, S.L., Kril, J.J. & Kovacs, G.G. (2021) Association Between Globular Glial Tauopathies and Frontotemporal Dementia-Expanding the Spectrum of Gliocentric Disorders: A Review. *JAMA Neurol*, **78**, 1004-1014.

Freir, D.B., Nicoll, A.J., Klyubin, I., Panico, S., Mc Donald, J.M., Risse, E., Asante, E.A., Farrow, M.A., Sessions, R.B., Saibil, H.R., Clarke, A.R., Rowan, M.J., Walsh, D.M. & Collinge, J. (2011) Interaction between prion protein and toxic amyloid beta assemblies can be therapeutically targeted at multiple sites. *Nat Commun*, **2**, 336.

Friedhoff, P., Schneider, A., Mandelkow, E.M. & Mandelkow, E. (1998) Rapid assembly of Alzheimer-like paired helical filaments from microtubule-associated protein tau monitored by fluorescence in solution. *Biochemistry*, **37**, 10223-10230.

Frost, B., Jacks, R.L. & Diamond, M.I. (2009) Propagation of tau misfolding from the outside to the inside of a cell. *J Biol Chem*, **284**, 12845-12852.

Furman, J.L., Vaquer-Alicea, J., White, C.L., 3rd, Cairns, N.J., Nelson, P.T. & Diamond, M.I. (2017) Widespread tau seeding activity at early Braak stages. *Acta Neuropathol*, **133**, 91-100.

Ganguly, P., Do, T.D., Larini, L., LaPointe, N.E., Sercel, A.J., Shade, M.F., Feinstein, S.C., Bowers, M.T. & Shea, J.E. (2015) Tau assembly: the dominant role of PHF6 (VQIVYK) in microtubule binding region repeat R3. *J Phys Chem B*, **119**, 4582-4593.

Garcia-Cabrero, A.M., Guerrero-Lopez, R., Giraldez, B.G., Llorens-Martin, M., Avila, J., Serratosa, J.M. & Sanchez, M.P. (2013) Hyperexcitability and epileptic seizures in a model of frontotemporal dementia. *Neurobiol Dis*, **58**, 200-208.

Gavin, R., Lidon, L., Ferrer, I. & Del Rio, J.A. (2020) The Quest for Cellular Prion Protein Functions in the Aged and Neurodegenerating Brain. *Cells*, **9**.

Ghetti, B., Oblak, A.L., Boeve, B.F., Johnson, K.A., Dickerson, B.C. & Goedert, M. (2015) Invited review: Frontotemporal dementia caused by microtubule-associated protein tau gene (MAPT) mutations: a chameleon for neuropathology and neuroimaging. *Neuropathol Appl Neurobiol*, **41**, 24-46.

Ghetti, B., Tagliavini, F., Masters, C.L., Beyreuther, K., Giaccone, G., Verga, L., Farlow, M.R., Conneally, P.M., Dlouhy, S.R., Azzarelli, B. & et al. (1989) Gerstmann-Straussler-Scheinker disease. II. Neurofibrillary tangles and plaques with PrP-amyloid coexist in an affected family. *Neurology*, **39**, 1453-1461.

Giachin, G., Mai, P.T., Tran, T.H., Salzano, G., Benetti, F., Migliorati, V., Arcovito, A., Della Longa, S., Mancini, G., D'Angelo, P. & Legname, G. (2015) The non-octarepeat copper binding site of the prion protein is a key regulator of prion conversion. *Sci Rep*, **5**, 15253.

Giasson, B.I., Forman, M.S., Higuchi, M., Golbe, L.I., Graves, C.L., Kotzbauer, P.T., Trojanowski, J.Q. & Lee, V.M. (2003) Initiation and synergistic fibrillization of tau and alpha-synuclein. *Science*, **300**, 636-640.

Gilvesy, A., Husen, E., Magloczky, Z., Mihaly, O., Hortobagyi, T., Kanatani, S., Heinsen, H., Renier, N., Hokfelt, T., Mulder, J., Uhlen, M., Kovacs, G.G. & Adori, C. (2022) Spatiotemporal characterization of cellular tau pathology in the human locus coeruleus-pericoerulear complex by three-dimensional imaging. *Acta Neuropathol*, **144**, 651-676.

Gimbel, D.A., Nygaard, H.B., Coffey, E.E., Gunther, E.C., Lauren, J., Gimbel, Z.A. & Strittmatter, S.M. (2010) Memory impairment in transgenic Alzheimer mice requires cellular prion protein. *J Neurosci*, **30**, 6367-6374.

Goedert, M. (2020) Tau proteinopathies and the prion concept. *Prog Mol Biol Transl Sci*, **175**, 239-259.

Goedert, M. (2021) Cryo-EM structures of tau filaments from human brain. *Essays Biochem*, **65**, 949-959.

Goedert, M., Clavaguera, F. & Tolnay, M. (2010) The propagation of prion-like protein inclusions in neurodegenerative diseases. *Trends Neurosci*, **33**, 317-325.

Goedert, M., Eisenberg, D.S. & Crowther, R.A. (2017a) Propagation of Tau Aggregates and Neurodegeneration. *Annu Rev Neurosci*, **40**, 189-210.

Goedert, M. & Jakes, R. (1990) Expression of separate isoforms of human tau protein: correlation with the tau pattern in brain and effects on tubulin polymerization. *EMBO J*, **9**, 4225-4230.

Goedert, M. & Jakes, R. (2005) Mutations causing neurodegenerative tauopathies. *Biochim Biophys Acta*, **1739**, 240-250.

Goedert, M., Jakes, R., Spillantini, M.G., Hasegawa, M., Smith, M.J. & Crowther, R.A. (1996) Assembly of microtubule-associated protein tau into Alzheimer-like filaments induced by sulphated glycosaminoglycans. *Nature*, **383**, 550-553.

Goedert, M., Masuda-Suzukake, M. & Falcon, B. (2017b) Like prions: the propagation of aggregated tau and alpha-synuclein in neurodegeneration. *Brain*, **140**, 266-278.

Goedert, M. & Spillantini, M.G. (2011) Pathogenesis of the tauopathies. *J Mol Neurosci*, **45**, 425-431.

Goedert, M., Spillantini, M.G., Jakes, R., Rutherford, D. & Crowther, R.A. (1989) Multiple isoforms of human microtubule-associated protein tau: sequences and localization in neurofibrillary tangles of Alzheimer's disease. *Neuron*, **3**, 519-526.

Goedert, M., Wischik, C.M., Crowther, R.A., Walker, J.E. & Klug, A. (1988) Cloning and sequencing of the cDNA encoding a core protein of the paired helical filament of Alzheimer disease: identification as the microtubule-associated protein tau. *Proc Natl Acad Sci U S A*, **85**, 4051-4055.

Gomes, L.A., Hipp, S.A., Rijal Upadhaya, A., Balakrishnan, K., Ospitalieri, S., Koper, M.J., Largo-Barrientos, P., Uytterhoeven, V., Reichwald, J., Rabe, S., Vandenberghe, R., von Arnim, C.A.F., Tousseyn, T., Feederle, R., Giudici, C.,

Willem, M., Staufenbiel, M. & Thal, D.R. (2019) Abeta-induced acceleration of Alzheimer-related tau-pathology spreading and its association with prion protein. *Acta Neuropathol*, **138**, 913-941.

Gomez-Ramos, A., Diaz-Hernandez, M., Cuadros, R., Hernandez, F. & Avila, J. (2006) Extracellular tau is toxic to neuronal cells. *FEBS Lett*, **580**, 4842-4850.

Gomez-Ramos, A., Diaz-Hernandez, M., Rubio, A., Miras-Portugal, M.T. & Avila, J. (2008) Extracellular tau promotes intracellular calcium increase through M1 and M3 muscarinic receptors in neuronal cells. *Mol Cell Neurosci*, **37**, 673-681.

Gong, C.X., Liu, F., Grundke-Iqbal, I. & Iqbal, K. (2005) Post-translational modifications of tau protein in Alzheimer's disease. *J Neural Transm (Vienna)*, **112**, 813-838.

Gonzalez, C., Armijo, E., Bravo-Alegria, J., Becerra-Calixto, A., Mays, C.E. & Soto, C. (2018) Modeling amyloid beta and tau pathology in human cerebral organoids. *Mol Psychiatry*, **23**, 2363-2374.

Gotz, J., Bodea, L.G. & Goedert, M. (2018) Rodent models for Alzheimer disease. *Nat Rev Neurosci*, **19**, 583-598.

Gotz, J., Streffer, J.R., David, D., Schild, A., Hoerndli, F., Pennanen, L., Kurosinski, P. & Chen, F. (2004) Transgenic animal models of Alzheimer's disease and related disorders: histopathology, behavior and therapy. *Mol Psychiatry*, **9**, 664-683.

Gousset, K., Schiff, E., Langevin, C., Marijanovic, Z., Caputo, A., Browman, D.T., Chenouard, N., de Chaumont, F., Martino, A., Enninga, J., Olivo-Marin, J.C., Mannel, D. & Zurzolo, C. (2009) Prions hijack tunnelling nanotubes for intercellular spread. *Nat Cell Biol*, **11**, 328-336.

Griffoni, C., Toni, M., Spisni, E., Bianco, M., Santi, S., Riccio, M. & Tomasi, V. (2003) The cellular prion protein: biochemistry, topology, and physiologic functions. *Cell Biochem Biophys*, **38**, 287-304.

Grundke-Iqbal, I., Iqbal, K., Quinlan, M., Tung, Y.C., Zaidi, M.S. & Wisniewski, H.M. (1986) Microtubule-associated protein tau. A component of Alzheimer paired helical filaments. *J Biol Chem*, **261**, 6084-6089.

Guillot-Sestier, M.V., Sunyach, C., Ferreira, S.T., Marzolo, M.P., Bauer, C., Thevenet, A. & Checler, F. (2012) alpha-Secretase-derived fragment of cellular prion, N1, protects against monomeric and oligomeric amyloid beta (Abeta)-associated cell death. *J Biol Chem*, **287**, 5021-5032.

Gunther, E.C., Smith, L.M., Kostylev, M.A., Cox, T.O., Kaufman, A.C., Lee, S., Folta-Stogniew, E., Maynard, G.D., Um, J.W., Stagi, M., Heiss, J.K., Stoner, A., Noble, G.P., Takahashi, H., Haas, L.T., Schneekloth, J.S., Merkel, J., Teran, C., Naderi, Z.K., Supattapone, S. & Strittmatter, S.M. (2019) Rescue of Transgenic Alzheimer's Pathophysiology by Polymeric Cellular Prion Protein Antagonists. *Cell Rep*, **26**, 145-158 e148.

Guo, J.L., Buist, A., Soares, A., Callaerts, K., Calafate, S., Stevenaert, F., Daniels, J.P., Zoll, B.E., Crowe, A., Brunden, K.R., Moechars, D. & Lee, V.M. (2016a) The Dynamics and Turnover of Tau Aggregates in Cultured Cells: INSIGHTS INTO THERAPIES FOR TAUOPATHIES. *J Biol Chem*, **291**, 13175-13193.

Guo, J.L., Covell, D.J., Daniels, J.P., Iba, M., Stieber, A., Zhang, B., Riddle, D.M., Kwong, L.K., Xu, Y., Trojanowski, J.Q. & Lee, V.M. (2013) Distinct alpha-synuclein strains differentially promote tau inclusions in neurons. *Cell*, **154**, 103-117.

Guo, J.L. & Lee, V.M. (2011) Seeding of normal Tau by pathological Tau conformers drives pathogenesis of Alzheimer-like tangles. *J Biol Chem*, **286**, 15317-15331.

Guo, J.L. & Lee, V.M. (2014) Cell-to-cell transmission of pathogenic proteins in neurodegenerative diseases. *Nat Med*, **20**, 130-138.

Guo, J.L., Narasimhan, S., Changolkar, L., He, Z., Stieber, A., Zhang, B., Gathagan, R.J., Iba, M., McBride, J.D., Trojanowski, J.Q. & Lee, V.M. (2016b) Unique pathological tau conformers from Alzheimer's brains transmit tau pathology in nontransgenic mice. *J Exp Med*, **213**, 2635-2654.

Guo, T., Noble, W. & Hanger, D.P. (2017) Roles of tau protein in health and disease. *Acta Neuropathol*, **133**, 665-704.

Habes, M., Janowitz, D., Erus, G., Toledo, J.B., Resnick, S.M., Doshi, J., Van der Auwera, S., Wittfeld, K., Hegenscheid, K., Hosten, N., Biffar, R., Homuth, G., Volzke, H., Grabe, H.J., Hoffmann, W. & Davatzikos, C. (2016) Advanced brain aging: relationship with epidemiologic and genetic risk factors, and overlap with Alzheimer disease atrophy patterns. *Transl Psychiatry*, **6**, e775.

Hall, A.M., Throesch, B.T., Buckingham, S.C., Markwardt, S.J., Peng, Y., Wang, Q., Hoffman, D.A. & Roberson, E.D. (2015) Tau-dependent Kv4.2 depletion and dendritic hyperexcitability in a mouse model of Alzheimer's disease. *J Neurosci*, **35**, 6221-6230.

Hallinan, G.I., Vargas-Caballero, M., West, J. & Deinhardt, K. (2019) Tau Misfolding Efficiently Propagates between Individual Intact Hippocampal Neurons. *J Neurosci*, **39**, 9623-9632.

Han, J., Zhang, J., Yao, H., Wang, X., Li, F., Chen, L., Gao, C., Gao, J., Nie, K., Zhou, W. & Dong, X. (2006) Study on interaction between microtubule associated protein tau and prion protein. *Sci China C Life Sci*, **49**, 473-479.

Hanes, J., Zilka, N., Bartkova, M., Caletkova, M., Dobrota, D. & Novak, M. (2009) Rat tau proteome consists of six tau isoforms: implication for animal models of human tauopathies. *J Neurochem*, **108**, 1167-1176.

Haraguchi, T., Fisher, S., Olofsson, S., Endo, T., Groth, D., Tarentino, A., Borchelt, D.R., Teplow, D., Hood, L., Burlingame, A. & et al. (1989) Asparagine-linked glycosylation of the scrapie and cellular prion proteins. *Arch Biochem Biophys*, **274**, 1-13.

Harasta, A.E. & Ittner, L.M. (2017) Alzheimer's Disease: Insights from Genetic Mouse Models and Current Advances in Human IPSC-Derived Neurons. *Adv Neurobiol*, **15**, 3-29.

Harrington, C.R., Storey, J.M., Clunas, S., Harrington, K.A., Horsley, D., Ishaq, A., Kemp, S.J., Larch, C.P., Marshall, C., Nicoll, S.L., Rickard, J.E., Simpson, M., Sinclair, J.P., Storey, L.J. & Wischik, C.M. (2015) Cellular Models of Aggregation-dependent Template-directed Proteolysis to Characterize Tau Aggregation Inhibitors for Treatment of Alzheimer Disease. *J Biol Chem*, **290**, 10862-10875.

Harris, J.A., Koyama, A., Maeda, S., Ho, K., Devidze, N., Dubal, D.B., Yu, G.Q., Masliah, E. & Mucke, L. (2012) Human P301L-mutant tau expression in mouse entorhinal-hippocampal network causes tau aggregation and presynaptic pathology but no cognitive deficits. *PLoS One*, **7**, e45881.

Hernandez-Rapp, J., Martin-Lanneree, S., Hirsch, T.Z., Pradines, E., Alleaume-Butaux, A., Schneider, B., Baudry, A., Launay, J.M. & Mouillet-Richard, S. (2014) A PrP(C)-caveolin-Lyn complex negatively controls neuronal GSK3beta and serotonin 1B receptor. *Sci Rep*, **4**, 4881.

Hernandez, F., Merchan-Rubira, J., Valles-Saiz, L., Rodriguez-Matellan, A. & Avila, J. (2020) Differences Between Human and Murine Tau at the N-terminal End. *Front Aging Neurosci*, **12**, 11.

Hickman, R.A., Faustin, A. & Wisniewski, T. (2016) Alzheimer Disease and Its Growing Epidemic: Risk Factors, Biomarkers, and the Urgent Need for Therapeutics. *Neurol Clin*, **34**, 941-953.

Hitt, B.D., Vaquer-Alicea, J., Manon, V.A., Beaver, J.D., Kashmer, O.M., Garcia, J.N. & Diamond, M.I. (2021) Ultrasensitive tau biosensor cells detect no seeding in Alzheimer's disease CSF. *Acta Neuropathol Commun*, **9**, 99.

Hochgrafe, K., Sydow, A. & Mandelkow, E.M. (2013) Regulatable transgenic mouse models of Alzheimer disease: onset, reversibility and spreading of Tau pathology. *FEBS J*, **280**, 4371-4381.

Hoglinger, G.U., Respondek, G. & Kovacs, G.G. (2018) New classification of tauopathies. *Rev Neurol (Paris)*, **174**, 664-668.

Holmes, B.B., DeVos, S.L., Kfoury, N., Li, M., Jacks, R., Yanamandra, K., Ouidja, M.O., Brodsky, F.M., Marasa, J., Bagchi, D.P., Kotzbauer, P.T., Miller, T.M., Papy-Garcia, D. & Diamond, M.I. (2013) Heparan sulfate proteoglycans mediate internalization and propagation of specific proteopathic seeds. *Proc Natl Acad Sci U S A*, **110**, E3138-3147.

Holmes, B.B., Furman, J.L., Mahan, T.E., Yamasaki, T.R., Mirbaha, H., Eades, W.C., Belaygorod, L., Cairns, N.J., Holtzman, D.M. & Diamond, M.I. (2014) Proteopathic tau seeding predicts tauopathy in vivo. *Proc Natl Acad Sci U S A*, **111**, E4376-4385.

Holth, J.K., Bomben, V.C., Reed, J.G., Inoue, T., Younkin, L., Younkin, S.G., Pautler, R.G., Botas, J. & Noebels, J.L. (2013) Tau loss attenuates neuronal network hyperexcitability in mouse and Drosophila genetic models of epilepsy. *J Neurosci*, **33**, 1651-1659.

Holzer, M., Schade, N., Opitz, A., Hilbrich, I., Stieler, J., Vogel, T., Neukel, V., Oberstadt, M., Totzke, F., Schachtele, C., Sippl, W. & Hilgeroth, A. (2018) Novel Protein Kinase Inhibitors Related to Tau Pathology Modulate Tau Protein-Self Interaction Using a Luciferase Complementation Assay. *Molecules*, **23**.

Honey, C.J., Sporns, O., Cammoun, L., Gigandet, X., Thiran, J.P., Meuli, R. & Hagmann, P. (2009) Predicting human resting-state functional connectivity from structural connectivity. *Proc Natl Acad Sci U S A*, **106**, 2035-2040.

Hosokawa, M., Arai, T., Masuda-Suzukake, M., Nonaka, T., Yamashita, M., Akiyama, H. & Hasegawa, M. (2012) Methylene blue reduced abnormal tau accumulation in P301L tau transgenic mice. *PLoS One*, **7**, e52389.

Hou, Z., Chen, D., Ryder, B.D. & Joachimiak, L.A. (2021) Biophysical properties of a tau seed. *Sci Rep*, **11**, 13602.

Hu, W., Zhang, X., Tung, Y.C., Xie, S., Liu, F. & Iqbal, K. (2016) Hyperphosphorylation determines both the spread and the morphology of tau pathology. *Alzheimers Dement*, **12**, 1066-1077.

Hutton, M., Lendon, C.L., Rizzu, P., Baker, M., Froelich, S., Houlden, H., Pickering-Brown, S., Chakraverty, S., Isaacs, A., Grover, A., Hackett, J., Adamson, J., Lincoln, S., Dickson, D., Davies, P., Petersen, R.C., Stevens, M., de Graaff, E., Wauters, E., van Baren, J., Hillebrand, M., Joosse, M., Kwon, J.M., Nowotny, P., Che, L.K., Norton, J., Morris, J.C., Reed, L.A., Trojanowski, J., Basun, H., Lannfelt, L., Neystat, M., Fahn, S., Dark, F., Tannenberg, T., Dodd, P.R., Hayward, N., Kwok, J.B., Schofield, P.R., Andreadis, A., Snowden, J., Craufurd, D., Neary, D., Owen, F., Oostra, B.A., Hardy, J., Goate, A., van Swieten, J., Mann, D., Lynch, T. & Heutink, P. (1998) Association of missense and 5'-splice-site mutations in tau with the inherited dementia FTDP-17. *Nature*, **393**, 702-705.

Hwang, S.C., Jhon, D.Y., Bae, Y.S., Kim, J.H. & Rhee, S.G. (1996) Activation of phospholipase C-gamma by the concerted action of tau proteins and arachidonic acid. *J Biol Chem*, **271**, 18342-18349.

Iba, M., Guo, J.L., McBride, J.D., Zhang, B., Trojanowski, J.Q. & Lee, V.M. (2013) Synthetic tau fibrils mediate transmission of neurofibrillary tangles in a transgenic mouse model of Alzheimer's-like tauopathy. *J Neurosci*, **33**, 1024-1037.

Iba, M., McBride, J.D., Guo, J.L., Zhang, B., Trojanowski, J.Q. & Lee, V.M. (2015) Tau pathology spread in PS19 tau transgenic mice following locus coeruleus (LC) injections of synthetic tau fibrils is determined by the LC's afferent and efferent connections. *Acta Neuropathol*, **130**, 349-362.

Ismail, T. & Kanapathipillai, M. (2018) Effect of cellular polyanion mimetics on tau peptide aggregation. *J Pept Sci*, **24**, e3125.

Jackson, S.J., Kerridge, C., Cooper, J., Cavallini, A., Falcon, B., Cella, C.V., Landi, A., Szekeres, P.G., Murray, T.K., Ahmed, Z., Goedert, M., Hutton, M., O'Neill, M.J. & Bose, S. (2016) Short Fibrils Constitute the Major Species of Seed-Competent Tau in the Brains of Mice Transgenic for Human P301S Tau. *J Neurosci*, **36**, 762-772.

Jankowsky, J.L., Fadale, D.J., Anderson, J., Xu, G.M., Gonzales, V., Jenkins, N.A., Copeland, N.G., Lee, M.K., Younkin, L.H., Wagner, S.L., Younkin, S.G. & Borchelt, D.R. (2004) Mutant presenilins specifically elevate the levels of the 42 residue beta-amyloid peptide in vivo: evidence for augmentation of a 42-specific gamma secretase. *Hum Mol Genet*, **13**, 159-170.

Jarrett, J.T. & Lansbury, P.T., Jr. (1993) Seeding "one-dimensional crystallization" of amyloid: a pathogenic mechanism in Alzheimer's disease and scrapie? *Cell*, **73**, 1055-1058.

Jeganathan, S., Chinnathambi, S., Mandelkow, E.M. & Mandelkow, E. (2012) Conformations of microtubule-associated protein Tau mapped by fluorescence resonance energy transfer. *Methods Mol Biol*, **849**, 85-99.

Jeganathan, S., Hascher, A., Chinnathambi, S., Biernat, J., Mandelkow, E.M. & Mandelkow, E. (2008) Proline-directed pseudo-phosphorylation at AT8 and PHF1 epitopes induces a compaction of the paperclip folding of Tau and generates a pathological (MC-1) conformation. *J Biol Chem*, **283**, 32066-32076.

Jeganathan, S., von Bergen, M., Brutlach, H., Steinhoff, H.J. & Mandelkow, E. (2006) Global hairpin folding of tau in solution. *Biochemistry*, **45**, 2283-2293.

Kamath, T.V., Klickstein, N., Commins, C., Fernandes, A.R., Oakley, D.H., Frosch, M.P., Hyman, B.T. & Dujardin, S. (2021) Kinetics of tau aggregation reveals patient-specific tau characteristics among Alzheimer's cases. *Brain Commun*, **3**, fcab096.

Kampers, T., Friedhoff, P., Biernat, J., Mandelkow, E.M. & Mandelkow, E. (1996) RNA stimulates aggregation of microtubule-associated protein tau into Alzheimer-like paired helical filaments. *FEBS Lett*, **399**, 344-349.

Kanai, Y., Takemura, R., Oshima, T., Mori, H., Ihara, Y., Yanagisawa, M., Masaki, T. & Hirokawa, N. (1989) Expression of multiple tau isoforms and microtubule bundle formation in fibroblasts transfected with a single tau cDNA. *J Cell Biol*, **109**, 1173-1184.

Kaniyappan, S., Chandupatla, R.R., Mandelkow, E.M. & Mandelkow, E. (2017) Extracellular low-n oligomers of tau cause selective synaptotoxicity without affecting cell viability. *Alzheimers Dement*, **13**, 1270-1291.

Kaniyappan, S., Tepper, K., Biernat, J., Chandupatla, R.R., Hubschmann, S., Irsen, S., Bicher, S., Klatt, C., Mandelkow, E.M. & Mandelkow, E. (2020) FRET-based Tau seeding assay does not represent prion-like templated assembly of Tau filaments. *Mol Neurodegener*, **15**, 39.

Karch, C.M., Jeng, A.T. & Goate, A.M. (2012) Extracellular Tau levels are influenced by variability in Tau that is associated with tauopathies. *J Biol Chem*, **287**, 42751-42762.

Katsikoudi, A., Ficulle, E., Cavallini, A., Sharman, G., Guyot, A., Zagnoni, M., Eastwood, B.J., Hutton, M. & Bose, S. (2020) Quantitative propagation of assembled human Tau from Alzheimer's disease brain in microfluidic neuronal cultures. *J Biol Chem*, **295**, 13079-13093.

Katsinelos, T., Zeitler, M., Dimou, E., Karakatsani, A., Muller, H.M., Nachman, E., Steringer, J.P., Ruiz de Almodovar, C., Nickel, W. & Jahn, T.R. (2018) Unconventional Secretion Mediates the Trans-cellular Spreading of Tau. *Cell Rep*, **23**, 2039-2055.

Kaufman, S.K., Sanders, D.W., Thomas, T.L., Ruchinskas, A.J., Vaquer-Alicea, J., Sharma, A.M., Miller, T.M. & Diamond, M.I. (2016) Tau Prion Strains Dictate Patterns of Cell Pathology, Progression Rate, and Regional Vulnerability In Vivo. *Neuron*, **92**, 796-812.

Kaufman, S.K., Thomas, T.L., Del Tredici, K., Braak, H. & Diamond, M.I. (2017) Characterization of tau prion seeding activity and strains from formaldehyde-fixed tissue. *Acta Neuropathol Commun*, **5**, 41.

Kazim, S.F., Chuang, S.C., Zhao, W., Wong, R.K., Bianchi, R. & Iqbal, K. (2017) Early-Onset Network Hyperexcitability in Presymptomatic Alzheimer's Disease Transgenic Mice Is Suppressed by Passive Immunization with Anti-Human APP/Abeta Antibody and by mGluR5 Blockade. *Front Aging Neurosci*, **9**, 71.

Kessels, H.W., Nguyen, L.N., Nabavi, S. & Malinow, R. (2010) The prion protein as a receptor for amyloid-beta. *Nature*, **466**, E3-4; discussion E4-5.

Kfoury, N., Holmes, B.B., Jiang, H., Holtzman, D.M. & Diamond, M.I. (2012) Trans-cellular propagation of Tau aggregation by fibrillar species. *J Biol Chem*, **287**, 19440-19451.

Khlistunova, I., Biernat, J., Wang, Y., Pickhardt, M., von Bergen, M., Gazova, Z., Mandelkow, E. & Mandelkow, E.M. (2006) Inducible expression of Tau repeat domain in cell models of tauopathy: aggregation is toxic to cells but can be reversed by inhibitor drugs. *J Biol Chem*, **281**, 1205-1214.

Kim, D., Lim, S., Haque, M.M., Ryoo, N., Hong, H.S., Rhim, H., Lee, D.E., Chang, Y.T., Lee, J.S., Cheong, E., Kim, D.J. & Kim, Y.K. (2015) Identification of disulfide cross-linked tau dimer responsible for tau propagation. *Sci Rep*, **5**, 15231.

Kirk, R.G.W. (2018) Recovering The Principles of Humane Experimental Technique: The 3Rs and the Human Essence of Animal Research. *Sci Technol Human Values*, **43**, 622-648.

Klyubin, I., Nicoll, A.J., Khalili-Shirazi, A., Farmer, M., Canning, S., Mably, A., Linehan, J., Brown, A., Wakeling, M., Brandner, S., Walsh, D.M., Rowan, M.J. & Collinge, J. (2014) Peripheral administration of a humanized anti-PrP antibody blocks Alzheimer's disease Abeta synaptotoxicity. *J Neurosci*, **34**, 6140-6145.

Kolar, K., Dondorp, D., Zwiggelaar, J.C., Hoyer, J. & Chatzigeorgiou, M. (2021) Mesmerize is a dynamically adaptable user-friendly analysis platform for 2D and 3D calcium imaging data. *Nat Commun*, **12**, 6569.

Kostylev, M.A., Kaufman, A.C., Nygaard, H.B., Patel, P., Haas, L.T., Gunther, E.C., Vortmeyer, A. & Strittmatter, S.M. (2015) Prion-Protein-interacting Amyloid-beta Oligomers of High Molecular Weight Are Tightly Correlated with Memory Impairment in Multiple Alzheimer Mouse Models. *J Biol Chem*, **290**, 17415-17438.

Kovacs, G.G. (2015) Invited review: Neuropathology of tauopathies: principles and practice. *Neuropathol Appl Neurobiol*, **41**, 3-23.

Kovacs, G.G. (2017) Tauopathies. *Handb Clin Neurol*, **145**, 355-368.

Kovacs, G.G., Ferrer, I., Grinberg, L.T., Alafuzoff, I., Attems, J., Budka, H., Cairns, N.J., Crary, J.F., Duyckaerts, C., Ghetti, B., Halliday, G.M., Ironside, J.W., Love, S., Mackenzie, I.R., Munoz, D.G., Murray, M.E., Nelson, P.T., Takahashi, H., Trojanowski, J.Q., Ansorge, O., Arzberger, T., Baborie, A., Beach, T.G., Bieniek, K.F., Bigio, E.H., Bodi, I., Dugger, B.N., Feany, M., Gelpi, E., Gentleman, S.M., Giaccone, G., Hatanpaa, K.J., Heale, R., Hof, P.R., Hofer, M., Hortobagyi, T.,

Jellinger, K., Jicha, G.A., Ince, P., Kofler, J., Kovari, E., Kril, J.J., Mann, D.M., Matej, R., McKee, A.C., McLean, C., Milenkovic, I., Montine, T.J., Murayama, S., Lee, E.B., Rahimi, J., Rodriguez, R.D., Rozemuller, A., Schneider, J.A., Schultz, C., Seeley, W., Seilhean, D., Smith, C., Tagliavini, F., Takao, M., Thal, D.R., Toledo, J.B., Tolnay, M., Troncoso, J.C., Vinters, H.V., Weis, S., Wharton, S.B., White, C.L., 3rd, Wisniewski, T., Woulfe, J.M., Yamada, M. & Dickson, D.W. (2016) Aging-related tau astrogliopathy (ARTAG): harmonized evaluation strategy. *Acta Neuropathol*, **131**, 87-102.

Kovacs, G.G., Ghetti, B. & Goedert, M. (2022) Classification of diseases with accumulation of Tau protein. *Neuropathol Appl Neurobiol*, **48**, e12792.

Kovacs, G.G., Robinson, J.L., Xie, S.X., Lee, E.B., Grossman, M., Wolk, D.A., Irwin, D.J., Weintraub, D., Kim, C.F., Schuck, T., Yousef, A., Wagner, S.T., Suh, E., Van Deerlin, V.M., Lee, V.M. & Trojanowski, J.Q. (2017a) Evaluating the Patterns of Aging-Related Tau Astrogliopathy Unravels Novel Insights Into Brain Aging and Neurodegenerative Diseases. *J Neuropathol Exp Neurol*, **76**, 270-288.

Kovacs, G.G., Xie, S.X., Lee, E.B., Robinson, J.L., Caswell, C., Irwin, D.J., Toledo, J.B., Johnson, V.E., Smith, D.H., Alafuzoff, I., Attems, J., Bencze, J., Bieniek, K.F., Bigio, E.H., Bodi, I., Budka, H., Dickson, D.W., Dugger, B.N., Duyckaerts, C., Ferrer, I., Forrest, S.L., Gelpi, E., Gentleman, S.M., Giaccone, G., Grinberg, L.T., Halliday, G.M., Hatanpaa, K.J., Hof, P.R., Hofer, M., Hortobagyi, T., Ironside, J.W., King, A., Kofler, J., Kovari, E., Kril, J.J., Love, S., Mackenzie, I.R., Mao, Q., Matej, R., McLean, C., Munoz, D.G., Murray, M.E., Neltner, J., Nelson, P.T., Ritchie, D., Rodriguez, R.D., Rohan, Z., Rozemuller, A., Sakai, K., Schultz, C., Seilhean, D., Smith, V., Tacik, P., Takahashi, H., Takao, M., Rudolf Thal, D., Weis, S., Wharton, S.B., White, C.L., 3rd, Woulfe, J.M., Yamada, M. & Trojanowski, J.Q. (2017b) Multisite Assessment of Aging-Related Tau Astrogliopathy (ARTAG). *J Neuropathol Exp Neurol*, **76**, 605-619.

Kovacs, G.G., Xie, S.X., Robinson, J.L., Lee, E.B., Smith, D.H., Schuck, T., Lee, V.M. & Trojanowski, J.Q. (2018) Sequential stages and distribution patterns of aging-related tau astrogliopathy (ARTAG) in the human brain. *Acta Neuropathol Commun*, **6**, 50.

Krammer, C., Schatzl, H.M. & Vorberg, I. (2009) Prion-like propagation of cytosolic protein aggregates: insights from cell culture models. *Prion*, **3**, 206-212.

Kruger, L. & Mandelkow, E.M. (2016) Tau neurotoxicity and rescue in animal models of human Tauopathies. *Curr Opin Neurobiol*, **36**, 52-58.

Kuhn, R., Mahajan, A., Canoll, P. & Hargus, G. (2021) Human Induced Pluripotent Stem Cell Models of Frontotemporal Dementia With Tau Pathology. *Front Cell Dev Biol*, **9**, 766773.

Kumar, S., Tepper, K., Kaniyappan, S., Biernat, J., Wegmann, S., Mandelkow, E.M., Muller, D.J. & Mandelkow, E. (2014) Stages and conformations of the Tau repeat domain during aggregation and its effect on neuronal toxicity. *J Biol Chem*, **289**, 20318-20332.

Kuret, J., Congdon, E.E., Li, G., Yin, H., Yu, X. & Zhong, Q. (2005) Evaluating triggers and enhancers of tau fibrillization. *Microsc Res Tech*, **67**, 141-155.

Kurz, A., Riemenschneider, M., Buch, K., Willoch, F., Bartenstein, P., Muller, U. & Guder, W. (1998) Tau protein in cerebrospinal fluid is significantly increased at the earliest clinical stage of Alzheimer disease. *Alzheimer Dis Assoc Disord*, **12**, 372-377.

La Vitola, P., Beeg, M., Balducci, C., Santamaria, G., Restelli, E., Colombo, L., Caldinelli, L., Pollegioni, L., Gobbi, M., Chiesa, R. & Forloni, G. (2019) Cellular prion protein neither binds to alpha-synuclein oligomers nor mediates their detrimental effects. *Brain*, **142**, 249-254.

Lauren, J., Gimbel, D.A., Nygaard, H.B., Gilbert, J.W. & Strittmatter, S.M. (2009) Cellular prion protein mediates impairment of synaptic plasticity by amyloid-beta oligomers. *Nature*, **457**, 1128-1132.

Laurent, C., Buee, L. & Blum, D. (2018) Tau and neuroinflammation: What impact for Alzheimer's Disease and Tauopathies? *Biomed J*, **41**, 21-33.

Lee, G., Neve, R.L. & Kosik, K.S. (1989) The microtubule binding domain of tau protein. *Neuron*, **2**, 1615-1624.

Lee, G., Newman, S.T., Gard, D.L., Band, H. & Panchamoorthy, G. (1998) Tau interacts with src-family non-receptor tyrosine kinases. *J Cell Sci*, **111 (Pt 21)**, 3167-3177.

Lee, V.M., Daughenbaugh, R. & Trojanowski, J.Q. (1994) Microtubule stabilizing drugs for the treatment of Alzheimer's disease. *Neurobiol Aging*, **15 Suppl 2**, S87-89.

Legname, G. (2017) Elucidating the function of the prion protein. *PLoS Pathog*, **13**, e1006458.

Legname, G. & Moda, F. (2017) The Prion Concept and Synthetic Prions. *Prog Mol Biol Transl Sci*, **150**, 147-156.

Legname, G. & Scialo, C. (2020) On the role of the cellular prion protein in the uptake and signaling of pathological aggregates in neurodegenerative diseases. *Prion*, **14**, 257-270.

Li, W. & Lee, V.M. (2006) Characterization of two VQIXXK motifs for tau fibrillization in vitro. *Biochemistry*, **45**, 15692-15701.

Lidon, L., Llao-Hierro, L., Nuvolone, M., Aguzzi, A., Avila, J., Ferrer, I., Del Rio, J.A. & Gavin, R. (2021) Tau Exon 10 Inclusion by PrP(C) through Downregulating GSK3beta Activity. *Int J Mol Sci*, **22**.

Lima, F.R., Arantes, C.P., Muras, A.G., Nomizo, R., Brentani, R.R. & Martins, V.R. (2007) Cellular prion protein expression in astrocytes modulates neuronal survival and differentiation. *J Neurochem*, **103**, 2164-2176.

Linden, R., Martins, V.R., Prado, M.A., Cammarota, M., Izquierdo, I. & Brentani, R.R. (2008) Physiology of the prion protein. *Physiol Rev*, **88**, 673-728.

Liu, C. & Gotz, J. (2013) Profiling murine tau with 0N, 1N and 2N isoform-specific antibodies in brain and peripheral organs reveals distinct subcellular localization, with the 1N isoform being enriched in the nucleus. *PLoS One*, **8**, e84849.

Liu, C., Song, X., Nisbet, R. & Gotz, J. (2016) Co-immunoprecipitation with Tau Isoform-specific Antibodies Reveals Distinct Protein Interactions and Highlights a Putative Role for 2N Tau in Disease. *J Biol Chem*, **291**, 8173-8188.

Liu, L., Drouet, V., Wu, J.W., Witter, M.P., Small, S.A., Clelland, C. & Duff, K. (2012) Trans-synaptic spread of tau pathology in vivo. *PLoS One*, **7**, e31302.

Liu, Y., Senatore, A., Sorce, S., Nuvolone, M., Guo, J., Gumus, Z.H. & Aguzzi, A. (2022) Brain aging is faithfully modelled in organotypic brain slices and accelerated by prions. *Commun Biol*, **5**, 557.

Lo, C.H. (2021) Recent advances in cellular biosensor technology to investigate tau oligomerization. *Bioeng Transl Med*, **6**, e10231.

Lo, C.H., Lim, C.K., Ding, Z., Wickramasinghe, S.P., Braun, A.R., Ashe, K.H., Rhoades, E., Thomas, D.D. & Sachs, J.N. (2019) Targeting the ensemble of heterogeneous tau oligomers in cells: A novel small molecule screening platform for tauopathies. *Alzheimers Dement*, **15**, 1489-1502.

Louros, N., Ramakers, M., Michiels, E., Konstantoulea, K., Morelli, C., Garcia, T., Moonen, N., D'Haeyer, S., Goossens, V., Thal, D.R., Audenaert, D., Rousseau, F. & Schymkowitz, J. (2022) Mapping the sequence specificity of heterotypic amyloid interactions enables the identification of aggregation modifiers. *Nat Commun*, **13**, 1351.

Madhavan, M., Nevin, Z.S., Shick, H.E., Garrison, E., Clarkson-Paredes, C., Karl, M., Clayton, B.L.L., Factor, D.C., Allan, K.C., Barbar, L., Jain, T., Douvaras, P., Fossati, V., Miller, R.H. & Tesar, P.J. (2018) Induction of myelinating oligodendrocytes in human cortical spheroids. *Nat Methods*, **15**, 700-706.

Maeda, S., Djukic, B., Taneja, P., Yu, G.Q., Lo, I., Davis, A., Craft, R., Guo, W., Wang, X., Kim, D., Ponnusamy, R., Gill, T.M., Masliah, E. & Mucke, L. (2016) Expression of A152T human tau causes age-dependent neuronal dysfunction and loss in transgenic mice. *EMBO Rep*, **17**, 530-551.

Maeda, S. & Takashima, A. (2019) Tau Oligomers. *Adv Exp Med Biol*, **1184**, 373-380.

Magnoni, S., Esparza, T.J., Conte, V., Carbonara, M., Carrabba, G., Holtzman, D.M., Zipfel, G.J., Stocchetti, N. & Brody, D.L. (2012) Tau elevations in the brain extracellular space correlate with reduced amyloid-beta levels and predict adverse clinical outcomes after severe traumatic brain injury. *Brain*, **135**, 1268-1280.

Mandelkow, E.M. & Mandelkow, E. (2012) Biochemistry and cell biology of tau protein in neurofibrillary degeneration. *Cold Spring Harb Perspect Med*, **2**, a006247.

Manson, J.C., Clarke, A.R., Hooper, M.L., Aitchison, L., McConnell, I. & Hope, J. (1994) 129/Ola mice carrying a null mutation in PrP that abolishes mRNA production are developmentally normal. *Mol Neurobiol*, **8**, 121-127.

Mantuano, E., Azmoon, P., Banki, M.A., Lam, M.S., Sigurdson, C.J. & Gonias, S.L. (2020) A soluble derivative of PrP(C) activates cell-signaling and regulates cell physiology through LRP1 and the NMDA receptor. *J Biol Chem*, **295**, 14178-14188.

Martin, L., Latypova, X. & Terro, F. (2011) Post-translational modifications of tau protein: implications for Alzheimer's disease. *Neurochem Int*, **58**, 458-471.

Martin, L., Latypova, X., Wilson, C.M., Magnaudeix, A., Perrin, M.L. & Terro, F. (2013a) Tau protein phosphatases in Alzheimer's disease: the leading role of PP2A. *Ageing Res Rev*, **12**, 39-49.

Martin, L., Latypova, X., Wilson, C.M., Magnaudeix, A., Perrin, M.L., Yardin, C. & Terro, F. (2013b) Tau protein kinases: involvement in Alzheimer's disease. *Ageing Res Rev*, **12**, 289-309.

Martinez, J., Sanchez, R., Castellanos, M., Makarava, N., Aguzzi, A., Baskakov, I.V. & Gasset, M. (2015) PrP charge structure encodes interdomain interactions. *Sci Rep*, **5**, 13623.

Masliah, E., Terry, R.D., DeTeresa, R.M. & Hansen, L.A. (1989) Immunohistochemical quantification of the synapse-related protein synaptophysin in Alzheimer disease. *Neurosci Lett*, **103**, 234-239.

Matamoros-Angles, A., Gayosso, L.M., Richaud-Patin, Y., di Domenico, A., Vergara, C., Hervera, A., Sousa, A., Fernandez-Borges, N., Consiglio, A., Gavin, R., Lopez de Maturana, R., Ferrer, I., Lopez de Munain, A., Raya, A., Castilla, J., Sanchez-Pernaute, R. & Del Rio, J.A. (2018) iPS Cell Cultures from a Gerstmann-Straussler-Scheinker Patient with the Y218N PRNP Mutation Recapitulate tau Pathology. *Mol Neurobiol*, **55**, 3033-3048.

McCarthy, J.M., Virdee, J., Brown, J., Ursu, D., Ahmed, Z., Cavallini, A. & Nuthall, H.N. (2021) Development of P301S tau seeded organotypic hippocampal slice cultures to study potential therapeutics. *Sci Rep*, **11**, 10309.

McMillan, P., Korvatska, E., Poorkaj, P., Evstafjeva, Z., Robinson, L., Greenup, L., Leverenz, J., Schellenberg, G.D. & D'Souza, I. (2008) Tau isoform regulation is region- and cell-specific in mouse brain. *J Comp Neurol*, **511**, 788-803.

Medina, M. & Avila, J. (2014a) The need for better AD animal models. *Front Pharmacol*, **5**, 227.

Medina, M. & Avila, J. (2014b) The role of extracellular Tau in the spreading of neurofibrillary pathology. *Front Cell Neurosci*, **8**, 113.

Medina, M., Hernandez, F. & Avila, J. (2016) New Features about Tau Function and Dysfunction. *Biomolecules*, **6**.

Messing, L., Decker, J.M., Joseph, M., Mandelkow, E. & Mandelkow, E.M. (2013) Cascade of tau toxicity in inducible hippocampal brain slices and prevention by aggregation inhibitors. *Neurobiol Aging*, **34**, 1343-1354.

Michel, C.H., Kumar, S., Pinotsi, D., Tunnacliffe, A., St George-Hyslop, P., Mandelkow, E., Mandelkow, E.M., Kaminski, C.F. & Kaminski Schierle, G.S. (2014) Extracellular monomeric tau protein is sufficient to initiate the spread of tau protein pathology. *J Biol Chem*, **289**, 956-967.

Millington, C., Sonego, S., Karunaweera, N., Rangel, A., Aldrich-Wright, J.R., Campbell, I.L., Gyengesi, E. & Munch, G. (2014) Chronic neuroinflammation in Alzheimer's

disease: new perspectives on animal models and promising candidate drugs. *Biomed Res Int*, **2014**, 309129.

Mirbaha, H., Chen, D., Mullapudi, V., Terpack, S.J., White, C.L., 3rd, Joachimiak, L.A. & Diamond, M.I. (2022) Seed-competent tau monomer initiates pathology in a tauopathy mouse model. *J Biol Chem*, **298**, 102163.

Mirbaha, H., Holmes, B.B., Sanders, D.W., Bieschke, J. & Diamond, M.I. (2015) Tau Trimers Are the Minimal Propagation Unit Spontaneously Internalized to Seed Intracellular Aggregation. *J Biol Chem*, **290**, 14893-14903.

Mocanu, M.M., Nissen, A., Eckermann, K., Khlistunova, I., Biernat, J., Drexler, D., Petrova, O., Schonig, K., Bujard, H., Mandelkow, E., Zhou, L., Rune, G. & Mandelkow, E.M. (2008) The potential for beta-structure in the repeat domain of tau protein determines aggregation, synaptic decay, neuronal loss, and coassembly with endogenous Tau in inducible mouse models of tauopathy. *J Neurosci*, **28**, 737-748.

Montejo de Garcini, E., Serrano, L. & Avila, J. (1986) Self assembly of microtubule associated protein tau into filaments resembling those found in Alzheimer disease. *Biochem Biophys Res Commun*, **141**, 790-796.

Mori, T., Koyama, N., Segawa, T., Maeda, M., Maruyama, N., Kinoshita, N., Hou, H., Tan, J. & Town, T. (2014) Methylene blue modulates beta-secretase, reverses cerebral amyloidosis, and improves cognition in transgenic mice. *J Biol Chem*, **289**, 30303-30317.

Moser, M., Colello, R.J., Pott, U. & Oesch, B. (1995) Developmental expression of the prion protein gene in glial cells. *Neuron*, **14**, 509-517.

Mudher, A., Colin, M., Dujardin, S., Medina, M., Dewachter, I., Alavi Naini, S.M., Mandelkow, E.M., Mandelkow, E., Buee, L., Goedert, M. & Brion, J.P. (2017) What is the evidence that tau pathology spreads through prion-like propagation? *Acta Neuropathol Commun*, **5**, 99.

Nakai, J., Ohkura, M. & Imoto, K. (2001) A high signal-to-noise Ca(2+) probe composed of a single green fluorescent protein. *Nat Biotechnol*, **19**, 137-141.

Nam, W.H. & Choi, Y.P. (2019) In vitro generation of tau aggregates conformationally distinct from parent tau seeds of Alzheimer's brain. *Prion*, **13**, 1-12.

Narasimhan, S., Guo, J.L., Changolkar, L., Stieber, A., McBride, J.D., Silva, L.V., He, Z., Zhang, B., Gathagan, R.J., Trojanowski, J.Q. & Lee, V.M.Y. (2017) Pathological Tau Strains from Human Brains Recapitulate the Diversity of Tauopathies in Nontransgenic Mouse Brain. *J Neurosci*, **37**, 11406-11423.

Necula, M. & Kuret, J. (2005) Site-specific pseudophosphorylation modulates the rate of tau filament dissociation. *FEBS Lett*, **579**, 1453-1457.

Neto, E., Leitao, L., Sousa, D.M., Alves, C.J., Alencastre, I.S., Aguiar, P. & Lamghari, M. (2016) Compartmentalized Microfluidic Platforms: The Unrivaled Breakthrough of In Vitro Tools for Neurobiological Research. *J Neurosci*, **36**, 11573-11584.

Nieznanska, H., Boyko, S., Dec, R., Redowicz, M.J., Dzwolak, W. & Nieznanski, K. (2021) Neurotoxicity of oligomers of phosphorylated Tau protein carrying

tauopathy-associated mutation is inhibited by prion protein. *Biochim Biophys Acta Mol Basis Dis*, **1867**, 166209.

Nishimiya, J. & Yuasa, T. (1999) [Progressive supranuclear palsy (PSP)]. *Ryoikibetsu Shokogun Shirizu*, 45-48.

Nizynski, B., Nieznanska, H., Dec, R., Boyko, S., Dzwolak, W. & Nieznanski, K. (2018) Amyloidogenic cross-seeding of Tau protein: Transient emergence of structural variants of fibrils. *PLoS One*, **13**, e0201182.

Noji, M., Samejima, T., Yamaguchi, K., So, M., Yuzu, K., Chatani, E., Akazawa-Ogawa, Y., Hagihara, Y., Kawata, Y., Ikenaka, K., Mochizuki, H., Kardos, J., Otzen, D.E., Bellotti, V., Buchner, J. & Goto, Y. (2021) Breakdown of supersaturation barrier links protein folding to amyloid formation. *Commun Biol*, **4**, 120.

Nonaka, T., Watanabe, S.T., Iwatsubo, T. & Hasegawa, M. (2010) Seeded aggregation and toxicity of {alpha}-synuclein and tau: cellular models of neurodegenerative diseases. *J Biol Chem*, **285**, 34885-34898.

Nuvolone, M., Hermann, M., Sorce, S., Russo, G., Tiberi, C., Schwarz, P., Minikel, E., Sanoudou, D., Pelczar, P. & Aguzzi, A. (2016) Strictly co-isogenic C57BL/6J-Prnp-/- mice: A rigorous resource for prion science. *J Exp Med*, **213**, 313-327.

Oakley, D.H., Klickstein, N., Commins, C., Chung, M., Dujardin, S., Bennett, R.E., Hyman, B.T. & Frosch, M.P. (2021) Continuous Monitoring of Tau-Induced Neurotoxicity in Patient-Derived iPSC-Neurons. *J Neurosci*, **41**, 4335-4348.

Olazaran, J., Prieto, J., Cruz, I. & Esteban, A. (2010) Cortical excitability in very mild Alzheimer's disease: a long-term follow-up study. *J Neurol*, **257**, 2078-2085.

Ondrejcak, T., Hu, N.W., Qi, Y., Klyubin, I., Corbett, G.T., Fraser, G., Perkinton, M.S., Walsh, D.M., Billinton, A. & Rowan, M.J. (2019) Soluble tau aggregates inhibit synaptic long-term depression and amyloid beta-facilitated LTD in vivo. *Neurobiol Dis*, **127**, 582-590.

Ondrejcak, T., Klyubin, I., Corbett, G.T., Fraser, G., Hong, W., Mably, A.J., Gardener, M., Hammersley, J., Perkinton, M.S., Billinton, A., Walsh, D.M. & Rowan, M.J. (2018) Cellular Prion Protein Mediates the Disruption of Hippocampal Synaptic Plasticity by Soluble Tau In Vivo. *J Neurosci*, **38**, 10595-10606.

Opitz, T., De Lima, A.D. & Voigt, T. (2002) Spontaneous development of synchronous oscillatory activity during maturation of cortical networks in vitro. *J Neurophysiol*, **88**, 2196-2206.

Ordonez-Gutierrez, L., Torres, J.M., Gavin, R., Anton, M., Arroba-Espinosa, A.I., Espinosa, J.C., Vergara, C., Del Rio, J.A. & Wandosell, F. (2013) Cellular prion protein modulates beta-amyloid deposition in aged APP/PS1 transgenic mice. *Neurobiol Aging*, **34**, 2793-2804.

Orlandi, J.G., Stetter, O., Soriano, J., Geisel, T. & Battaglia, D. (2014) Transfer entropy reconstruction and labeling of neuronal connections from simulated calcium imaging. *PLoS One*, **9**, e98842.

Osinde, M., Clavaguera, F., May-Nass, R., Tolnay, M. & Dev, K.K. (2008) Lentivirus Tau (P301S) expression in adult amyloid precursor protein (APP)-transgenic mice leads to tangle formation. *Neuropathol Appl Neurobiol*, **34**, 523-531.

Palop, J.J. & Mucke, L. (2010) Synaptic depression and aberrant excitatory network activity in Alzheimer's disease: two faces of the same coin? *Neuromolecular Med*, **12**, 48-55.

Palop, J.J. & Mucke, L. (2016) Network abnormalities and interneuron dysfunction in Alzheimer disease. *Nat Rev Neurosci*, **17**, 777-792.

Pampuscenko, K., Morkuniene, R., Krasauskas, L., Smirnovas, V., Tomita, T. & Borutaite, V. (2021) Distinct Neurotoxic Effects of Extracellular Tau Species in Primary Neuronal-Glial Cultures. *Mol Neurobiol*, **58**, 658-667.

Pan, K.M., Baldwin, M., Nguyen, J., Gasset, M., Serban, A., Groth, D., Mehlhorn, I., Huang, Z., Fletterick, R.J., Cohen, F.E. & et al. (1993) Conversion of alpha-helices into beta-sheets features in the formation of the scrapie prion proteins. *Proc Natl Acad Sci U S A*, **90**, 10962-10966.

Pasquale, V., Massobrio, P., Bologna, L.L., Chiappalone, M. & Martinoia, S. (2008) Self-organization and neuronal avalanches in networks of dissociated cortical neurons. *Neuroscience*, **153**, 1354-1369.

Pellegrini, L. & Lancaster, M.A. (2021) Modeling neurodegeneration with mutant-tau organoids. *Cell*, **184**, 4377-4379.

Philiastides, A., Ribes, J.M., Yip, D.C., Schmidt, C., Benilova, I. & Klohn, P.C. (2019) A New Cell Model for Investigating Prion Strain Selection and Adaptation. *Viruses*, **11**.

Pooler, A.M. & Hanger, D.P. (2010) Functional implications of the association of tau with the plasma membrane. *Biochem Soc Trans*, **38**, 1012-1015.

Pooler, A.M., Phillips, E.C., Lau, D.H., Noble, W. & Hanger, D.P. (2013) Physiological release of endogenous tau is stimulated by neuronal activity. *EMBO Rep*, **14**, 389-394.

Poorkaj, P., Bird, T.D., Wijsman, E., Nemens, E., Garruto, R.M., Anderson, L., Andreadis, A., Wiederholt, W.C., Raskind, M. & Schellenberg, G.D. (1998) Tau is a candidate gene for chromosome 17 frontotemporal dementia. *Ann Neurol*, **43**, 815-825.

Porzoor, A. & Macreadie, I.G. (2013) Application of yeast to study the tau and amyloid-beta abnormalities of Alzheimer's disease. *J Alzheimers Dis*, **35**, 217-225.

Probst, A. & Tolnay, M. (2002) [Argyrophilic grain disease (AgD), a frequent and largely underestimated cause of dementia in old patients]. *Rev Neurol (Paris)*, **158**, 155-165.

Prusiner, S.B. (1982) Novel proteinaceous infectious particles cause scrapie. *Science*, **216**, 136-144.

Prusiner, S.B. (1991) Molecular biology of prion diseases. *Science*, **252**, 1515-1522.

Prusiner, S.B. (1998) Prions. *Proc Natl Acad Sci U S A*, **95**, 13363-13383.

Prusiner, S.B. (2012) Cell biology. A unifying role for prions in neurodegenerative diseases. *Science*, **336**, 1511-1513.

Prusiner, S.B. & DeArmond, S.J. (1994) Prion diseases and neurodegeneration. *Annu Rev Neurosci*, **17**, 311-339.

Puckett, C., Concannon, P., Casey, C. & Hood, L. (1991) Genomic structure of the human prion protein gene. *Am J Hum Genet*, **49**, 320-329.

Puzzo, D., Piacentini, R., Fa, M., Gulisano, W., Li Puma, D.D., Staniszewski, A., Zhang, H., Tropea, M.R., Cocco, S., Palmeri, A., Fraser, P., D'Adamio, L., Grassi, C. & Arancio, O. (2017) LTP and memory impairment caused by extracellular Abeta and Tau oligomers is APP-dependent. *Elife*, **6**.

Raj, A., Kuceyeski, A. & Weiner, M. (2012) A network diffusion model of disease progression in dementia. *Neuron*, **73**, 1204-1215.

Ramachandran, G. & Udgaonkar, J.B. (2011) Understanding the kinetic roles of the inducer heparin and of rod-like protofibrils during amyloid fibril formation by Tau protein. *J Biol Chem*, **286**, 38948-38959.

Ramsden, M., Kotilinek, L., Forster, C., Paulson, J., McGowan, E., SantaCruz, K., Guimaraes, A., Yue, M., Lewis, J., Carlson, G., Hutton, M. & Ashe, K.H. (2005) Age-dependent neurofibrillary tangle formation, neuron loss, and memory impairment in a mouse model of human tauopathy (P301L). *J Neurosci*, **25**, 10637-10647.

Rankin, C.A., Sun, Q. & Gamblin, T.C. (2005) Pseudo-phosphorylation of tau at Ser202 and Thr205 affects tau filament formation. *Brain Res Mol Brain Res*, **138**, 84-93.

Rauch, J.N., Chen, J.J., Sorum, A.W., Miller, G.M., Sharf, T., See, S.K., Hsieh-Wilson, L.C., Kampmann, M. & Kosik, K.S. (2018) Tau Internalization is Regulated by 6-O Sulfation on Heparan Sulfate Proteoglycans (HSPGs). *Sci Rep*, **8**, 6382.

Rauch, J.N., Luna, G., Guzman, E., Audouard, M., Challis, C., Sibih, Y.E., Leshuk, C., Hernandez, I., Wegmann, S., Hyman, B.T., Gradinaru, V., Kampmann, M. & Kosik, K.S. (2020) LRP1 is a master regulator of tau uptake and spread. *Nature*, **580**, 381-385.

Ren, Y. & Sahara, N. (2013) Characteristics of tau oligomers. *Front Neurol*, **4**, 102.

Resenberger, U.K., Harmeier, A., Woerner, A.C., Goodman, J.L., Muller, V., Krishnan, R., Vabulas, R.M., Kretzschmar, H.A., Lindquist, S., Hartl, F.U., Multhaup, G., Winklhofer, K.F. & Tatzelt, J. (2011) The cellular prion protein mediates neurotoxic signalling of beta-sheet-rich conformers independent of prion replication. *EMBO J*, **30**, 2057-2070.

Resenberger, U.K., Winklhofer, K.F. & Tatzelt, J. (2012) Cellular prion protein mediates toxic signaling of amyloid beta. *Neurodegener Dis*, **10**, 298-300.

Roberson, E.D., Halabisky, B., Yoo, J.W., Yao, J., Chin, J., Yan, F., Wu, T., Hamto, P., Devidze, N., Yu, G.Q., Palop, J.J., Noebels, J.L. & Mucke, L. (2011) Amyloid-

beta/Fyn-induced synaptic, network, and cognitive impairments depend on tau levels in multiple mouse models of Alzheimer's disease. *J Neurosci*, **31**, 700-711.

Rohan, Z., Milenkovic, I., Lutz, M.I., Matej, R. & Kovacs, G.G. (2016) Shared and Distinct Patterns of Oligodendroglial Response in alpha-Synucleinopathies and Tauopathies. *J Neuropathol Exp Neurol*, **75**, 1100-1109.

Rosener, N.S., Gremer, L., Wordehoff, M.M., Kupreichyk, T., Etzkorn, M., Neudecker, P. & Hoyer, W. (2020) Clustering of human prion protein and alpha-synuclein oligomers requires the prion protein N-terminus. *Commun Biol*, **3**, 365.

Rosler, T.W., Tayaranian Marvian, A., Brendel, M., Nykanen, N.P., Hollerhage, M., Schwarz, S.C., Hopfner, F., Koeglsperger, T., Respondek, G., Schweyer, K., Levin, J., Villemagne, V.L., Barthel, H., Sabri, O., Muller, U., Meissner, W.G., Kovacs, G.G. & Hoglinger, G.U. (2019) Four-repeat tauopathies. *Prog Neurobiol*, **180**, 101644.

Saito, T., Mihira, N., Matsuba, Y., Sasaguri, H., Hashimoto, S., Narasimhan, S., Zhang, B., Murayama, S., Higuchi, M., Lee, V.M.Y., Trojanowski, J.Q. & Saido, T.C. (2019) Humanization of the entire murine Mapt gene provides a murine model of pathological human tau propagation. *J Biol Chem*, **294**, 12754-12765.

Sala-Jarque, J., Mesquida-Veny, F., Badiola-Mateos, M., Samitier, J., Hervera, A. & Del Rio, J.A. (2020) Neuromuscular Activity Induces Paracrine Signaling and Triggers Axonal Regrowth after Injury in Microfluidic Lab-On-Chip Devices. *Cells*, **9**.

Sala-Jarque, J., Zimkowska, K., Avila, J., Ferrer, I. & Del Rio, J.A. (2022) Towards a Mechanistic Model of Tau-Mediated Pathology in Tauopathies: What Can We Learn from Cell-Based In Vitro Assays? *Int J Mol Sci*, **23**.

Saman, S., Kim, W., Raya, M., Visnick, Y., Miro, S., Saman, S., Jackson, B., McKee, A.C., Alvarez, V.E., Lee, N.C. & Hall, G.F. (2012) Exosome-associated tau is secreted in tauopathy models and is selectively phosphorylated in cerebrospinal fluid in early Alzheimer disease. *J Biol Chem*, **287**, 3842-3849.

Sanders, D.W., Kaufman, S.K., DeVos, S.L., Sharma, A.M., Mirbaha, H., Li, A., Barker, S.J., Foley, A.C., Thorpe, J.R., Serpell, L.C., Miller, T.M., Grinberg, L.T., Seeley, W.W. & Diamond, M.I. (2014) Distinct tau prion strains propagate in cells and mice and define different tauopathies. *Neuron*, **82**, 1271-1288.

Sanders, D.W., Kaufman, S.K., Holmes, B.B. & Diamond, M.I. (2016) Prions and Protein Assemblies that Convey Biological Information in Health and Disease. *Neuron*, **89**, 433-448.

Santacruz, K., Lewis, J., Spires, T., Paulson, J., Kotilinek, L., Ingelsson, M., Guimaraes, A., DeTure, M., Ramsden, M., McGowan, E., Forster, C., Yue, M., Orne, J., Janus, C., Mariash, A., Kuskowski, M., Hyman, B., Hutton, M. & Ashe, K.H. (2005) Tau suppression in a neurodegenerative mouse model improves memory function. *Science*, **309**, 476-481.

Scheres, S.H., Zhang, W., Falcon, B. & Goedert, M. (2020) Cryo-EM structures of tau filaments. *Curr Opin Struct Biol*, **64**, 17-25.

Schindelin, J., Arganda-Carreras, I., Frise, E., Kaynig, V., Longair, M., Pietzsch, T., Preibisch, S., Rueden, C., Saalfeld, S., Schmid, B., Tinevez, J.Y., White, D.J., Hartenstein, V., Eliceiri, K., Tomancak, P. & Cardona, A. (2012) Fiji: an open-source platform for biological-image analysis. *Nat Methods*, **9**, 676-682.

Schmitz, M., Cramm, M., Llorens, F., Muller-Cramm, D., Collins, S., Atarashi, R., Satoh, K., Orru, C.D., Groveman, B.R., Zafar, S., Schulz-Schaeffer, W.J., Caughey, B. & Zerr, I. (2016) The real-time quaking-induced conversion assay for detection of human prion disease and study of other protein misfolding diseases. *Nat Protoc*, **11**, 2233-2242.

Schmitz, M., Wulf, K., Signore, S.C., Schulz-Schaeffer, W.J., Kermer, P., Bahr, M., Wouters, F.S., Zafar, S. & Zerr, I. (2014) Impact of the cellular prion protein on amyloid-beta and 3PO-tau processing. *J Alzheimers Dis*, **38**, 551-565.

Scholl, M., Lockhart, S.N., Schonhaut, D.R., O'Neil, J.P., Janabi, M., Ossenkoppele, R., Baker, S.L., Vogel, J.W., Faria, J., Schwimmer, H.D., Rabinovici, G.D. & Jagust, W.J. (2016) PET Imaging of Tau Deposition in the Aging Human Brain. *Neuron*, **89**, 971-982.

Scholl, M., Maass, A., Mattsson, N., Ashton, N.J., Blennow, K., Zetterberg, H. & Jagust, W. (2019) Biomarkers for tau pathology. *Mol Cell Neurosci*, **97**, 18-33.

Schweers, O., Schonbrunn-Hanebeck, E., Marx, A. & Mandelkow, E. (1994) Structural studies of tau protein and Alzheimer paired helical filaments show no evidence for beta-structure. *J Biol Chem*, **269**, 24290-24297.

Scott-McKean, J.J., Surewicz, K., Choi, J.K., Ruffin, V.A., Salameh, A.I., Nieznanski, K., Costa, A.C.S. & Surewicz, W.K. (2016) Soluble prion protein and its N-terminal fragment prevent impairment of synaptic plasticity by Abeta oligomers: Implications for novel therapeutic strategy in Alzheimer's disease. *Neurobiol Dis*, **91**, 124-131.

Seeley, W.W., Crawford, R.K., Zhou, J., Miller, B.L. & Greicius, M.D. (2009) Neurodegenerative diseases target large-scale human brain networks. *Neuron*, **62**, 42-52.

Seidler, P.M., Boyer, D.R., Murray, K.A., Yang, T.P., Bentzel, M., Sawaya, M.R., Rosenberg, G., Cascio, D., Williams, C.K., Newell, K.L., Ghetti, B., DeTure, M.A., Dickson, D.W., Vinters, H.V. & Eisenberg, D.S. (2019) Structure-based inhibitors halt prion-like seeding by Alzheimer's disease-and tauopathy-derived brain tissue samples. *J Biol Chem*, **294**, 16451-16464.

Seidler, P.M., Boyer, D.R., Rodriguez, J.A., Sawaya, M.R., Cascio, D., Murray, K., Gonen, T. & Eisenberg, D.S. (2018) Structure-based inhibitors of tau aggregation. *Nat Chem*, **10**, 170-176.

Sharma, A.M., Thomas, T.L., Woodard, D.R., Kashmer, O.M. & Diamond, M.I. (2018) Tau monomer encodes strains. *Elife*, **7**.

Shi, Y., Zhang, W., Yang, Y., Murzin, A.G., Falcon, B., Kotecha, A., van Beers, M., Tarutani, A., Kametani, F., Garringer, H.J., Vidal, R., Hallinan, G.I., Lashley, T., Saito, Y., Murayama, S., Yoshida, M., Tanaka, H., Kakita, A., Ikeuchi, T., Robinson, A.C., Mann, D.M.A., Kovacs, G.G., Revesz, T., Ghetti, B., Hasegawa,

M., Goedert, M. & Scheres, S.H.W. (2021) Structure-based classification of tauopathies. *Nature*, **598**, 359-363.

Shimada, H., Sato, Y., Sasaki, T., Shimozawa, A., Imaizumi, K., Shindo, T., Miyao, S., Kiyama, K., Kondo, T., Shibata, S., Ishii, S., Kuromitsu, J., Aoyagi, H., Ito, D. & Okano, H. (2022) A next-generation iPSC-derived forebrain organoid model of tauopathy with tau fibrils by AAV-mediated gene transfer. *Cell Rep Methods*, **2**, 100289.

Shin, W.S., Di, J., Murray, K.A., Sun, C., Li, B., Bitan, G. & Jiang, L. (2019) Different Amyloid-beta Self-Assemblies Have Distinct Effects on Intracellular Tau Aggregation. *Front Mol Neurosci*, **12**, 268.

Simon, D., Garcia-Garcia, E., Gomez-Ramos, A., Falcon-Perez, J.M., Diaz-Hernandez, M., Hernandez, F. & Avila, J. (2012) Tau overexpression results in its secretion via membrane vesicles. *Neurodegener Dis*, **10**, 73-75.

Sipe, J.D. & Cohen, A.S. (2000) Review: history of the amyloid fibril. *J Struct Biol*, **130**, 88-98.

Siskova, Z., Justus, D., Kaneko, H., Friedrichs, D., Henneberg, N., Beutel, T., Pitsch, J., Schoch, S., Becker, A., von der Kammer, H. & Remy, S. (2014) Dendritic structural degeneration is functionally linked to cellular hyperexcitability in a mouse model of Alzheimer's disease. *Neuron*, **84**, 1023-1033.

Sohn, P.D., Huang, C.T., Yan, R., Fan, L., Tracy, T.E., Camargo, C.M., Montgomery, K.M., Arhar, T., Mok, S.A., Freilich, R., Baik, J., He, M., Gong, S., Roberson, E.D., Karch, C.M., Gestwicki, J.E., Xu, K., Kosik, K.S. & Gan, L. (2019) Pathogenic Tau Impairs Axon Initial Segment Plasticity and Excitability Homeostasis. *Neuron*, **104**, 458-470 e455.

Sokolow, S., Henkins, K.M., Bilousova, T., Gonzalez, B., Vinters, H.V., Miller, C.A., Cornwell, L., Poon, W.W. & Gylys, K.H. (2015) Pre-synaptic C-terminal truncated tau is released from cortical synapses in Alzheimer's disease. *J Neurochem*, **133**, 368-379.

Soriano, J., Rodriguez Martinez, M., Tlusty, T. & Moses, E. (2008) Development of input connections in neural cultures. *Proc Natl Acad Sci U S A*, **105**, 13758-13763.

Spangenberg, E.E. & Green, K.N. (2017) Inflammation in Alzheimer's disease: Lessons learned from microglia-depletion models. *Brain Behav Immun*, **61**, 1-11.

Spillantini, M.G., Crowther, R.A., Kamphorst, W., Heutink, P. & van Swieten, J.C. (1998) Tau pathology in two Dutch families with mutations in the microtubule-binding region of tau. *Am J Pathol*, **153**, 1359-1363.

Stamer, K., Vogel, R., Thies, E., Mandelkow, E. & Mandelkow, E.M. (2002) Tau blocks traffic of organelles, neurofilaments, and APP vesicles in neurons and enhances oxidative stress. *J Cell Biol*, **156**, 1051-1063.

Stancu, I.C., Vasconcelos, B., Ris, L., Wang, P., Villers, A., Peeraer, E., Buist, A., Terwel, D., Baatsen, P., Oyelami, T., Pierrot, N., Casteels, C., Bormans, G., Kienlen-Campard, P., Octave, J.N., Moechars, D. & Dewachter, I. (2015) Templated misfolding of Tau by prion-like seeding along neuronal connections impairs

neuronal network function and associated behavioral outcomes in Tau transgenic mice. *Acta Neuropathol*, **129**, 875-894.

Stirling, D.R., Swain-Bowden, M.J., Lucas, A.M., Carpenter, A.E., Cimini, B.A. & Goodman, A. (2021) CellProfiler 4: improvements in speed, utility and usability. *BMC Bioinformatics*, **22**, 433.

Su, A.I., Wiltshire, T., Batalov, S., Lapp, H., Ching, K.A., Block, D., Zhang, J., Soden, R., Hayakawa, M., Kreiman, G., Cooke, M.P., Walker, J.R. & Hogenesch, J.B. (2004) A gene atlas of the mouse and human protein-encoding transcriptomes. *Proc Natl Acad Sci U S A*, **101**, 6062-6067.

Tagliavini, F., Giaccone, G., Prelli, F., Verga, L., Porro, M., Trojanowski, J.Q., Farlow, M.R., Frangione, B., Ghetti, B. & Bugiani, O. (1993) A68 is a component of paired helical filaments of Gerstmann-Straussler-Scheinker disease, Indiana kindred. *Brain Res*, **616**, 325-329.

Tak, H., Haque, M.M., Kim, M.J., Lee, J.H., Baik, J.H., Kim, Y., Kim, D.J., Grailhe, R. & Kim, Y.K. (2013) Bimolecular fluorescence complementation; lighting-up tau-tau interaction in living cells. *PLoS One*, **8**, e81682.

Takahashi, R.H., Tobiume, M., Sato, Y., Sata, T., Gouras, G.K. & Takahashi, H. (2011) Accumulation of cellular prion protein within dystrophic neurites of amyloid plaques in the Alzheimer's disease brain. *Neuropathology*, **31**, 208-214.

Takahashi, R.H., Yokotsuka, M., Tobiume, M., Sato, Y., Hasegawa, H., Nagao, T. & Gouras, G.K. (2021) Accumulation of cellular prion protein within beta-amyloid oligomer plaques in aged human brains. *Brain Pathol*, **31**, e12941.

Takeda, S., Commins, C., DeVos, S.L., Nobuhara, C.K., Wegmann, S., Roe, A.D., Costantino, I., Fan, Z., Nicholls, S.B., Sherman, A.E., Trisini Lipsanopoulos, A.T., Scherzer, C.R., Carlson, G.A., Pitstick, R., Peskind, E.R., Raskind, M.A., Li, G., Montine, T.J., Frosch, M.P. & Hyman, B.T. (2016) Seed-competent high-molecular-weight tau species accumulates in the cerebrospinal fluid of Alzheimer's disease mouse model and human patients. *Ann Neurol*, **80**, 355-367.

Takeda, S., Wegmann, S., Cho, H., DeVos, S.L., Commins, C., Roe, A.D., Nicholls, S.B., Carlson, G.A., Pitstick, R., Nobuhara, C.K., Costantino, I., Frosch, M.P., Muller, D.J., Irimia, D. & Hyman, B.T. (2015) Neuronal uptake and propagation of a rare phosphorylated high-molecular-weight tau derived from Alzheimer's disease brain. *Nat Commun*, **6**, 8490.

Tanzi, R.E. & Bertram, L. (2001) New frontiers in Alzheimer's disease genetics. *Neuron*, **32**, 181-184.

Tardivel, M., Begard, S., Bousset, L., Dujardin, S., Coens, A., Melki, R., Buee, L. & Colin, M. (2016) Tunneling nanotube (TNT)-mediated neuron-to neuron transfer of pathological Tau protein assemblies. *Acta Neuropathol Commun*, **4**, 117.

Taylor, A.M. & Jeon, N.L. (2010) Micro-scale and microfluidic devices for neurobiology. *Curr Opin Neurobiol*, **20**, 640-647.

Tepper, K., Biernat, J., Kumar, S., Wegmann, S., Timm, T., Hubschmann, S., Redecke, L., Mandelkow, E.M., Muller, D.J. & Mandelkow, E. (2014) Oligomer formation of tau protein hyperphosphorylated in cells. *J Biol Chem*, **289**, 34389-34407.

Terwel, D., Lasrado, R., Snauwaert, J., Vandeweert, E., Van Haesendonck, C., Borghgraef, P. & Van Leuven, F. (2005) Changed conformation of mutant Tau-P301L underlies the moribund tauopathy, absent in progressive, nonlethal axonopathy of Tau-4R/2N transgenic mice. *J Biol Chem*, **280**, 3963-3973.

Thom, T., Schmitz, M., Fischer, A.L., Correia, A., Correia, S., Llorens, F., Pique, A.V., Mobius, W., Domingues, R., Zafar, S., Stoops, E., Silva, C.J., Fischer, A., Outeiro, T.F. & Zerr, I. (2022) Cellular Prion Protein Mediates alpha-Synuclein Uptake, Localization, and Toxicity In Vitro and In Vivo. *Mov Disord*, **37**, 39-51.

Tian, H., Davidowitz, E., Lopez, P., Emadi, S., Moe, J. & Sierks, M. (2013) Trimeric tau is toxic to human neuronal cells at low nanomolar concentrations. *Int J Cell Biol*, **2013**, 260787.

Tibau, E., Valencia, M. & Soriano, J. (2013) Identification of neuronal network properties from the spectral analysis of calcium imaging signals in neuronal cultures. *Front Neural Circuits*, **7**, 199.

Urrea, L., Segura-Feliu, M., Masuda-Suzukake, M., Hervera, A., Pedraz, L., Garcia Aznar, J.M., Vila, M., Samitier, J., Torrents, E., Ferrer, I., Gavin, R., Hagesawa, M. & Del Rio, J.A. (2018) Involvement of Cellular Prion Protein in alpha-Synuclein Transport in Neurons. *Mol Neurobiol*, **55**, 1847-1860.

Usenovic, M., Niroomand, S., Drolet, R.E., Yao, L., Gaspar, R.C., Hatcher, N.G., Schachter, J., Renger, J.J. & Parmentier-Batteur, S. (2015) Internalized Tau Oligomers Cause Neurodegeneration by Inducing Accumulation of Pathogenic Tau in Human Neurons Derived from Induced Pluripotent Stem Cells. *J Neurosci*, **35**, 14234-14250.

Vanhelmont, T., Vandebroek, T., De Vos, A., Terwel, D., Lemaire, K., Anandhakumar, J., Franssens, V., Swinnen, E., Van Leuven, F. & Winderickx, J. (2010) Serine-409 phosphorylation and oxidative damage define aggregation of human protein tau in yeast. *FEMS Yeast Res*, **10**, 992-1005.

Vascellari, S. & Manzin, A. (2021) Parkinson's Disease: A Prionopathy? *Int J Mol Sci*, **22**.

Vasconcelos, B., Stancu, I.C., Buist, A., Bird, M., Wang, P., Vanoosthuyse, A., Van Kolen, K., Verheyen, A., Kienlen-Campard, P., Octave, J.N., Baatsen, P., Moechars, D. & Dewachter, I. (2016) Heterotypic seeding of Tau fibrillization by pre-aggregated Abeta provides potent seeds for prion-like seeding and propagation of Tau-pathology in vivo. *Acta Neuropathol*, **131**, 549-569.

Vergara, C., Ordonez-Gutierrez, L., Wandosell, F., Ferrer, I., del Rio, J.A. & Gavin, R. (2015) Role of PrP(C) Expression in Tau Protein Levels and Phosphorylation in Alzheimer's Disease Evolution. *Mol Neurobiol*, **51**, 1206-1220.

Vogelsberg-Ragaglia, V., Bruce, J., Richter-Landsberg, C., Zhang, B., Hong, M., Trojanowski, J.Q. & Lee, V.M. (2000) Distinct FTDP-17 missense mutations in tau produce tau aggregates and other pathological phenotypes in transfected CHO cells. *Mol Biol Cell*, **11**, 4093-4104.

von Bergen, M., Barghorn, S., Li, L., Marx, A., Biernat, J., Mandelkow, E.M. & Mandelkow, E. (2001) Mutations of tau protein in frontotemporal dementia

promote aggregation of paired helical filaments by enhancing local beta-structure. *J Biol Chem*, **276**, 48165-48174.

von Bergen, M., Friedhoff, P., Biernat, J., Heberle, J., Mandelkow, E.M. & Mandelkow, E. (2000) Assembly of tau protein into Alzheimer paired helical filaments depends on a local sequence motif ((306)VQIVYK(311)) forming beta structure. *Proc Natl Acad Sci U S A*, **97**, 5129-5134.

Vossel, K.A., Beagle, A.J., Rabinovici, G.D., Shu, H., Lee, S.E., Naasan, G., Hegde, M., Cornes, S.B., Henry, M.L., Nelson, A.B., Seeley, W.W., Geschwind, M.D., Gorno-Tempini, M.L., Shih, T., Kirsch, H.E., Garcia, P.A., Miller, B.L. & Mucke, L. (2013) Seizures and epileptiform activity in the early stages of Alzheimer disease. *JAMA Neurol*, **70**, 1158-1166.

Wagner, U., Utton, M., Gallo, J.M. & Miller, C.C. (1996) Cellular phosphorylation of tau by GSK-3 beta influences tau binding to microtubules and microtubule organisation. *J Cell Sci*, **109 (Pt 6)**, 1537-1543.

Wang, C., Fan, L., Khawaja, R.R., Liu, B., Zhan, L., Kodama, L., Chin, M., Li, Y., Le, D., Zhou, Y., Condello, C., Grinberg, L.T., Seeley, W.W., Miller, B.L., Mok, S.A., Gestwicki, J.E., Cuervo, A.M., Luo, W. & Gan, L. (2022) Microglial NF-kappaB drives tau spreading and toxicity in a mouse model of tauopathy. *Nat Commun*, **13**, 1969.

Wang, J.Z., Grundke-Iqbal, I. & Iqbal, K. (2007) Kinases and phosphatases and tau sites involved in Alzheimer neurofibrillary degeneration. *Eur J Neurosci*, **25**, 59-68.

Wang, X.F., Dong, C.F., Zhang, J., Wan, Y.Z., Li, F., Huang, Y.X., Han, L., Shan, B., Gao, C., Han, J. & Dong, X.P. (2008) Human tau protein forms complex with PrP and some GSS- and fCJD-related PrP mutants possess stronger binding activities with tau in vitro. *Mol Cell Biochem*, **310**, 49-55.

Wang, Y., Balaji, V., Kaniyappan, S., Kruger, L., Irsen, S., Tepper, K., Chandupatla, R., Maetzler, W., Schneider, A., Mandelkow, E. & Mandelkow, E.M. (2017) The release and trans-synaptic transmission of Tau via exosomes. *Mol Neurodegener*, **12**, 5.

Watts, J.C., Bourkas, M.E.C. & Arshad, H. (2018) The function of the cellular prion protein in health and disease. *Acta Neuropathol*, **135**, 159-178.

Waxman, E.A. & Giasson, B.I. (2011) Induction of intracellular tau aggregation is promoted by alpha-synuclein seeds and provides novel insights into the hyperphosphorylation of tau. *J Neurosci*, **31**, 7604-7618.

Wegmann, S., Maury, E.A., Kirk, M.J., Saqran, L., Roe, A., DeVos, S.L., Nicholls, S., Fan, Z., Takeda, S., Cagsal-Getkin, O., William, C.M., Spires-Jones, T.L., Pitstick, R., Carlson, G.A., Pooler, A.M. & Hyman, B.T. (2015) Removing endogenous tau does not prevent tau propagation yet reduces its neurotoxicity. *EMBO J*, **34**, 3028-3041.

Wegmann, S., Nicholls, S., Takeda, S., Fan, Z. & Hyman, B.T. (2016) Formation, release, and internalization of stable tau oligomers in cells. *J Neurochem*, **139**, 1163-1174.

Willbold, D., Strodel, B., Schroder, G.F., Hoyer, W. & Heise, H. (2021) Amyloid-type Protein Aggregation and Prion-like Properties of Amyloids. *Chem Rev*, **121**, 8285-8307.

Wille, H., Drewes, G., Biernat, J., Mandelkow, E.M. & Mandelkow, E. (1992) Alzheimer-like paired helical filaments and antiparallel dimers formed from microtubule-associated protein tau in vitro. *J Cell Biol*, **118**, 573-584.

Wischik, C.M., Novak, M., Edwards, P.C., Klug, A., Tichelaar, W. & Crowther, R.A. (1988a) Structural characterization of the core of the paired helical filament of Alzheimer disease. *Proc Natl Acad Sci U S A*, **85**, 4884-4888.

Wischik, C.M., Novak, M., Thogersen, H.C., Edwards, P.C., Runswick, M.J., Jakes, R., Walker, J.E., Milstein, C., Roth, M. & Klug, A. (1988b) Isolation of a fragment of tau derived from the core of the paired helical filament of Alzheimer disease. *Proc Natl Acad Sci U S A*, **85**, 4506-4510.

Wiseman, F.K., Cancellotti, E., Piccardo, P., Iremonger, K., Boyle, A., Brown, D., Ironside, J.W., Manson, J.C. & Diack, A.B. (2015) The glycosylation status of PrPC is a key factor in determining transmissible spongiform encephalopathy transmission between species. *J Virol*, **89**, 4738-4747.

Woerman, A.L., Aoyagi, A., Patel, S., Kazmi, S.A., Lobach, I., Grinberg, L.T., McKee, A.C., Seeley, W.W., Olson, S.H. & Prusiner, S.B. (2016) Tau prions from Alzheimer's disease and chronic traumatic encephalopathy patients propagate in cultured cells. *Proc Natl Acad Sci U S A*, **113**, E8187-E8196.

Wu, J.W., Herman, M., Liu, L., Simoes, S., Acker, C.M., Figueroa, H., Steinberg, J.I., Margittai, M., Kayed, R., Zurzolo, C., Di Paolo, G. & Duff, K.E. (2013) Small misfolded Tau species are internalized via bulk endocytosis and anterogradely and retrogradely transported in neurons. *J Biol Chem*, **288**, 1856-1870.

Wu, J.W., Hussaini, S.A., Bastille, I.M., Rodriguez, G.A., Mrejeru, A., Rilett, K., Sanders, D.W., Cook, C., Fu, H., Boonen, R.A., Herman, M., Nahmani, E., Emrani, S., Figueroa, Y.H., Diamond, M.I., Clelland, C.L., Wray, S. & Duff, K.E. (2016) Neuronal activity enhances tau propagation and tau pathology in vivo. *Nat Neurosci*, **19**, 1085-1092.

Wulf, M.A., Senatore, A. & Aguzzi, A. (2017) The biological function of the cellular prion protein: an update. *BMC Biol*, **15**, 34.

Yamada, K., Cirrito, J.R., Stewart, F.R., Jiang, H., Finn, M.B., Holmes, B.B., Binder, L.I., Mandelkow, E.M., Diamond, M.I., Lee, V.M. & Holtzman, D.M. (2011) In vivo microdialysis reveals age-dependent decrease of brain interstitial fluid tau levels in P301S human tau transgenic mice. *J Neurosci*, **31**, 13110-13117.

Yamada, K., Holth, J.K., Liao, F., Stewart, F.R., Mahan, T.E., Jiang, H., Cirrito, J.R., Patel, T.K., Hochgrafe, K., Mandelkow, E.M. & Holtzman, D.M. (2014) Neuronal activity regulates extracellular tau in vivo. *J Exp Med*, **211**, 387-393.

Yang, S.H. (2019) Cellular and Molecular Mediators of Neuroinflammation in Alzheimer Disease. *Int Neurourol J*, **23**, S54-62.

Yoshiyama, Y., Higuchi, M., Zhang, B., Huang, S.M., Iwata, N., Saido, T.C., Maeda, J., Suhara, T., Trojanowski, J.Q. & Lee, V.M. (2007) Synapse loss and microglial

activation precede tangles in a P301S tauopathy mouse model. *Neuron*, **53**, 337-351.

Zahn, R., Liu, A., Luhrs, T., Riek, R., von Schroetter, C., Lopez Garcia, F., Billeter, M., Calzolai, L., Wider, G. & Wuthrich, K. (2000) NMR solution structure of the human prion protein. *Proc Natl Acad Sci U S A*, **97**, 145-150.

Zahs, K.R. & Ashe, K.H. (2010) 'Too much good news' - are Alzheimer mouse models trying to tell us how to prevent, not cure, Alzheimer's disease? *Trends Neurosci*, **33**, 381-389.

Zhang, H., Wei, W., Zhao, M., Ma, L., Jiang, X., Pei, H., Cao, Y. & Li, H. (2021) Interaction between Abeta and Tau in the Pathogenesis of Alzheimer's Disease. *Int J Biol Sci*, **17**, 2181-2192.

Zhang, W., Falcon, B., Murzin, A.G., Fan, J., Crowther, R.A., Goedert, M. & Scheres, S.H. (2019) Heparin-induced tau filaments are polymorphic and differ from those in Alzheimer's and Pick's diseases. *Elife*, **8**.

Zhang, W., Tarutani, A., Newell, K.L., Murzin, A.G., Matsubara, T., Falcon, B., Vidal, R., Garringer, H.J., Shi, Y., Ikeuchi, T., Murayama, S., Ghetti, B., Hasegawa, M., Goedert, M. & Scheres, S.H.W. (2020) Novel tau filament fold in corticobasal degeneration. *Nature*, **580**, 283-287.

Zhang, X., Lin, Y., Eschmann, N.A., Zhou, H., Rauch, J.N., Hernandez, I., Guzman, E., Kosik, K.S. & Han, S. (2017) RNA stores tau reversibly in complex coacervates. *PLoS Biol*, **15**, e2002183.

Zhou, J., Gennatas, E.D., Kramer, J.H., Miller, B.L. & Seeley, W.W. (2012) Predicting regional neurodegeneration from the healthy brain functional connectome. *Neuron*, **73**, 1216-1227.